PhD degree in Systems Medicine (curriculum in Molecular Oncology)

European School of Molecular Medicine (SEMM),

University of Milan and University of Naples "Federico II"

Settore disciplinare: BIO/11

Polycomb Repressive Complex 1 is required to maintain stem cell identity and to preserve adult tissue homeostasis.

Pivetti Silvia

IEO, Milan

Matricola n. R11473

Supervisor: Dr. / Prof. Pasini Diego IEO, Milan

Anno accademico 2018-2019

TABLE OF CONTENTS

LIST OF ABBREVIATIONS

APC	Adenomatous Polyposis Coli
BL	Basal Layer
BMP	Bone Morphogenetic Protein
CBC	Crypt Base Columnar
CBX	Chromobox
ChIP	Chromatin Immuno-Precipitation
CreERT2	Cre-recombinase Estrogen Receptor T2
Ctrl	Control
DEG	Differentially expressed genes
DP	Dermal Papilla
dKO	double Knock-Out
DUB	DeUbiquitinase
EED	Embryonic Ectoderm Development
EGF	Epidermal Growth Factor
EZH1	Enhancer of Zeste 1
EZH2	Enhancer of Zeste 1
FACS	Fluorescence Activated Cell Sorting
FBS	Fetal Bovine Serum
FGF	Fybroblast Growth Factor
GFP	Green Fluorescent Protein
HF	Hair Follicle
HFSC	Hair Follicle stem cell
HG	Hair Germ
HOX	Homeotic

HSC	Hematopoietic Stem cell
IFE	Interfollicular Epidermis
IP	Immunoprecipitation
IP injection	Intaperitoneal injection
Ires	Internal ribosome entry site
IRS	Inner Root Sheath
ISC	Intestinal Stem Cells
KO	Knock-Out
LoxP	Locus of Crossover in Phage P1
LGR5	Leucine-Rich Repeat Containing G Protein- Coupled Receptor 5
Me	Methylation
MEDS	Mosaic Ends Double-Stranded oligonucleotides
mESC	murine Embryonic Stem Cell
Mx	Matrix
O.C.T	Optimal Cutting Temperature
ORS	Outer Root Sheath
PCR	Polymerase Chain Reaction
PCG	Polycomb group of proteins
PCGF	Polycomb Group Ring Finger protein
PHC	Polyhomeotic-like protein
PLA	Proximity Ligation Assay
PRC1	Polycomb Repressive Complex 1
PRC2	Polycomb Repressive Complex 2
RING1A	Really Interesting New Gene 1A
RING1B	Really Interesting New Gene 1B

RPKM	Read Per Kilobases of Million Mapped Reads
RT	Room Temperature
RT-qPCR	Real Time quantitative PCR
RYBP	Ring and YY1 Binding Protein
SG	Sebaceous Gland
SHH	Sonic Hedgehog
SUZ12	Suppressor of Zeste
TAC	Transient amplifying cell
TF	Transcription Factor
TN5	Transposase 5
TrxG	Trithorax group of protein
TSS	Transcription Start Site
Ub	Ubiquitin
WNT	Wingless Integration site
YAF2	YY1 associated factor 2

FIGURE INDEX

2. INTRODUCTION

3. MATERIALS AND METHODS

4. RESULTS

1. ABSTRACT

Polycomb Repressive Complex 1 (PRC1) is an evolutionary conserved transcriptional repressive complex, fundamental for lineage fate decisions and maintenance during development. PRC1 acts by depositing a moiety of Ubiquitin on lysine 119 on histone H2A, promoting nucleosome compaction and transcriptional repression. Cell identity is a fundamental feature, not only during development, but it has to be maintained throughout the entire individual lifespan. Importantly, loss of cell identity is associated with pathologies, primarily with cancer.

We recently described that, in homeostatic condition, PRC1 loss of function in LGR5 expressing intestinal stem cells, led to severe defects in tissue maintenance due to loss of stem cell identity and stem cell self-renewal. This places PRC1 as a fundamental complex in stem cell preservation. In this context, PRC1 is necessary to repress non-lineage specific transcription factors, whose upregulation not only perturbs the transcriptome of stem cells, thus leading to identity loss, but also impairs the transcriptional control of the WNT pathway that is essential for stem cell self-renewal.

The landscape is even more complicated by the evidence that tissue context plays a critical role in protein function. In pathological conditions, primarily in cancer, several reports have described opposite roles for epigenetic players, including PRC1 subunits, depending on the cancer type. This highlights the importance of context dependency for the correct choice of the therapeutic approach. This opens up the possibility that PRC1 function, or PRC1 activity loss, could be different among different tissue types.

To address this point we evaluated PRC1 activity and function in a different LGR5 expressing stem cell populations that derives from a different embryonic layer, the hair follicle, analyzing the phenotype of loss of PRC1 activity in this context and comparing the

transcriptional outcomes in the different stem cell populations to describe the influence of context on PRC1-loss.

Our data support a general role of PRC1 in stem cell identity maintenance, that is accomplished through the regulation of the same targets. However, we show that, differently from intestinal stem cells, PRC1 activity loss in the hair follicle leads to the activation of a specific epidermal program, showing that the pool of transcription factors present in different stem cell population alters the transcriptional outcome of PRC1 loss.

To add a layer of complexity to the Polycomb field and to its role in identity maintenance, PRC1 is composed by several subunits that define at least 5 different biochemical sub-complexes. These complexes are specified by 6 different mutually exclusive PCGF proteins (PCGF1-6) that determine the ancillary subunits composing the complexes. Their role in embryonic development is matter of several studies, however their involvement in adult tissue maintenance is still obscure. Exploiting different PCGFs conditional knock out mouse models we aim to address the specific role of different sub complexes in the maintenance of tissue homeostasis, in order to define the contribution of these Polycomb complexes in the phenotypic outcome observed in PRC1 loss of function intestinal and hair follicle LGR5 stem cells.

2. INTRODUCTION

2.1 POLYCOMB GROUP OF PROTEINS

2.1.1 CELL IDENTITY

Cell identity is an important cell feature in both the research field and clinic, due to its connection to homeostasis preservation and pathology development. Importantly, establishment and maintenance of the correct identity is critical for organism development and for whole tissue homeostasis in adult life. A single cell, the zygote, gives rise to all of the hundreds of cell types composing the human body in a spatially and temporally coordinated and precise manner during embryogenesis and later development (Mohammad and Baylin 2010, Mortimer, Wainwright et al. 2019).

This process involves different regulatory elements and mechanisms, such as morphogens, transcription factors and epigenetic players, that cooperate to determine the correct cell fate. Among them, epigenetic regulators plays a fundamental regulatory role, by integrating different signals at the chromatin level, shaping DNA accessibility and dictating genes activation and repression, thus leading to a fine regulation of all cellular processes and ensuring that genetically identical cells acquire different identities (Cheung, Allis et al. 2000, Mortimer, Wainwright et al. 2019).

Remarkably, these mechanisms are also conserved in adulthood where they are necessary to control stem cells function and whole tissue homeostasis, highlighting the importance of epigenetic regulation of transcription throughout the entire lifespan (Rinaldi and Benitah 2015). However, in recent years, several studies have shown that factors involved in chromatin regulation can act differently in adulthood compared to development.

Throughout life, adult stem cells have to be carefully preserved due to their fundamental role in replenishing the tissue from dying and, importantly, damaged cells. In this view, it is clear that their identity has to be tightly regulated and preserved in order to maintain homeostasis

within the tissue. Intriguingly, different organs present dissimilar cell turnover and damage rate. Indeed, several mechanisms have evolved differently in adult stem cell to integrate different stimuli to ensure the maintenance of homeostasis (Rinaldi and Benitah 2015) highlighting the importance of studying homeostatic processes *in vivo* in different organs.

Importantly, how adult stem cells retain their identity while self-renewing, or lose it while differentiating, during homeostasis is still largely unexplored.

Due to epigenetic players strict relation with cell identity, it is indeed not surprising that their deregulation is involved in aging and in the pathogenesis of different diseases, primarily in tumors. Cancer is a heterogeneous disease and is considered a multistep process that gradually leads to the loss of cellular identity meanwhile acquiring typical cancer cell features (Hanahan and Weinberg 2000, Hanahan and Weinberg 2011). Epigenetic players are affected at different levels and in a highly context dependent manner, reaching almost half of the total altered proteins in different cancers (Vogelstein, Papadopoulos et al. 2013).

2.1.2 EPIGENETIC

The term epigenetic was coined to define *"the heritable traits that are not linked to DNA sequence"* but its definition has been modified over time and is accepted a more comprehensive meaning is accepted in which *"epigenetic is used to describe the mechanisms by which chromatin-associated proteins and post-translational modification of histones regulates transcription"* (Helin and Dhanak 2013). Genomic DNA is folded inside the nucleus by histones and non-histone proteins that constitute the chromatin. Based on the grade of compaction, two main forms of chromatin have been described: the heterochromatin, which is highly compacted and transcriptionally less permissive, and the euchromatin, which in turn is more relaxed and accessible. However, except for a few genomic regions, such as repeated and non-coding regions, centromeres and telomeres, that constitute the "constitutive heterochromatin", the remaining DNA portions are not static and

it is possible to switch between condensed “facultative heterochromatin” and decondensed euchromatin status by actively changing chromatin conformation (Trojer and Reinberg 2007) with different mechanisms in order to obtain the activation or the repression of the genes needed.

The nucleosome is the basic unit of chromatin and was described more than 40 years ago by Kornberg (Kornberg and Thomas 1974). It is composed by an octamer of histone proteins, whose core is made by a tetramer of histones H3-H4 and two dimers of histones H2A-H2B, around which are wrapped ~147 bp of left-handed DNA. This structure is stabilized by both protein-protein interaction, within the histone core, and several electrostatic and hydrogen bonds, among the DNA helix and the histones (Richmond and Davey 2003, Rohs, West et al. 2009). Beside the structured core of the histones, these proteins possess flexible tails that protrude outside the nucleosome core structure and are used as scaffold for other non-protein interactions. These tails can be post-translationally modified by different classes of epigenetic proteins, affecting histone-DNA and protein-protein interaction thus enabling chromatin modulation of its structure and functions.

Nucleosomes are spaced from each other by free DNA that can be associated with the linker histone H1, that is attached outside the nucleosome core, where DNA exit and enter the nucleosome. Histone H1 is involved in chromatin compaction and is found to be present in the constitutive heterochromatin and in short discrete genomic regions that should be transcriptionally repressed, while transcribed regions are devoid of histone H1 (Trojer and Reinberg 2007).

Indeed, this complex organization and its surrounding proteins interaction and modification is fundamental to tightly regulate gene expression. Chromatin plays an important regulatory role as an integrative platform for several different signaling pathways, that ultimately converge on histones, regulating all the cellular processes. This transcriptional fine tuning requires rapid rearrangements of the chromatin to allow or impede DNA accessibility

(Cheung, Allis et al. 2000). Four are the principal mechanisms of epigenetic controls: Chromatin remodeling, histone variants, DNA modification and Histones modification (Fig 2.1).

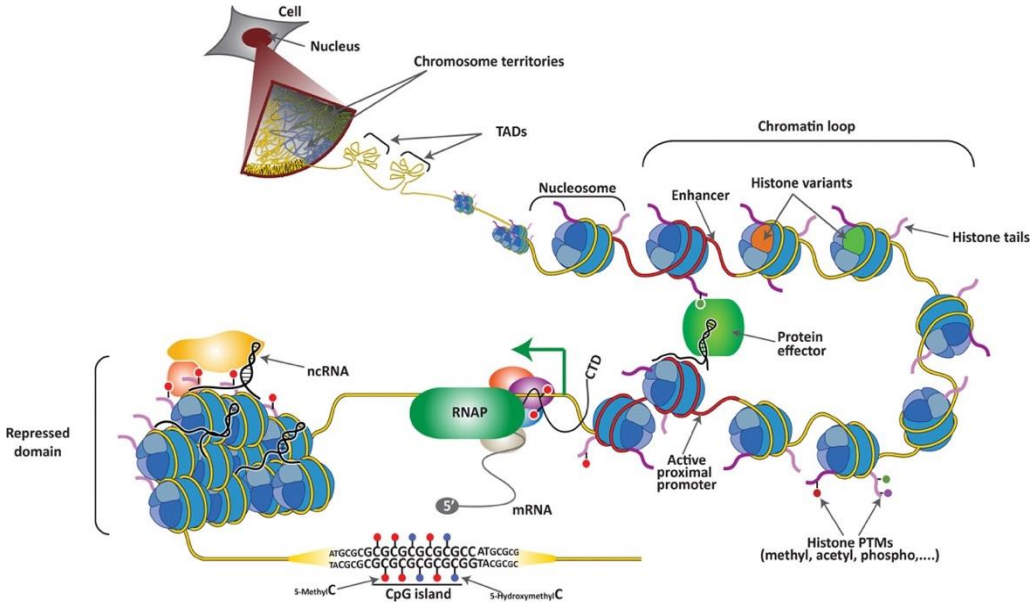

Figure 2.1 Chromatin and Epigenetic modifications

Schematic view of chromatin structure and compaction. In the figure are represented different epigenetic modifications and chromatin associated proteins and structures. Image from (Aranda, Mas et al. 2015).

This dynamic reorganization of nucleosomes is achieved through the activity of different remodeling proteins and complexes which rely on the use of adenosine triphosphate (ATP) as source of energy to disrupt nucleosome-DNA contacts, move the nucleosome on the DNA filament and remove or substitute the nucleosomes. Based on protein homologies, chromatin remodeling players can be divided in at least 4 major families. All these proteins share the ATPase domain, and are characterized by unique domains, within or adjacent to the catalytic residues, that guarantee tissue specific expression patterns, as well as a large variety of different peculiar functions (Hargreaves and Crabtree 2011). Overall their function results in a fine regulation of nucleosome occupancy along the DNA, causing both increased or reduced accessibility of a genomic site, thereby affecting the transcriptional outcome (Sudarsanam and Winston 2000, Levine and Tjian 2003).

Another epigenetic mechanism that regulates the transcriptional control is the incorporation of different histone variants within the nucleosome core. In eukaryotes several histones variants exist, all resembling the canonical counterpart but exhibiting differences both in expression patterns and in their genomic recruitment and organization (Szenker, Ray-Gallet et al. 2011). Canonical histone proteins are encoded by large gene clusters, containing multiple copies that lack introns and 3'PolyA and their mRNA ends with a stem-loop structure needed for their stability and translation during S-phase (Dominski and Marzluff 2007, Talbert and Henikoff 2017). On the contrary, histone variants are more similar to a general mRNA, as they have introns and a polyadenylated 3'end. Typically histones are incorporated in the DNA during replication, by contrast their variants are deposited and substituted throughout the cell cycle (Marzluff and Duronio 2002, Talbert and Henikoff 2017). The replacement of canonical histone forms alters the nucleosome distribution and the interacting proteins, for example chromatin remodelers and modifiers, thus affecting the chromatin landscape with different outcomes. Histone variants, like their classical counterparts, are subjected to several post-translational modification, that can be either the same as their replication dependent canonical histone, or can be newly acquired or lost (Szenker, Ray-Gallet et al. 2011, Talbert and Henikoff 2017) greatly increasing the range of possible transcriptional outcome.

Overall the biochemical diversity introduced with histone variants shows the importance of histones, they represent not only a scaffold protein for DNA compaction, but also a fine tool for epigenetic regulation of gene transcription through different mechanisms.

Together with histones, DNA covalent modifications are the most influential epigenetic alteration that is able to affect the association and the downstream function of factor that binds DNA. Four different DNA modification have been described: 5-methyl cytosine (5mC), 5-hydroxymethylcytosine (5hmC), 5-formylcytosine (5fC) and 5-carboxylcytosine

(5aC) (Rothbart and Strahl 2014). However, the most studied and represented in the genome is the DNA methylation that occurs primarily at the 5-position of cytosine residues (5mC) in the context of CpG dinucleotides. 5mC is widespread throughout the mammalian genome approximately marking the 70-80% of total CpG. However, CpG island (CGIs), which are CpG-rich regions that are mainly found in gene promoters, are particularly refractory to this modification, indeed they are generally unmethylated (Illingworth and Bird 2009). DNA methylation is performed by specialized enzymes named DNA-methyltransferases (DNMTs). Two types of DNA methylation exist: one is associated with DNA-replication, necessary to maintains the correct methylation pattern in the newly formed cells, and the second, that ensures "de novo" methylation deposition, (Okano, Xie et al. 1998, Okano, Bell et al. 1999). Both are fundamental for the correct organism development (Okano, Bell et al. 1999, Li 2002). Importantly, DNA methylation is a crucial epigenetic modification and its deregulation leads to several different pathologies including cancer (Helin and Dhanak 2013).

Beside all the histone forms, nucleosomal proteins encounter several different covalent modification occurring not only on various residues on their tails, but also in their globular domain, thus enormously increasing the number of regulatory epigenetic signals (Jenuwein and Allis 2001, Rothbart and Strahl 2014). Lysine acetylation, Lysine/Arginine methylation and Serine/Threonine/Tyrosine phosphorylation are the best characterized histone modifications. However several others modification exists, such as Ubiquitination, Sumoilation, and Succinylation which are less abundant and their roles have been started to be elucidated (Arnaudo and Garcia 2013).

Histone modifications are deposited by different proteins families called "chromatin writers". These post-translational modifications can either act directly or indirectly (Kouzarides 2007). The deposition of acetylation and phosphorylation can directly influence

the chromatin structure altering the histone positive charge and leading to a more accessible chromatin status. Also, the addition of the large molecules such as ubiquitin can induce a change in chromatin conformation by itself. Moreover, the deposited histone modification can be recognized by other specialized proteins called “chromatin readers” that can recruit to the genome Transcription Factors (TFs) and cofactors needed for the transcriptional and epigenetic regulation. Histone covalent modification can be actively removed by the “chromatin erasers” proteins, creating a complex network of proteins and histone modifications that ultimately lead to the precise control of transcription (Kouzarides 2007). Additionally, more than one modification can be present on the same histone, and can influence the deposition or the stability of the other histone marks and the binding affinity of readers and TFs in several ways creating a real histone code for transcriptional regulation (Jenuwein and Allis 2001, Kouzarides 2007).

All of these mechanisms contribute to create a powerful platform necessary to integrate the cellular and extracellular signal and to promptly respond to environmental changes and their correct function must be accurately preserved, to prevent epigenetic and transcriptional deregulation that ultimately can lead to pathologies such as cancer.

2.1.3 POLYCOMB PROTEINS

Among all the epigenetic modifiers Polycomb Group of Proteins (PcG) are the most widely studied. Polycomb proteins are essential epigenetic regulators of embryonic development and cell fate differentiation. They regulate this process by repressing gene transcription of developmental and differentiation genes in a highly precise spatial and temporal manner.

PcG were discovered almost 70 years ago in *Drosophila melanogaster*, where they control the expression of Homeotic (Hox) genes during development and differentiation. In 1942 a single male fly with ectopic sex combs present on each of its six legs was observed, which

led to the identification of the first PcG mutant, *extra sex combs* (*esc*). A few years later P.H. Lewis named another heterozygous mutant with extra sex comb that were lethal in homozygous conditions *Polycomb* (*Pc*), and in the following years other mutants were discovered (Poynter and Kadoch 2016). However, it was only years later that the function of PcG genes was fully appreciated, when in *Pc* mutant embryos drastic homeotic transformations of thoracic and abdominal segments which were posteriorly shifted were observed (Lewis 1978, Poynter and Kadoch 2016). This phenotype was shown to antagonize mutations in BX-C, a gene cluster encoding for *Hox* genes, suggesting that Pc plays a role as BX-C inhibitor, a theory confirmed by later studies (Poynter and Kadoch 2016, Schuettengruber, Bourbon et al. 2017). Years later from PcG discovery, other regulators of Hox genes were discovered. Their mutation caused embryonic segments transformation into a more anterior ones, thus antagonizing the Polycomb phenotype. This new set of genes where named Trithorax group of proteins (TrxG) (Ingham 1983, Ingham 1985, Ingham 1985, Struhl and Akam 1985, Kennison and Tamkun 1988). Crosstalk among PcG and TrxG ensure the correct establishment of segmentation along the anteroposterior axis of drosophila melanogaster body.

PcGs function in the regulation of developmental genes trough repression, is also strongly conserved in mammals (Morey and Helin 2010). Moreover, in the last few decades Polycomb proteins were found to be implicated in several different processes including control of cell cycle progression, senescence, X-chromosome inactivation, stem cell differentiation and, importantly, pathologies such as cancer (Morey and Helin 2010). Mammalian orthologues of fly PcGs began to be acknowledged in early 90's with the identification of Bmi1 (Psc in Drosophila) and its role in cancer development (Haupt, Alexander et al. 1991, Haupt, Bath et al. 1993). Based on biochemical purification in drosophila melanogaster, PcG proteins were divided into two different complexes Polycomb Repressive Complex 1 and 2 (PRC1 and 2). This division is maintained also in mammals

where the PRCs possess additional subunits and their structures and composition became more complex and context dependent (Aranda, Mas et al. 2015).

PRC1 and PRC2 have specific catalytic functions and mediate transcriptional repression via modification of histones tails and chromatin compaction. PRC1 catalyzes the deposition of a moiety of ubiquitin on lysine 119 of histone H2A (H2AK119Ub1) while PRC2 is responsible for the deposition of mono-, di-, tri-methylation on lysine 27 of histone H3 (H3K27me1/me2/me3) (Cao, Wang et al. 2002, Muller, Hart et al. 2002, Cao, Tsukada et al. 2005, Stock, Giadrossi et al. 2007).

In line with their essential role in drosophila also during development, mammalian PcGs plays a fundamental role in development also. PRC2 complex ablation results in early embryonic lethality and the same is true for the loss Rnf2/RING1B for PRC1 subunit (Faust, Schumacher et al. 1995, O'Carroll, Erhardt et al. 2001, Voncken, Roelen et al. 2003, Pasini, Bracken et al. 2004). Of note, it is increasingly evident that genes important for development largely overlap with those that govern adult renewal potential and identity of stem cells (Mohammad and Baylin 2010), emphasizing the importance of Polycomb regulation of developmental genes also in adult tissue. In the last few years the characterization of PRCs composition, structure, functions and regulation has started to take place, not only for the importance of these complexes in development, but also for the evidence of their involvement in human disease including cancer.

2.1.3.1 POLYCOMB REPRESSIVE COMPLEX 2

Drosophila PRC2 core is composed by Enhancer of Zeste (E(z)), Suppressor of Zeste (Su(z)) and Extra sex combs (Esc). In mammals the subunits composing the core complex are well conserved, and it is composed of either EZH1 or EZH2 (homolog of E(z)), SUZ12 (homolog

of Su(z)) and EED (Embryonic Ectoderm Development, homolog of Esc) (Pasini, Bracken et al. 2004, Morey and Helin 2010, Poynter and Kadoch 2016). EZH1/2, which are mutually exclusive within the complex, exert the catalytic activity through their SET domain performing al the three methylation status of H3K27 (Margueron, Li et al. 2008), while the SUZ12 and EED scaffold proteins are necessary for the enzymatic activity of the complex (Cao and Zhang 2004, Pasini, Bracken et al. 2004). In particular, the EED subunit, through its WD40 domain, is able to recognize H3K27me3, thus establishing a positive feedback loop that enhance the PRC2 activity up to 7-fold suggesting a mechanism for PRC2 mark level maintenance throughout the cell cycle (Margueron, Justin et al. 2009). These three subunits are present in a 1:1:1 stoichiometry within the complex and constitute the minimal composition for the catalytic activity of PRC2 (Smits, Jansen et al. 2013) (Fig 2.2).

The mutually exclusive catalytic subunits are the only two core proteins that are paralog. Interestingly EZH2 loss causes early embryonic lethality, while EZH1 knock out mice are viable, fertile and shows a normal phenotype, meaning that EZH2 can fully compensate for EZH1 activity. On the contrary, EZH1 can only partially complement EZH2 in H3K27 methylation. Moreover, the two proteins show dissimilar expressions patterns. EZH1 is ubiquitously expressed at constant levels during the cell cycle, whereas EZH2 seems to be more expressed in actively dividing cells (Margueron, Li et al. 2008). Their expression patterns are also different at temporal and differentiation levels, in fact, while EZH2 decreases during cell differentiation, EZH1 increases (Margueron, Li et al. 2008, Mousavi, Zare et al. 2012, Xu, On et al. 2015). Moreover, although both EZH1 and EZH2 have H3K27 methylation ability, EZH2 shows 20-fold greater ability in mark deposition, compared to EZH1 that, in turn, seems to be more efficient in chromatin compaction. EZH1 and EZH2 shows only partial redundancy also in terms of catalytic activity. EZH1 seem to be associated to H3K27 mono-methylation on region of active transcription, while EZH2 is commonly associated to di- and tri-methylation deposition in transcriptional repressed genomic loci (Mousavi, Zare et al. 2012, Xu, On et al. 2015). These evidences imply a non-redundant

functionality for the two different PRC2 complexes, increasing the complexity of PRC2 in mammalian organism.

Histone methylation plays a key role in transcriptional regulation by acting through different mechanisms. Overall it can influence the chromatin architecture leading to a differential modulation and interaction with TFs and proteins involved in the transcription initiation and elongation (Wagner and Carpenter 2012, Helin and Dhanak 2013).

Remarkably, in contrast to other histone modifications, methylation does not have an univocal effect and, depending on the methylation degree, it can result in either active or repressive transcription (Bannister and Kouzarides 2011). Historically, PRC2 functionality has been associated only to H3K27me3 and gene repression, however it sequentially deposits all the three methylation-status on H3K27 with different specific outcome (Ferrari, Scelfo et al. 2014). H3K27me3 is preferentially deposited in correspondence of CpG-rich promoter region of silenced genes, H3K27me2, is associated to large transcriptional silenced regions and H3K27me1 is deposited throughout all the gene bodies of actively transcribed genes.

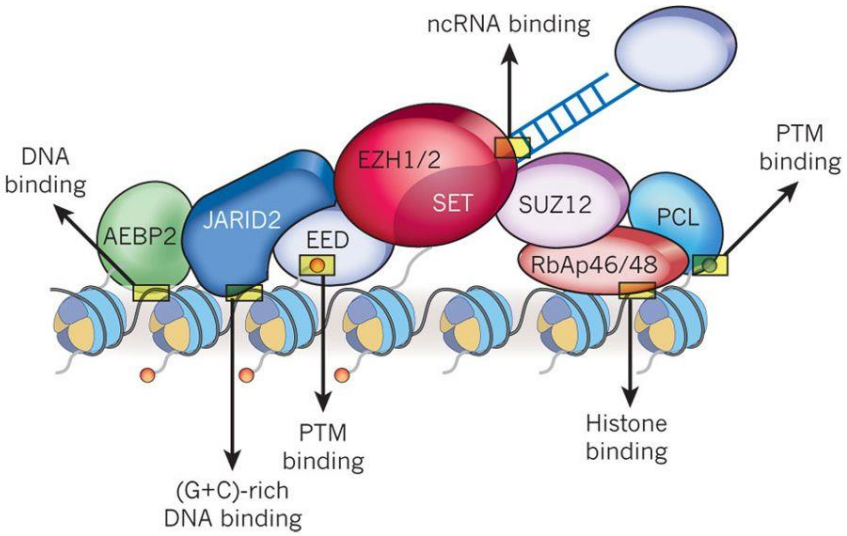

Figure 2.2 Schematic representation of Polycomb repressive complex 2

In the cartoon, taken from (Margueron and Reinberg 2011), are shown PRC2 core and ancillary subunits with their putative interaction with chromatin.

Significantly, combinatorial patterns provide an important regulatory platform to regulate expression. In the case of H3K4me3, deposited by the COMPASS complexes (Shilatifard 2012), and H3K27me3 concomitant modifications, found together in murine Embryonic Stem Cells (mESCs) at the so called "poised" or "bivalent" genes. These genes are typically related to development, which, owning both active and repressive status, are able to be promptly switched on and off when needed during differentiation (Brookes, de Santiago et al. 2012, Voigt, Tee et al. 2013). In differentiated cells these domains tend to disappear, retaining only active or repressive marks depending on their role in specific tissue (Ku, Koche et al. 2008), however new bivalent genes are formed (Mikkelsen, Ku et al. 2007, Mohn, Weber et al. 2008, Oguro, Yuan et al. 2010, Jadhav, Nalapareddy et al. 2016, Cohen, Zhao et al. 2018, Pivetti, Fernandez-Perez et al. 2019).

PRC2 core is associated with several accessory subunits, that are dispensable for its enzymatic activity, but participate in the regulation of its histone modification deposition, by modulating the catalytic activity or the complex association to the genome. Among all, the most important are the histone chaperone RbAp48/46 (retinoblastoma associated proteins 48/46) which are required for catalytic activity *in vivo* (Ketel, Andersen et al. 2005), AEBP2 which enhance KTM activity *in vitro* (Cao, Wang et al. 2008), three different Polycomb-like proteins (PCLs; PHF1, MTF2, PHF19) that through their TUDOR domain recognize the H3K36me3 mark, suggesting a role in silencing initiation of active gene (Ballare, Lange et al. 2012), and JARID2 that recognizing the GC-GA rich DNA elements is involved in PRC2 recruitment at genes for proper ESC differentiation (Pasini, Cloos et al. 2010).

2.1.3.2 POLYCOMB REPRESSIVE COMPLEX 1

Polycomb repressive complex 1 (PRC1) is composed by numerous subunits and these proteins form several different subcomplexes that are biochemically different among each other and are potentially different in terms of biological function (Gao, Zhang et al. 2012). In Drosophila melanogaster PRC1 core is composed by Polycomb (Pc), Polyhomeotic (Ph), Posterior sex combs (Psc) and Sex comb extra (Sce, also known as dRING) (Morey and Helin 2010). In mammals, the situation is extremely more complicated. For each subunit at least two homologues have been discovered. Mammalian PRC1 core is composed by one catalytic subunit that deposits a single molecule of ubiquitin on lysine 119 of histone H2A, mutually exclusive among Really Interesting New Gene 1A and 1B (RING1A and RING1B, Sce homolog), one out of six different Polycomb Group Ring Finger protein (PCGF, Psc homolog) (Fig 2.3) and one out of three Polyhomeotic-like protein (PHC1, PHC2 and PHC3, Ph homolog) (Morey and Helin 2010). PRC1 complex then can be further subdivided into two major classes of complexes named “canonical” and “non canonical” PRC1 based on the presence respectively of the CBX subunit (Chromobox, Pc homolog) or its mutually

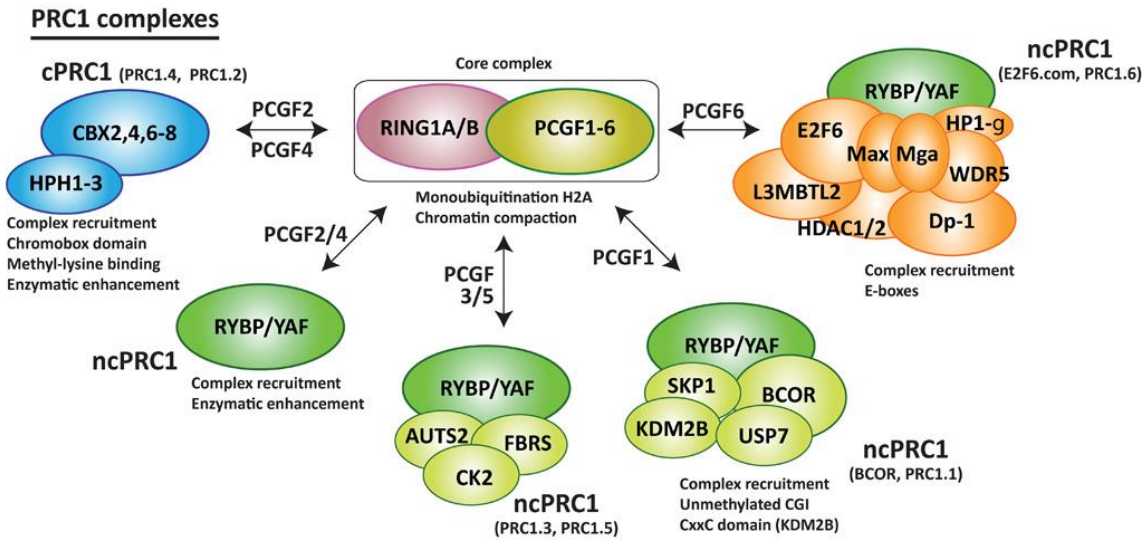

Figure 2.3 Schematic representation of Polycomb repressive complex 1

In the cartoon, modified from (Aranda, Mas et al. 2015), are shown PRC1 core and ancillary subunits with respect to the specific PCGFs associated to the complex and their recruitment specificity oh chromatin.

exclusive counterpart, RYBP, that determines the mechanisms of PRC1 recruitment to chromatin. Moreover, in mammals several different CBX paralogues exist (CBX2,4,6,7,8) and RYBP can be substitute by YAF2 (Morey and Helin 2010, Gao, Zhang et al. 2012). Accordingly to mass spectrometry analyses performed in mammalian cells by Gao and colleagues (Gao, Zhang et al. 2012), at least 5 different biochemical, and probably functional, PRC1 sub-complexes exist. Each of these sub-complexes can interact with specific proteins that can direct the complex to specific targets.

All of these complexes catalyze for H2AK119 Ubiquitin (Ub) deposition, that is a 76-aminoacid protein conserved among all eukaryotic organisms, implicated in several mechanisms including protein degradation, cell cycle, protein trafficking and transcriptional regulation (Zhang 2003). Ub is attached to a lysine residue through an isopeptide bond, and this addition is a complex process involving three different enzymes: E1 activating protein, E2 conjugating enzyme and lastly an E3 ligase, that is responsible for target recognition and catalyze the binding reaction (Pickart 2001), that in PRC1 complex are either RING1A or RING1B. This modification is implicated in transcriptional regulation and is associated with gene repression and chromatin compaction (Ogawa, Ishiguro et al. 2002, Cao, Tsukada et al. 2005, Zhou, Zhu et al. 2008, Zhou, Wang et al. 2009). As for other modifications, histone ubiquitination is reversible, and several specific deubiquitinating enzymes exist (DUBs). Polycomb protein BAP1 has been identified as H2A-specific histone DUB and its loss significantly increase the levels of H2AK119Ub1 on PRC1 targets (Scheuermann, de Ayala Alonso et al. 2010). However, DUBs roles are poorly investigated. Importantly, BAP1 is commonly found to be mutated in mesotheliomas and uveal melanomas (Carbone, Yang et al. 2013, Murali, Wiesner et al. 2013), highlighting the importance of maintaining the correct epigenetic mark deposition to prevent neoplastic pathology.

Based on Gao's and coworker's data, the minimal canonical PRC1 complexes contains either RING1A or RING1B, Mel18/ PCGF2 or Bmi1/ PCGF4 and one CBX subunit (Gao, Zhang et al. 2012).

The different CBXs proteins are mutually exclusive within the complex, and their inclusion in PRC1 seems to be regulated during development. CBX7 seems to be the main component in ESCs and is substituted by CBX2 and CBX4 in differentiated cells (Morey, Pascual et al. 2012, O'Loghlen, Munoz-Cabello et al. 2012). CBX subunit is considered the determinant for canonical PRC1 recruitment on the chromatin (Aranda, Mas et al. 2015) in fact through its Chromobox domain, is able to recognize and bind H3K27me3 PRC2 deposited mark, thereby recruiting PRC1 on PRC2 targets, where the two complexes cooperate in silencing the target locus. This mechanism is supported by the large overlap between PRC2 and RING1B targets and by the loss of RING1B from the chromatin in absence of PRC2 activity.

However, in recent years a new paradigm arise, and by ChIP-seq analyses performed by Gao and colleagues, and in accordance with other studies, emerged that RING1B peaks only partially overlap with H3K27me3, all of which colocalized with Mel18/ PCGF2 or Bmi1/ PCGF4 and CBX proteins, suggesting distinct role for CBX- and RYBP (Boyer, Plath et al. 2006, Pasini, Bracken et al. 2007, Trojer, Cao et al. 2011, Gao, Zhang et al. 2012). Moreover, it is important to know that upon loss of PRC2 activity, the global H2AK119Ub1 levels remains largely unaffected, suggesting that PRC1 activity does not require PRC2 (Tavares, Dimitrova et al. 2012).

Non canonical PRC1 complexes incorporate RYBP (Ring and YY1 Binding protein) or YAF2 (YY1 Associated Factor 2) instead of CBX. These complexes lack the subunit that recognize PRC2 mark, meaning that they are tethered to chromatin in a PRC2 independent manner (Tavares, Dimitrova et al. 2012). Moreover, RYBP containing complexes, beside the classical PRC1-PRC2 targets, can binds different subsets of targets, suggesting that PRC1 possess other mechanisms for its recruitment on the genetic material and can regulate

different cellular processes (Morey, Aloia et al. 2013). Differently from canonical complexes, where only Mel18/ PCGF2 and Bmi1/ PCGF4 can bound CBX subunit, all PCGFs proteins are able to interact with RYBP and YAF2 (Gao, Zhang et al. 2012).

PCGFs proteins are mutually exclusive within the complex, defining different non canonical complexes core, that associate with different ancillary proteins.

PRC1 containing PCGF1/NSPC1 (also named PRC1.1), is the homolog of dRAF complex in Drosophila. A fundamental subunit of the complex is the histone H3K36 demethylase KDM2B, that, through its CxxC domain, drives the complex on CpG rich DNA regions (Blackledge, Zhou et al. 2010, Barrero and Izpisua Belmonte 2013, Scelfo, Piunti et al. 2015).

PCGF3 and PCGF5 have been found to bind the same interactors, thereby defining two biochemically redundant complexes. AUTS2, together with FBRS and FBRSL1, which has no previous association with PRC1, have been recovered in Mass spectrometry analyses for the two PcG proteins (Gao, Zhang et al. 2012, Scelfo, Piunti et al. 2015). Interestingly, in a study in central nervous system development, AUTS2 is able to tether PCGF5 to chromatin where it can activate transcription via CK2 and P300 recruitment, opening a new field on active transcription and polycomb complexes (Gao, Lee et al. 2014). Moreover, a recent work carried out in our laboratory in ES cells define a novel interaction of PCGF3 with USF1 transcription factor and demonstrated that this interaction is necessary for PCGF3 chromatin localization, thus introducing a novel player in polycomb recruitment field (Scelfo, Fernandez-Perez et al. 2019).

Lastly, PCGF6/MBLR can associate with several different proteins defining a huge complex containing E2F6, DP1, MGA, MAX, WDR5 and L3MBTL2. In the past years, it has been demonstrated that PRC1.6 occupies E2F6 binding sites and recently that MGA mediates PRC1.6 recruitment on chromatin on T-box sequences (Trojer, Cao et al. 2011, Gao, Zhang et al. 2012).

Despite all these new advances our PRC1 knowledge about the biology and the molecular functions is still largely not understood.

2.1.4 POLYCOMB RECRUITMENT

Polycomb complexes must be recruited on chromatin to exert their function. In *Drosophila Melanogaster* PcG recruitment is mediated by Polycomb Responsive Elements (PREs), as demonstrated at Hox genes (Busturia and Bienz 1993, Sengupta, Kuhrs et al. 2004). PREs are distal cis-regulatory elements, few hundred bp long, that are devoid of nucleosomes and can be present upstream or downstream of their target promoter, in introns or in the majority of cases close to the transcriptional start site (TSS).

In mammal the recruitment represents a major issue. Despite PRCs core are well conserved, mammals lack PRE- binding proteins and PRE-elements remains elusive in the genome. In general, mammalian PcGs preferentially bind non methylated CpG rich promoters of their target genes and CpG-rich sequence itself mediates PRC2 recruitment (Mendenhall, Koche et al. 2010, Lynch, Smith et al. 2012, Riising, Comet et al. 2014).

The classical model of Polycomb recruitment is a two-step mechanism: first PRC2 is recruited on its targets and mediates the methylation of histone H3K27, which is recognize by CBX subunit that subsequently tether PRC1 complex on the chromatin where RING1B ubiquitinates the K119 of histone H2A. These two modifications lead to chromatin compaction and transcriptional silencing.

However, with the new discovery of CBX lacking non canonical PRC1 complexes, this model remains valid only for canonical complexes targets.

Moreover, it has been demonstrated that H3K27me3 distribution does not completely fit the binding of PRC1, and example of PRC1 peaks devoid of H3K27me3 exist (Gao, Zhang et al. 2012, Tavares, Dimitrova et al. 2012). Furthermore, H2AK119Ub1 deposited by PRC1

has been suggested to play a key role in PRC2 recruitment (Schwartz and Pirrotta 2014), shedding a new light on the complexity of Polycomb recruitment on chromatin.

Since PRC1 and PRC2 core component do not have DNA binding properties, several alternative recruitment mechanisms have been proposed for their engagement to the chromatin that includes the association with other ancillary proteins (such as PCL1-3, AEBP2, JARID2, KDM2B…) or with specific transcription factors, the influence of chromatin signatures (apart from CpG-island also histone variants and histone modifications), the interaction with long non-coding RNAs and the status of Polymerase II (PolII).

PRC1.1 component BCOR (BCL6 Co-repressor) is able to recruits PCGF1 containing complex on BCL6 targets (Morey and Helin 2010), and KDM2B demethylase is able to tether PRC1.1 on H3K36 methylated histones (Barrero and Izpisua Belmonte 2013 , He, Shen et al. 2013, Xu, On et al. 2015). On the other hand, PRC1.6 associate with several proteins and it has been demonstrated that either MGA, E2F6 and L3MBTL2 can drive PCGF6 localization on chromatin (Stielow, Finkernagel et al. 2018, Scelfo, Fernandez-Perez et al. 2019). Last, PCGF5 has been reported to interact with AUTS2, that mediates it recruitment on DNA. Moreover, our laboratory has demonstrated that PCGF3 is able to interact with USF1 that mediates PCGF3 tethering on the chromatin on its specific E-box motifs (Scelfo, Fernandez-Perez et al. 2019).

PRC2 can be targeted to the DNA through JARID2 protein that have been shown to binds most of PcG target genes and to be necessary for binding. This interactor protein contains an AT-rich interaction domain (ARID) and a Zn-finger domain, both with the potential to bind DNA. Despite some studies have shown that JARID2 is necessary for PRC2 binding, inhibition of JARID2 has only minor effect on H3K27me3 and *Jarid2* KO mice shows a milder effect on development compared to PRC2 KO ones, indicating that other mechanisms

can regulates PRC2 genomic targeting (Ku, Koche et al. 2008, Li, Margueron et al. 2010, Pasini, Cloos et al. 2010).

As previously mentioned, other mechanisms can recruit Polycomb complexes on the chromatin. It has been reported that both long non-coding RNA *HOTAIR*, expressed in *HOXC* cluster and necessary for efficient silencing of *HODX* locus (Rinn, Kertesz et al. 2007), and, *Xist* non-coding RNA, that initiate the process of X Chromosome inactivation, can directly recruit PRC1 on the genes or chromosome that should be inactivated (Schoeftner, Sengupta et al. 2006). Also, the phosphorylation status of Polymerase II has been shown to affect PcG occupancy. PolII can be modified within its carboxyl-terminal domain and exclusive phosphorylation of Serine 5 in ESCs, is associated with developmental genes that are in a poised status, with transcription ready to be initiated or repressed upon differentiation stimuli and PRC1 and PRC2 marks co-occurrency (Brookes, de Santiago et al. 2012, Voigt, Tee et al. 2013, Ferrai, Torlai Triglia et al. 2017).

From 2010 many groups focused on a deep characterization of PRC1 subcomplexes molecular mechanisms and functions and their interdependency with PRC1 and PRC2. It has to be mention that accordingly to new studies non canonical PRC1 complexes can localizes on active chromatin, with roles that can be different from the classical Polycomb transcriptional repression (Cohen, Zhao et al. 2018, Fursova, Blackledge et al. 2019, Pivetti, Fernandez-Perez et al. 2019, Scelfo, Fernandez-Perez et al. 2019) and that, least for PCGF3 and PCGF5, their involvement in active transcription has been validate (Zhao, Huang et al. 2017, Scelfo, Fernandez-Perez et al. 2019).

2.1.5 POLYCOMB BIOLOGY

mESCs derive from the inner mass of the pre-implantation embryos at the stage of blastocyst and represent an excellent model system to study the mechanisms for establishing the correct

cell-fate acquisition and transitions, in fact they are pluripotent cells that when cultured in the correct environment can self-renew or can be induced to differentiate, recapitulating *in vitro* the three embryonal layers found *in vivo* (Aloia, Di Stefano et al. 2013). Polycomb complexes are highly expressed in ESCs where they are bound preferentially to CpG-rich promoters of genes encoding for developmental factors (Boyer, Plath et al. 2006, Bracken, Dietrich et al. 2006). Generally, ESCs possess an open chromatin structure with low levels of DNA methylation and high levels of activating histone modification that must be finely regulated to balance self-renewal and pluripotency, and differentiation (Orkin and Hochedlinger 2011). Upon differentiation the chromatin shift from a more open status to a more closed one with the concomitant accumulation of H3K27me3.

For these reasons ESCs, are widely used in Polycomb field to perform mechanistic and biological studies. Moreover, both straight and conditional KO mouse models have been developed to study phenotypes arising from PcG loss, during embryogenesis and later development. Importantly, only in recent years Polycomb complexes started to be investigated in adulthood, thus only little is known about PRCs roles in adult tissue maintenance.

PRC2 core subunits are necessary for early step of embryogenesis *in vivo* and straight KO mice for these subunits died early in post-implantation stages (Faust, Schumacher et al. 1995, O'Carroll, Erhardt et al. 2001, Pasini, Bracken et al. 2004). Notably, deficient mESCs can be derived from KO mice blastocysts. These mESCs do not display self-renewal impairment despite the loss of H3K27me2/3 and a pervasive activation of genes related to differentiation (Richly, Aloia et al. 2011). On the contrary ancillary proteins *Jarid2* deletion cause defects in neural tube formation (at 15.5 dpc), and Pcl2 (Mtf2) results in loss of left-right symmetry in chicken embryos but results dispensable in mouse (Takeuchi, Yamazaki et al. 1995, Wang, Wang et al. 2004, Wang, He et al. 2007). Nevertheless, PRC2 plays an important role in embryonic and adult hematopoietic stem cells (HSCs). *Ezh2* loss impairs embryonic HSCs

self-renewal but does not affect adult stem cell function in the bone marrow, except for lymphopoiesis. By contrast, in line with the different expression pattern of EZH1 and EZH2 which are more expressed in differentiated and undifferentiated status respectively, *Ezh1* depletion highly affect adult HSCs total numbers, impairing HSCs self-renewal and quiescence, alleviating the repression of *Ink4a/Arf* locus and *Bmp2* (Margueron and Reinberg 2011, Mousavi, Zare et al. 2012, Aloia, Di Stefano et al. 2013, Xu, On et al. 2015).

Regarding PRC1, loss of RING1B activity results in embryonic lethality due to gastrulation arrest, while *Ring1a* KO mice are viable (de Napoles, Mermoud et al. 2004). *Ring1b* deficient ESCs shows reduced levels of H2AK119Ub1 and the deregulation of some target genes but maintain the expression of pluripotency markers (Richly, Aloia et al. 2011). Notably depletion of both PRC1 catalytic subunits severely impairs ES self-renewal (Endoh, Endo et al. 2008).

In later development, mice in which *Ring1b, Ezh2* or *Eed* is depleted in central nervous system shows impairment of this transition leading to an incorrect neuronal development (Hirabayashi, Suzki et al. 2009). Moreover, it has been demonstrated that RING1B is required for maintenance of neural stem cell in an undifferentiated status (Roman-Trufero, Mendez-Gomez et al. 2009).

In accordance with the dispensability of PRC1 subunits, except for RING1B in mouse development, single PCGFs depletion in ESCs does not affect self-renewal properties, however it affects cell differentiation. This is the case for PCGF1 which is dispensable for ES colony formation and maintenance but PCGF1 KO cells fail to repress stem cell markers upon induction of differentiation (Yan, Zhao et al. 2017). Moreover, it has been demonstrated that PCGF1 is needed in HSCs to repress *HoxA* gene promoter in order to terminate self-renewal program in progenitor cells (Ross, Sedello et al. 2012).

Mel18/ PCGF2 and Bmi1/ PCGF4 KO have been studied for long time, and their single genetic ablation results in defects in anterior-posterior specification of skeleton, while the

concomitant deletion of both canonical PCGFs results in a more severe developmental defects that results in mice death at 9.5 dpc (van der Lugt, Domen et al. 1994, Alkema, van der Lugt et al. 1995, Akasaka, Kanno et al. 1996). Moreover, Bmi1/PCGF4 has been largely investigated in hematological pathology and in hematopoietic stem cells (HSCs). It has been reported to inhibit the *Ink4a/Arf* locus, that encodes for p16 and p19 cell cycle inhibitors, and mice depleted for *Bmi1* in HSCs show a reduced postnatal population of stem cells and impaired self-renewal (Park, Qian et al. 2003). Moreover, *Bmi1* loss causes an aberrant activation of *Ebf1* and *Pax5* developmental genes that promotes a premature lymphoid lineage specification (Oguro, Yuan et al. 2010). Interestingly, even though is reported as BMI1 paralog, Mel18 has been proposed as tumor suppressor via BMI1 downregulation (Zhang, Sheng et al. 2010), while in other cancer it can act as oncogene (Wiederschain, Chen et al. 2007), highlighting again the extreme variability of PRCs proteins among different contexts.

Endoh and colleagues investigated the role of PCGF6 in mESCs and found that Pcgf6 KO affects the rate of cell proliferation without affecting the morphology of cells. Moreover, according to MAX ablation in ESCs, PCGF6 depletion leads to the ectopic expression of meiosis-related and germ-cell related genes. They also reported that ablation of *Pcgf6* results in viable and fertile mice, although not at normal mendelian ratio. Lethality was observed at blastocyst stage of embryonic development and in post-implantation stages. Moreover, one third of embryos at 10.5 dpc exhibit growth retardation (Endoh, Endo et al. 2017).

Lastly a role for PGF3/5 in correct ESCs development have been reported. Indeed loss of *Pcgf3/5* results in a pronounced decrease of mesoderm markers, thus implying an active role in transcription of PCGF3 and PCGF5, as suggested by other reports (Gao, Zhang et al. 2012, Zhao, Huang et al. 2017, Scelfo, Fernandez-Perez et al. 2019).

Polycomb proteins have been shown to act also in skin development and maintenance. Interestingly, *Ezh2* loss during embryonic skin development accelerates the differentiation process by transcriptionally upregulating epidermal-related genes, without affecting other PcG pathways. However, by birth, PRC2 histone mark reappears, shedding light on the possible compensatory effect of EZH1 postnatally. Importantly, loss of both *Ezh1* and *Ezh2* affects general skin development, in two opposite ways: Hair follicles appendages, which derives from epidermal progenitors, shows a compromised formation and maintenance, in contrast the epidermis is hyperproliferative and survives long-term engraftment (Ezhkova, Pasolli et al. 2009, Ezhkova, Lien et al. 2011). Among the two complexes, PRC1 exert a major role in skin compartment. It has been reported recently that during epidermal development, PRC1 ablation in epidermal progenitors leads to fragile skin phenotype, with tissue thinning and mechanical stress susceptibility (Cohen, Zhao et al. 2019). Moreover, impaired hair follicle formation during epidermal development has been recently reported also for PRC1 ablation (Cohen, Zhao et al. 2018).

Adult tissues are maintained by stem cells that sustain the cells renewal. Intestinal tissue are renewed in 5 days and stem cells located at the bottom of the tissues sustain this regeneration (Barker, van Es et al. 2008). PRC1 and PRC2 accomplish two different roles during adult intestinal homeostasis, as demonstrated by their respectively KOs in intestinal epithelium and intestinal stem cells (Chiacchiera, Rossi et al. 2016, Chiacchiera, Rossi et al. 2016, Chiacchiera and Pasini 2017). PRC1 depletion in intestinal stem cells (ISCs) leads to loss of stem cell identity and stem cell exhaustion affecting ISCs self-renewal potential, independently from *Ink4a/Arf*. On the contrary PRC2 is necessary to maintain the correct balance among secretory and absorptive lineage in the intestinal epithelium. Moreover, PRC2 ablation does not affect ISCs maintenance but is required for regeneration of the tissue upon irradiation.

Taken together this study highlight the extreme context dependency of PcGs and the need to deeply investigate these complexes in other models and in several tissues. Additionally, a deep knowledge about Polycomb roles in adult stem cell homeostasis and in their role in regeneration upon damage is still missing.

2.1.6 POLYCOMB DEREGULATION AND CANCER

Due to Polycomb role in development and differentiation regulation is not surprising that their deregulation frequently occurs in several cancer (Jones and Baylin 2007).

Overexpression of PcG genes have been observed in either hematological malignances and solid tumors including Medulloblastoma and tumors originating from colon, liver, lung, breast and prostate (Raaphorst 2005). Moreover Polycomb genes have been shown to be recruited on chromatin by interacting with multiple chimeric fusion proteins such as PLZF-RARA and TMPRSS2-ERG (Boukarabila, Saurin et al. 2009, Yu, Yu et al. 2010).

Compare to PRC2, PRC1 seems to be less affected in cancer development probably for its fundamental role in stem cell maintenance, however some subunits have been found important in cancer development. Bmi1/PCGF4 collaborate with c-Myc oncogene in lymphomagenesis (Haupt, Bath et al. 1993), and is aberrantly expressed also in solid tumors including squamous cell carcinoma (Sparmann and van Lohuizen 2006). Bmi1/PCGF4 role as oncogene is further confirmed by its enhanced expression correlation with poor prognosis (Mohty, Yong et al. 2007, Shafaroudi, Mowla et al. 2008). Its oncogenic function has been mainly attributed to *Ink4a/arf* locus repression, however its paralog Mel18/PCGF2 shows tumor-suppressor features being frequently lost in cancer (Zhang, Sheng et al. 2010, Schwartz and Pirrotta 2013). However, as mentioned above, these differences are context dependent and Mel18 acts as oncogene in some cancer type. The same duality is maintained also for CBX7 that have been proposed as both oncogene and tumor suppressor in solid and

hematological tumors (Scott, Gil et al. 2007, Forzati, Federico et al. 2012, Klauke, Radulovic et al. 2013, Shinjo, Yamashita et al. 2014).

PRC2 components are more involved and compromised in cancer. EZH2, SUZ12 and PCL3 are frequently overexpressed in different tumors (Sparmann and van Lohuizen 2006). EZH2 overexpression has been linked to aggressive and advanced metastatic stages of the pathology and is typically associated poor prognosis (Kleer, Cao et al. 2003).

However, recent studies suggest a complex scenario for EZH2, which can act both as oncogene and tumor suppressor depending on the cellular context. For this reason, either activating or inactivating mutations can be found for EZH2. Interestingly, its overexpression seems to correlate more with solid tumors, while hyperactivating and inactivating mutation with hematological malignances (Ernst, Chase et al. 2010, Morin, Johnson et al. 2010, Sneeringer, Scott et al. 2010, Ntziachristos, Tsirigos et al. 2012).

Of note, PRCs are involved in the regulation of pathways implicated in the emergence of cancer stem cells, such as Hedgehog, WNT and Notch pathways. Due to this role Polycomb deregulation has important implications. As an example, it has been demonstrated that WNT pathways is a major factor in colorectal cancer development (Zhao, Chen et al. 2009, Vermeulen, De Sousa et al. 2010, Takebe, Harris et al. 2011). Of note PRC1 depletion studies in murine intestinal epithelium has underly the necessity of a functional PRC1 for WNT driven intestinal cancer (Chiacchiera, Rossi et al. 2016).

2.2 THE HAIR FOLLICLE

The skin is the largest organ of the body and is the first barrier protecting animals against several insults, such as UV radiation, pathogens, dehydration and is constantly subjected to

several traumas (Fuchs 2016). In adults the tissue is maintained by stem cells that provides new cells to substitute the older and damaged ones.

The skin is composed by two major compartments: the Interfollicular Epidermis (IFE) and the hair follicles (HFs), with its associated appendage, the Sebaceous Gland (SG).

The IFE, or epidermis, is a stratified epithelium whose innermost layer, that is called Basal Layer (BL), is attached to a basement membrane, a structure composed by extracellular matrix and that is rich in growth factors. Among all the different layers that compose the epidermis, only the BL has the ability to proliferate. Once a cell divides, it detaches from the BL and migrate upward while differentiating. The outermost layer is composed by dead keratinocytes, the cells that compose the vast majority of the epithelium, that forms flattened scales that are sloughed from the skin and replaced continuously by the underlying keratinocytes (Fuchs 2016).

Most mammals have hairs that guaranties warmth and protection (Fuchs 2016). Differently from IFE the hair follicle does not regenerate continuously. Instead, it encounters cyclical bouts of proliferation and hair growth (Anagen), followed by the destruction of exceeding cells (Catagen) and finally the quiescent phase (Telogen). Due to their abundance in mouse and their peculiar cycle, which stages are well characterized (Paus, Muller-Rover et al. 1999, Saxena, Mok et al. 2019), it emerged as one of the best systems to explore homeostasis and stem cells of adult tissue, with the possibility to explore both quiescent and resting phase of the stem cells and their differentiation.

Murine HFs are specified during late embryogenesis and mostly develops after birth in a synchronized process called morphogenesis, that start the first cycle. By the end of the morphogenesis, approximately 16 days after delivery (Postnatal day 16, P16), the follicles are formed, and after catagen and telogen a new synchronized hair cycle begins at P28 (Paus,

Muller-Rover et al. 1999, Muller-Rover, Handjiski et al. 2001). This is the last synchronized wave of hair regeneration during mouse life and ends with a long quiescent phase named "long telogen" that last at least four weeks (from week 7, or from P49). After the long telogen phase, mouse fur starts to regenerate in an asynchronous way, forming patches of anagen, telogen and catagen follicles (Muller-Rover, Handjiski et al. 2001). However, it is possible to re-synchronize the hair cycle by waxing mouse back-skin and forcing the hairs to re-enter the anagen phase, that occurs normally without differences respect to spontaneous anagen (Muller-Rover, Handjiski et al. 2001). At each cycle a new hair shaft is formed and the older one is eventually shed, for the vast majority of time in an active process called exogen (Schneider, Schmidt-Ullrich et al. 2009).

Mature hair follicle is composed by several specialized parts that can be divided in two compartments: the first, that constitute the upper part of the HF, remains static throughout the cycle, and it is composed by the infundibulum, that is a transition zone between HF and

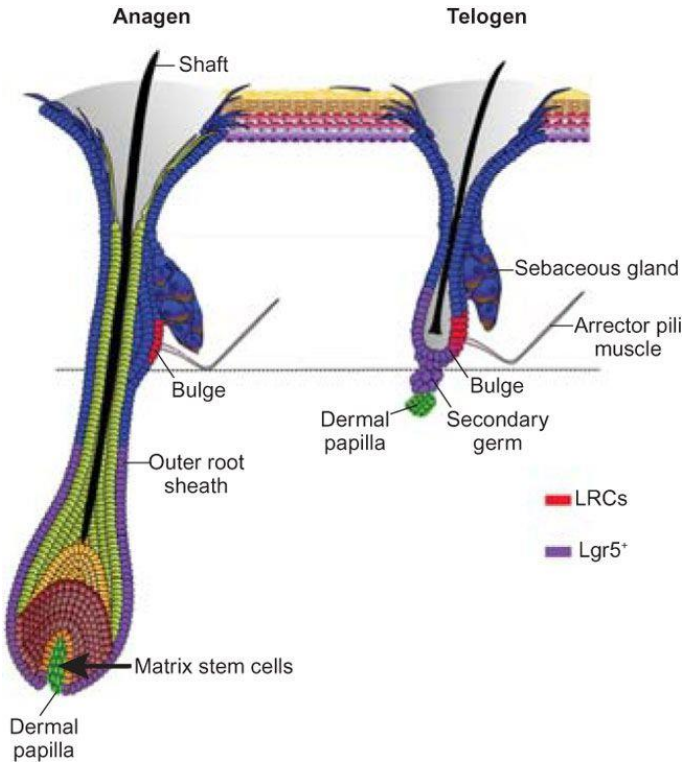

Figure 2.4 Schematic representation of Hair follicle

In the figure, taken from (Morgan 2008), are represented HFs during the proliferating (anagen) and resting (telogen) phase, showing the different cellular population within the HF.

IFE, the isthmus, where the arrector pili muscle is inserted, and the HF associated sebaceous gland; the second, the lower part of the hair follicle, changes during the cycle and actively participate to this process, and its composition changes during the different cycle phases (Schneider, Schmidt-Ullrich et al. 2009) (Fig 2.4). The quiescent follicle presents, in its lower part, the bulge, that houses stem cells and melanocytes, and the secondary hair germ, or hair germ (HG), that contains other stem cells, that will be discussed in the next sections. Anagen induces many changes in this lower follicle part, that greatly extend downward in the subcutis forming the bulb, that contains all the proliferating cells, the matrix keratinocytes and the HF pigmentary units that cooperate to form the new hair shaft. Also the bulge participate in this processes, although it do not change in morphology and positioning. Anagen phase will be discussed in detail in the following sections.

Outside the HF structure an important associated mesenchymal structure is the Dermal Papilla (DP) that is composed by mesenchymal cells that cluster together forming a defined structure. Its role is to sustain anagen progression through the production and diffusion of signaling molecules, such as Fgf7 and Fgf10, that stimulate proliferation in the associated HF (Greco, Chen et al. 2009, Driskell, Clavel et al. 2011).

2.2.1 MORPHOGENESIS

Hair follicle cycle does not create new follicles, but only regenerate the hairs. HFs are specified in late embryonic development in a temporally and spatially tightly controlled process called morphogenesis (Paus, Muller-Rover et al. 1999, Saxena, Mok et al. 2019), that leads to the creation of adult HFs.

Historically, the guide written by Paus and colleagues in 1999 dictated the basis for morphogenesis stage recognition (Paus, Muller-Rover et al. 1999). However, in the last 20 years advanced mouse genetics, molecular and imaging methods have enabled numerous studies that increased our knowledge at phenotypical, functional and molecular levels, that

have been summarized by Saxena and coworker this year (Saxena, Mok et al. 2019). Morphogenesis requires the formation of two important structures, the placode (PC), in the developing epidermis, and the dermal condensate (DC) in the underlying mesenchymal subcutis. These two structures necessitate the activity of the WNT pathway to be specified, as demonstrated by the glabrous phenotype of mice depleted for WNT signaling mediator Wintless (Wls) in the epidermal progenitors and by beta-catenin ablation in the dermis (Zhang, Tomann et al. 2009, Chen, Jarrell et al. 2012). Before morphogenesis begin, at stage 0, epidermis is a uniform layer of cells without any morphological signs or molecular specification of HFs formation. What is known is the presence of a widespread WNT signaling activity in the upper dermis, which is critical HF specification signal, called "first dermal signal", that is still not identified (Zhang, Tomann et al. 2009). Absence of WNT signaling, either in epidermis or in the dermal compartment, results in absence of pre-PC in the epidermis (Saxena, Mok et al. 2019). During the first stages, the unknown dermal signal induces the specification of the pre-PC, that is morphologically undistinguishable from the epidermis, that still present a peculiar molecular pattern with active WNT signaling (Huelsken, Vogel et al. 2001, Andl, Reddy et al. 2002, Zhang, Tomann et al. 2009), Edar (Barsh 1999, Headon and Overbeek 1999, Schmidt-Ullrich, Tobin et al. 2006) and Fgf20 (Huh, Narhi et al. 2013) expression. This specification induces the gradual formation of the DC that enlarge while the PC, that appears thicker and composed by tightly packed vertically oriented cells, starts to move downward in the underlying dermis. This invagination is concomitant with the expression of a master regulator of hair follicle cycle, *Shh* (Huelsken, Vogel et al. 2001, Rhee, Polak et al. 2006, Zhang, Tomann et al. 2009, Tomann, Paus et al. 2016). Particularly, asymmetric division creates 2 layers of PC, the upper one expressing *Sox9* and with diminished WNT signaling, that will specify for bulge-HFSCs, and the lower one that maintain *Shh* expression and active-WNT pathway that will specify for matrix (Mx) cells, and, at the end of morphogenesis for a second HFSCs population (Nowak, Polak et al. 2008). At later stage hair peg is similar to an adult HF. Basal PC cells continue to express

Shh and *Pcad*, while the Outer Root Sheath (ORS) is starting to differentiate (Saxena, Mok et al. 2019) and the inner Mx start to produce the Inner Root Sheath (IRS) that develop the hair. In the next stages, the hair shaft is elongating and will exit from the hair canal emerging from the epidermis.

After morphogenesis, the anagen hair follicles enter the first catagen phase. The ORS and the IRS shrink due to programmed apoptotic events. However, not all cells are lost during this process, but some ORS cells will constitute the HG that, together with the bulge, houses the HFSCs populations (Jaks, Barker et al. 2008).

2.2.2 ADULT HAIR FOLLICLE: ANAGEN AND TELOGEN

Anagen hair follicle is an elongated structure composed by several different concentric layers. The bulge characterizes the end of the permanent non-cycling region and is separated from the anagen bulb by a long stretch of suprabulbar epithelium. The bulb is composed by the Mx cells that rapidly proliferates to give rise to all the differentiated cells of the hair shaft. Full anagen hair follicle is composed by eight different concentric layers, each one expressing a peculiar keratins pattern (Schneider, Schmidt-Ullrich et al. 2009). At the outermost part of the HF it is identifiable the ORS, marked by LGR5 expression. Deeper in the HF, the IRS is composed by the companion layer, Henle's layer, Huxely's layer and IRS cuticle. In the middle of the follicle reside the new hair shaft that is composed by the hair cuticle, the cortex, and finally the medulla (Schneider, Schmidt-Ullrich et al. 2009, Genander, Cook et al. 2014). To date, many molecular markers of HFs lineages have been discovered: among them, *Gata3*, *Cut1* and BMPs are important for IRS formation, while *Sox9* and *Shh* for ORS maintenance and formation (Schneider, Schmidt-Ullrich et al. 2009).

Telogen can last up to several weeks. During this phase HFs are at their minimal size and comprises only quiescent stem cells in the bulge and in the HG, which is in close contact

with the DP. To date most of the transcriptomic studies on telogen follicles have been performed in bulk on the whole population of HFSCs, or on subsets of cell enriched for specific markers. However, recently, Joost and coworkers profiles the whole epidermis and the hair follicle at single cell level (Joost, Zeisel et al. 2016). This work revealed that telogen HFs are extremely heterogenous and different subpopulation can be identified within the follicle, confirming already known markers and expression gradients, but also discovering new markers and new cell populations.

Hair follicle stem cells can be divided in two populations: a quiescent population in the bulge region, and a primed population in the lower bulge and in the HG (Hsu, Li et al. 2014).
Stem cells in the bulge are characterized by the expression of K15 and CD34 surface marker (Cotsarelis, Sun et al. 1990, Trempus, Morris et al. 2003, Blanpain, Lowry et al. 2004, Morris, Liu et al. 2004) and shows the potential to retain histone labels over a long period (Braun, Niemann et al. 2003, Tumbar, Guasch et al. 2004). Initial studies, led to the creation of the "bulge activation hypothesis" model that foresaw, at the anagen onset, the activation of a subset of stem cells and their progeny-derived migration that ultimately creates the matrix (Cotsarelis, Sun et al. 1990, Oshima, Rochat et al. 2001, Cotsarelis 2006).
In 2008, Jaks and colleagues identified a stem cell population marked by LGR5 expression, an orphan receptor previously identified as WNT target gene in colon cancer (Barker, van Es et al. 2007, Barker, van Es et al. 2008, Jaks, Barker et al. 2008). Through *in vivo* lineage tracing analyses carried out in Lgr5-CreERT2-Rosa26-LoxSTOPLox-LacZ mouse strain, the authors demonstrated that this population resides in the lower bulge area, where it partially overlaps with CD34 expressing cells, and in the HG. This population forms the ORS in anagen follicle, and part of these cells are maintained after catagen constituting the new lower bulge and HG (Ito, Kizawa et al. 2004). Moreover, they described that LGR5-HFSCs are the first cells that proliferates during anagen and expresses genes indicative of an active Hedgehog pathway, such as *Gli1* and *Gli2*, and importantly also *Shh* itself. In

contrast with the previous literature, CD34 or Bulge-HFSC population do not actively participate to anagen progression and they remain in the bulge area while anagen progress (Jaks, Barker et al. 2008). Importantly, bulk RNA-seq analyses revealed that bulge-HFSCs and HG-HFSCs are transcriptionally largely indistinguishable and interchangeable (Greco, Chen et al. 2009, Rompolas, Mesa et al. 2013).

During anagen onset and progression LGR5-HFSCs are the first cells to respond to the proliferation stimuli, and importantly they have been shown to be necessary for hair follicle regeneration, and their loss impair HF cycle. However, CD34 bulge-HFSCs are able to reconstitute LGR5-HFSCs population, restoring HF cycle (Hoeck, Biehs et al. 2017), further demonstrating that LGR5 stem cells are necessary for anagen progression.

The molecular detail of stem cell activation still remains unknown. However, telogen phase set a critical threshold for anagen induction that anagen-promoting factors must overcome to start a new hair cycle (Blanpain, Lowry et al. 2004, Lin, Chudova et al. 2004, Morris, Liu et al. 2004, Tumbar, Guasch et al. 2004, Rendl, Lewis et al. 2005). During telogen, BMP and WNT inhibition by TCF3 and DKKs impede stem cell activation. Cycle start when WNT activation, and consequently beta-catenin stabilization, combined with focal expression of BMP inhibitors in the DP is reached. Nevertheless, is not known how WNT signal is initiated (Fuchs 2007, Fuchs 2008), but it has been demonstrated that waves of BMP signals occurs in the telogen dermis, thus defining high BMP telogen phases, during which HFs are refractory to proliferation, and low BMP telogen phases which render HFs competent to anagen induction (Plikus, Mayer et al. 2008). At the anagen onset, HG promptly proliferates as first (Greco, Chen et al. 2009, Lien, Polak et al. 2014), develops into the Mx, a pool of Transient Amplifying cells (TACs) that rapidly proliferate and terminally differentiate to form the IRS and the hair shaft. Lower bulge stem cells proliferate to form the ORS, that envelop the other HF structures (Hsu, Pasolli et al. 2011, Rompolas, Mesa et al. 2013). During early anagen phases, the upper bulge starts to cycle few times, induced by short-

living progenitors derived from the lower bulge that start to express *Shh*, generating the new bulge for the next hair cycle and replenishing the niche, however, the bulge progressively moves away from the DP thus returning to quiescence (Hsu, Pasolli et al. 2011, Hsu, Li et al. 2014, Hsu, Li et al. 2014). Matrix cells, in contrast move downward engulfing the DP and continue to proliferate, sustained by active WNT and SHH pathways. Moving away, due to their division, from the proliferating part of the bulb and entering into the pre-cortical matrix, the cells start to terminally differentiate and to create the hair shaft (Schneider, Schmidt-Ullrich et al. 2009).

During catagen, TAC undergoes apoptosis, however some ORS sparse cells remains, forming the new HG. Nevertheless, one inner layer of terminally differentiated K6 positive cells, the companion layer, remain in the telogen follicle, anchoring the hair and providing inhibitory signals to the HFSCs of both bulge and HG, through BMP6 and FGF18 expression (Hsu, Pasolli et al. 2011).

2.2.3 PATHWAYS IN HAIR FOLLICLE STEM CELLS

Several pathways are important for the correct maintenance of HF during all cycle phases. Among them the most important are Hedgehog pathway, specifically SHH, WNT/beta-catenin and BMP-antagonist, that boost the cell cycle, and BMP and FGF that, conversely, induce cycle arrest or catagen (Hebert, Rosenquist et al. 1994, Paus and Foitzik 2004, Cotsarelis 2006).

Hedgehog signaling pathway controls several different processes, among them cell growth, survival, cell fate, and pattern specification (Varjosalo and Taipale 2008). SHH molecule binds to its receptor Patched (Ptc) activating a signaling cascade that drive the activation of zinc-finger TFs GLI1-3, that in turn modulate the expression of their target genes. In the

absence of SHH, Ptc inhibit Smoothened (Smo) transmembrane proteins, that is required for GLI2 and GLI3 stabilization and *Gli1* transcription (Cohen, Kicheva et al. 2015).

In HF, SHH pathway is essential for its formation and its proliferation during anagen progression (St-Jacques, Dassule et al. 1998, Chiang, Swan et al. 1999). LGR5-HFSCs express high levels of GLI1 and GLI2, and importantly also present abundancy of *Shh* transcript level, addressing a possible autocrine function to reinforcing this pathway in LGR5-HFSCs (Jaks, Barker et al. 2008). In a recent work by Zhang and colleagues (Zhang, Tsai et al. 2016), *in vivo* depletion of *Shh* from K15 expressing cells, that specify for both bulge and HG stem cell population, shows the essential role of this pathway also in the flanking environment. Particularly, *Shh* deletion in K15 generates a TAC population deprived for this molecule that is impaired in proliferation, resulting in early anagen block.

Another important player governing HFs development and adult cycle is the WNT pathway. This pathway is activated when WNT ligand engage its receptor complex Frizzled-LPR5-LPR6. This binding inhibits beta-catenin destruction, continuously exerted by Adenomatous Polyposis Coli (APC) within the so called “destruction complex”, leading to beta-catenin nuclear accumulation. In the nucleus TCF/LEF family members, already localized on chromatin are repressed by Groucho binding. When beta-catenin enters the nucleus it is able to bind TCF/LEF protein unseating TLE/Groucho from the complex, thus leading to transcriptional regulation of beta-catenin targets (Nusse and Clevers 2017). As previously mentioned, WNT pathway exert a major role in HF development. Indeed, mice that ectopically express WNT inhibitor that impede LPR binding to Frizzled, shows a complete impairment of HFs morphogenesis, preventing the expression of PC molecular markers and its specification (Andl, Reddy et al. 2002).

Interestingly, mice expressing the non-degradable form of beta-catenin in epidermal progenitors shows an accelerated and excessive PC formation, however, most of the developing HFs failed to produce hair, suggesting that a tight regulation of beta-catenin in both proliferation and differentiation is needed (Narhi, Jarvinen et al. 2008).

WNT pathway is counteracted by BMP inhibitory signal. Indeed, the balance between these two pathways set a critical threshold that has to be overcome to induce HF in anagen (Schneider, Schmidt-Ullrich et al. 2009).

BMP belongs to the TGF-Beta family of secreted signaling molecules. BMP binds to its membrane receptor BMPRI or ALK2-6, activating the signaling pathway. This receptor-ligand binding is followed by the recruitment of BMPRII which phosphorylate BMPRI leading to its activation, thus starting a cascade of phosphorylation events that involves receptor-regulated SMAD (R-SMAD1/5/8), that in turn activates SMAD4, the effector SMAD protein, that translocate into the nucleus and activates transcription of its target.

BMP signaling is important to tightly regulate the resting phase of the HF cycle. During telogen BMP2/4 are expressed, thus making HFs refractory to growth stimulation (Schneider, Schmidt-Ullrich et al. 2009). Importantly when quiescent HFSCs are depleted for *Bmpr1a* they rapidly adopt features of activated HFSCs, progressing in the cell cycle, without the possibility to return to quiescence, however, these bulbs do not form any hair shaft and most of them transform in cyst structure, highlighting BMPs important role, not only in governing quiescence, but also in differentiation programs (Genander, Cook et al. 2014).

2.2.4 POLYCOMB AND HAIR FOLLICLES

The high grade of stem cell plasticity is tightly governed at epigenetic and transcriptional level. In 2009 Ezhkova and colleagues showed that lineage definition and progression of the hair follicle is governed, at least in part, by PRC2 complex, through the repression and the de-repression of chromatin (Ezhkova, Pasolli et al. 2009, Ezhkova, Lien et al. 2011). In the same year, Lien and colleagues analyzed the different chromatin states of various HFs populations: anagen HFSCs, quiescent HFSCs and the derived TAC (Lien, Guo et al. 2011). They identify some genes whose transcriptional repression change during lineage progression, as an example, matrix related genes are silenced in both quiescent and anagen HFSCs, while become activate in TAC population. On the contrary stemness genes are repressed in TAC and devoid of H3K27me3 PRC2 mark in both quiescent and anagen HFSCs, showing that epigenetics plays a fundamental role in tightly regulate lineage choices.

Recently, it has been demonstrated that both PRC2 or PRC1 loss, severely affected HFSCs formation (Ezhkova, Lien et al. 2011, Dauber, Perdigoto et al. 2016, Cohen, Zhao et al. 2018). Remarkably, these works were performed during morphogenesis, the process that define stem cell population within the HF, while PRC1 role in adult HFSCs is still largely unexplored.

2.3 INTESTINE

Intestine is the second most extended epithelial tissue of the body (Gehart and Clevers 2019). Being an interface with the external environment, it accomplishes two main functions: it is deputed to nutrients uptake meanwhile guaranties protection against the harsh environment. Several insults from luminal content damage intestinal cells, inducing a high rate of cell

death every day. Thus, tissue must be renewed constantly throughout the entire life, without losing its absorptive and protective function, and it has been estimated that a new epithelial tissue is renewed and formed in 3 to 5 days. Intestine divides into two major parts: the small intestine, that exert the absorptive role, which is further subdivided in duodenum, jejunum and ileum, and the large intestine, which functions are water re-absorption and undigested contents compaction, and is composed by caecum, proximal and distal colon and rectum.

The intestinal epithelium is structured in functional modules constituted by crypts-villus units (Barker 2014) (Fig 2.5). Absorptive function is mainly carried out by enterocytes that are present on the villi, that compose the differentiated part of the intestinal tissue. Villi are finger-like protrusion that spread from the intestinal surface toward the lumen, enormously increasing the absorptive surface of the epithelium. In the opposite direction, epithelial invaginations form the less differentiated and staminal part of the tissue, the intestinal crypts of Lieberkün, where the intestinal stem cells (ISCs) that sustain tissue regeneration are housed (Barker 2014). Each villus is surrounded by at least six crypts cooperating to maintain the villus cell population.

Intestinal epithelium is composed by several different cell populations that are more or less represented in the tissue depending on the intestinal tract.

Differentiated cells are located mainly along the villi and comprise: the Enterocytes, that accomplish the absorptive role; the Goblets cells, that produce the mucins, needed for modulating the interaction among intestinal epithelium and intestinal bacterial population and, in the last part of the small intestine, to help the passage of compact stools in the colon (Birchenough, Johansson et al. 2015); the Enteroendocrine cells, that produce hormones needed to regulates the digestive system (Worthington, Reimann et al. 2018). Rarer populations are the Tuft cells, which role is to rapidly increase in cell number and to promptly activate type 2 immune response during helminths inflammation (Howitt, Lavoie et al. 2016), the Cup cells, whose function is not known and the M cells, that reside on

lymphoid Peyer's patches and transport antigens from the gut lumen to the underlying lymphoid tissue.

At the crypts base, a high cycling stem cell population fuels tissue regeneration producing transient amplifying cells that are pushed upward in the luminal compartment and exit the crypt within two days. Paneth cells, the only differentiated cells in the crypts, contribute to protective role producing and secreting defensins and lysozyme to help the antimicrobial protective role (Bevins and Salzman 2011). Importantly, Paneth cells escape this upward migration and conversely migrate downward to re-occupy the crypt base where they can remain from 6 to 8 weeks (Scoville, Sato et al. 2008, Barker, van Oudenaarden et al. 2012) (Fig 2.5).

As mentioned above, intestine encounters high damage rate and cell death. Therefore, crypts containing stem cells must be well protected from the harsh environment to minimize their damage. First, crypts are not in close contact with digestive and absorptive system, and they are connected to the lumen only with a 6um opening that limited the exchange. Secondly, mucus produced by Goblet cells, physically creates a barrier over this opening.

Within the crypt, Paneth cells plays a fundamental role in ISCs protection. This cell type produces a wide variety of antimicrobial products such as lysozyme, defensins and phospholipase A2 that, not only protect the stem cells but are exported in the lumen as integral part of mucosal protection (Gehart and Clevers 2019). Despite the protective environment, stem cells can suffer mutations, toxins and other environmental factors. Stem cell competition provide another mechanism for tissue protection, limiting the ability of deteriorated cells to create their progeny. The limited space of the crypt creates this competition that stochastically leads to either loss or dominance of one clone in a single crypt. Cells that displays mutations that delay their division or provoke irregular cell cycle or enhance apoptosis, are displaced from the intestinal tissue, limiting the insurgence of

neoplastic proliferation to those cells that can proliferate outside the stem cell niche (Gehart and Clevers 2019).

Paneth cells are interspersed with ISCs, putting in close contact ISCs with at least one Paneth cell. At the crypt base, Paneth cells do not contribute only to stem cells and intestine defense, but they also provide nourishment for ISCs. Paneth cells are source of WNT ligand, epidermal growth factor (EGF) and Notch signaling (Sato, van Es et al. 2011). Recently it

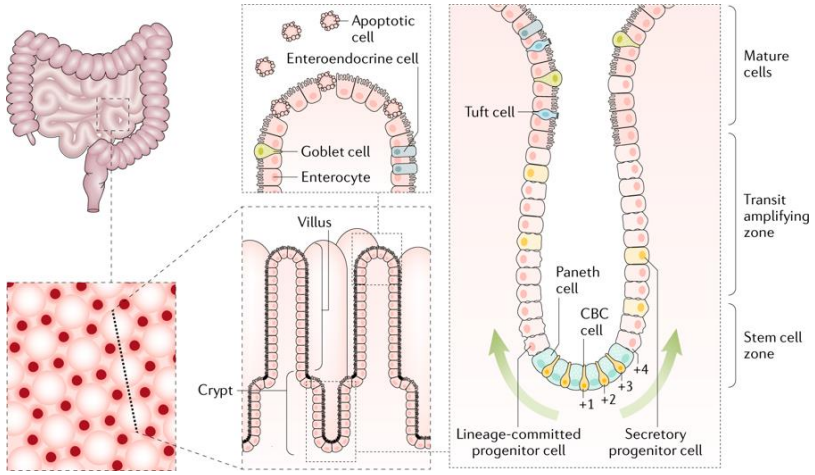

Figure 2.5 Schematic representation of intestinal tissue

In the figure, taken from (Gehart and Clevers 2019), the intestinal tissue, with enlargement on the crypts and villi structures. In the pictures are represented the major cell types constituting the differentiated and the undifferentiated compartment.

has been discovered that Paneth cells and ISCs has different metabolism: while stem cells depend on mitochondrial oxidative stress, Paneth cells undergoes glycolysis with lactate as end product (Rodriguez-Colman, Schewe et al. 2017). Importantly, lactate is used in ISCs as substrate for mitochondrial metabolism. Of note, oxidative metabolism is a source of DNA damage, however lactate has been shown to act as a radical scavenger and antioxidant in vitro, open the possibility that lactate can both boost ISCs metabolism and protect them from oxidative stress.

Mesenchymal cells provide another important source of signals for stem cell niche specification and maintenance. Fibroblast, myofibroblast, pericytes, neural cells, vascular cells and smooth muscle, do not create only a physical and structural support for the tissue,

but they provide signals that help to regulates stem cell behavior (Gehart and Clevers 2019). Several studies have pointed out the important role of mesenchymal cells as source of WNT, R-Spondin, BMPs and BMP inhibitor, however, a deep characterization of cell population is still lacking. Importantly, also crypts influence the microenvironment through ligands secretion such as Sonic and Indian Hedgehog, that are important for smooth muscle maintenance in adult tissue.

During homeostasis ISCs, also known as Crypt base columnar (CBCs) cells for their morphology, give rise to all differentiated cells types in the intestinal tissue meanwhile maintaining the ISCs population. To face the high rate of cell death and damage that occurs at the top of the villi, they proliferate every 24 hours, generating the transit amplifying (TA) progeny that localize in the middle of the crypts and that in turn divide every 12-16 hours to sustain the massive intestinal cells loss, migrating upward while differentiating (Barker 2014, Leung, Tan et al. 2018).

However, adult stem cells are crucial also for tissue regeneration after injury. In adult intestinal tissue two different stem cell population have been described: beside CBCs, committed precursors derived from columnar cells, the so called +4 cells, can dedifferentiate into a multipotent state and participate to intestinal regeneration. This mechanism requires a high rate of cell plasticity that is established and maintained through particular chromatin state that characterize intestinal crypts cells (Elliott and Kaestner 2015, Beumer and Clevers 2016, Leung, Tan et al. 2018). This high plasticity give rise to two different models for tissue homeostasis: the “stem cell zone mode” and the “+4 model”.

Initially, in 1977, the mapping of long-lived cells containing all cell lineages, drived the postulation of “+4 model” as stem cells governing tissue homeostasis. In this model stem cells were positioned just above Paneth cell at the +4 position from the crypt base (Potten 1977). CBCs as intestinal stem cells were discovered in the same years by Cheng and Leblond (Cheng and Leblond 1974), however, it was only twenty years later that Bjerknes

and colleagues challenged the "+4 model" proposing the "stem cell model" where CBCs were identified as the intestinal stem cells (Bjerknes and Cheng 1999).

Despite the great advance in intestinal stem cells identification, only in 2007 Barker and colleagues, provides, through genetic mouse model and lineage tracing analyses, the proof for CBCs stemness (Barker, van Es et al. 2007, Barker, van Es et al. 2008). As first, based on a study of WNT pathway in cancer cell lines, *Lgr5* (Leucine-rich repeat-containing G-protein coupled Receptor 5) was identified as one of the best targets of this signaling cascade. The generation of the mouse model Lgr5-CreERT2-Rosa26-LoxSTOPLox-LacZ, that enable the visualization of the progeny derived from LGR5 expressing cells, reveals that LGR5 is an effective marker of CBCs intestinal stem cells and that from these proliferating cells, ribbons of LacZ marked cells progressively extend from crypts bottom to the villi tips (Barker, van Es et al. 2007, Barker, van Es et al. 2008).

However, other genetic studies, addressed +4 cells as a second long-term stem population within the crypts and in the last years new studies contributed to clarify the molecular identity of this stem cell reserve (Sangiorgi and Capecchi 2008, Montgomery, Carlone et al. 2011, Takeda, Jain et al. 2011, Powell, Wang et al. 2012). Buckzaki and colleagues demonstrated that after a transient H2B-GFP expression, that is diluted and lost in several cell division, two distinct population retains GFP expression: Paneth cells and a cell population characterized by both *Lgr5* and +4 markers expression. Additionally, these cells express markers of differentiated secretory cells and contribute to Paneth cells formation during physiological tissue renewal. However, after irradiation, these long-lived cells revert to a multipotent state regenerating the whole intestinal epithelium (Buczacki, Zecchini et al. 2013). Further experiments demonstrated that upon LGR5 expressing cell loss, by irradiation or with genetic models to induce specific cellular death, CBCs are depleted from the tissue and the homeostatic regeneration is lost. Indeed, within few days after CBCs loss, LGR5-expressing cells reappears and perfectly reconstitute the tissue. This regeneration is impaired if reappearance of LGR5 expressing cells is continuously blocked, meaning that CBCs are

essential for tissue regeneration (Dekaney, Gulati et al. 2009, Tian, Biehs et al. 2011, van Es, Haegebarth et al. 2012, Metcalfe, Kljavin et al. 2014).

In this new model two coexisting stem cell populations participate to intestinal epithelium maintenance, the LGR5-CBCs expressing cells that replenish the intestinal tissue during homeostatic conditions, and long-lived cells serve as a stem cells reserve-pool in case LGR5-ISCs are lost upon tissue damage or generally when needed (Tetteh, Farin et al. 2015).

Still, this ability of dedifferentiate to drive tissue regeneration, seems to be wider than expected and other reports identified new precursors of both absorptive and secretory lineages as cells involved in stem cell pool and tissue regeneration after damage, highlighting the importance of dedifferentiation to ensure the tissue maintenance (Gehart and Clevers 2019).

2.3.1 PATHWAYS IN INTESTINAL TISSUE

This elaborate organization is maintained throughout a complex network of interactions among different cell types.

The most important and studied are Wingless integration site (WNT), Bone Morphogenetic Protein (BMP), NOTCH and Epidermal Growth Factor (EGF) pathways.
To ensure tissue regeneration different pathways tightly regulates cells fate determination. The most important and studied are Wingless integration site (WNT), Bone Morphogenetic Protein (BMP), NOTCH and Epidermal Growth Factor (EGF) pathways.

The WNT pathway is tightly correlated with stemness, in fact mutations in its components are the first cause of colorectal cancer onset and development. WNT ligands binds to Frizzled-LPR5-LPR6 receptor complex, that inhibit beta-catenin destruction, leading to

nuclear accumulation and, upon binding with TCF/LEF family members, transcriptional regulation (Nusse and Clevers 2017).

The role of WNT pathway during homeostasis has been intensively investigated with different approaches both *in vivo* and *in vitro*. A gradient of WNT ligands is established in intestinal compartment, starting from the crypt base, where it reaches the higher concentration, and being lost at the interface between crypt and lumen. Importantly, during development WNT is necessary for Paneth cells specification, that subsequently become the main source of WNT ligands (van Es, Jay et al. 2005). Inhibition of WNT signaling severely affects intestinal epithelium leading to stem cell loss and rapid animal death (Fevr, Robine et al. 2007, van Es, Haegebarth et al. 2012). Others important players in WNT signaling are R-Spondins soluble proteins. Despite the abundance of WNT ligands at the crypt base, their ability to activate the pathway rely on R-spondin binding to LGR5 receptor. This binding provokes the sequester of RNF3 or ZNRF3 E3 ligase that, when free, ubiquitinates the Frizzled receptor, thus leading to its degradation. Indeed, R-Spondin/LGR5 interaction results in increased sensitivity to WNT pathway (de Lau, Peng et al. 2014).

BMP belongs to the TGF-Beta family of secreted signaling molecules, and the pathway is activated when BMP engages its membrane receptor BMPRI or ALK2-6, followed by the recruitment of BMPRII which phosphorylate BMPRI leading to its activation. A sequent cascade of phosphorylation events involves R-SMAD1/5/8, that activate the effector SMAD4, that translocate into the nucleus and activate transcription of its targets. Conversely to WNT, BMP restricts the stemness potential in the crypts, and its gradient is opposed to the WNT ones, starting from the villus and diminish reaching the crypt base. BMP signal cascade is able to negatively regulate the stem cell specific transcriptional program (He, Zhang et al. 2004, Qi, Li et al. 2017).

In the crypt, BMP inhibitor molecules, such as Noggin and Gremlin 1-2, tightly titrate the free BMP, thus impeding stem cell exhaustion.

NOTCH pathway is one of the most direct form of cell-to-cell communication. The canonical transduction molecule involves a ligand, tethered on the cell membrane that binds the transmembrane receptor on the adjacent cell. In mammals five different ligands (DLL1, 3, 4 and Jagged1, 2) and four notch receptors (NOTCH1-4) exist. Ligand-receptor binding induces Notch cleavage by gamma-secretase and the release of notch intracellular domain (NCID) that translocate into the nucleus. RBPJ is a transcriptional repressor in absence of signal, however, upon NCID binding, the dimers recruit MALM1-4 resulting in transcriptional activation of the target genes. NOTCH signaling is able to activate either proliferation, differentiation or cell death depending on the context. In the small intestine NOTCH ligands are expressed by secretory precursors and Paneth cells, while stem cells express NOTCH1 and 2. Genetic ablation of NOTCH 1 and 2 or their ligands DLL1 and 4 induces stem cells and TA cells to differentiate toward the secretory lineage, severely impairing the absorptive ability of the intestinal epithelium (Sato, van Es et al. 2011, Guruharsha, Kankel et al. 2012, Sancho, Cremona et al. 2015).

Last, EGF-ERBB pathway comprises four transmembrane receptor tyrosine kinases (EGFR/ERBB1, ERBB2-4) and 13 secreted ligands, all sharing the epidermal growth factor domain. Upon ligand binding, ERBB1 and ERBB4 can form homodimers or heterodimers, that activate the signaling cascade. Phospho-activated receptors can bind different adaptor proteins responsible for RAS GTPase recruitment and MAPK cascade activation.

EGF signaling pathway promotes intestinal cell growth and proliferation, as demonstrated by mice lacking or defective for EGF pathway components (Miettinen, Berger et al. 1995, Threadgill, Dlugosz et al. 1995, Lee, Yu et al. 2009).

2.3.2 POLYCOMB AND INTESTINE

Signaling pathways converge on chromatin to tightly regulate cell differentiation. Several are the TFs and the epigenetic players involved in this tight and complex network, and some of them shows fundamental roles.

Secretory lineage specification is controlled by NOTCH signaling pathway through HES1, a direct NCID target. *Hes1* is expressed in proliferating cells and is required for ISCs and TA cells maintenance (Kayahara, Sawada et al. 2003, Suzuki, Fukui et al. 2005). Loss of NOTCH signaling or *Hes1* deletion leads to the upregulation of ATOH1 TF (Jensen, Pedersen et al. 2000, Ueo, Imayoshi et al. 2012), that can be considered the master regulator of secretory lineage, as demonstrated by the lethality due to the complete absence of secretory cells in *Atoh1* deficient mice (Yang, Bermingham et al. 2001). On the contrary ATOH1 ectopic expression results in prenatal death due to the complete transformation of intestinal cells in secretory cells (VanDussen and Samuelson 2010). These data demonstrate that ATOH1 is necessary and sufficient to specify for secretory lineage, and its expression must be strictly regulated.

Epigenetic analyses of H3K27me3 PRC2 mark along the crypts-villus axis revealed that almost 40% of repressed genes in enterocytes are active in ISCs, among them *Myc*, *Ascl2* and *Lgr5* (Jadhav, Nalapareddy et al. 2016). In non-secretory cells *Atoh1* promoter is enriched for H3K27me3 and inhibition of NOTCH signaling correlates with PRC2 mark decrease and Atoh1 increase (Chiacchiera, Rossi et al. 2016). Accordingly, EED loss, leading to the disruption of PRC2 activity, increases *Atoh1* levels and expand goblet and enteroendocrine cells populaitons, meaning that PRC2 activity is essential to maintain repressed *Atoh1* in cells where it should be silenced.

However, Polycomb plays other important role in intestinal tissue. PRC2 is required for intestinal regeneration when LGR5 population is lost, as upon irradiation, by repressing INK4A/ARF locus (Chiacchiera, Rossi et al. 2016). On the other hand, independently from p16 and p19 activation, PRC1 is strictly required to maintain stem cell identity, preserving

the correct transcriptional profile, by repressing non-lineage-specific genes. In PRC1 deficient mice, the massive upregulation of genes belonging to other cell types, directly interfere with TCF4/beta-catenin binding, leading to stem cell loss (Chiacchiera, Rossi et al. 2016) identifying PRC1 as a fundamental complex for ISC identity and self-renewal preservation.

2.4 AIMS

Cell identity is an essential feature that is preserved, controlled and modulated throughout life. In this context, PcG proteins exert a critical role defining transcriptional identity during development as well as during adult tissue homeostasis. Our laboratory has previously demonstrated that PRC1 activity is fundamental for ISCs identity and for the integrity of the whole intestinal tissue. An important aspect of Polycomb biology, starting from its pathological behavior in cancer settings, suggest that PcG activity in adult tissue is highly context dependent. This may also involve the high biochemical heterogeneity that exist among Polycomb Repressive complexes with a particular emphasis on PRC1 activity that can exist in six distinct sub-forms. Therefore, taking advantage of LGR5-GFP-ires-CreERT2/Ring1a$^{-/-}$/Ring1b$^{fl/fl}$/Rosa26Lox-stop-Lox LacZ mouse model, the major aim of this project is to investigate the role of PRC1 in a different stem cell compartment in which the LGR5 receptor is expressed: the hair follicle. This tool allowed us to compare two different adult cycling stem cells, that develop from different embryonic layers, during adult tissue homeostasis. This will provide understanding about PRC1functional similarities and specificities in these two stem cell populations at a molecular level, thus defining if and how cell identity and the associated environment are able to reshape Polycomb activity.

Furthermore, since PRC1 activity is divided in six different biochemical complexes that are specified by the expression of the six distinct and mutually exclusive PCGFs paralogues, the second aim of my project is to translate the knowledge generated in our laboratory in more simple models such as embryonic stem cell in a more complex biological system like the intestinal epithelium. To achieve this, we decided to deeply investigate PCGFs biological function taking advantage of tissue-specific conditional KO mouse models to define the role of each PCGF protein, thus of PRC1 sub-complexes, respect to the general role that PRC1 activity exert in this tissue.

3. MATERIALS AND METHODS

3.1 ETHIC STATEMENT

Mice were maintained accordingly to the guidelines set out in Commission Recommendation 2007/526/EC, 18 June 2007, on guidelines for the accommodation and care of animals used for experimental and other scientific purposes. All experiments were performed in accordance with the Italian Laws (D.L.vo 116/92 and following additions), which enforces EU Directive 86/609 (Council Directive 86/609/EEC of 24 November 1986 on the approximation of laws, regulation, and administrative provisions of the member states regarding the protection of animals used for experimental and other scientific purposes.

3.2 MOUSE MODELS

LGR5-specific conditional knockout mice were generated crossing a C57BL6 strain straight knockout for Ring1a ($Ring1a^{-/-}$) through the insertion of a PGK-HPRT deletion cassette (del Mar Lorente, Marcos-Gutierrez et al. 2000), and with LoxP sites flanking exons 3 to 5 of Ring1b ($Ring1b^{fl/fl}$) (Cales, Roman-Trufero et al. 2008) with LGR5-GFP-ires-CreERT2 (Barker, van Es et al. 2007). These mice were further crossed with Rosa26lox-stop-lox LacZ transgenic mice for in vivo lineage tracing (Barker, van Es et al. 2007). Specific PCGFs conditional KO mice, that allow the depletion of different exons of the various genes, were bred either with LGR5-CreERT2 and Rosa26lox-stop-lox Lacz or AhCre background strains, which are described below. The correctness of the genotype was confirmed by polymerase chain reaction (PCR) with specific primers performed on genomic DNA extracted and purified from tail or ear skin, as described in the next paragraph.

Cre-recombinase protein is an enzyme that directs recombination between two strands of DNA with specific sequences called loxP sites (“locus of crossover in Phage P1”) (Oumard, Qiao et al. 2006). Upon Cre activity, the removal of the genomic region between the loxP sites induces the deregulation of the target genes. Ring1b recombination elicits the start codon of the transcript thereby, inhibit the start recognition and consequently the transcription and the protein production. On the contrary, LacZ transcript is blocked by the

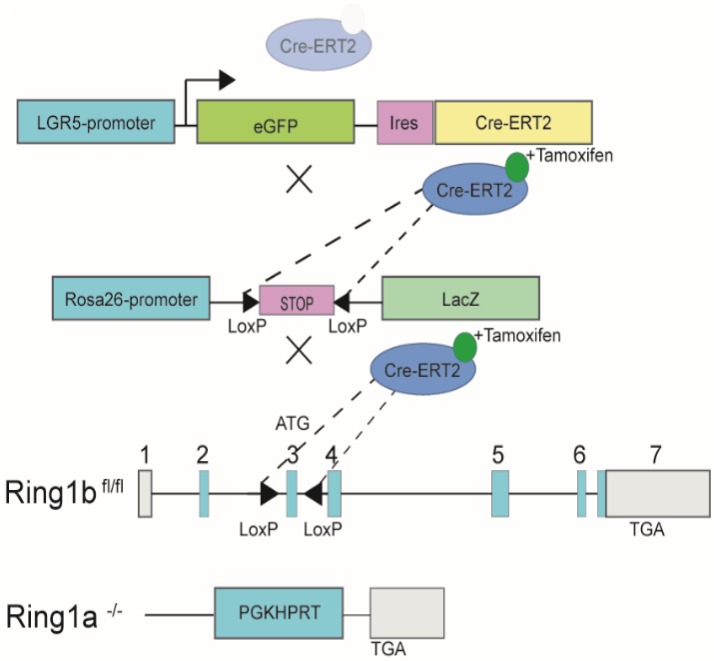

Figure 3.1 Schematic representation of the mouse model used

The mouse strain is homozygous straight knock-out for Ring1a gene and harbor floxables alleles for Ring1b genes. It has been further complemented with a lineage tracing construct, in homozygosity, that allows the expression of LacZ gene after the removal of a stop cassette inserted before the LacZ start codon.

Cre Recombinase and GFP are under the LGR5 promoter that allows their expression only in cells where the receptor is expressed. Cre-ERT2 encodes for a cytoplasmic therefore inactive form of the enzyme that is translocated in the nucleus upon tamoxifen metabolites binding.

presence of an upstream STOP codon that is removed by Cre cleavage, thus permitting beta-galactosidase expression and translation.

LGR5-GFP-ires-CreERT2 transgene constitutively expresses, only in LGR5-expressing cells, a Cre-recombinase protein fused to a modified fragment of the Estrogen Receptor, that

sequesters the enzyme in the cytoplasm, where it cannot exert its function. The estrogen receptor antagonists (i.e. Tamoxifen molecule) (Fig 3.1) binds the ERT2 fragment of the fusion protein, enabling its nuclear translocation where it can actively cleave loxP sites.

Differently from LGR5-specific CreERT2 expression, Rosa26lox-stop-lox LacZ possess a more ubiquitous expression potential thanks to ROSA26 promoter, however beta-galactosidase transcript can be expressed only upon Cre nuclear import, thus limiting LacZ expression only in LGR5 stem cells and their progeny in our mouse model.

Cre mediated recombination of LGR5-CreERT2 strains was induced by performing four intraperitoneal injection of Tamoxifen (Sigma-Aldrich) dissolved at 75mg/kg in corn oil. Tamoxifen is a prodrug that possess little affinity for the ER, indeed, to obtain the active molecule is metabolized in the liver by Cytochrome P450 to 4-hydroxytamoxifen (4-OHT) or N-desmethyl-4-hydroxytamoxifen (Desta, Ward et al. 2004).

AhCre mouse model (Ireland, Kemp et al. 2004) mediate Cre recombinase expression upon CYP1A1 promoter which is highly activated by lipophilic xenobiotic binding. Induction of Cre transcription is obtained by 4 intraperitoneal injection of beta-naphthoflavone dissolved at 80 mg/kg in corn oil. This mouse model allows Cre expression in whole intestinal epithelium, with the only exception of Paneth cells.

3.3 GENOTYPES

Skin from tails or ears were conserved at RT for few days in 100% ethanol until the extraction. Ethanol was discarded and the samples were washed with 1X PBS to remove the remaining alcohol. Samples were digested in 200 μL Digestion buffer (TRIS-HCl pH 7,5 10 mM, EDTA pH8 10 mM, NaCl 10 mM, SDS 0,5%) with 0.5 mg/ml Proteinase K at 52°C for at least 5 hours or overnight shaking. Digested tissues were then purified by adding 1 volume of each Guanidine thiocyanate solution (Guanidine Thiocyanate 0,345 g/ml, EDTA

pH8 10 mM, TRIS-HCl pH 7,5 10 mM, NaCl 10 mM) and 75% Ethanol. The mixture was vortexed, transferred to EconoSpin™ Spin Column for DNA (Epoch Life Science), fudge to 13000 RPM for 3' at RT and the flow-through was discarded. The column was then washed with 500 μL of Washing Buffer (Ethanol 25%, 2-Propanol 25%, NaCl 100 mM, TRIS-HCl pH8 10 mM) and subsequently with 600 μL of 75% Ethanol, removing the flow-through after each centrifugation. The column was dried fudging 5' at 13000 RPM at RT and the DNA were eluted in 50 μl of DNase-RNase free water.

5 μL of this DNA were used for each PCR.

3.4 HAIR FOLLICLE PURIFICATION

LGR5 positive stem cells were purified from back skin of treated mice at different time points according to the experimental plan. After mice were euthanized, the fur was removed with razor and back skin near the tail were lifted with tweezer and cut, gently peeling the skin from the underlying tissue. Back-skin obtained were washed in ice cold PBS, laid and pin, without over-stretching the tissue, with intern facing up. Under a stereomicroscope, subcutaneous fat and blood vessels were accurately removed to expose the hair bulbs, and the tissue were digested using Collagenase (0,8 μg/μL) in Dulbecco's Modified Eagle's Medium (DMEM) for 45 minutes at 37°C. After this incubation, back-skin were scraped off and the collected HFs were further digested to obtain a single cell suspension with 2.5% trypsin in PBS with the addition of Deoxyribonuclease 1 (DNse1: 1600 U/ml) for 10' at 37°C. Fetal bovine serum (FBS) was added to the single cell suspension to neutralize trypsin. Cells were pelleted at 2000 RPM at 4°C for 5 minutes and washed in ice-cold PBS to remove FBS and trypsin residues. To remove hairs and aggregates the single cell, suspension was filtered with a 70 μm cell strainer. The obtained suspension, enriched for HFs single cells, were resuspended in the correct buffer depending on the application.

3.5 CRYPTS PURIFICATION

Small intestine was taken from mice and immediately processed due to its fast degradation. Intestine was flashed with ice-cold PBS twice, opened longitudinally and the villi were manually removed by scraping the tissue. Intestine was then chopped into around 5mm pieces and incubated in 30 ml of cold PBS containing 2mM EDTA, and kept on ice for 15 minutes. After this incubation, the falcon was inverted twice to move the mixture and release remaining villi in the supernatant, that was carefully removed. Intestinal pieces were further incubated with 5mM EDTA in PBS for 45 minutes rocking at 4°C, after which fragments were let sit on the falcon base and the supernatant was removed. Tissue containing crypts was resuspended in 20 ml of ice-cold PBS containing 1% of FBS and vigorously shacked ten times, and supernatant containing the released crypts were filtered using a 70 μM cell strainer. This passage was performed twice with new 20 ml of PBS-FBS 1% solution. Crypts were pelleted at 1000 RPM at 4°C and washed with ice-cold PBS-FBS 1%, and pelleted at 800 RPM at 4°C to clean the purification from small fragmented tissue.

Obtained crypts were used for lysate preparation or processed for other techniques, or alternatively incubated for 15 minutes in DMEM solution containing Trypsin 0.1%, DNaseI 800 U/ml and 10 μM Rock inhibitor Y-27632 (Selleck chemicals) to obtain a single cells suspension. Dissociated cells were resuspended in the buffer needed for further analyses.

3.6 VILLI PURIFICATION

Villi that were manually removed during crypts extraction were collected in ice cold PBS. Once pelleted, the supernatant was removed, and the villi were carefully resuspended in 50 mL of ice-cold PBS with 3mM EDTA. Villi were incubated 10 minutes rocking at 4° C and fudged at 1200 RPM at 4° C for 10 minutes. Supernatant was removed, and the villi

resuspended and washed in 50 mL of ice-cold PBS with 1% FBS, and passed through a 100 μM cell strainer, changing the strainer when mucus stuck the flow, in order to recover only villi. The purified villi were pelleted as previously described, and washed in PBS. Next, the pellet was lysed as described in the next paragraph.

3.7 LYSATES PREPARATION AND WESTERN BLOTTING ANALYSES

The obtained pellet, from either crypts or villi, was lysed with S300 extraction buffer (TRIS-HCl pH 8 20 mM, NaCl 300 mM, Glycerol 10%, Igepal 0.2%) with protease inhibitors, sonicated to disrupt DNA, fudged at 13000 RPM for 30 minutes at 4° C. After the centrifugation, the supernatant was quantified. Lysate was then diluted and preserved with LAEMLLI buffer to 1x concentration to reach the desired protein concentration, usually 1 or 2 μg/μL. 40ug of total lysate were separated on SDS-PAGE and transferred on Nitrocellulose membrane. The membranes were then saturated with 5% low-fat dried milk in TBS-Tween 0.01% and incubated with the specific antibody following time and dilution reported in Table1.

After primary antibody binding membranes were washed in TBS-Tween 0.01% and incubated with the correct secondary antibody as reported in Table 2. Excess of milk and secondary antibodies were washed prior to signal revelation, which was carried out with Clarity™ Western ECL Substrate (Bio Rad) and acquired using ChemiDoc XRS+ (Bio Rad).

3.8 TOTAL RNA EXTRACTION

Total RNA extraction was performed lysing the cells with TriZol and following the Direct-zol RNA MiniPrep protocol (Zymo research) and then retrotranscribed to obtain cDNA. Briefly, crypts were lysed in TriZol and an equal volume of 95% ethanol was added to the

lysate. RNA was applied to a Zymo-spin column and washed by centrifugation, and then DNA was removed by a short DNase I treatment directly on the column. Pure RNA was washed twice and recovered in a sterile collection tube and quantified at NanoDrop.

500 to 1000 nanograms of purified RNA was used for each retro-transcription reaction. RT was performed with ImProm-II™ Reverse Transcriptase reagents, following Promega standard transcription protocol.

Retrotranscribed cDNA was analyzed by RT-qPCR with Gotaq(r) Qpcr Master Mix (Promega) with the primers list described in Table 3.

3.9 FLOW CYTOMETRY

Single cell suspensions obtained following the protocol described above were fixed 10’ at RT, with 4% Paraformaldehyde (PFA) in PBS without Methanol to crosslink the cells avoiding damaging the membrane, and preventing GFP leaking from the cytoplasm. PFA were blocked by adding the same volume of Glycine solution (Glycine 0,1 M, NaN3 0,01% in PBS) to the crosslinking reaction, in order to saturate the crosslinker, pelleted by centrifugation at 2000 RPM for 5’ at RT and washed with PBS. Cells were then permeabilized with Triton buffer (Triton 0,25% in PBS) for 7’ at RT at dark, washed and blocked for 30’ at RT at dark, with a solution of 5% FBS in PBS to diminish antibody non-specific binding.

Cells were then pelleted, and primary antibody diluted in PBS were added to the cells according to Table 1. After primary antibody binding, cells were pelleted and washed with BSA 1% in PBS to remove any residual primary antibody, followed by incubation with secondary antibody (Table 2) performed at dark. Cells were finally washed to remove the excess of secondary antibody, diluted in PBS and the fluorescence were read on FACS Calibur.

3.10 FACS

In order to obtain a pure population of HFSCs, we exploited the GFP expression of LGR5-GFP-ires-CreERT2 mouse strain. Single cell suspensions obtained following the protocol of hair follicle purification were washed once in PBS and resuspended in Sorting Medium (DMEM, 1;100 Penicillin and streptomycin (17-602, Lonza), 1:100 L-Glutamine (17-605E, Lonza), Hepes, EDTA pH8 2 mM, DNase1 (800 U/mL) and Y27632 (selleck Chemicals) 20 μM)). Cells were further filtered with 40 μM cell strainer prior Sorting.

Single cells from intestinal purification were resuspended in Sorting Medium (Advanced-DMEM, 1:100 Penicillin and Streptomycin (17-602, Lonza), 1:100 L-Glutamine (17-605E, Lonza), Hepes, EDTA pH8 2 mM, DNase1 (800 U/mL), Y27632 (Selleck Chemicals), N2 50x, B27 200x and NAC (N-Acetyl Cysteine) 100x and further filtered with 40 μM cell strainer prior Sorting.

Single GFP positive LGR5-HFSC were FACS-sorted using either FACSMelody or FACSJazz cell sorters (BD Biosciences). To discriminate between living and dead cells, we added Propidium Iodide to a final concentration of 25 μg/ml.

3.11 IMMUNOFLUORSCENCE

Back-skin from ctrl and dKO mice were harvested as described in the first passage of "Hair follicle purification" protocol. The back skin obtained were briefly fixed in 4% PFA for 3 hours at 4°C covering all the skin and gently shaking. The materials were then incubated at least overnight in 30% Sucrose in PBS to cryopreserve the tissues and avoid freezing damages. Back-skins were then embedded in O.C.T (Tissue-Tek 4583), that is a water soluble mixture of glycols and resins that provides an optimal matrix for cryostat sectioning,

and stored at -80°C. Embedded tissue were cut at 7um and slides were collected and stored at -80°C until staining.

Sections were prewarmed at RT for few minutes and washed twice with 0,1% Tween 20 in Tris-Buffered Saline (TBS-T) to eliminate the residual matrix, and blocked with 5% donkey serum in TBS-T for one hour at RT. Primary antibody were then incubated overnight at 4°C (specified in Table.1). The following day, slices were washed twice with TBS-T and incubated for 1 hour at RT with secondary antibody (specified in Table 2) and 4',6-diamidino-2-phenylindole dihydrochloride (DAPI, 32670, Sigma- Aldrich) and mounted with Mowiol 4-88 (81381, Sigma-Aldrich). Images of back-skin were taken with Leica SP8 confocal microscope.

3.12 PROXIMITY LIGATION ASSAY

The proximity ligation assay (PLA) is a powerful technique that enables both the visualization of endogenous proteins, or proteins modification, and the protein-protein interactions directly in situ on histological section and with high sensitivity. With the collaboration of another lab member we set up the following protocol to perform this assay on anagen induced pure HFSCs populations.

Anagen-induced HF were purified as described and were sorted to obtain LGR5-HFSCs from Ctrl and dKO mice. Collected cells were spotted on a coverslip pre-coated with Cell-Tak (Corning) adhesive, that is composed by polyphenolic proteins extracted from marine mussel (*Mytilus edulis*), that creates a not-charged adhesion matrix suitable for PLA which, in turn, requires the use of charged molecules. Briefly, the correct amount of Cell Tak adhesive was resuspended in a sufficient volume of filtered Sodium bicarbonate 0,1M pH 8 necessary to overlay the coverslip lied down in a 24 wells plate, incubated for 30 minutes at RT, then the mixture was removed, and the coverslip washed with pure water.

Cells were pelleted after sorting and resuspended in 300 μL of sorting medium, and gently applied to the coated coverslip. After 4 hours at 4°C, cells were efficiently anchored to the matrix and were fixed with 4% PFA in PBS for 10' at RT, washed and permeabilized with Triton 0.1% in PBS. Excess of permeabilization buffer were washed out with fresh PBS and the cells were subjected to Sigma-Aldrich PLA protocol using Duolink In Situ Orange Starter Kit Mouse/Rabbit. Cells were incubated with 1 drop of Duolink Blocking Solution for one hour at 37°C in a humidity chamber (Figure 3.2 step 1). Blocked samples were then subjected to specific antibodies binding (Figure 3.2 step 2), diluting both primary antibodies,

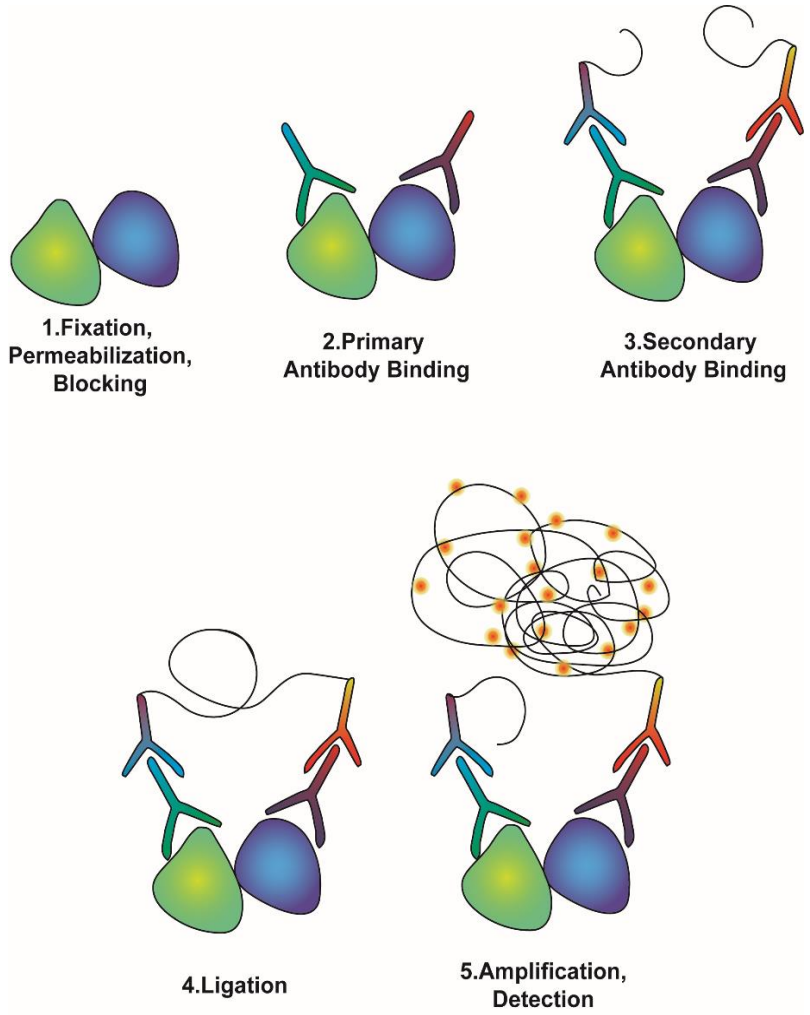

Figure 3.2 Proximity ligation assay protocol

Schematic workflow of PLA protocol highlighting the principal steps of the technique.

which were raised in different animals (Ring1B-Mouse and Bmi1 or Rybp-Rabbit), together in Duolink Antibody diluent, as specified in Table 2, and incubating cells in humidity

chamber for 1hours at RT. Primary antibody solution was then removed and the samples were washed twice to take away any antibody trace. To detect whether two different proteins can interact, PLA involves the usage of PLUS and MINUS charged PLA Probes, that are oligonucleotides-labelled secondary antibody that when in close proximity (less than 40nm) can interact (Figure 3.2 step 3). The probe binding requires one-hour incubation in pre-warmed humidity chamber at 37°C followed by two washes to eliminate the residual probes. If the proteins are in close proximity, so that the DNA probes can interact, during the ligation step (Figure 3.2 Step 4), that is carried out for 30' at 37°C in humidity chamber, Ligase enzyme is able to close the loop among the two probes. After ligation step, the enzyme and the reaction buffer were washed out. The circular loop created by the probes is a suitable platform for the Polymerase to work, and the loops are amplified several times during the reaction, that is carried out at 37°C and last 100 minutes, incorporating in the nascent concatenamer fluorescent oligonucleotides that amplify the ligation signal (Figure 3.2 Step 5). The treated coverslips were the mounted on a slide with the mounting medium added with DAPI, to counterstain the Nuclei. Stained samples were acquired with Leica SP8 confocal microscope and interactions a visualized as discrete dots in the cell nuclei.

3.13 HISTOLOGY

Back skin and intestinal tissues from treated mice were collected at the indicated time points depending on the experimental work. Isolated samples were immediately fixed overnight at 4°C in Formaldehyde (FA), flattened in the inclusion cassettes without overstretching the tissue. Tissues were then dehydrated in Ethanol solution, at increasing concentrations, to substitute the water present in the tissue, incubated with Xylene and included in Paraffin. Embedded samples were then cut with microtome at 5 μm thickness, and the slices were subjected to Hematoxylin\Eosin Y staining. Briefly, samples were rehydrated, tissue were stained with Hematoxylin (Harris Hematoxylin Solution, Sigma Aldrich) for 2' at RT and

coloration excess were removed with EtOH/ 0.5% HCl and were fixed, after two washes, with Ammonium Hydroxide 0,2% in water for 15' at RT. Cell cytoplasm were counter stained with Eosin Y, and the excessive coloration were removed with 95% Ethanol in water, and slices were then processed with ethanol 100% and Xylene. Stained sections were then mounted with Eukitt (Bio-Optica) and images were acquired with either Olympus BX51 or Leica DM6 widefield microscopes.

3.14 LINEAGE TRACING: HAIR FOLLICLE

Our mouse model LGR5-GFP-ires-CreERT2/Ring1a$^{-/-}$/Ring1b$^{fl/fl}$/Rosa26Lox-stop-Lox LacZ, thanks to Rosa26 Lox-stop-Lox Lacz transgene allows the tracing of LGR5 stem cell progeny through the production of Beta-galactosidase molecule.

Freshly prepared back-skin of treated mice, collected at the time point, indicated in the experimental workflow, were prefixed for 30' at RT in PBS containing Gluteraldehyde 0.2%, NP-40 0,02% and PFA 2%. Tissues were washed three times for 10' with fresh PBS, and incubated gently shacking for 30 minutes at RT in the equilibration buffer (MgCl2 2mM, NP-40 0,02% and Sodium Deoxycholate 0,1% in PBS). Equilibrated back-skin was then stained overnight at RT with 5 mM $K_3Fe(CN)_6$, 5 mM $K_4Fe(CN)_6$ and 1mg/ml X-Gal (5-bromo-4-chloro-3-indolyl-beta-D-galactopyranoside) diluted in equilibration buffer. Cells that derive from stem cells in which CreERT2 was nuclear, will express beta-galactosidase, which in turn catalyzes the hydrolysis of X-Gal into galactose and 5-bromo-4-chloro-3-hydoxyndolo. This latter compound is further oxidized into 5,5'-dibromo-4,4'-dichloro-indigo, which possesses the characteristic blue color, providing a visual assay for lacZ activity. Stained samples were then washed abundantly in PBS at RT, and the skin were fixed overnight with 4% PFA in PBS before paraffin embedding, that is carried out as described in Histology section. Embedded tissue was cut at 5um section and rehydrated following the standard rehydration steps for histology, gradually decreasing the Xylene and

the alcohol in the tissue. Section were then counter-stained with Nuclear Fast Red solution for 10’ at RT under chemical hood, dehydrated and mounted.

3.15 LINEAGE TRACING: INTESTINE

Freshly recovered intestinal tissues were washed once in ice cold PBS, and prefixed for 2 hours at 4°C in PBS containing Gluteraldehyde 0.2%, NP-40 0,02% and PFA 2%. Tissues were washed three times for 10’ with fresh PBS and incubated gently shacking for 30 minutes at RT in the equilibration buffer (MgCl2 2mM, NP-40 0,02% and Sodium Deoxycholate 0,1% in PBS). Equilibrated intestinal tissues were stained overnight at RT with 5 mM $K_3Fe(CN)_6$, 5 mM $K_4Fe(CN)_6$ and 1mg/ml X-Gal (5-bromo-4-chloro-3-indolyl-beta-D-galactopyranoside) diluted in equilibration buffer. The day after staining, intestinal tissue was abundantly washed with PBS and fixed over-night in 4% PFA. Before beginning the dehydration step, intestines were flattened and embedded as described in the Histology section.

3.16 RNA-SEQUENCING

Singlets of HFSCs, isolated from mice back-skin as previously described, were FACS-sorted thanks to GFP protein and collected in 0,5ml tubes, previously coated with 20% FBS in PBS. Cells were immediately processed in sorting tubes following Smart-seq2 protocol (Switching Mechanism at the 5’ end of the RNA Transcript) (Picelli, Faridani et al. 2014) with minor modification. This protocol is extremely useful, first because the amount of material needed is extremely small, compared to other RNA sequencing protocol, as it is designed to work with less than 1000 cells, and secondly allowing the operator to reduce the material waste, by coupling sample collection and processing without wash and fudge alternation. We collected 3000 cells per sample that were directly lysed in 2 μL of Lysis

buffer composed of Triton X-100 0,2% and Ribonuclease inhibitor (4 U/μL) in pure water. One microliter of each 10 mM oligo-dT30Vn and 10 mM deoxynucleotide triphosphate were added to the samples that were then incubated for 3' at 72°C, to allow RNA unfolding and oligo annealing with the polyA end of messenger-RNA. After this step, Reverse Transcription coupled with Template switching was performed by adding to the sample a mix containing SuperScript III reverse transcriptase enzyme 100U/μL (Invitrogen) and buffer, RNase Inhibitor 10U/μL, Betaine 1M, DTT 5 mM, MgCl2 6 mM and TSO 1 μM (Template Switching Oligo) (Fig 3.3) RT was performed following the published protocol. cDNA was then Pre-Amplified using KAPA taq HotStart enzyme working in High Fidelity buffer. To perform the Pre-amplification, 15 μL of the preamplification mix (KAPA taq HotStart, KAPA HiFi Buffer, MgCl2 0,5 mM, dNTPs 0,3 mM, ISPCR primer 0,1 μM) were directly added to the retro-transcribed samples and were incubated in the thermal cycler for 14 amplification cycles following temperature of the published protocol (Fig 3.3). Samples were then purified with AMPure XP beads (Agencourt AMPure XP, Beckman Coulter) equilibrated at RT for at least 30 minutes. An equal volume of AMPure beads was added to pre-amplified cDNA and the mix was incubated at RT for 8' to let the DNA binds the beads. Beads with DNA were immobilized with a magnet and were washed with 100 μL of 80% Ethanol and dried for 10 minutes to remove any alcohol residue. cDNA was eluted with 20 μL of pure water and eventually stored at -20°C. Eluted cDNA was quantified with Qubit colorimetric quantitation assay (Thermo Fisher Scientific, Q32854), and the quality was checked with High-sensitivity DNA assay of Bioanalyzer instrument (Invitrogen). Poor quality cDNA, presenting short DNA fragments at the Bioanalyzer, possibly derived from degraded RNA and was discarded. 2 nanograms of good quality pre-amplified cDNA were used for fragmentation reaction (Tagmentation) and library preparation (Fig 3.3). Smart-seq protocol enables DNA cutting and the ligation of adapters, needed for amplification of the library and the sequencing, at the same time. cDNA was tagmented with 100 ng of

homemade Tn5 enzyme pre-annealed with A/B-MEDS (Mosaic End Double-Stranded) oligonucleotides in working buffer containing TAPS-NaOH pH 8.5 5mM , PEG 8000 8%for 5 minutes at 55°C. Immediately after tagmentation reaction, the samples were put in ice to inhibit the enzyme that were further stripped 5' at RT with 5 µl of SDS 0,2%. Enzyme and buffer were removed by a quick AMPure purification (AMPure beads 1:1 ratio, 8' at RT for

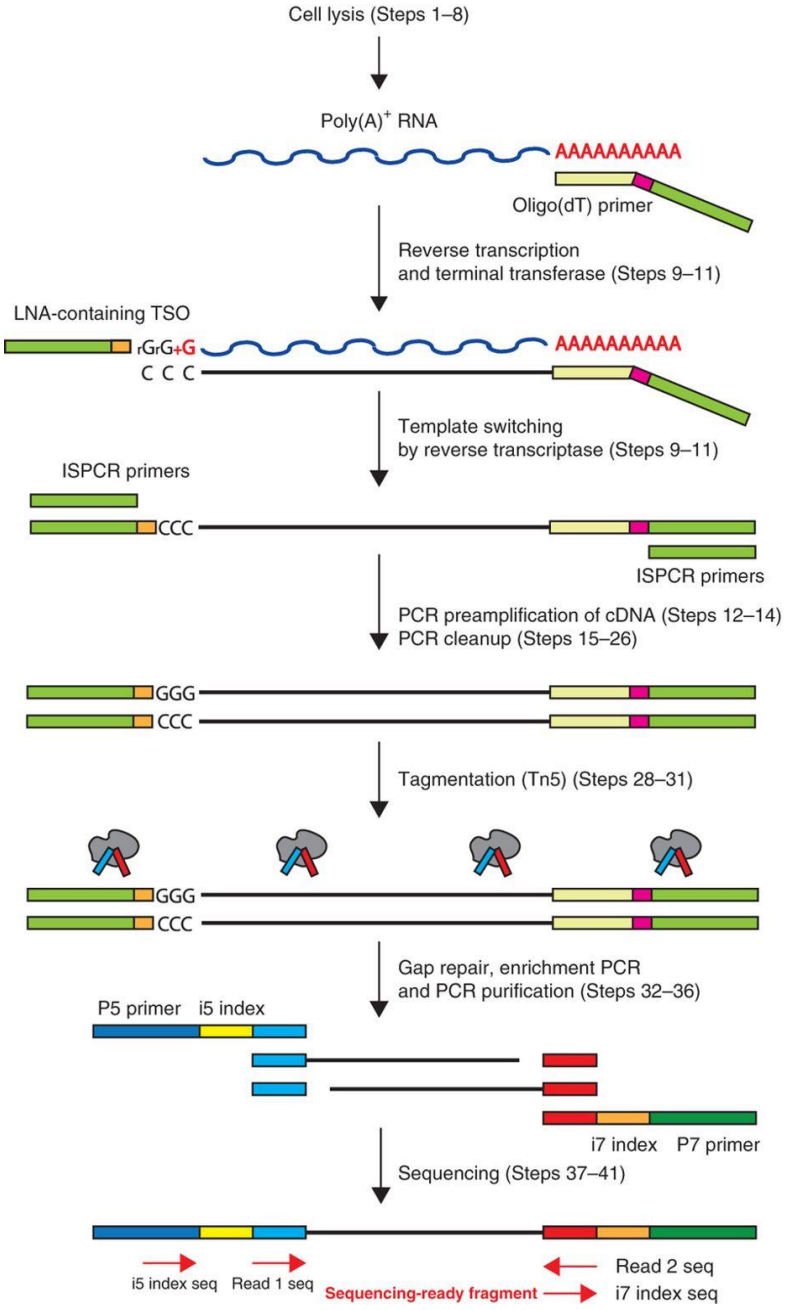

Figure 3.3 SMART-Seq2 library preparation protocol

Brief and schematic workflow of SMART-seq2 protocol highlighting the principal steps for library preparation. Figure from (Picelli, Faridani et al. 2014).

DNA binding, 5’ on the magnet (flow-through were discarded), 17,75 μL of pure water for DNA elution). PCR mix (KAPA HiFi buffer, KAPA Taq HotStart, dNTPs 0,3mM, Ad1 Primer (i5 primer for Illumina sequencing Without Barcode) 2 μM and Ad2.X Primer 2 μM (i7 primer for Illumina sequencing containing different Barcodes) were directly added to the eluted tagmented DNA and were amplified following the program: 72°C 3’, 98°C 30’’, 14 cycles of three steps amplification 98°C 10’, 62°C 30’’, 72°C 30’’, followed by the final elongation at 72°C for 5’. Amplified library DNA were then purified with AMPure, as for the pre-amplification step, quantified by Qubit and the quality was checked with High-sensitivity DNA assay for Bioanalyzer. Libraries that showed enrichment of DNA fragments that span around 200 and 800 bp length, were then sequenced using Illumina HiSeq 2000.

3.17 RNA SEQUENCING ANALYSES

The RNA sequencing analyses were performed by a bioinformatic of the lab. Reads were aligned to the mouse reference genome mm9 using TopHat v2.1.1 (Trapnell, Pachter et al. 2009) with parameters *--no-coverage-search* and *--library-type-fr-unstranded*. PCR duplicates were removed using Picard tool from Broad Institute (http://broadinstitute.github.io/picard/).

Gene counts were calculated using HTSeq-count v0.8.0 (Anders, Pyl et al. 2015) with parameters *--stranded=no --mode=intersection-nonempty* using RefSeq mm9 annotation downloaded from the University of California, Santa Cruz (USCS genome browser). Differential expression analyses were carried out using R package DESeq2 v1.20 (Love, Huber et al. 2014) using default parameters. Genes with an absolute log2(fold change) of 1 and false discovery rate of <0.1 were considered ad Differentially expressed and used for analyses. Gene enrichment analyses on down- and up- regulated genes were performed using DAVID 6.8 online tool (Huang da, Sherman et al. 2009). Pre-ranked Gene Set Enrichment Analyses (GSEA) (Subramanian, Tamayo et al. 2005) were performed using gene lists

(Signature Gene Lists) from multiple skin cell population obtained from (Rezza, Wang et al. 2016). The analysis was performed using default parameters (weighted as enrichment statistic) and ranking the input gene list using log2(fold change) data obtained from DESeq2.

To assess the expression of differentially expressed genes in dKO vs Ctrl HFSC in other mouse tissues, we used public RNA-seq data (Bam Files) deposited by ENCODE at https://hgdownload.soe.ucsc.edu/goldenPath/mm9/encodeDCC/wgEncodeLicreRnaSeq/. Bam files were processed with the pipeline described previously and RPKM (Read Per Kilobases of Million Mapped Reads) data were normalized with the function *normalize.quantiles()* from R package processCore (https://github.com/bmbolstad/preprocessCore).

3.18 CHIP SEQUENCING

LGR5 expressing HFSCs from anagen synchronized Ctrl mice were purified as described in "Hair follicle purification" and sorted for GFP expression. Intestinal cells were purified as described in "Crypts purification" and sorted for GFP expression in order to isolate only LGR5 stem cells. A total of 2.5 millions of sorted cells were used for each Chromatin Immuno-Precipitation (ChIP) and were crosslinked with 1% FA for 10' at RT followed by 5' incubation with Glycine 0.125 M. Cells were then pelleted and resuspended in IP buffer (NaCl 100 mM, Tris-HCl pH8.6 100 mM, EDTA pH8.0 5 mM, NaN3 0.2%, SDS 0.3% Triton X-100 1,7%).

Cells were lysed 20' in ice, and then sonicated to brake DNA by Branson sonicator with 10% of amplitude for 30' for 4 times with 1-minute rest to preserve sample's integrity.

Sonicated cells were then pelleted, and the supernatant is used for immunoprecipitation. The correct amount of Antibody (listed in Table 1) was added to the lysate, and the IPs were performed over-night. The day after, the immunocomplexes were recovered with protein A-

conjugated magnetic beads (Dynabeads,Life Technoligies) at 4°C for 3 hours rocking, and then washed 5 times with washing buffer containing 150 mM salt, and once with 500 mM salt (NaCl 150 or 500 mM, Tris-HCl pH 8.0 20 mM, EDTA pH 8.0 2 mM, SDS 0,1%, Triton X-100 1%). Samples were decrosslinked overnight in NaHCO3 0.1 M and SDS 1% at 65°C shacking. Decrosslinked DNA was purified with PCR purification Kit from Qiagen and sequenced with Illumina HiSeq2000.

ChIP performed in crypts was carried out on 500/1000 μg of total chromatin, following the same protocol as previously reported, but Protein A sepharose beads were used instead of the magnetic ones.

3.19. CHIP SEQUENCING ANALYSES

The ChIP sequencing analyses were performed by a bioinformatic of the lab. Sequenced reads were aligned to mouse reference genome mm9 using Bowtie v1.2.2 (Langmead, Trapnell et al. 2009) with default parameters and not allowing multimapping (-m1). PCR duplicates were removed using Picard tool (http://broadinstitute.github.io/picard/), and peaks were called using MACS2 v2.1.1 (Zhang, Liu et al. 2008) with parameters *–g-mm –nomodel –p 1e10 –B.*

Genomic peaks annotation was performed using R package ChIPpeakAnno v3.15 (Zhu, Gazin et al. 2010), considering the promoter region major or equal to 2.5kb around TSS (Transcription start site). Overlaps of ChIP-seq targets were performed as following: Genes with peaks in their promoter regions (+/- 2.5kb around TSS) were considered as targets. Then, the overlap between target gene lists were performed using the R package VennDiagram v1.6.20 (Chen and Boutros 2011). For heatmap representation of ChIP-seq signals, bigwig files, subtracted by input signal, were generated using function *bamCompare* from deepTools 2.0 (Ramirez, Ryan et al. 2016) with parameters *–ratio subtract –bs 30 –*

extendReads200. To normalize for differences in sample library size, a scaling factor for each sample was calculated as (1/total mapped reads) x 1 milion, and applied during bigwig file generation with the parameter –*scaleFactors* from bamCompare.

RING1B ChIP-seq targets were clustered in four groups according to their RPKM expression in Ctrl mice using the *dplyr* function *ntile()*. Tracks for H3K27me3 from ISC and HFSCs were obtained from (Chiacchiera, Rossi et al. 2016, Chiacchiera, Rossi et al. 2016) and (Lien, Guo et al. 2011) respectively, and processed with the pipeline described previously.

3.20 ANTIBODIES

Table 1 Primary antibody list

Name		FACS	IF	PLA	ChIP	WB
H2AK119	D27C4, Cell Signaling	1:600 1h30' RT	1:100 o/n 4°C	\\	10µg	\\
RING1B	Home made	\\	1:100 o/n 4°C	1:100	10µg	\\
PCGF4	Home made	\\	\\	1:100	10µg	1:1000; 5% milk in TBS\T; Rabbit; o/n 4°C
DEDAF/RYBP	AB3637, Millipore	\\	\\	1:100	10µg	\\
CBX8	Home made	\\	\\	\\	10µg	\\
H3K4Me3	39159, Active Motif	\\	\\	\\	5µg	\\
PCGF1	Home Made	\\	\\	\\	5µg	1:1000; 5% milk in TBS\T; Rabbit; o/n 4°C
PCGF2	Home Made	\\	\\	\\	5µg	1:1000; 5% milk in TBS\T; Rabbit; o/n 4°C

PCGF3	Home Made	\\	\\	\\	5µg	1:1000; 5% milk in TBS\T; Rabbit; o/n 4°C
PCGF5	Home Made	\\	\\	\\	5µg	1:1000; 5% milk in TBS\T; Rabbit; o/n 4°C
PCGF6	Home Made	\\	\\	\\	5µg	1:1000; 5% milk in TBS\T; Rabbit; o/n 4°C
Vinculin	V9131-.2ML, Sigma Aldrich	\\	\\	\\	\\	1:20000; 5% milk in TBS\T; Mouse; o/n 4°C

Table 2 Secondary antibody list

Name		FACS	IF	PLA	WB
Alexa 647	705-605-147 Alexa Fluor 647 AffiniPure, Jackson ImmunoResearch	1:400 30’ RT	\\	\\	\\
CY3	715-165-147 Cy3 AffiniPure, Jackson ImmunoResearch	\\	1:400 1h RT	\\	\\
Rabbit PLUS probe	Duolink, Sigma-Aldrich	\\	\\	5x	\\
Mouse MINUS probe	Duolink, Sigma-Aldrich	\\	\\	5x	\\
Anti Rabbit	Agilent Technologies Italia S.p.a	\\	\\	\\	1:5000 Milk 5% TBS\T
Anti Mouse	Agilent Technologies Italia S.p.a	\\	\\	\\	1:5000 Milk 5% TBS\T

3.21 PRIMERS

Primers were designed with Primer3 Plus or Primer Blast with the following parameters:

Amplicon length 100-150 bp; Primer size: 18-23; Primer Tm: 57°C -63°C; designed on two different exons, in order to avoid genomic recognition.

Table 3 List of qPCR primers

Primer name	Sequence
PCGF1 Fw	GGCTGAGTTCTGGCAAAGAC
PCGF1 Rv	GGAGCTGTACATGCTGTGGA
PCGF2 Fw	AATCACGGAGCTGAACCCTC
PCGF2 Rv	AGCGTACGATGCAGGTTTTG
PCGF3 Fw	TCCAGAGGAGAAGCCAAAGA
PCGF3 Rv	ACTGTGGTTGCGTCAATGAG
PCGF4 Fw	TGTCCAGGTTCACAAAACCA
PCGF4 Rv	CGGGTGAGCTGCATAAAAAT
PCGF5 Fw	CTGATCAAGCCCACGACAGT
PCGF5 Rv	TGAACTTGGTTGCCACACCT
PCGF6 Fw	TCCACCAGACTCAGCCTCTT
PCGF6 Rv	GGCTTGGGGACTTCTAGACC
TBP Fw	TGGAGATCACAACAGCCAAA
TBP Rv	CTTCTTCCGTTTTCCAGGTG
Rplp0 Fw	TTCATTGTGGGAGCAGAC
Rplp0 Rv	CAGCAGTTTCTCCAGAGC

3.22 SPECIAL AKNOWLEDGEMENT

Bioinformatics analyses presented in this thesis have been performed by a bioinformatician of the laboratory, that aligned all the sequencing tracks and performed the subsequent analyses, such as peaks calling, comparison among different peaks, for chip seq tracks and gene expression analyses for RNA-seq tracks. Gene Ontology analyses were performed in collaboration with the bioinformatician person using DAVID online Tools.

4. RESULTS

4.1 HAIR FOLLICLE REGENERATION REQUIRES PRC1-DEPENDENT H2AK119UB1.

PRC1 is a well-established regulator of lineage identity in embryonic stem cells (Morey and Helin 2010) and recently we described a fundamental role in adult Intestinal Stem Cells maintenance (ISC) (Chiacchiera, Rossi et al. 2016). However, nothing is known about PRC1 functions in other adult tissue homeostasis. Indeed, our goal was to unveil whether PRC1 role and function is conserved among different adult stem cells or not. We took advantage of the mouse models LGR5-GFP-ires-CreERT2/Rosa26Lox-stop-Lox LacZ (hereof *Ring1a/b* ctrl after tamoxifen administration) and LGR5-GFP-ires-CreERT2/Ring1a$^{-/-}$/Ring1b$^{fl/fl}$/Rosa26Lox-stop-LoxLacZ (hereof *Ring1a/b* dKO after tamoxifen administration) that was previously generated in our laboratory. This mouse model expresses both GFP and Cre-recombinase under the control of the LGR5 promoter, enabling the visualization and the excision of LoxP sites only in stem cells expressing LGR5 marker. Our mouse model was further crossed with the LacZ reporter gene whose expression is enabled only in cells where the Cre-recombinase enzyme is nuclear and active, tracing in this case LGR5 stem cells their progeny. Furthermore, our LGR5-GFP-ires-CreERT2/Ring1a$^{-/-}$/Ring1b$^{fl/fl}$/Rosa26Lox-stop-LoxLacZ mice are straight Knock-Out (KO) for *Ring1a* gene and possess homozygous-floxable alleles for the *Ring1b* gene allowing for the complete loss of PRC1 functionality through the inactivation of the two catalytic subunits of the complex (Fig 3.1, Materials and Method).

Due to the reported redundancy of *Ring1a* and *Ring1b* (del Mar Lorente, Marcos-Gutierrez et al. 2000; de Napoles, Mermoud et al. 2004; Roman-Trufero, Mendez-Gomez et al. 2009), we directly investigated the dKO mice. Moreover, during development and through adult

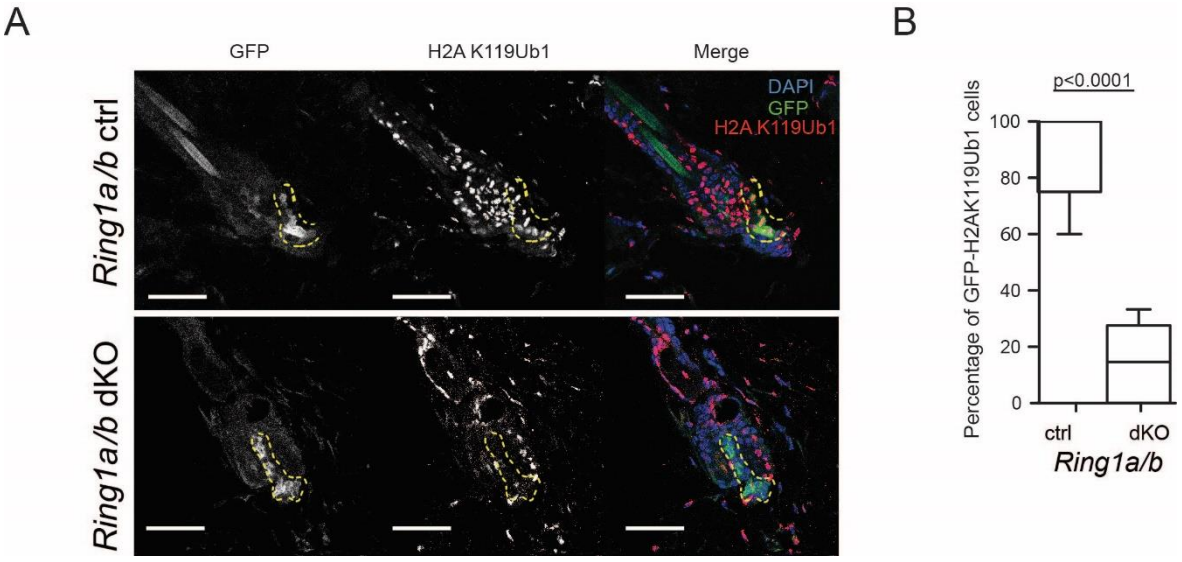

Figure 4.1 H2AK119 ubiquitin loss upon PRC1 activity abrogation

A) Immunofluorescence analyses of hair follicle in *Ring1a/b* ctrl and dKO condition, showing the loss of H2AK119Ub1 modification in PRC1 depleted mice. Green: GFP expressed by LGR5-HFSCs; Red: H2AK119Ub1; Blue: DAPI
B) Quantification of the percentage of GFP-H2AK119Ub1 double positive cells on total GFP cells in HFs of both ctrl and dKO mice.

P value was calculated with a two-side t test. Box plot graphs were generated with Prism software.

life, until tamoxifen injection, our mouse model, LGR5-GFP-ires-CreERT2/Ring1a$^{-/-}$/Ring1b$^{fl/fl}$/Rosa26Lox-stop-LoxLacZ do not show any severe impairment in hair follicle morphogenesis and regeneration, as demonstrated by their ability to maintain the fur, suggesting that the deletion of *Ring1a* catalytic subunit does not affect the hair cycle.

The LGR5 transgene is expressed in Hair Follicle (HF) in a long-lived stem cell subpopulation that is actively cycling during hair regeneration. In the non-proliferative stage of the hair cycle, LGR5 stem cells are located at the base of the HFs in the secondary hair germ and in the lower part of the bulge region. During regeneration, LGR5-HFSCs expand downward generating a single cell layer called Outer Root Sheat (ORS) and giving rise to Transient Amplifying matrix-cells (TAC) (Jaks, Barker et al. 2008) that will further differentiate in all hair structures. We use the described genetic model to acutely abrogate

PRC1 activity in 8-12 weeks old, sex-matched mice in LGR5-HFSC. We treated the mice with 4 daily IP injection of Tamoxifen, to induce Cre-recombinase nuclear localization and function, and we were able to obtain a great loss of PRC1 activity, as demonstrated by the loss of the H2AK119Ub1 histone mark in GFP+ cells of telogen HFs (Fig 4.1A, B), proving that our system works.

Mice fur is maintained during the entire lifespan by HF regeneration. This process is

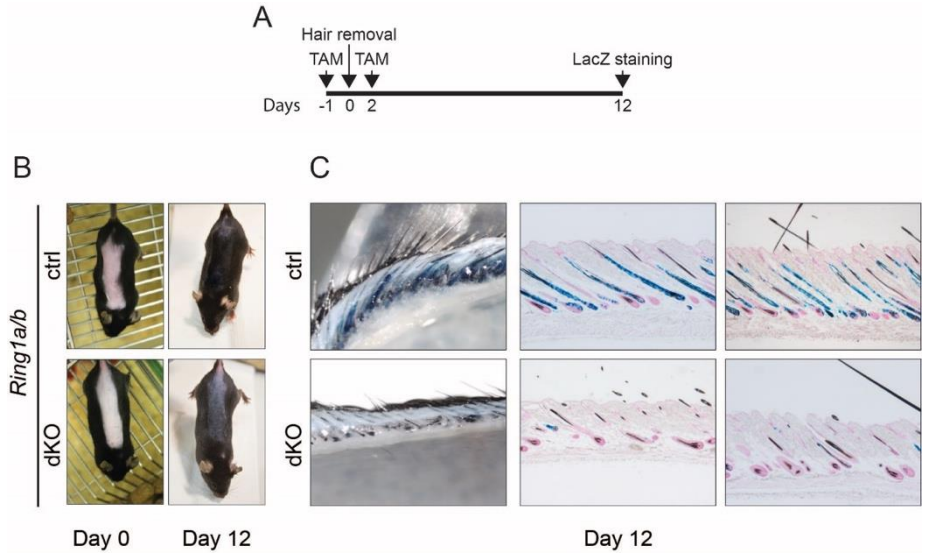

Figure 4.2 PRC1 depletion severely affect hair follicle regeneraion

A) Schematic representation of PRC1 depletion and anagen induction protocol. Mice back-skins were recovered at 12 days post wax. TAM: Tamoxifen
B) Image showing mice back-skin at day 0 (post wax) and at the end of the experimental work, showing hair follicle regeneration impairment in dKO compared to ctrl mice.
C) In vivo lineage tracing of LGR5-HFSCs progeny. Tissues were stained with X-Gal. Wholemount images were taken before paraffin embedding and the obtained section were counterstained with neutral red.

regulated in a synchronous way during the first 10 to 11 weeks of age, however, after a long telogen (resting) phase the hair follicle start to gradually lose their synchrony without affecting their regenerating capabilities (Paus, Muller-Rover et al. 1999, Muller-Rover, Handjiski et al. 2001, Jaks, Barker et al. 2008). In order to investigate the role of PRC1 in adult LGR5-HFSCs in the process of HF regeneration we forced re-synchronization by means of follicle plucking. HF removing starts a signaling cascade that rapidly and synchronously induces cells to start cycling and to proliferate, thus entering the anagen phase

(Muller-Rover, Handjiski et al. 2001). In order to abrogate PRC1 activity in the very first phases of HF regeneration, to explore its function in telogen to anagen transition, we administered Tamoxifen via IP injection in adult mice 1 day before waxing the back skin (Fig 4.2A) and we recovered it after 12 days from hair removal.

Ctrl mice completely regenerate the hairs (Fig 4.2B, top panels), while in the absence of PRC1 activity, dKO mice presented severe defects in hair follicle regeneration (Fig 4.2B, bottom panel) showing a delayed hair follicle cycle.

With the aim to better characterize this delayed hair growth phenotype we performed the same experiment following in this case the HFSCs progeny (lacZ positive staining) in presence or absence of PRC1 complexes. Our mouse model expresses the Rosa26-Lox-STOP-Lox LacZ construct in all cells of the body, however LacZ production is inhibited by a STOP codon upstream to the gene, so that its expression is restrained only in cells where Cre-recombinase efficiently floxed the LoxP sites of the transgene. In our model, only LGR5 expressing cells produce the enzyme, therefore leading to the expression of lacZ gene in stem cells and all their derived progeny. Indeed, chemical retrieval of beta-galactosidase allows the visualization of cell populations derived from floxed stem cells. Lineage tracing analyses further confirm our result and 12 days after waxing we obtained a marked reduction of the number of beta-galactosidase expressing HFs in *Ring1a/b* dKO animals, suggesting that the remaining hair growth is derived from wild-type HFs (Fig 4.2C).

4.2 PRC1 LOSS AFFECTS HAIR FOLLICLE CYCLE AND ANAGEN ONSET

With this first experiment, we showed that PRC1 loss is able to severely affect hair follicle regeneration process and anagen progression. To further characterize PRC1 activity in adult

HFs maintenance, we took advantage of different hair follicle cycles taking place during mouse life. Murine fur undergoes two synchronous proliferative boosts in the first 7 weeks of life, the morphogenesis and the first hair cycle. After these two proliferative events, HFs encounter a long resting phase, called the "long telogen" phase, that can last up to 4 weeks (Muller-Rover, Handjiski et al. 2001, Jaks, Barker et al. 2008). At the end of this long quiescent phase hair follicle start to regenerate in an asynchronous way. With the aim to elucidate whether PRC1 activity is necessary for entering into or to progress through the anagen phase we induced Cre-mediated recombination, with 4 consecutive tamoxifen IP injection, during long telogen phase at P49 (post-delivery day 49) in order to reach PRC1 depletion when all HFs are in their resting phase. After two weeks from tamoxifen delivery we induce anagen in order to synchronize HFs entering in proliferative phase of the cycle and we recovered the mice back-skin at either 8 days and 12 days post-waxing to perform histological analyses and lineage tracing staining to follow stem cell progeny fate (Fig 4.3).

8 days after waxing, we observed a substantial delay in hair growth of *Ring1a/b* dKO mice compared to ctrl (Fig 4.4A). It is reported that, during HFs regeneration, C57bl/6 mice back-

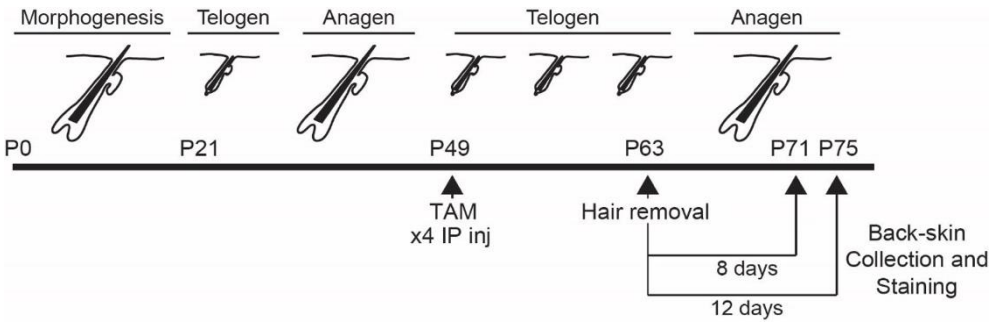

Figure 4.3 Hair follicle cycles in mouse

Schematic representation of the experiment. The temporal bar shows HFs morphogenesis, first telogen and first anagen, which are synchronized. At day P49 (post-delivery) all follicles are in long telogen phase and PRC1activity were abrogated with 4 intraperitoneal injection of Tamoxifen (TAM). After 2 weeks anagen were induced by waxing mice back-skin and samples were recovered at both 8- and 12-days post wax and processed for IHC and Lineage tracing analyses.

skin full of proliferative follicles becomes darker, due to the strict coupling of hair cycle progression and follicular melanogenesis (Slominski, Paus et al. 1991, Muller-Rover,

Handjiski et al. 2001) (Fig 4.4A). While ctrl mice back-skin presented a grey black color (Fig 4.4A left image), at this time point, *Ring1a/b* dKO still remains pink, suggesting that follicles are at earlier anagen phases compared to PRC1 proficient mice.

This delayed phenotype is further confirmed by histological analyses showing an altered morphology of hair follicle in *Ring1a/b* dKO mice (Fig 4.4B).

Detailed observation of histological section reveals that *Ring1a/b* dKO mice shows shorter HFs (Fig 4.4B, top panel and Fig 4.5A), with a morphology that, according to the Müller-Röver et al., classification (Muller-Rover, Handjiski et al. 2001) seems to be blocked in the early anagen phases (I and IIIA) compared to ctrl HFs. Moreover, at 8 days post waxing the total number of beta-galactosidase positive HFs are strongly reduced in *Ring1a/b* dKOs (Fig

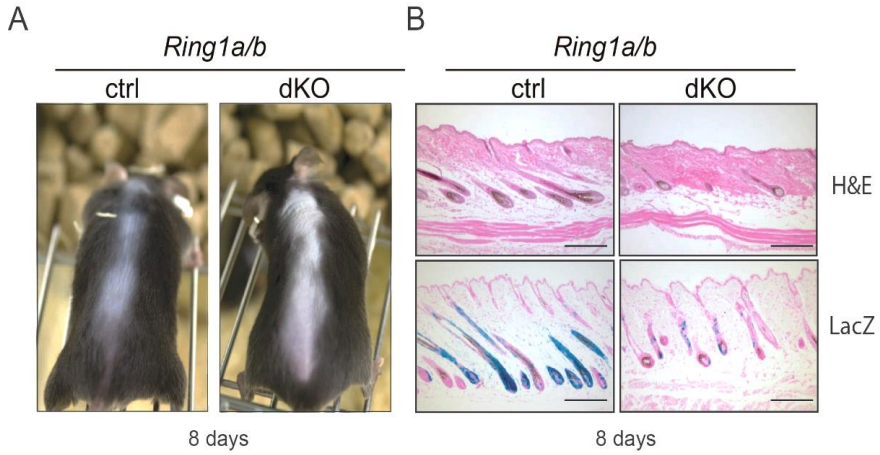

Figure 4.4 PRC1 is required for anagen onset and progression

A) Picture showing defective HF regrowth in *Ring1a/b* dKO mice compared to ctrl mice after 8 days from anagen induction.
B) Top panel: Hematoxylin/Eosin Y staining of paraffin embedded tissue from ctrl and dKO mice showing the drastic changes in HF morphology upon PRC1 depletion.
Bottom panel: back-skin from *Ring1a/b* ctrl and dKO mice were stained with X-gal prior paraffin embedding. Slices were counterstained with neutral red. Pictures shows the loss of LacZ staining in dKO mice compared to ctrl mice.

Mice were treated as described in Figure 4.3 and back-skin was recovered at 8d post wax. Scale bars 250 μm.

4.4B, bottom panel and Fig 4.5B). Since LacZ is expressed in stem cell progeny, this staining defect suggested an impairment of LGR5-HFSCs proliferation.

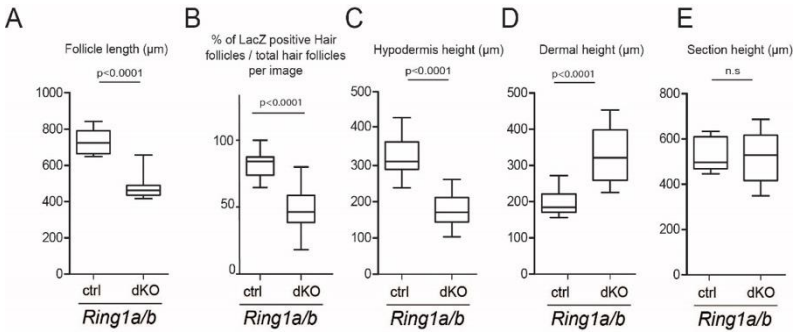

Figure 4.5 Measurement of HFs length and tissue morphology 8 days post wax

A) Quantification of hair follicle length after 8 days from anagen induction. Measurements were taken with ImageJ software from the bulb base to the surface-exposure of follicular channel.
B) Quantification of beta-gal positive follicles in *Ring1a/b* ctrl and dKO mice after 8 days from anagen induction.
C) Quantification of hypodermal fat. Measurements were taken with ImageJ software from the lowest part of the dermis to the panniculus carnosus.
D) Quantification of dermal height in *Ring1a/b* ctrl and dKO mice. Measurement were calculated with ImageJ software from the upper part of the subcutis to the lowest part of epidermis.
E) Total sections heights were measured from the lowest part of the subcutis to the upper part of the dermal compartment.

All p-values were calculated with two side t test. N.s., not significant. Box plot graphs were generated with Prism software.

Several different layers constitute the skin. Under the epidermal tissue, the presence of hypodermal fat guarantees thermal isolation, functions as an energy reservoir and plays a role in mechanical protection and skin wound healing (Rosen and Spiegelman 2014). In the process of HFs regeneration it is well established that the hypodermal adipocyte layer fluctuates in thickness according to the different stages of hair cycle (Muller-Rover, Handjiski et al. 2001, Festa, Fretz et al. 2011, Foster, Nicu et al. 2018), and in particular this specialized tissue increases during anagen phase and reduces throughout catagen to reach a resting phase until a new hair cycle begins. Looking at histological sections, it is evident that *Ring1a/b* dKOs display a clear imbalance between hypodermis fat (Fig 4.5C) and dermis thickness (Fig 4.5D) despite the skin having a similar width among ctrl and dKOs conditions (Fig 4.5E), reinforcing the evidence that PRC1 loss severely affects HF regeneration.

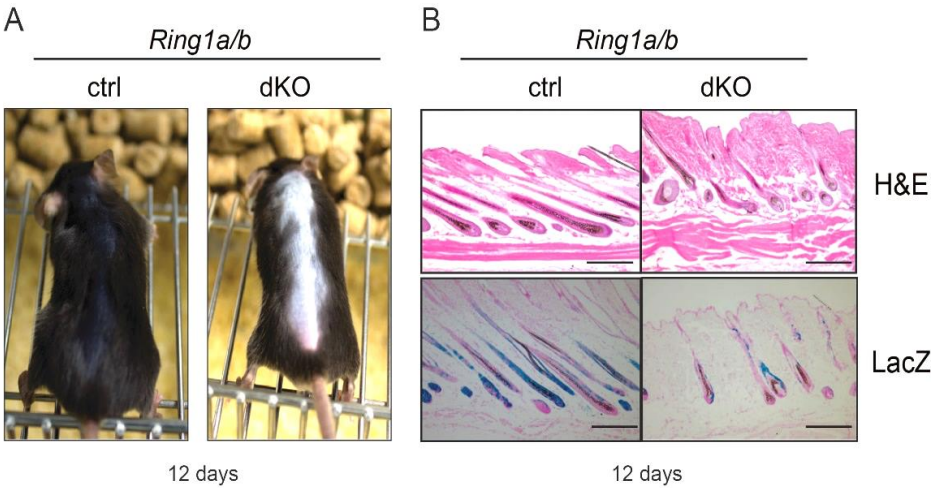

Figure 4.6 PRC1 is required for anagen onset and progression

A) Picture showing defective HF regrowth in *Ring1a/b* dKO mice compared to ctrl mice after 12 days from anagen induction.
B) Top panel: Hematoxylin/Eosin Y staining of paraffin embedded tissue from ctrl and dKO mice showing the drastic changes in HF morphology upon PRC1 depletion.
Bottom panel: back-skin from *Ring1a/b* ctrl and dKO mice were stained with X-gal prior paraffin embedding. Slices were counterstained with neutral red. Pictures shows the loss of LacZ staining in dKO mice compared to ctrl mice.

Mice were treated as described in Figure 4.3 and back-skin were recovered at 12d post wax. Scale bars 250 μm.

This phenotype was confirmed and more evident 12 days after waxing when *Ring1a/b* ctrl mice fully regenerate the fur, while dKO mice failed to correctly progress through HF proliferative phase, resulting in a severe hair regeneration delay (Fig 4.6A). Hematoxylin/eosin staining highlights drastic morphological HFs defects that ultimately results in defective regeneration (Fig 4.6B top). According to Müller-Röver et al. classification (Muller-Rover, Handjiski et al. 2001), *Ring1a/b* ctrl mice showed all features of full anagen follicles (anagen phase VI) (Fig 4.6B), while *Ring1a/b* dKO still resembled primary stages of anagen follicles and they seems to be slowly proceeding to anagen phases II and III (Fig 4.6B).

Lineage tracing experiments on mouse back-skin 12 days after anagen induction revealed a marked reduction in *Ring1a/b* dKO of LGR5-HFSCs derived progeny, as demonstrated by the severe loss of beta-galactosidase staining compared to *Ring1a/b* ctrl mice (Fig 4.6B, bottom panel and Fig 4.7A). Consistently with 8 days post waxing, hair follicles showed

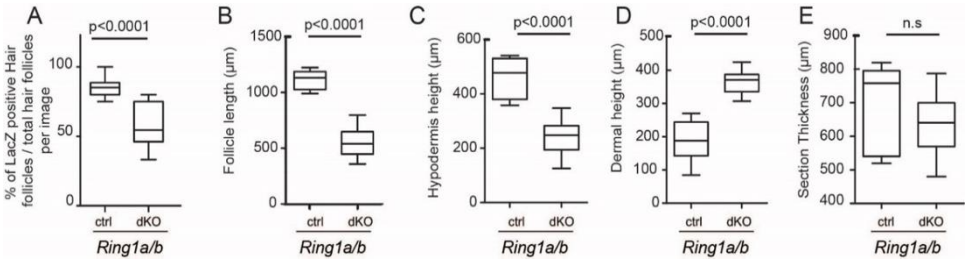

Figure 4.7 Measurement of HFs length and tissue morphology 12 days post wax

A) Quantification of beta-gal positive follicles in *Ring1a/b* ctrl and dKO mice after 12 days from anagen induction.
B) Quantification of hair follicle length after 12 days from anagen induction. Measurements were taken with ImageJ software from the bulb base to the surface-exposure of follicular channel.
C) Quantification of hypodermal fat. Measurements were taken with ImageJ software from the lowest part of the dermis to the panniculus carnosus.
D) Quantification of dermal height in *Ring1a/b* ctrl and dKO mice. Measurement were calculated with ImageJ software from the upper part of the subcutis to the lowest part of epidermis.
E) Total section heights were measured from the lowest part of the subcutis to the upper part of the dermal compartment.

All p-values were calculated with two side t test. N.s., not significant. Box plot graphs were generated with Prism software.

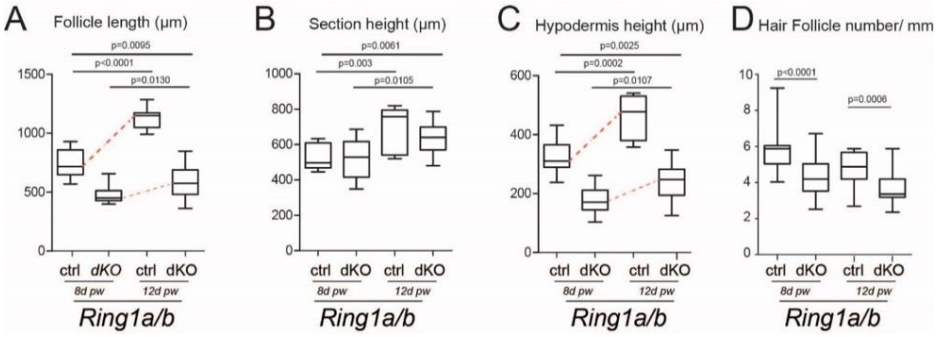

Figure 4.8 PRC1 dKO impairs HFs progression during anagen

A) Quantification of hair follicle length after 8 and 12 days from anagen induction. Measurements were taken with ImageJ software from the bulb base to the surface-exposure of follicular channel. Red line indicates the increase in hair follicle length in *Ring1a/b* ctrl and dKO mice.
B) Quantification of total section height in Ring1a/b ctrl and dKO condition showing no differences in skin thickness.
C) Quantification of hypodermal fat. Measurements were taken with ImageJ software from the lowest part of the dermis to the panniculus carnosus. Red line indicates the increase in hair follicle length in *Ring1a/b* ctrl and dKO mice.
D) Quantification of HF number per mm in *Ring1a/b* ctrl and dKO mice showing that PRC1 depleted mice display a reduced number of follicles.

All p-values were calculated with two side t test. N.s., not significant. Box plot graph were extrapolated with Prism software.

reduced follicle length (Fig 4.7B) as well as for the imbalance among hypodermis and dermis

(Fig 4.7C-D).

Comparing 8 and 12 days, it is clear that the differences of follicle length (Fig 4.8A) and dermis-hypodermis thickness unbalance are further increased (Fig 4.8B-C) during time, with a similar reduction in the number of HFs (Fig 4.8D). Taken together these data suggest that, rather than impair anagen entry, PRC1 activity loss severely affects the regenerative potential of LGR5-HFSCs and anagen progression.

4.3 CONSERVED PRC1-REPRESSED TRANSCRIPTIONAL PROGRAMS ARE REQUIRED TO MAINTAIN HFSCs AND ISCs.

These newly obtained data suggests that PRC1 loss in HFSCs induces similar phenotypic outcomes that was previously generated and observed by our lab in Intestinal Stem Cells (ISCs) (Chiacchiera, Rossi et al. 2016). With the aims to better define whether PRC1 loss of activity leads to an analogous phenotype through similar or different processes, we decided to deeper investigate the molecular effects of *Ring1a/b* dKO in two stem cells population that shares different common features despite arising from different embryonic layers (de Santa Barbara, van den Brink et al. 2003, Liu, Zhang et al. 2013). Even though ISC continuously regenerate the tissue while LGR5-HFSCs encounter cycles of proliferation and resting, both stem cell population are characterized by LGR5 receptor and rapidly divides to regenerate the tissue during their own proliferative phase, providing a perfect tool to study PRC1 mechanism in different context.

To investigate the transcriptional changes induced by PRC1 loss of function in anagen-activated LGR5 expressing stem cells, we collected both *Ring1a/b* ctrl and dKO mice back-skins 8 days after hair plucking (Fig 4.9A). HFs were isolated from the tissue, reduced to single cells and 3000 LGR5-HFSCs per sample were isolated by Fluorescence Activated Cell Sorting (FACS), thanks to LGR5-GFP expression. The remaining sample was stained

for H2AK119Ub1 PRC1 mark and analyzed by FACS, demonstrating that tamoxifen treatment results in >70% loss of PRC1 activity in LGR5 expressing cells (Fig 4.9B).

Sorted cells were processed with SMART-seq2 (Switching Mechanism at the 5' end of the RNA Transcript) protocol to perform RNA sequencing. This protocol published by Picelli et al in 2014 (Picelli, Faridani et al. 2014) allows us to perform RNA-sequencing starting from low material amount, performing the Retro-transcription step directly in lysed cells, minimizing the steps critical for material waste. The library was obtained with transposase 5 that simultaneously cuts the amplified cDNA and adds two DNA primers for sequencing

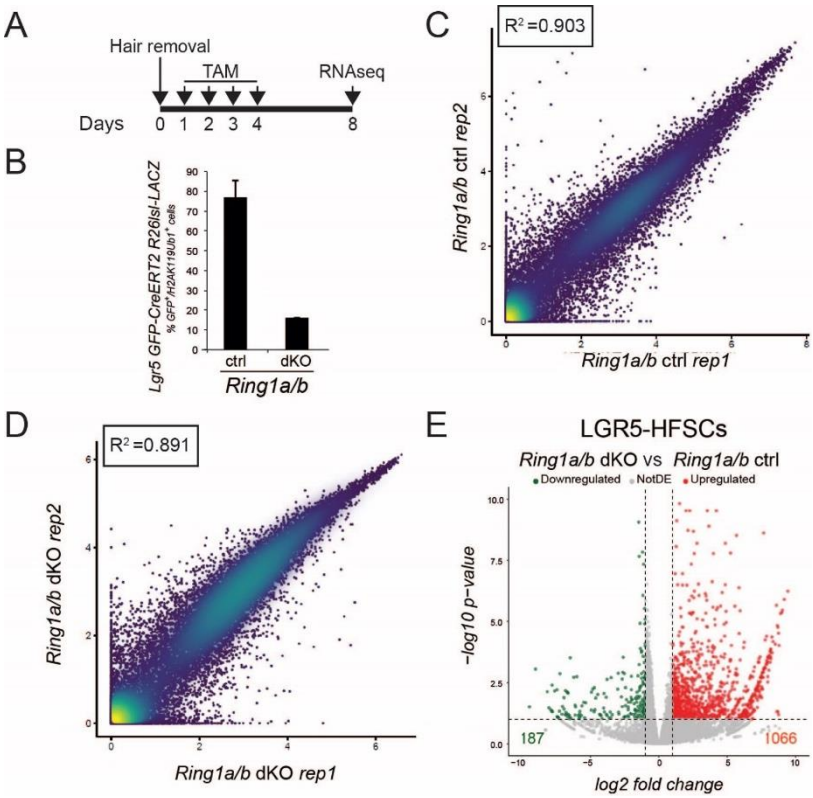

Figure 4.9 PRC1 loss induce a massive gene upregulation

A) Schematic view of the experimental procedure to induce anagen and perform PRC1 ablation in HFSCs. Mice back skins were recovered after 8 days from anagen induction.
B) Quantification of GFP-H2AK119Ub1 positive cells in *Ring1a/b* ctrl and dKO HFs. Single cell suspension was stained with H2AK119Ub1 antibody and analyzed by FACS.
C) Correlation plot of RPKM values of detected genes from two independent biological replicates of *Ring1a/b* ctrl samples.
D) Correlation plot of RPKM values of detected genes from two independent biological replicates of *Ring1a/b* dKO samples.
E) Volcano plot showing deregulated genes in *Ring1a/b* dKO vs ctrl cells. (tresholds: p-value < 0.05, absolute log2(fold change)>1).

index addition. In order to minimize the biological variance among different mice, we purified and processed 2 independent biological replicates for *Ring1a/b* ctrl and dKO mice and both the replicates correlated well (Fig 4.9C and D).

Consistently with the general role of PRC1 complex as transcriptional repressor, RNA-seq analyses revealed a >5-fold bias in genes up-regulation (1066 up-regulated genes versus only 187 down-regulated genes) also in HFSCs compartment (Fig 4.9E). To elucidate which category of transcript was mostly affected by PRC1 loss, we first analyzed the Differentially Expressed Genes (DEG) with David Tool (Huang da, Sherman et al. 2009) to obtain the list of deregulated processes and pathways in our samples.

Gene ontology analyses (GO) on upregulated genes revealed that they are associated with general developmental processes (Fig 4.10A) such as multicellular organism development and embryonic limb morphogenesis that are linked to PRC1 classical function during

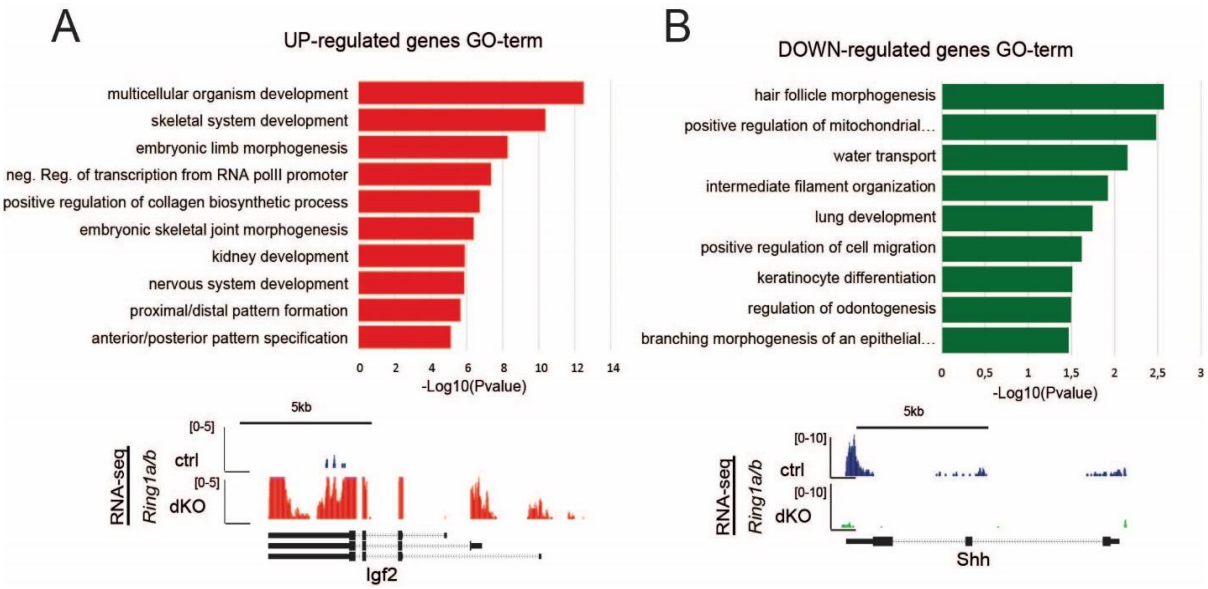

Figure 4.10 PRC1 loss induces upregulation of developmental genes and downregulation of lineage-related ones

A) GO-term analyses of upregulated genes in *Ring1a/b* dKO HFSCs compared to ctrl. Top: Bar plot shows the genes-related pathways affected upon PRC1 depletion. Bottom: representative genomic view of RNA-seq tracks for one upregulated gene.
B) GO-term analyses of downregulated genes in *Ring1a/b* dKO HFSCs compared to ctrl. Top: Bar plot shows the genes-related pathways affected upon PRC1 depletion. Bottom: representative genomic view of RNA-seq tracks for one upregulated gene.

development, such as IGF2 (Fig 4.10A bottom panel) and some HOX clusters genes. In contrast, down-regulated genes were specifically enriched for hair follicle morphogenesis and hair follicles related processes (Fig 4.10B). Among these down-regulated mRNAs we found the Sonic Hedgehog gene (SHH) (Fig 4.10B bottom panel) that is a well know regulator of HF anagen promotion and progression (St-Jacques, Dassule et al. 1998, Hsu, Li et al. 2014). SHH is upregulated in LGR5 and LGR5-derived matrix cells and is necessary to progress through anagen (Greco, Chen et al. 2009, Zhang, Tomann et al. 2009, Rompolas,

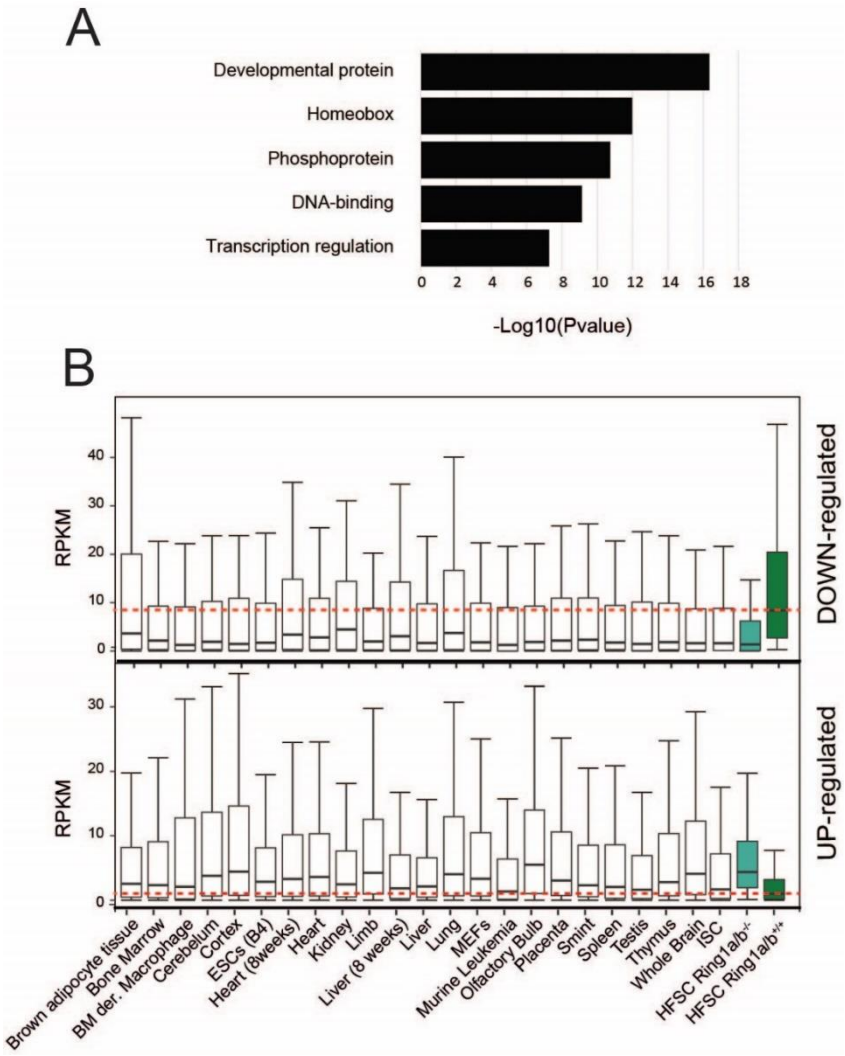

Figure 4.11 PRC1 loss induces deregulation of non-lineage specific homeobox TFs

A) GO-term analyses of upregulated genes in *Ring1a/b* dKO compared to ctrl. Bar plot shows the class of genes affected upon PRC1 depletion.

B) Box plot showing the expression of downregulated (top panel) and upregulated genes (bottom panel), in *Ring1a/b* dKO compared to ctrl, among different tissues, organs and cell lines, showing that downregulated genes are specific for HFSCs while upregulated genes are already expressed in several different cell types.

Mesa et al. 2013) Its downregulation is in line with our block in the early phases of anagen, where matrix cells are emerging from LGR5-HFSCs, providing a possible explanation for the proliferative arrest of *Ring1a/b* dKOs HFs.

Functional annotation analyses further revealed that DNA binding TFs, in particular homeotic and development-related transcription factors, were enriched in *Ring1a/b* dKO up-regulated genes (Fig 4.11A) suggesting a massive deregulation of different TFs involved in developmental processes. To investigate whether these deregulated transcripts belong to specific tissues or were expressed in various compartments we decided to compare transcriptional data obtained from several different tissues (ENCODE) with up- or down-regulated genes in our LGR5-HFSCs. *Ring1a/b* dKO down-regulated genes (Fig 4.11B, top panel) are primarily expressed (Dark green box) in HFSCs compared to other tissues (White boxes), further confirming that down-regulated genes were essential to maintain HFSC identity.

In contrast, upregulated genes, that were lowly expressed in HFCS ctrl cells (Dark green box), were already expressed in many tissue types, highlighting that loss of PRC1 activity results in massive upregulation of non-lineage-specific genes.

In agreement with our previous finding obtained in ISCs (Chiacchiera, Rossi et al. 2016), these data strongly support a central role of PRC1 in maintaining lineage identity in stem cells of adult tissues.

However, whether this involves common or specific mechanism still remains an open question.

To elucidate this mechanism, we searched for common classes of genes that could be potentially involved in the regulation and the maintenance of lineage identity in ISCs and HFSCs upon PRC1 inactivation.

We compared RNA-seq profiles in adult LGR5 stem cells from intestine and anagen HFs and we found that none of the downregulated genes were in common between the two populations, in accordance with the role of these genes in maintaining the distinct identity

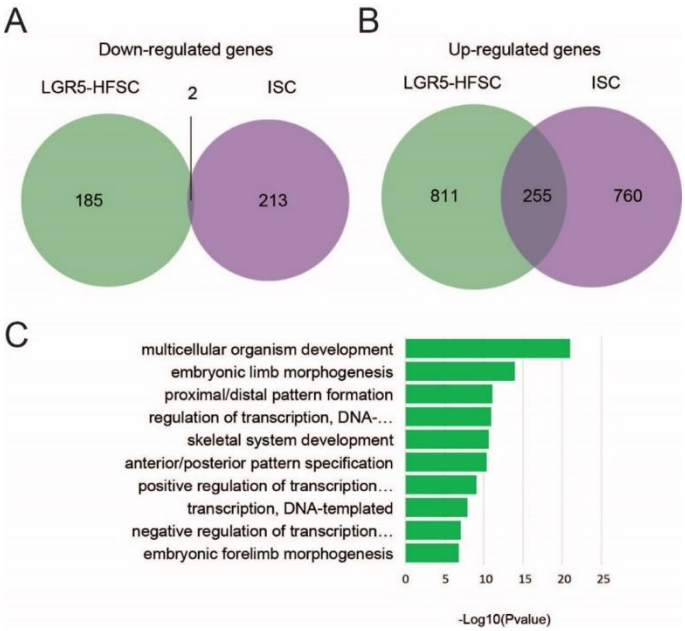

Figure 4.12 Common upregulated genes are development related genes

A) Venn-diagram showing the overlap of downregulated genes, upon PRC1 loss of activity, among LGR5-HFSCs and ISCs.
B) Venn-diagram showing the overlap of upregulated genes, upon PRC1 loss of activity, among LGR5-HFSCs and ISCs.
C) GO-term analyses of common upregulated genes (255genes) between LGR5-HFSCs and ISCs showing their role in development and differentiation.

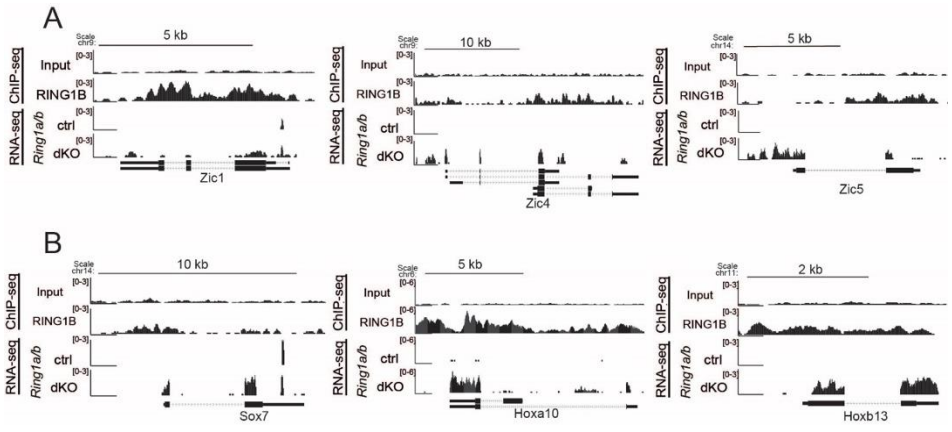

Figure 4.13 PRC1 dKO upregulates development-related TFs

A) Genomic snapshots of ZIC1, ZIC4 and ZIC5 showing RING1B binding and the gene transcription upon PRC1 depletion.
B) Genomic snapshots of SOX7, HOXA10 and HOXB13 showing RING1B binding and the gene transcription upon PRC1 depletion.

of the two different stem cell populations (Fig 4.12A). On the contrary, we found that among the up-regulated genes (Fig 4.12B), approximately one-fourth (255 genes) are common between ISCs and HFSCs. We performed a GO-term analyses of this common set of genes and they result to be for the vast majority homeobox containing TFs related to the regulation of developmental processes (Fig 4.12C). Among these genes we found several ZIC (zinc finger protein of cerebellum) TFs, such as *Zic1*, *Zic4* and *Zic5* (Fig 4.13A), as well as *Sox7*, *Hoxa10* and *Hoxb13* (Fig 4.13B), that are known regulators of development in several different tissues (Grinberg and Millen 2005, Mallo and Alonso 2013). These data suggest that PRC1 is able to repress and to prevent the activation of common non-lineage specific homeobox-containing TFs in different stem cells populations.

4.4 PRC1 GUARANTEES STEM CELL IDENTITY MAINTENANCE BY REPRESSING A SUBSET OF CANONICAL PRC1 TARGETS.

Two major classes of PRC1 have been recently described (Gao, Zhang et al. 2012), based on their biochemical composition. PRC1 complexes core contains RING1A or RING1B and one out of six mammalian Polycomb Group Ring Finger Protein (PCGF) (Gao, Zhang et al.

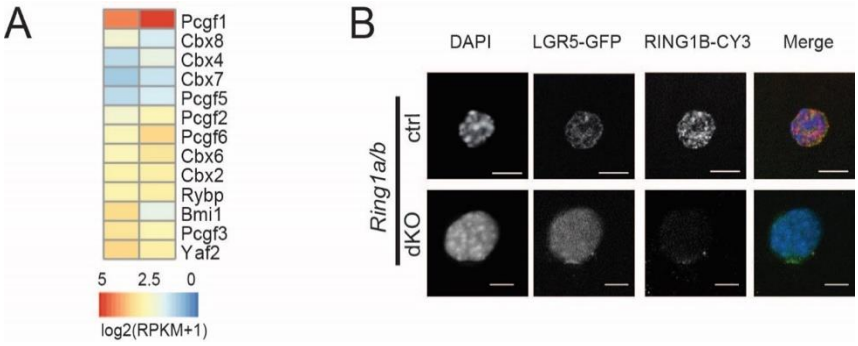

Figure 4.14 different PRC1 subunits are expressed in LGR5-HFSCs

A) Heatmap showing expression levels of PRC1 canonical and non-canonical subunits of two independent biological replicates of HFSCs from *Ring1a/b* ctrl mice.
B) Immunofluorescence analysis of RING1B in a pure population of sorted *Ring1a/b* ctrl and dKO HFSCs.

Scale bars 5um.

2012). Canonical PRC1 complexes contains CBX proteins, which are responsible for PRC1 tethering on the chromatin, recognizing the H3K27me3 histone mark, deposited by PRC2, thus resulting in a PRC1 recruitment on its targets that is PRC2-dependent. Of note only PCGF2/Mel18 and PCGF4/Bmi1 are found to take part in PRC1 canonical complexes. On the other hand, all PCGFs can be part of non-canonical PRC1 complexes, that do not contain the CBX subunit and are recruited to chromatin independently from PRC2. These complexes are characterized by the presence of either RING1 and YY1 Binding Protein (RYBP) or YY1 Associated Factor 2 (YAF2). Different components both of canonical and non-canonical PRC1 complexes are expressed in HFSCs (Fig 4.14A), suggesting the presence of all the existing subcomplexes.

To investigate the ability of RING1B to form both canonical and non-canonical subcomplexes in LGR5-HFSCs, we decided to perform the Proximity Ligation Assay (PLA) in sorted anagen induced-HFSCs, from *Ring1a/b* ctrl and dKO mice (Fig 4.14B). PLA is a powerful technique that enable the visualization of proteins interactions directly *in situ*, exploiting the use of secondary antibodies conjugated with DNA probes that can be amplified, with Fluorescent labelled nucleotides, only if they are in proximity (less than 40nm) to each other. We used this technique to evaluate the ability of RING1B to interact with RYBP (non-canonical PRC1, Fig 4.15 A, B) and Bmi1 (canonical PRC1, Fig 4.15 C, D) in our stem cells

PLA-foci formation indicates that, in LGR5 expressing HFSCs, both canonical and non-canonical complexes are formed and the deletion of both PRC1 catalytic subunits results in the disruption of PLA foci. Indeed, the phenotype observed upon Ring1a/b depletion could be ascribed to an impaired activity of both canonical and non-canonical complexes.

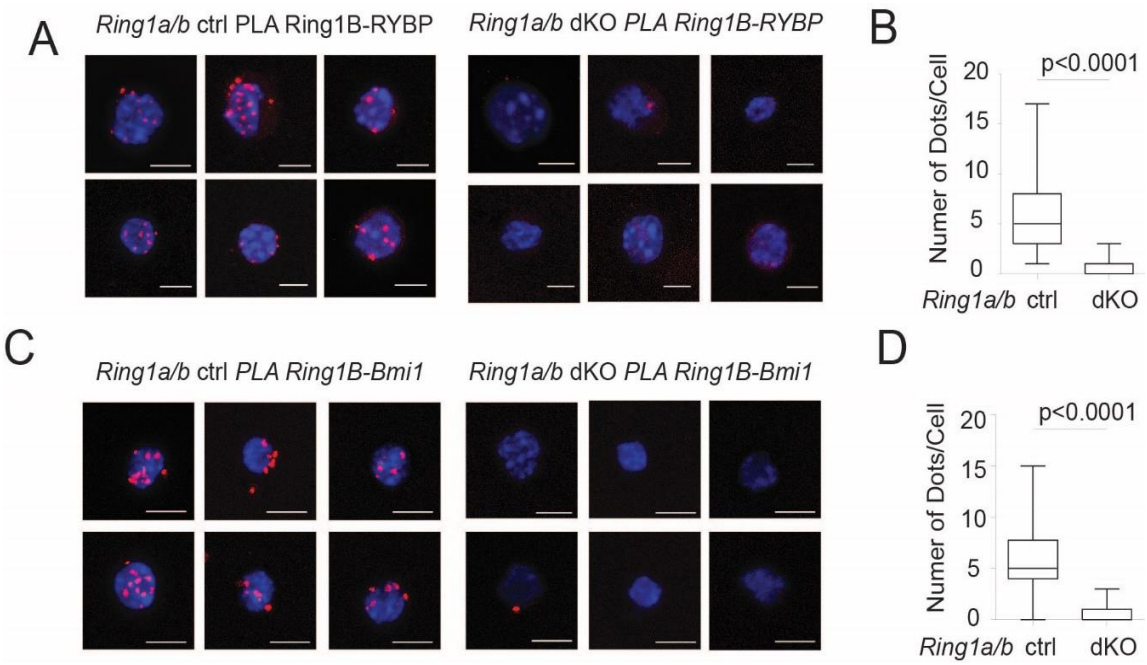

Figure 4.15 Both canonical and non-canonical PRC1 are present in LGR5-HFSCs

A) PLA between RING1B and RYBP on *Ring1a/b* ctrl and dKO sorted LGR5-HFSCs
B) Quantification of RING1B-RYBP dots per cell in *Ring1a/b* ctrl and dKO HFSCs
C) PLA between RING1B and RYBP on *Ring1a/b* ctrl and dKO sorted LGR5-HFSCs
D) Quantification of RING1B-RYBP dots per cell in *Ring1a/b* ctrl and dKO HFSCs

Scale bars 5 μm. All p-values were calculated with two side t test. N.s., not significant. Box plot graphs were generated with Prism software.

To identify the common mechanisms through which PRC1 regulates cell fate determination in different stem cell population we performed chromatin immunoprecipitation followed by sequencing analysis (ChIP-seq) for RING1B in HFSCs.

We collected FACS-sorted activated LGR5-HFSCs after 8 days from anagen induction from *Ring1a/b* crtl mice (Fig 4.16A, B). A total amount of 2.5M cells were fixed in 1% Formaldehyde, resuspended in the IP buffer (refer to material and methods), sonicated to fragment the genomic DNA and used for a single immunoprecipitation.

RING1B ChIP-seq analyses identified nearly 3900 RING1B peaks that were mainly associated to promoter regions (Fig 4.16C), resembling the chromatin association distribution of RING1B in ISCs (Fig 4.16D) and in accordance with other cellular system (Scelfo, Fernandez-Perez et al. 2019).

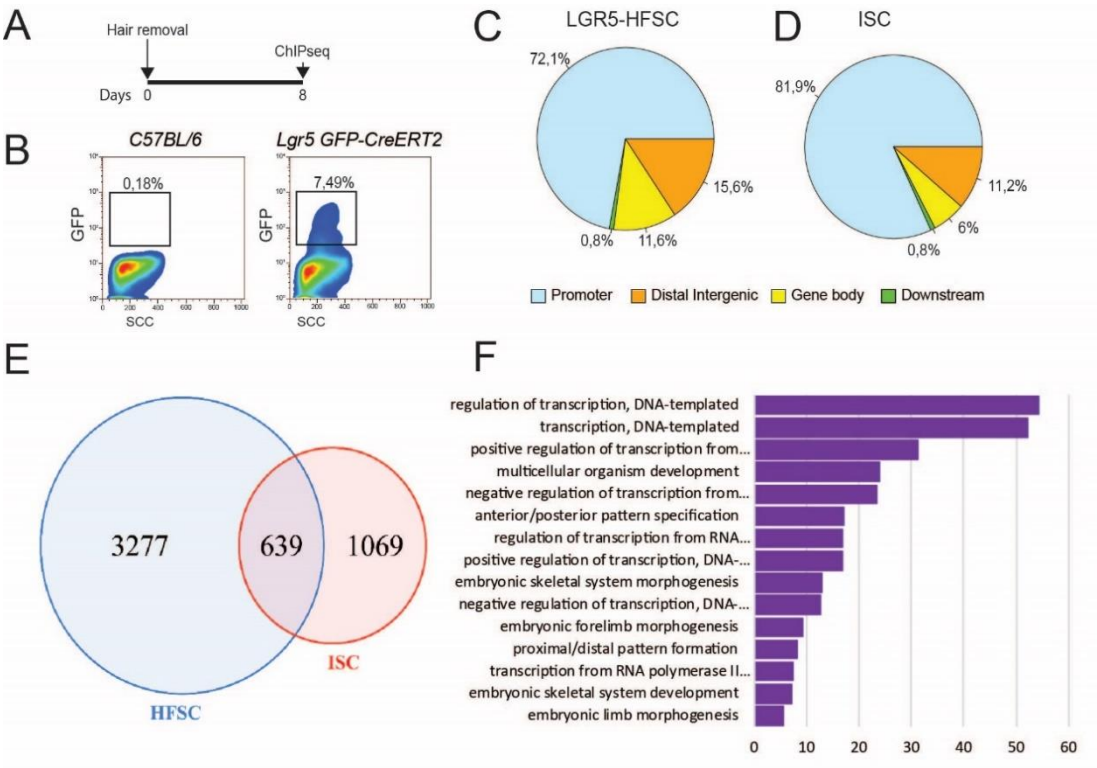

Figure 4.16 PRC1 preferentially binds promoters in different stem cell population

A) Schematic view of the experimental workflow for LGR5-HFSCs collection.
B) FACS analyses of GFP expression in anagen hair follicle of C57BL/6 and Lgr5-GFP CreERT2 mice.
C) Pie chart showing the percentage of RING1B peaks on Promoters, Distal intergenic regions, Gene body and Downstream gene regions in anagen LGR5-HFSCs. (Total peaks = 3917)
D) Pie chart showing the percentage of RING1B peaks on Promoters, Distal intergenic regions, Gene body and Downstream gene regions in ISCs. (Total peaks = 1293)
E) Venn diagram showing overlapping HFSCs ChIP-seq Peaks respect to ISCs.
F) GO analyses on genes related to the common ChIP peaks in HFSCs and ISCs.

Between the two stem cells population RING1B is able to bind different sets of genes (Fig 4.16E), as demonstrated by the overlapping peaks-related genes, however the common ones are related to development and differentiation (Fig 4.16F), highlighting that the classical role of PRC1 is maintained in different adult stem cells.

Since PRC1 can form both canonical and non-canonical complexes, that are functionally distinct and can localize differently along the genome (Gao, Zhang et al. 2012) we decided to map the genomic localization of RING1B, in both stem cells population, comparing them with H3K27me3 deposition in order to define the PRC1 repressed domains (Lien, Guo et al. 2011, Chiacchiera, Rossi et al. 2016). We took advantage of published data of H3K27me3

ChIP-seq performed in anagen HFSCs (Lien, Guo et al. 2011) and our previous obtained data in ISC (Chiacchiera, Rossi et al. 2016). We found that the extent of overlap with canonical Polycomb-repressed domains was restricted to only 20% of RING1B peaks in HFSCs (Fig 4.17A left) and 10% in ISCs (Fig 4.17A right), thus suggesting that a large fraction of RING1B activity does not require prior PRC2 mark deposition.

H3K27me3 repressive mark can be present within the same histone decorated with H3K4me3 transcriptional activatory modification. In ESCs, these two histone modifications together are enriched at promoters of development-related genes, defining the "bivalent" or "poised" status (Bernstein, Mikkelsen et al. 2006). These concomitant modifications are resolved when ESCs are triggered to differentiate by the acquisition of totally active (H3K4me3 only) or repressed (H3K27me3 only) state. Stem cells give rise to all cell populations in the tissue and should be able to efficiently switch on and off gene transcription in response to different stimuli. For this reason, we investigated the status of H3K4me3 of PRC1 repressed domain, and we found that, while only 30% of H3K27me3 sites in LGR5-HFSCs are poised (Fig 4.17B left), this proportion reaches the 80% of RING1B-H3K27me3 sites in ISCs (Fig 4.17B right). We also observed a large fraction of RING1B-bound sites

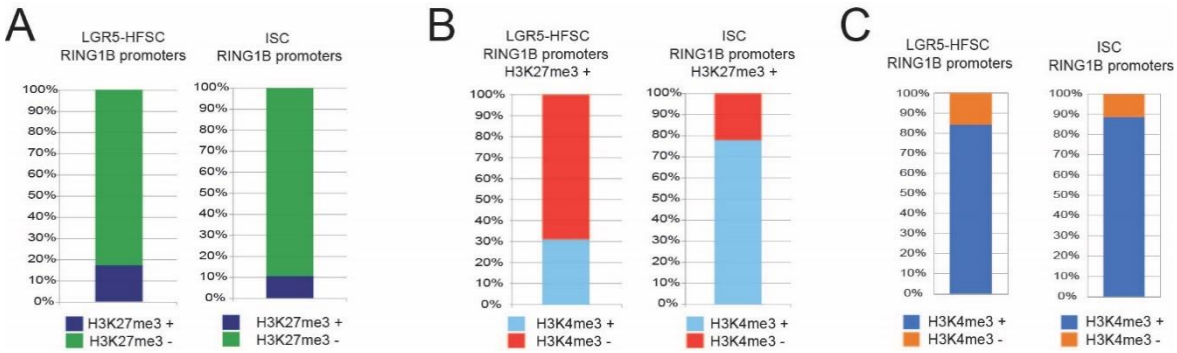

Figure 4.17 PRC1 preferentially binds active genes promoters in different stem cell population

A) Quantification of LGR5-HFSCs and ISCs RING1B promoter peaks that contains the H3K27me3 histone modification.
B) Quantification of LGR5-HFSCs and ISCs RING1B-H3K27me3 promoters peaks that are decorated by H3K4me3 modification.
C) Quantification of LGR5-HFSCs and ISCs RING1B promoter peaks that contains only H3K4me3 histone modification.

which are devoid of H3K27me3 but decorated with H3K4me3, suggesting in this context, an involvement of PRC1 in active transcription (Scelfo, Fernandez-Perez et al. 2019).

Among all PRC1 subcomplexes, non-canonical subcomplexes are described to binds actively transcribed genes while canonical PRC1 is more linked to repression (Scelfo, Piunti et al. 2015, Zhao, Huang et al. 2017, Scelfo, Fernandez-Perez et al. 2019). As we know that PRC1 in LGR5-HFSCs is able to form both canonical and non-canonical complexes, to discern which PRC1 subtype binds promoters with the two different histone marks, we performed ChIP against the discriminating subunits CBX8 and RYBP respectively.

We observed that in HFSCs, nearly 70% of RYBP peaks colocalize with RING1B (Fig 4.18A). However only a small fraction of co-occupied peaks (11%) also harbor H2AK119Ub1 (Fig 4.18B). We also observed that those regions that are occupied by both RING1B and H2AK119Ub1, are also characterized by the presence of H3K27me3 PRC2-deposited histone mark (Fig 4.18C) and by the presence of CBX8 subunits, specifying these sites as targets of canonical PRC1 complexes.

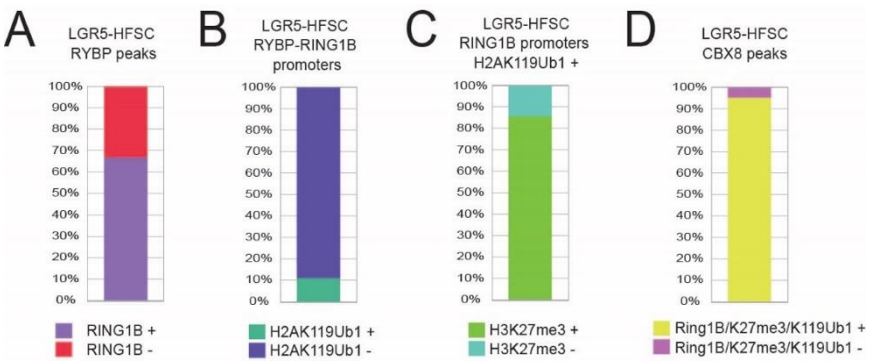

Figure 4.18 H2AK119Ub1 is preferentially deposited at canonical PRC1 sites

A) Quantification of LGR5-HFSCs RYBP peaks overlap with RING1B. (Total RYBP peaks = 811)
B) Quantification of LGR5-HFSCs RYBP-RING1B promoters peaks that are decorated with H2AK119Ub1
C) Quantification of LGR5-HFSCs RING1B- H2AK119Ub1 promoters peaks that harbor the H3K27me3 PRC2 mark.
D) Quantification of LGR5-HFSCs CBX8 peaks that contains RING1B and the 2 modification H3K27me3 and H2AK119Ub1.

These data suggest that both canonical and non-canonical PRC1 activities could possibly contribute to maintenance of stem cell identity by acting on both repressed and active genes.

To discern the complexes involvement in this crucial regulation, we decided to analyze ChIP-seq data relating gene expression differences in *Ring1a/b* ctrl and dKO mice.

We ranked all RING1B target promoters based on their expression in wild type stem cells from both HF and intestine. This analysis identified 4 clusters of genes each containing a quartile of gene expression. This divides all promoters in four groups: repressed, medium low, medium high and high expressed genes; that we used to determine transcriptional changes upon PRC1 loss of function in both HFSCs and ISCs (Fig 4.19A and Fig 4.20A). Repressed genes in *Ring1a/b* ctrl samples defined cluster 1 genes and were transcriptionally activated upon *Ring1a/b* dKO in both HFSCs and ISCs (Fig 4.19A and Fig 4.20A). Clusters 2 and 3 comprised genes with intermediate expression, that in turn does not shows significant changes or slightly decreased their expression in PRC1 depleted stem cells counterpart (Fig 4.19A and Fig 4.20A). The last group (Cluster 4) is composed of highly expressed genes that were slightly downregulated upon PRC1 depletion (Fig 4.19A and Fig 4.20A). Heatmaps of normalized ChIP signal around TSS (Fig 4.19B and Fig 4.20B), divided according to the previous identified expression clusters, shows that Cluster 1 transcripts belongs to gene that are fully silenced through canonical PRC1 complexes, as demonstrated by the concomitant presence of H2AK119Ub1, H3K27me3 and the relatively low presence of H3K4me3 active marks (Fig 4.19A and Fig 4.20A). Furthermore, the CBX8 canonical PRC1 subunit is localized only in this first gene cluster, thus providing additional evidence of canonical PRC1-mediated repression (Fig 4.19B).

H3K4me3 signal is enriched in all the other 3 clusters and colocalized with a sharper RING1B signal, proving that PRC1 is able to localize at active transcription sites on chromatin (Fig 4.19B and Fig 4.20B). This cluster also showed an intense signal of RYBP subunit, thus specifying for PRC1 non-canonical subcomplexes localization.

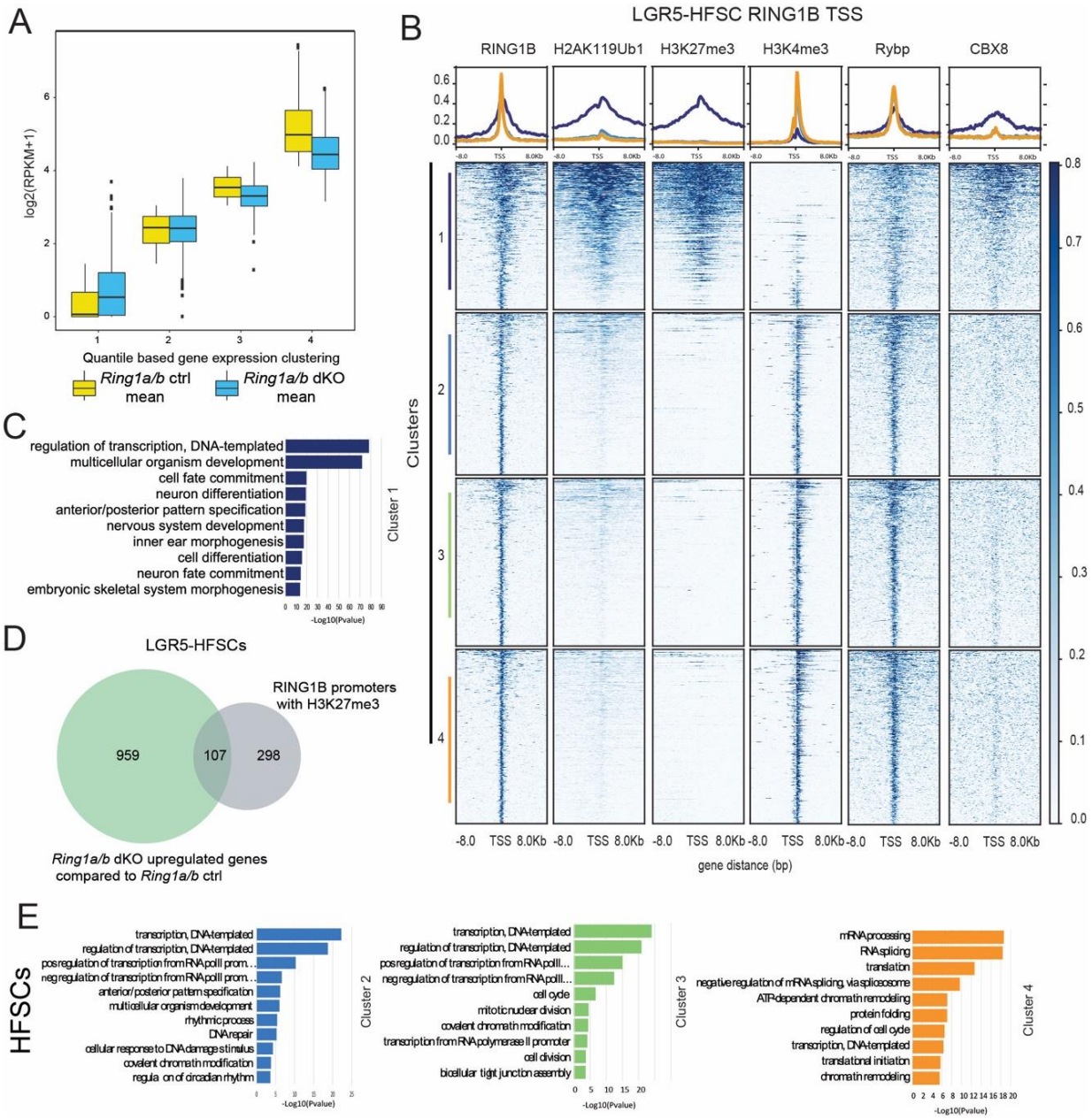

Figure 4.19 Genomic distribution of PRC1 binding in HFSCs

A) Quartile-based gene expression clustering performed using *Ring1a/b* ctrl RNA-seq data, showing expression variations between *Ring1a/b* dKO and ctrl HFSCs.
B) Heatmap representing normalized RING1B, H3K27me3, H3K4me3, H2AK119Ub1, CBX8 and RYBP ChIP-seq intensities of +/- 8Kb from TSS of RING1B target genes in HFSCs.
C) GO analyses of genes belonging to HFSCs cluster 1
D) Venn- diagram showing the overlap between up-regulated genes in *Ring1a/b* dKO mice with total RING1B/H3K27me3-enriched regions.
E) GO analyses of genes belonging to HFSCs clusters 2,3 and 4

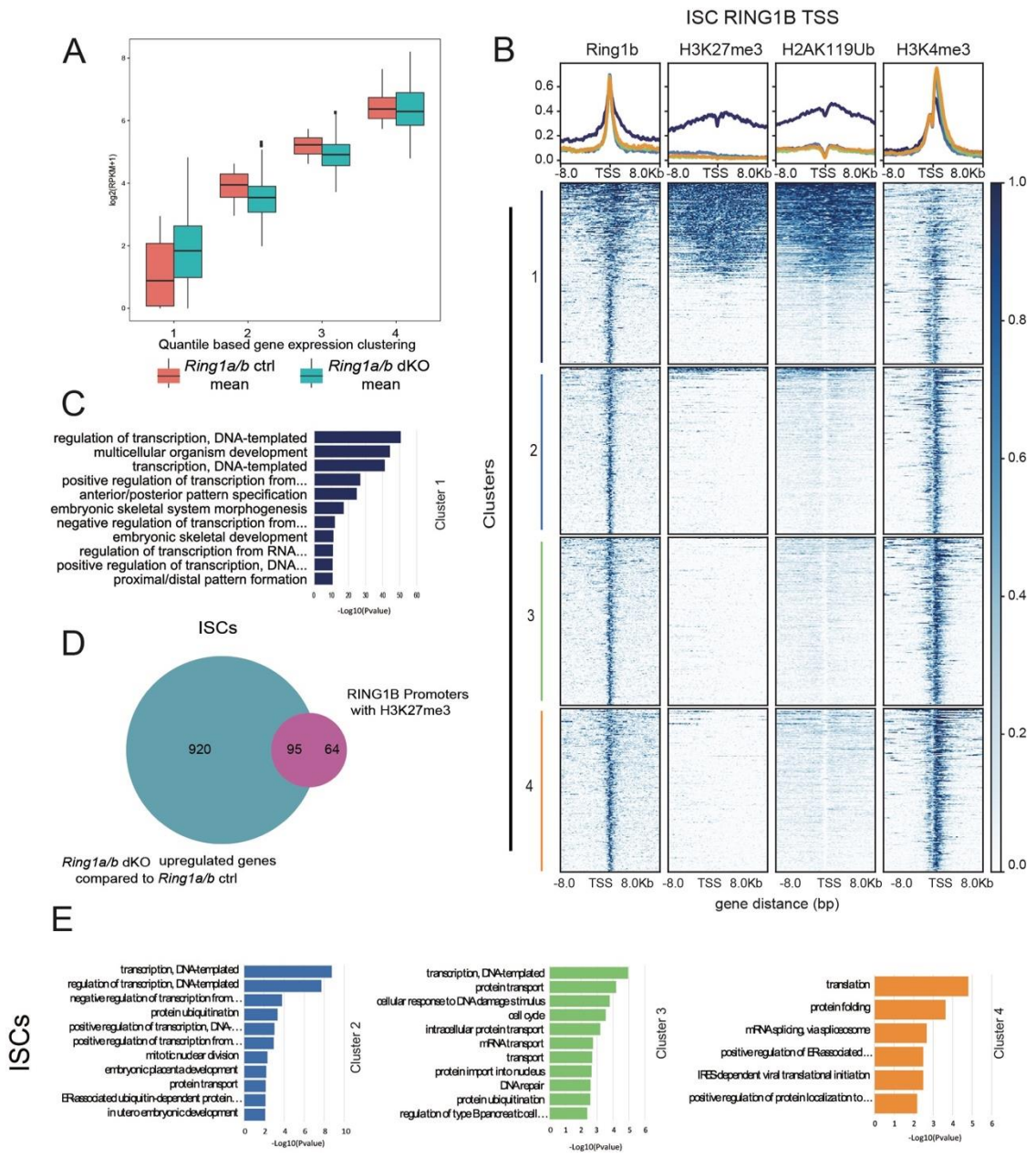

Figure 4.20 Genomic distribution of PRC1 binding in ISCs.

A) Quartile-based gene expression clustering performed using *Ring1a/b* ctrl RNA-seq data, showing expression variations between *Ring1a/b* dKO and ctrl ISCs.
B) Heatmap representing normalized RING1B, H3K27me3, H3K4me3 and H2AK119Ub1 ChIP-seq intensities of +/- 8Kb from TSS of RING1B target genes in ISCs.
C) GO analyses of genes belonging to ISCs cluster 1
D) Venn- diagram showing the overlap between up-regulated genes in *Ring1a/b* dKO mice with total RING1B/H3K27me3-enriched regions.
E) GO analyses of genes belonging to ISCs clusters 2,3 and 4

Accordingly to transcriptomic data and their related ontology analyses, we found that genes involved in development and differentiation were over-represented only in cluster 1 (Fig 4.19C and Fig 4.20C), which is characterized by the presence of canonical PRC1 and PRC2

marks and the respective components. While the remaining 3 clusters showed enrichment in more general processes such as transcription, translation and cell cycle regulation (Fig 4.19E and Fig 4.20E).

These data support a prominent role of canonical PRC1 activities compared to non-canonical ones in the maintenance of stem cell identity in both HFSCs and ISCs. However, it is important to stress that only a subset of RING1B /H3K27me3 double positive targets are derepressed upon PRC1 loss in stem cells from HFs and intestine (Fig 4.19D and Fig 4.20D).

This suggests that H3K27me3 is largely sufficient to prevent TF accessibility and the consequently activation of canonical Polycomb targets and that only a small proportion of PRC1-PRC2 target genes contributes to the observed phenotypes, underlying the complex crosstalk and interdependency of the two complexes.

4.5 LOSS OF PRC1 ACTIVATES AN EPIDERMAL-SPECIFIC PROGRAM IN HFSCs

To elucidate the direct mechanism by which PRC1 prevents differentiation of stem cells, maintaining their identity, we analyzed the RING1B targets that became derepressed upon *Ring1a/b* dKO. HFs derives from a single layer of embryonic epidermis, that under the correct stimuli is able to differentiate into a new tissue that is then maintained throughout life by CD34-HFSCs and LGR5-HFSCs that are necessary to regenerate all hair structures (Jaks, Barker et al. 2008, Saxena, Mok et al. 2019). To understand the role of PRC1 in the suppression of interfollicular epidermis related genes and the maintenance of HF lineage, we decided to look at genes that were implicated in skin specification in PRC1 depleted HFSCs. Among these genes we found Achaete-Scute family BHLH Transcription Factor 2

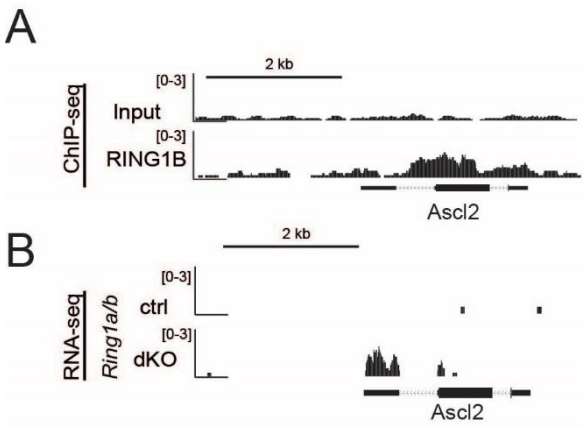

Figure 4.21 Ascl2 is repressed by PRC1 in HFSCs

A) Genomic snapshots of *Ascl2* gene, showing RING1B binding.
B) Genomic snapshots of *Ascl2* gene showing gene transcription upon PRC1 depletion.

(ASCL2) (Fig 4.12) that was previously shown to be sufficient and required for epidermal differentiation (Moriyama, Durham et al. 2008).

We decided to investigate whether an epidermal specific program is initiated upon PRC1 loss of activity and we performed a Gene Set Enrichment Analyses (GSEA) a bioinformatic a priori analyses that is able to determine whether a gene set list or database is enriched or not in the ranked gene list used as query. In our analyses we decided to compare signatures

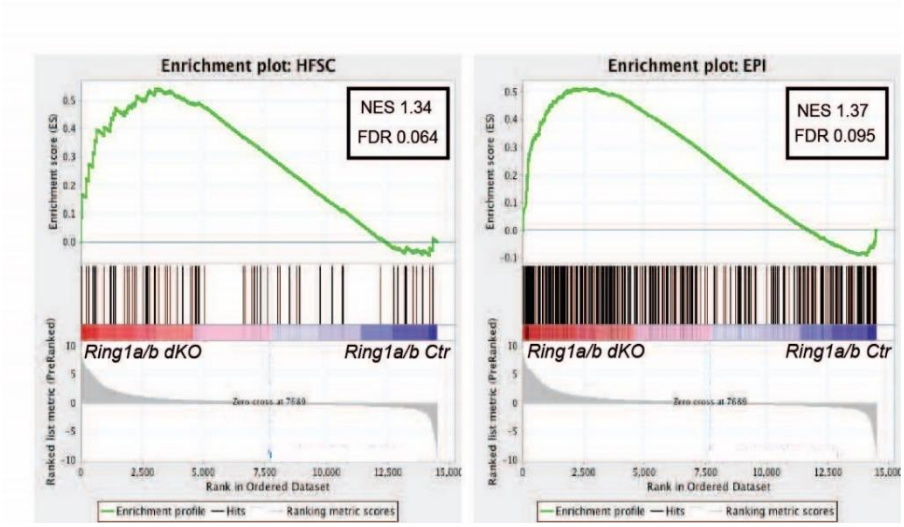

Figure 4.22 PRC1 activity depletion activates an epidermal program differentiation

Gene set enrichment analyses (GSEA) performed on *Ring1a/b* dKO HFSCs using signature specific for 14 major skin and HF cell population s (Rezza, Wang et al. 2016)

from different cells belonging to distinct skin compartments (Rezza, Wang et al. 2016) with *Ring1a/b* dKO vs ctrl transcriptional outcome in HFSCs.

This analysis pointed out that, together with stem cell signature (Fig 4.22 left panel, HFSC), genes related to epidermis (Fig 4.22 right panel, EPI) were enriched in our sample. Among this signature we confirm that some genes such as, *Krtdap*, *Calm5*, *Itgam* and *Gdpd2*, together with *Ascl2*, were activated and highly upregulated in depleted HFSCs compared to ctrl ones (Fig 4.23A and B).

Given the fact that Polycomb group proteins are epigenetics modifiers, and not TFs, that could actively start target genes transcription, removal of PRC1 suppression could be insufficient to activate gene transcription. To better characterize the mechanism of epidermal differentiation we decided to scan *Ascl2* promoter with LASAGNA-search 2.0 in order to find TFs that could be responsible for its activation.

Interestingly we found in the promoter of *Ascl2*, several binding motifs that are recognized by ZIC TFs family (Fig 4.24). Of note, we previously demonstrated that upon PRC1 loss of activity, several ZIC TFs, that are also directly bound by PRC1, are transcriptionally

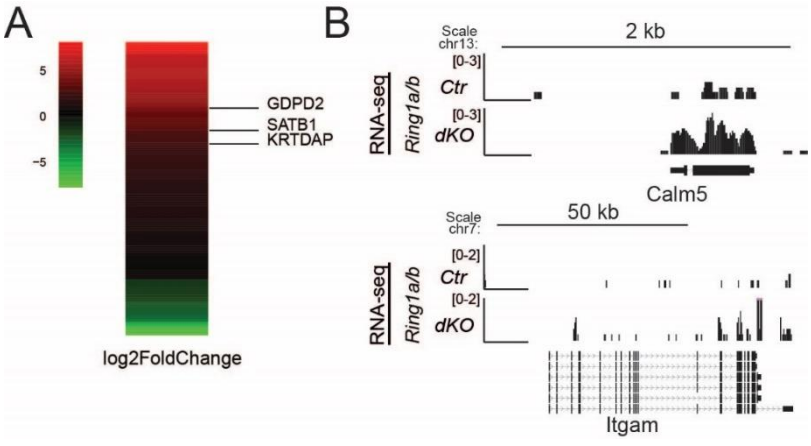

Figure 4.23 PRC1 depletion upregulates different Epidermal related genes

A) Heatmap representing epidermal-specific genes differentially regulated in *Ring1a/b* dKO LGR5-HFSCs (Log2 fold change).
B) Genomic snapshots of RNA-seq for *Calm5* and *Itgam* gene showing gene transcription upon PRC1 depletion.

upregulated (Fig 4.13A), possibly establishing a positive feedback loop for *Ascl2* activation and driving an epidermal differentiation program.

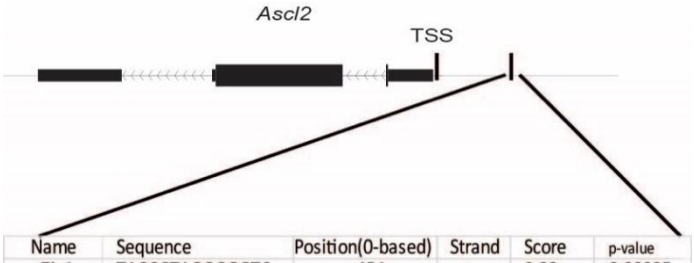

Name	Sequence	Position(0-based)	Strand	Score	p-value
Zic1	TACCCTAGGGGGTC	454	+	9.32	0.00025
Zic2	GCTACCCTAGGGGGT	452	+	8.41	0.0005
Zic2	GACCCCCTAGGGTAG	453	-	7.71	0.00095
Zic3	GCTACCCTAGGGGGT	452	+	8.42	0.000825

Figure 4.24 ZIC TFs binds Ascl2 promoter

Genomic snapshot of *Ascl2* gene showing the binding sequences for ZIC family member in its promoter region.

These results support a model in which PRC1 directly suppresses an epidermal-specific transcriptional program via suppression of master regulators of lineage specification thus contributing to preserve HF identity.

4.6 PCGFs PROTEINS LOCALIZE DIFFERENTLY IN INTESTINAL CRYPTS.

Loss of both PRC1 catalytic subunits, *Ring1a* and *Ring1b*, leads to a severe phenotype in intestinal and hair follicle tissues. However, Polycomb Repressive Complex 1 is composed by several different subcomplexes defined by a Polycomb Group Ring Finger protein (PCGF1-6) (Gao, Zhang et al. 2012, Scelfo, Piunti et al. 2015). Their mutual incorporation in the complex gives rise to at least 5 biochemically different PRC1 subcomplexes that could govern different cellular processes.

In recent years, PCGFs proteins became a central focus in the field of Polycomb research,

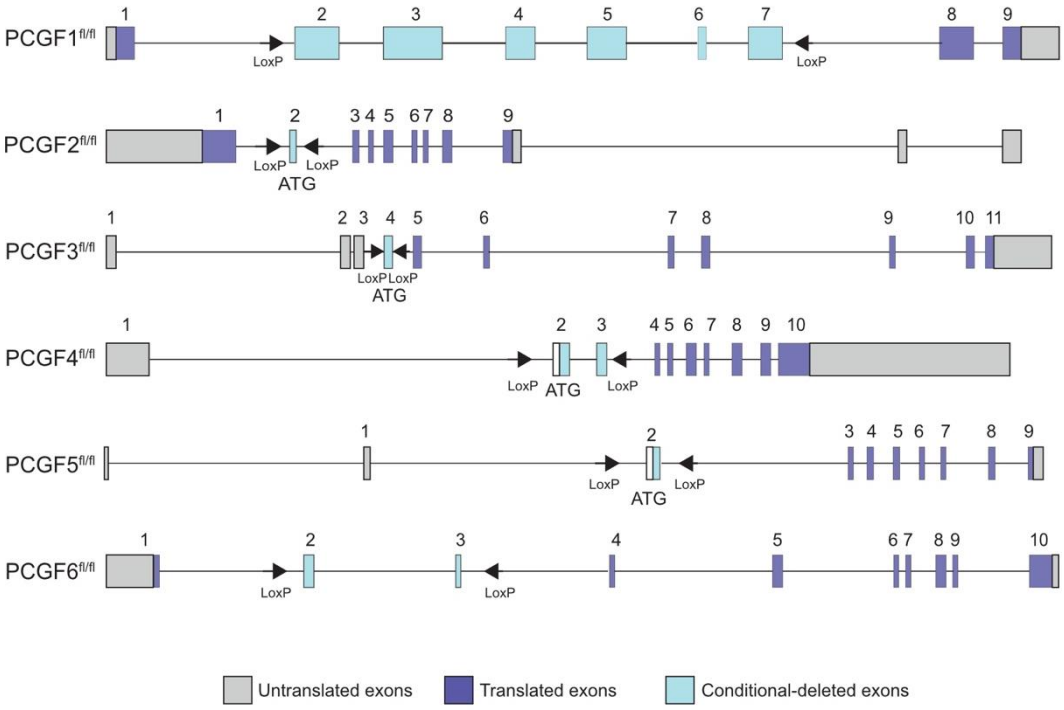

Figure 4.25 Schematic representation of PCGFs construct for conditional KOs

The figure shows the murine constructs for different PCGFs conditional KOs. These strains have been crossed with LGR5-CreERT2-Rosa26-LSL-LacZ to induce the KO specifically in stem cells, and with AhCre that allows for deletion in the intestinal epithelium.

The figure presents all the translated and non-translated exons for each PCGF gene and the ones that are delete upon Cre-mediated cleavage.

however their characterization has been performed mostly in-vitro, in mESC, and during murine embryonic development. Remarkably, a deep characterization of PCGFs proteins

biochemical and molecular functions in adult tissue homeostasis and adult stem cell maintenance is still lacking.

With the aim to better characterize PCGFs functions in adult tissue and to address their contribution in the phenotype driven by PRC1 loss of activity, we obtained all the genetic models for conditional deletion of specific PCGFs in mouse (Fig 4.25). Due to the presence of redundant complexes, we breed PCGF1 and PCGF6 alone, while PCGF2/4 and PCGF3/5 together to create the double KO.

To carry out this phenotypical and molecular analysis of PCGFs function in vivo, we first moved back to intestinal epithelium, a field where the laboratory has more expertise, to complement the analyses previously performed in *Ring1a/b* dKO. However, in order to understand if the different molecular outcome of PRC1 loss in HFs arise from different PCGFs functions in another stem cell compartment, the analyses will be further expanded in the hair follicle stem cell compartment.

We first assessed PCGFs expression within the intestinal tissue. Since commercial antibodies were not all available, we took advantage of antibodies risen against murine PCGFs, produced in our laboratory, which were tested for the major molecular analyses such as Western Blot, Chromatin Immuno-Precipitation and Immuno-Precipitation used in our laboratory (Scelfo, Fernandez-Perez et al. 2019).

Small intestines were harvested from Wild-type (WT or ctrl) mice and processed to isolate intestinal crypts and the villi.

Proteins and RNA were extracted and the different levels of PCGFs were compared among undifferentiated and differentiated cells. PCGF1 and PCGF5 proteins seems to be more expressed in the differentiated compartment of intestinal epithelium, while the remaining four PCGFs are more expressed in the staminal compartment of the crypt, suggesting a role

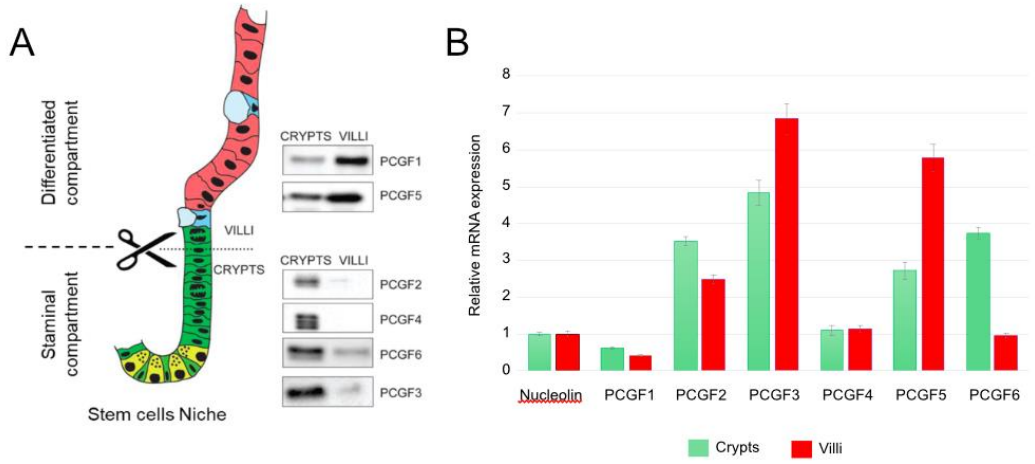

Figure 4.26 PCGFs expression in crypts and villi

A) Schematic picture of the intestinal differentiated (villi) and undifferentiated (crypts) and relative protein abundance of different PCGFs.
B) Relative mRNA expression of different PCGFs in Crypts (Green) and Villi (Red)

for these PcG proteins in cell differentiation programs. Importantly, also PCGF1 and PCGF5 are also expressed in the undifferentiated compartment, although their expression seems to increase in the villi, suggesting a role also in the maintenance of differentiated tissue (Fig 4.26A, B).

Within PRC1, PCGFs proteins dictate the ancillary proteins that will be recruited to assemble the final complex. This different composition leads to diverse chromatin localization of the subcomplexes, as previously demonstrated in mESCs and cell lines (Gao, Zhang et al. 2012, Scelfo, Piunti et al. 2015, Fursova, Blackledge et al. 2019, Scelfo, Fernandez-Perez et al. 2019).

In order to discover specific set of genes bound by the complexes, we map the different PRC1 sub-complexes binding sites along chromatin in the adult intestinal epithelium, we performed ChIP-seq experiments against all PCGFs protein from intestinal crypts compartment. With the exception of ChIP for PCGF1, purified crypts were fixed with 1% FA and sonicated to disrupt genomic DNA prior immuno-precipitation. Since the conventional crosslinking method with FA, which has a crosslinking radius of only ~2A and

does not always conserve protein-DNA interaction, was not successful for the PCGF1 ChIP, we tried a different cross-linking protocol. This complex was recovered in purified crypts subjected to a double crosslinking protocol with dissucinimidyl glutarate (DSG) molecule, that has a radius of 7.7A and acts by crosslinking the primary amine of proteins, followed by protein-DNA fixing with FA.

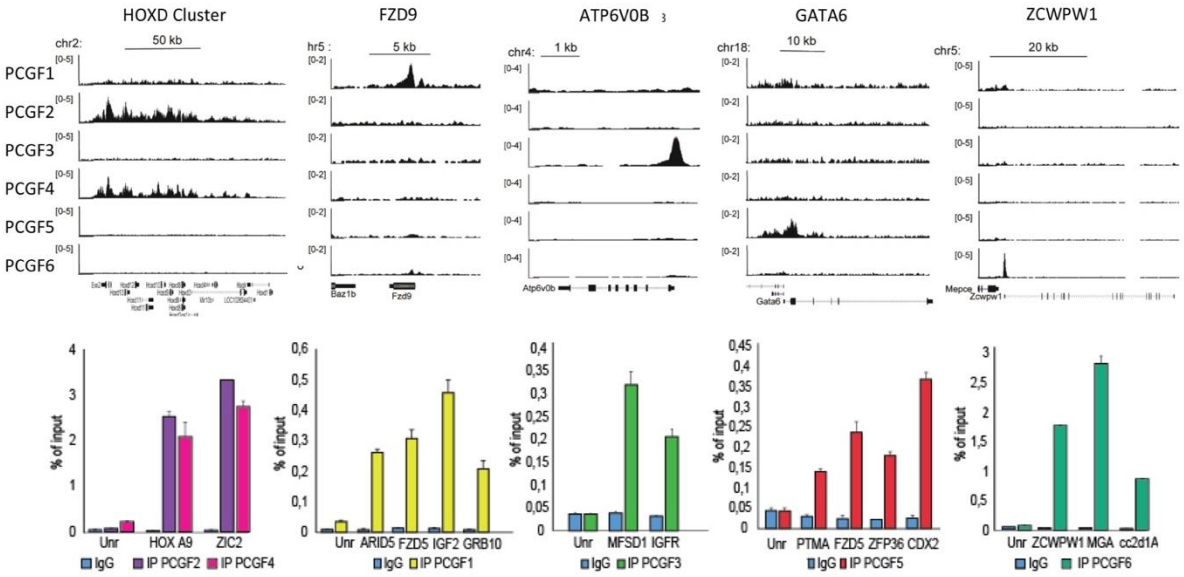

Figure 4.27 PCGFs localization in intestinal crypts

Genomic snapshots of ChIP-sequencing tracks for all the different PCGFs proteins in intestinal crypts and their relative RT-qPCR analyses of selected genes, showing the percentage of enrichment on the input.

We found that, as expected, canonical PRC1 complexes, containing PCGF2/Mel18 and PCGF4/Bmi1, localized on classical target genes, such as HOXD cluster and ZIC genes (Fig 4.27). Particularly, HOXD cluster seems devoid of any other PCGFs, that in turn binds discrete genes, demonstrating that PCGF proteins targets different genes, possibly regulating their transcription and governing different processes during intestinal tissue homeostasis.

Of note, PCGF2/Mel18 and PCGF4/Bmi1 among all PCGFs displays the widest peaks length (Fig 4.28A), spanning from hundreds of bp in length to 5000 bases, settling to a median of 1kb. On the other hand, non-canonical PCGFs showed narrower peaks, that are around

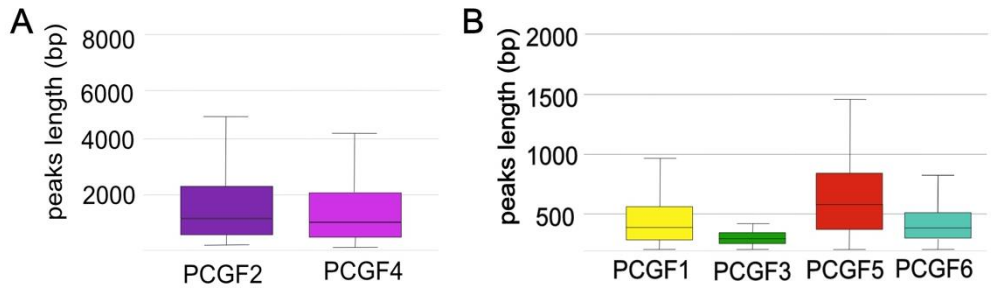

Figure 4.28 PCGFs genomic peaks shows differences in their length

Box plot representing the width of the different PCGFs peaks on their genomic targets.

(Total Peaks: PCGF1= 2114; PCGF2= 1064; PCGF3= 64; PCGF4= 1303; PCGF5= 56; PCGF6= 1900)

500bp (Fig 4.28B), except for PCGF3 that shows even sharper peaks, probably due to it binding to specific target sequences.

Unfortunately, PCGF5 immunoprecipitation was not efficient in intestinal crypts. Probably this is due to the low abundance of this protein expression that is consistent with the few peaks that we have detected along the genome, and localized on promoters (33 out of 56). Thus, we did not include PCGF5 in our genomic analyses.

In order to dissect the possible complementarity among the different PCGFs, we analyzed ChIP seq by performing a heatmap analysis of PCGF peaks (Fig 4.29). We found that overall the different PCGFs localize differently on the genome, and only a partial overlap exists, in particular among PCGF2/Mel18 and PCGF4/Bmi1 containing PRC1, consistently with their ability to form similar complexes. Surprisingly, we found a good overlap of PCGF2/4 targets with PCGF1-containing complexes.

A partial overlap of PCGF6 and PCGF3 also exist, but it is still restricted to few genes, due to low peaks number in the PCGF3 ChIP-seq. Remarkably, we ran a motifs enrichment analyses on promoters bound by PCGFs proteins and we found that, consistently with

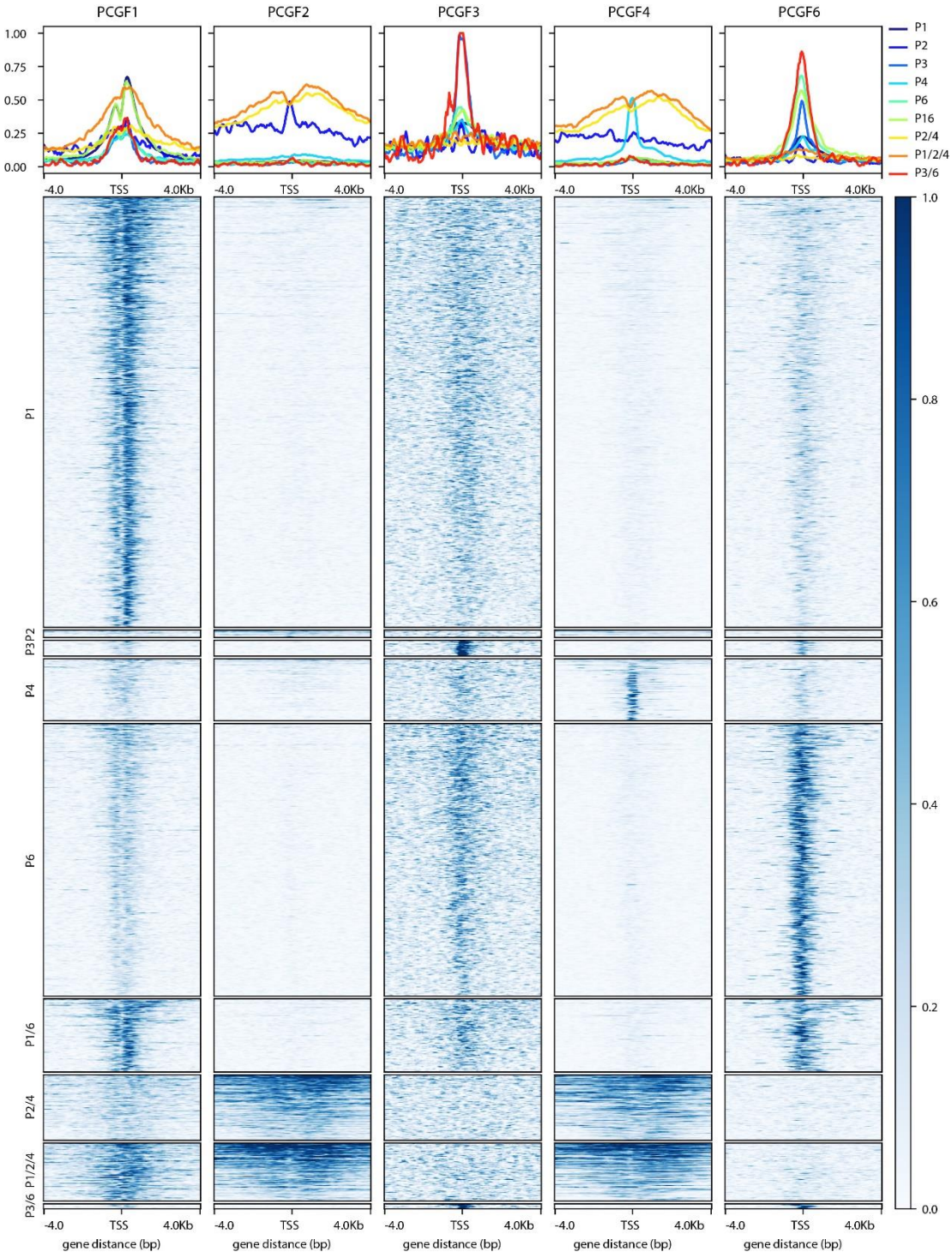

Figure 4.29 Different PCGFs shows partial overlaps on gene promoters

Heatmap showing the quantification of ChIP seq signals over PCGFs bound promoters (+/- 4kb from TSS) showing the grade of overlaps among PCGF1, PCGF2 PCGF3, PCGF4 and PCGF6.

mESCs literature, PCGF6 is found on E-box binding motif, that is also bound by c-Myc oncogene, and T-box sequences, that in turn is recognize by MGA, which is part of the

PRC1.6 complex. Moreover, PCGF3 motif enrichment discovery shows that, also in intestinal crypts it is able to bind another BHLH motif, similar to c-Myc E-box, that is recognized and bound by the newly described USF1 partner discovered by our laboratory (Scelfo, Fernandez-Perez et al. 2019).

To define the classes of genes possibly regulated by PCGFs proteins, we performed a GO term analyses on genes-related peaks for every PCGFs (Fig 4.30). We found that PCGF2 and PCGF4 largely overlap, governing genes involved in development and cell fate commitment.

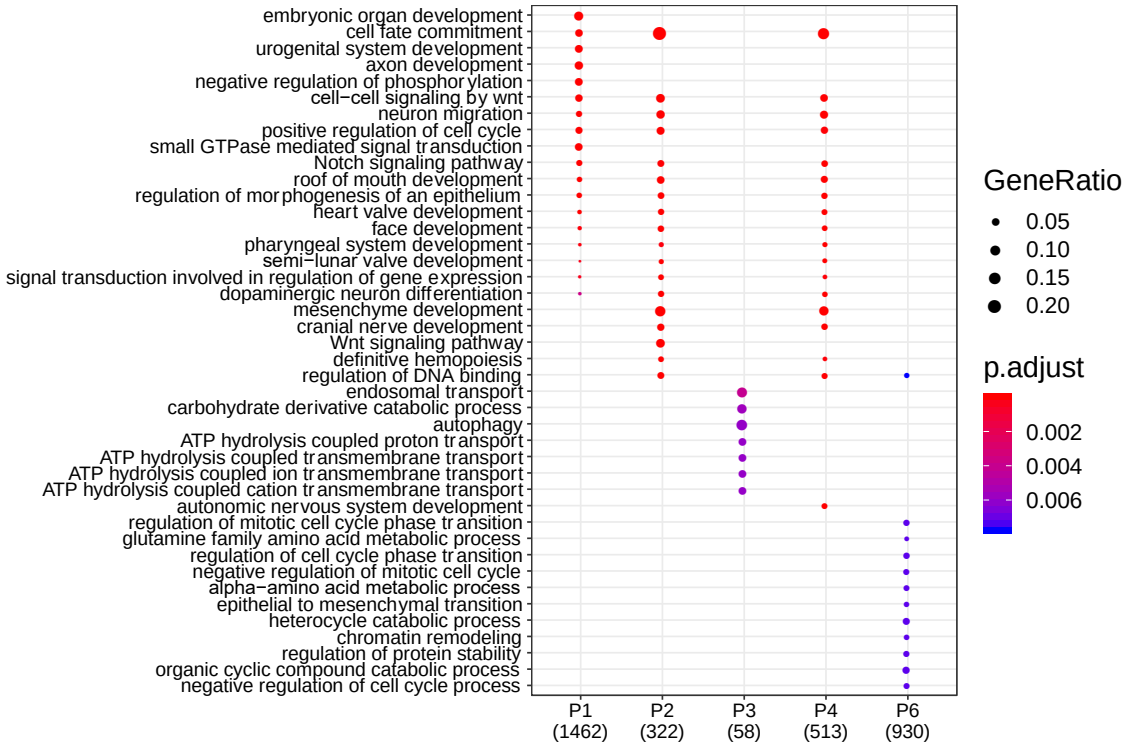

Figure 4.30 GO-Term analyses of PCGFs gene target reveals functional overlap among PCGF1, PCGF2 and PCGF4

Gene ontology analyses of PCGFs bound genes, showing their involvement in different cellular processes. PCGFs promoter peaks number are displayed in brackets.

Remarkably, also PCGF1 seems to bind genes related to development and differentiation, supporting the hypothesis that PCGF1 co-governs developmental genes together with

PCGF2/Mel18 and PCGF4/Bmi1, opening the possibility that PCGF1 is involved in canonical-gene regulation. On the other hands, PCGF3 and PCGF6 seems to regulate different cellular functions related to transport, and cell cycle/metabolism respectively.

In HFSCs, and accordingly to the recent literature (Morey, Aloia et al. 2013, Zhao, Huang et al. 2017, Cohen, Zhao et al. 2018, Fursova, Blackledge et al. 2019, Scelfo, Fernandez-Perez et al. 2019), we showed that PRC1 localize on active genes. To elucidate PCGFs functions and role in transcriptional regulation, we decided to investigate which PRC1 sub-complex localized on active or repressed genes. To do so, we compared PCGFs ChIP seq performed in intestinal crypts to RNA-seq obtained from ISCs of LGR5 ctrl mice.

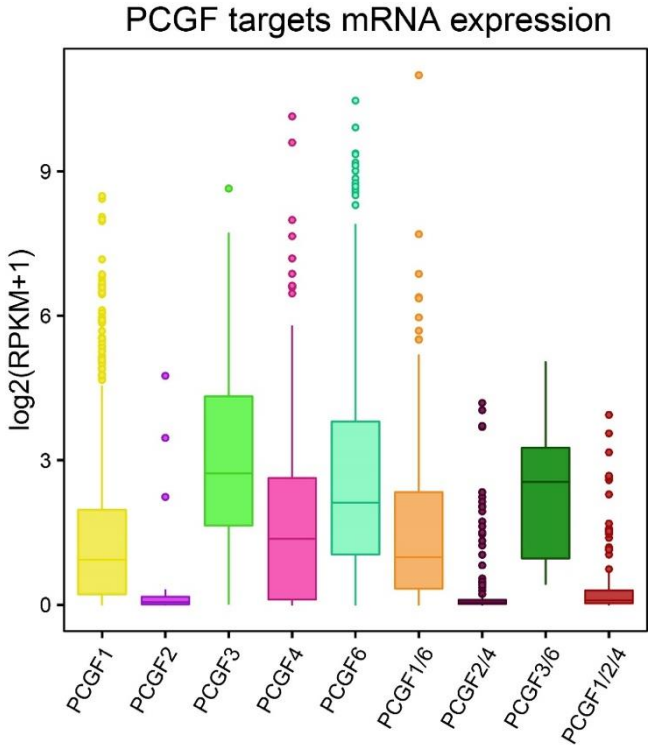

Figure 4.31 PCGFs proteins binds both expressed and repressed genes

Box plot representing PCGFs targets genes, retrieved by ChIP-seq analyses and their relative expression in ISCs, showing that single and combinations of PCGFs binds both active and repressed genes.

PCGF3 and PCGF6 localize on actively transcribed genes, suggesting a role in active transcription regulation also in intestinal epithelium. This is true also for PCGF1 targets genes which are enriched for medium-active genes. Strikingly, while PCGF2, consistently

with reported literature is found on transcriptionally repressed gene, PCGF4 seems to localize on active genes. Importantly, peaks containing PCGF2 and PCGF4 or PCGF1/2/4 are on totally silenced genes, suggesting that PCGF2 is the main effector in gene silencing in intestinal crypts (Fig 4.31).

However, to better characterize the epigenetic changes induced by specific PCGFs loss, and to elucidate to which extent PCGFs are able to compensate for each other, we are now breeding our conditional PCGFs KOs mice with AhCre transgenic mice, in order to perform ChIP sequencing analyses on PcG proteins and histone modifications among all PCGFs KO mice. These mouse models allow the deletion of PCGFs exons in all intestinal populations, with the only exception being Paneth cells. Moreover, these mice will be used for phenotypical analyses and transcriptomic analyses at single cell level, as well as in bulk.

4.7 PRC1-NULL PHENOTYPE IN ISCs IS A SUM OF DIFFERENT SUB-COMPLEXES ACTIVITY.

Intestinal tissue homeostasis and heterogeneity of intestinal cell populations arise from ISCs. Due to the fundamental role of PRC1 in adult stem cell identity maintenance we were interested in defining if a single PRC1 subcomplex or, alternatively, which combinations of complexes, were responsible for the loss of PRC1 activity phenotype.

To investigate PCGFs function in governing ISCs self-renewal and identity maintenance, we bred all the previously described mouse models (Fig 4.25) with the LGR5-GFP-ires-CreERT2 /Rosa26Lox-stop-Lox LacZ mouse strain (hereof LGR5 ctrl or LGR5 PCGFx KO after tamoxifen treatment), to obtain PCGFs excision only in LGR5 expressing stem cells.

The obtained strains, give us the possibility to carry out lineage tracing analysis and molecular analyses specifically in stem cells, allowing the definition of the phenotypic and transcriptomic changes arising from specific PCGF loss in the stem population.

To this purpose, we began with the generation and analyses of LGR5-PCGF1, LGR5-PCGF2/4, LGR5-PCGF3/5 and LGR5-PCGF6 conditional KO mice, focusing first on their ability to affect or impair stem cell self-renewal by performing a lineage tracing analysis. Importantly, in intestinal tissue, differently from hair follicle, the expression of LGR5-GFP-ires-CreERT2 /Rosa26Lox-stop-Lox LacZ construct is not homogeneous. Within the crypts base, different ISCs that randomly inactivate the transgene, always compete with other stem cells, resulting in crypt clonality (Gehart and Clevers 2019). Indeed, this leads to crypts that express GFP and CreERT2, that are capable to elicit recombination between LoxP sites of PCGF and Rosa26Lox-stop-Lox LacZ transgenes, and crypts that do not express the enzyme. Therefore, LacZ staining does not occur homogeneously in the tissue.

To verify whether PCGFs KOs are able to affect stem cell maintenance and tissue regeneration during homeostasis, mice were treated with four daily IP injection of tamoxifen and the intestine were harvested 30 days after the first injection, time point that showed a complete loss of traced cells derived from LGR5-PRC1 depleted stem cells (Chiacchiera, Rossi et al. 2016) . In fact, in our previous report, the ablation of all PRC1 subcomplexes, through the depletion of both catalytic subunits *Ring1a* and *Ring1b*, results in the loss of progeny derived from PRC1 defective ISCs, due to stem cell self-renewal impairment, as highlighted by the loss of LacZ staining in the tissue (Fig 4.32 top panel left). On the contrary, KOs for PCGF1, PCGF6, PCGF3, PCGF5 and the double KO for PCGF3/5 redundant subunits do not affect stem cell ability to maintain the tissue (Fig 4.32), as

demonstrated by the presence of LacZ staining, thus proving that the depletion of a single PRC1 subcomplex is not sufficient to phenocopy the loss of the entire Polycomb complex.

To define the role of PRC1 canonical subcomplexes we plan to perform the same lineage tracing experiment. However, preliminary data obtained by lineage tracing at 7 days post injection, suggest that also PRC1.2 and PRC1.4 concomitant ablation is not sufficient to phenocopy *Ring1a/b* dKO. In fact, while PRC1 loss of activity at 8 days display intestinal units that are only stained at the crypt base (Fig 4.33 left), while LGR5-PCGF2/4 KO derived progeny are found also in villi (Fig 4.33 right). This is due to the fact that impaired stem cells, are counter selected from the high competition at the crypt base, and the arising progeny, migrates in the villi is finally lost in lumen. LGR5-PCGF2/4 KO, are continuously

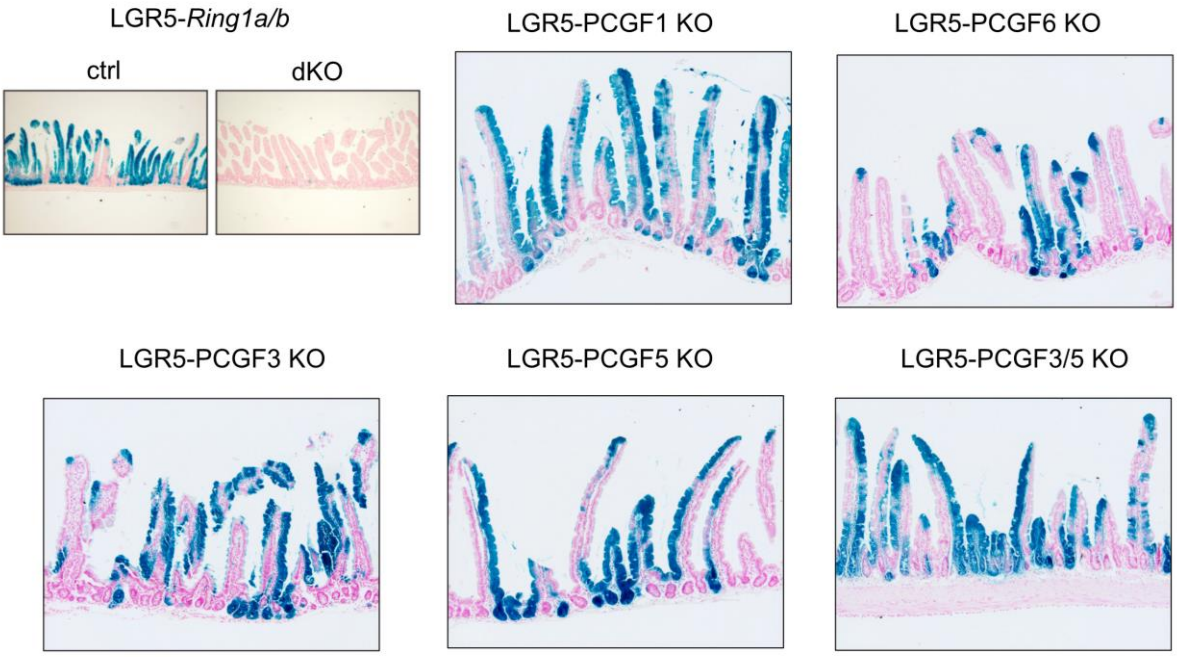

Figure 4.32 Lineage tracing analyses of non-canonical LGR5-PCGFs KO at 30 dpi

Lineage tracing analyses of non-canonical PRC1 subcomplexes KOs, showing that the depletion of these subcomplexes do not affect stem cell capability to maintain the tissue.

generating progeny without being counter-selected, indicating that these mutations do not

confer disadvantages in terms of self-renewal and proliferation. However, longer time point are needed to better define the phenotype.

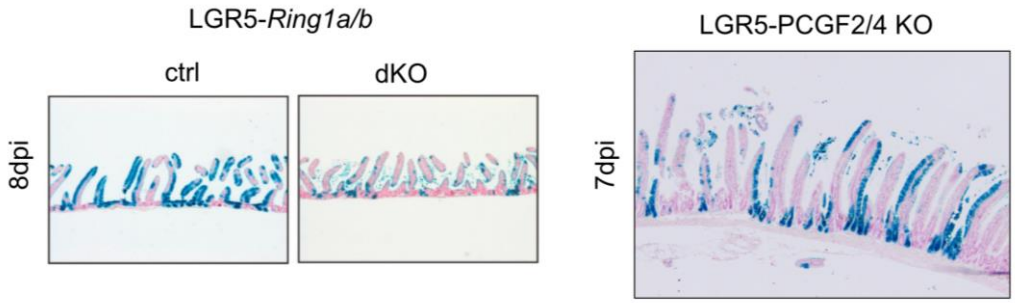

Figure 4.33 Lineage tracing analyses of canonical LGR5-PCGFs KO at 7 dpi

Lineage tracing analyses of canonical PRC1 subcomplexes KOs, showing that the depletion of these subcomplexes do not affect stem cell capability to maintain the tissue.

These results together suggest that single PRC1 subcomplex depletion is not sufficient to phenocopy the drastic phenotype observed in PRC1 deficient mice, indicating that more than one complex is involved in the maintenance of cellular identity and stem cell self-renewal.

4.8 TRANSCRIPTOMIC ANALYSES OF ISCs REVEALS THAT PRC1 SUBCOMPLEXES GOVERN SPECIFIC CELLULAR PROCESSES

To elucidate the molecular functions of the different PCGFs proteins in ISCs, we decided to evaluate the transcriptional changes arising from PCGF1, PCGF2/PCGF4, PCGF3/PCGF5 and PCGF6 depletion. To do this, we induced Cre-mediated excision of the transgenes in LGR5-ISCs by four daily intraperitoneal injection of Tamoxifen and we harvested the intestinal tissue after 7 days from the first injection (Fig 4.34A) and processed the crypts to single cells prior to sorting. 3000 to 5000 of sorted GFP-positive ISC from LGR5 ctrl mice,

2 biological replicates for LGR5-PCGF1 KO, LGR5-PCGF6 KO and LGR5-PCGF2/4, and 2 technical replicates for PCGF3/5 KO were processed with Smart-Seq2 protocol and the floxing efficiency for every PCGF was evaluated on the pre-amplified cDNA (Fig 4.34B-E).

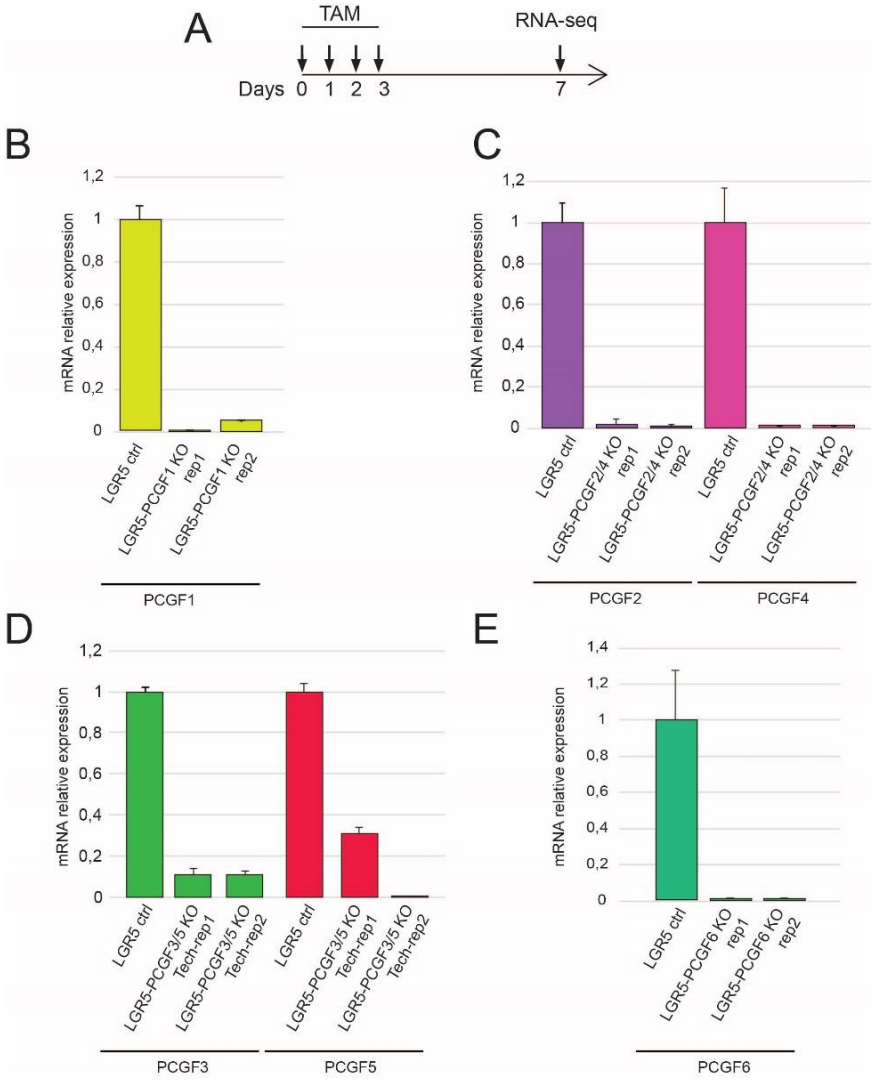

Figure 4.34 LGR5-PCGFs KO validation

A) Schematic representation of the experiment workflow.
B-E) RT-qPCR analyses of different PCGFs KO in pre-amplified cDNA obtained from 3-to-5 thousand sorted ISCs subjected to SMART-seq2 protocol. Bar plots represent mRNA relative expression plus Standard Deviation.

Sequencing analyses revealed that overall LGR5-PCGF2/4 KO, consistent with their known important role as transcriptional regulators, leads to the upregulation of more than 2000 genes and the downregulation of 1700 genes (Fig 4.35). Similarly, loss of PCGF1 in LGR5 stem cell causes the downregulation of 617 gene and almost an equal number of genes upregulated (437) (Fig 4.35). Conversely, consistent with the activatory roles reported for PCGF3/5 and PCGF6 PRC1 containing complexes (Morey, Aloia et al. 2013, Zhao, Huang et al. 2017, Cohen, Zhao et al. 2018, Fursova, Blackledge et al. 2019, Scelfo, Fernandez-Perez et al. 2019), their loss leads to a massive amount of genes downregulation, compared

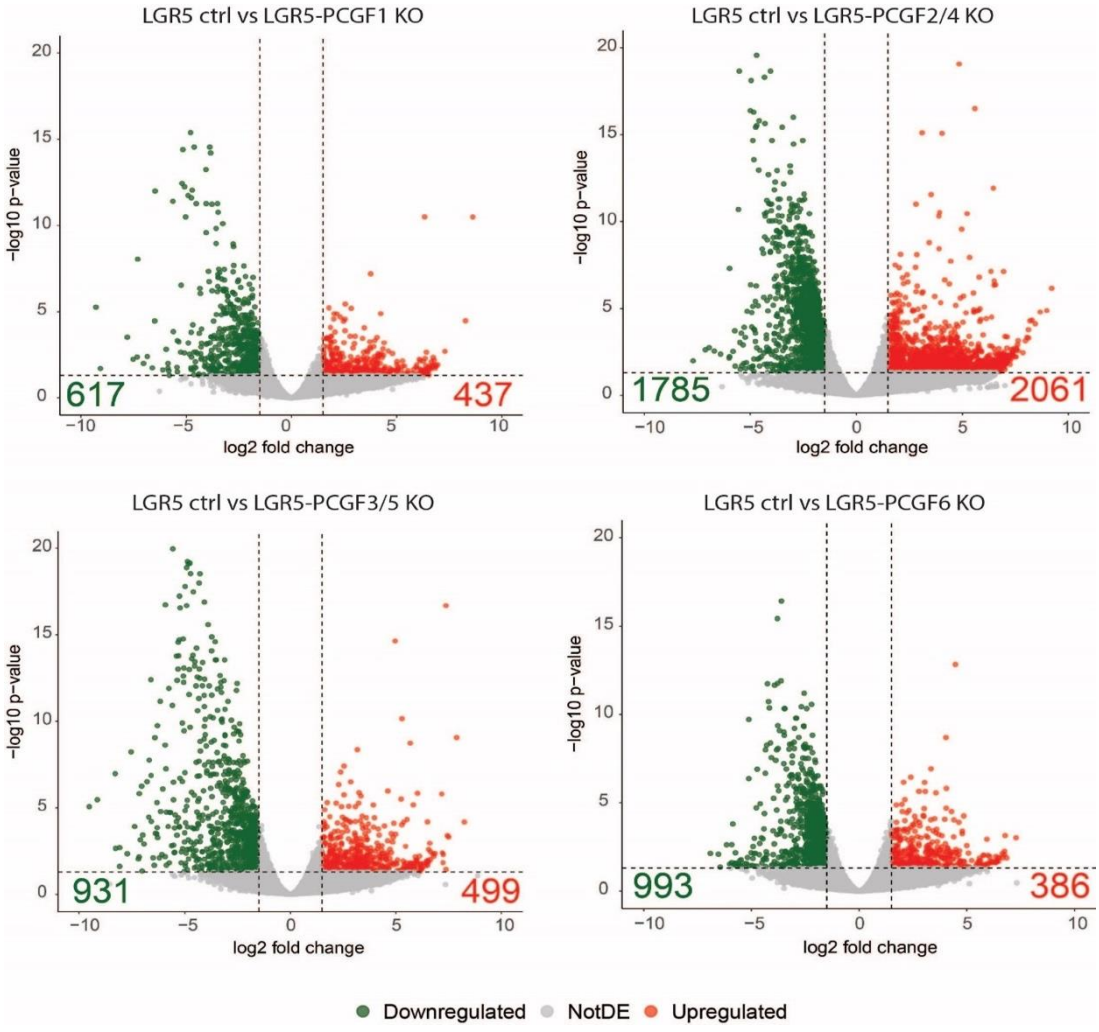

Figure 4.35 Volcano plots of different PCGFs KO showing the up and downregulated genes

Volcano plot analyses of PCGF1, PCGF2/4, PCGF3/5 and PCGF6 KO ISCs showing the different expressed genes of KOs compared to LGR5 ctrl ISCs. (tresholds: p-value < 0.05, absolute log2(fold change)>1).

to gene activation with respectively 931 vs 499 and 993 and 386 genes deregulated (Fig 4.35).

To define which pathways are altered upon different PCGFs KO in ISCs, we interrogated GO analyses for up and downregulated genes (Fig 4.36). Genes that decrease their expression upon PCGFs depletion are involved in different metabolic, transcriptional, cell cycle-related and viral response processes, that are only partially overlapping among different sub complexes, suggesting that their loss impairs specific cellular functions.

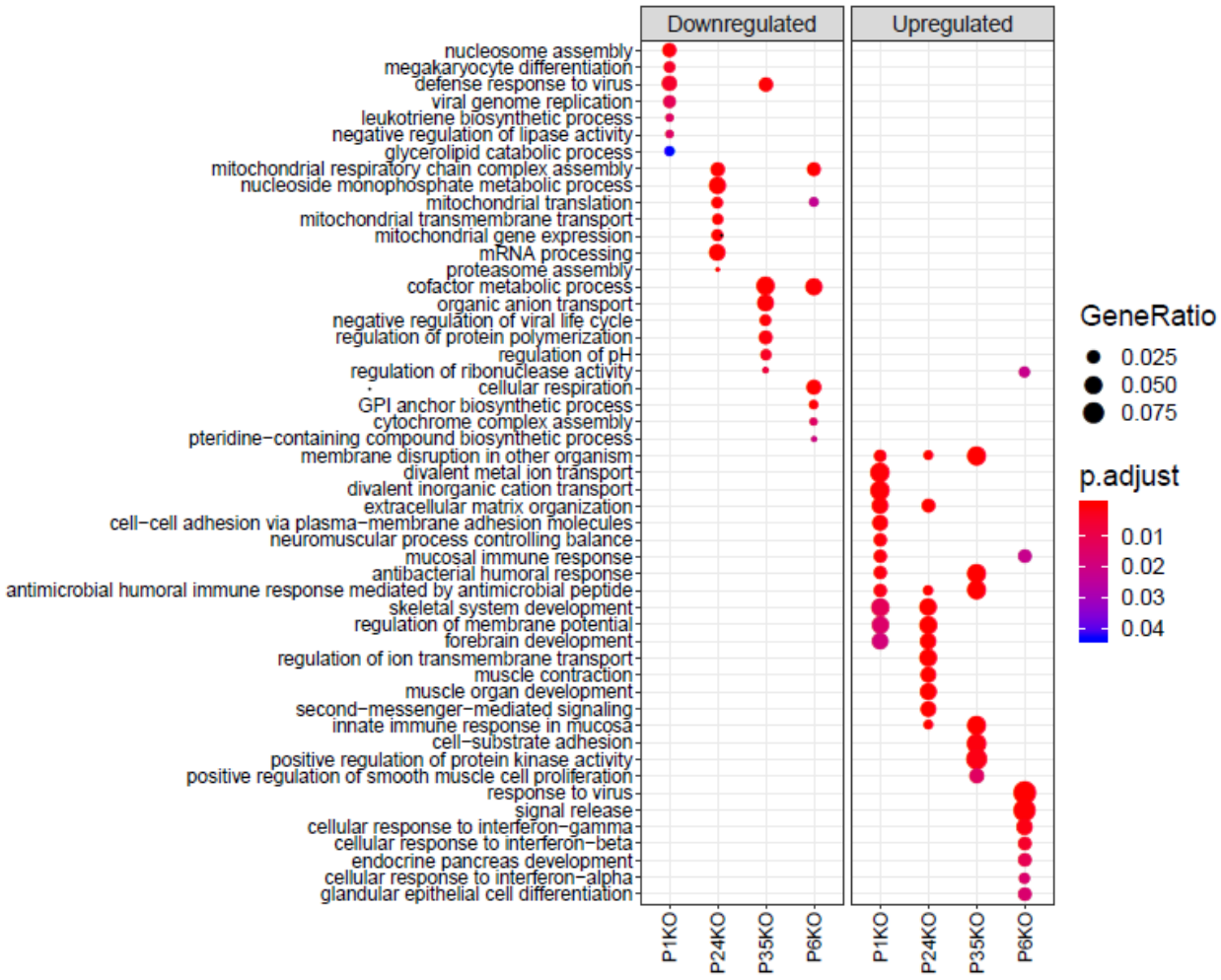

Figure 4.36 GO term analyses of deregulated genes in ISCs upon different PCGFs KO

Gene ontology analyses of ISCs PCGFs KOs deregulated genes, showing their involvement in different cellular processes.

On the other hand, ISCs abrogated for canonical PRC1 complexes activity shows up regulation of genes related to development and differentiation, further proving their classical PRC1 functions, biological processes that are partially shared with LGR5-PCGF1KO altered transcriptome. Moreover, PCGF1 loss also induces alteration in transport and microbial related processes. Differently from PCGF1 and PCGF2/4 KO, PCGF3 and PCGF6 do not share any biological process, in accordance with their ability to binds different targets.

4.9 FUTURE PERSPECTIVE AND ON-GOING CHARACTERIZATION

To date, we show that in vivo PRC1 complexes maintenance is necessary to regulates stem cell identity in different stem cells, and that this function is accomplished by the sum of different PRC1 subcomplexes activities, that remains to be defined, that acts together on different cellular processes. We showed that in the intestinal epithelium, PRC1-subcomplexes govern several different pathways and functions that are only partially shared among different PCGFs. This has to be proved also in HF-stem cell compartment, in order to dissect whether PRC1 subcomplexes features are similar or different in the two tissues.

To complement the phenotypic analyses of ISCs, we are investigating also the effect of PCGFs deletion in the whole intestinal epithelium, through the controlled induction of Cre-recombinase under CYP1A1 promoter, that is activated upon lipophilic xenobiotic administration. Preliminary analyses of single KO in epithelial tissue of intestine, showed that, consistent with their specific gene regulation, no major effects are evident when PCGFs are ablated in homeostatic conditions (Fig 4.37), further highlighting their interdependency.

Polycomb proteins are important cell identity regulators, and their alteration in cancer is well documented. Among the different PCGFs, Mel18 and Bmi1, despite their great overlapping features, are known as tumor suppressor and oncogene respectively (Zhang, Sheng et al.

2010). However, nothing is known about the other PCGFs proteins constituting the non-canonical complexes in both pathological and homeostatic condition.

Of note, PRC1.1 subcomplex seems to be related to canonical-PRC1 regulation, that together with the lack of phenotypic outcome of LGR5-PCGF2/4 KO leads to the hypothesis that PCGF1 is able to co-regulate canonical PRC1 genes. To validate this theory, we are now breeding PCGF1 and PCGF2/4 mouse models to ablate the three complexes together in LGR5 expressing stem cells and intestinal epithelium, in order to study the phenotypical addiction of PRC1.1 loss in PRC1.2 and PRC1.4 KO. These three PcG proteins are reported in literature as transcriptional repressors, and we showed that, when they colocalized, target gene transcription is completely absent. On the other hand, PCGF3/5 and PCGF6 containing

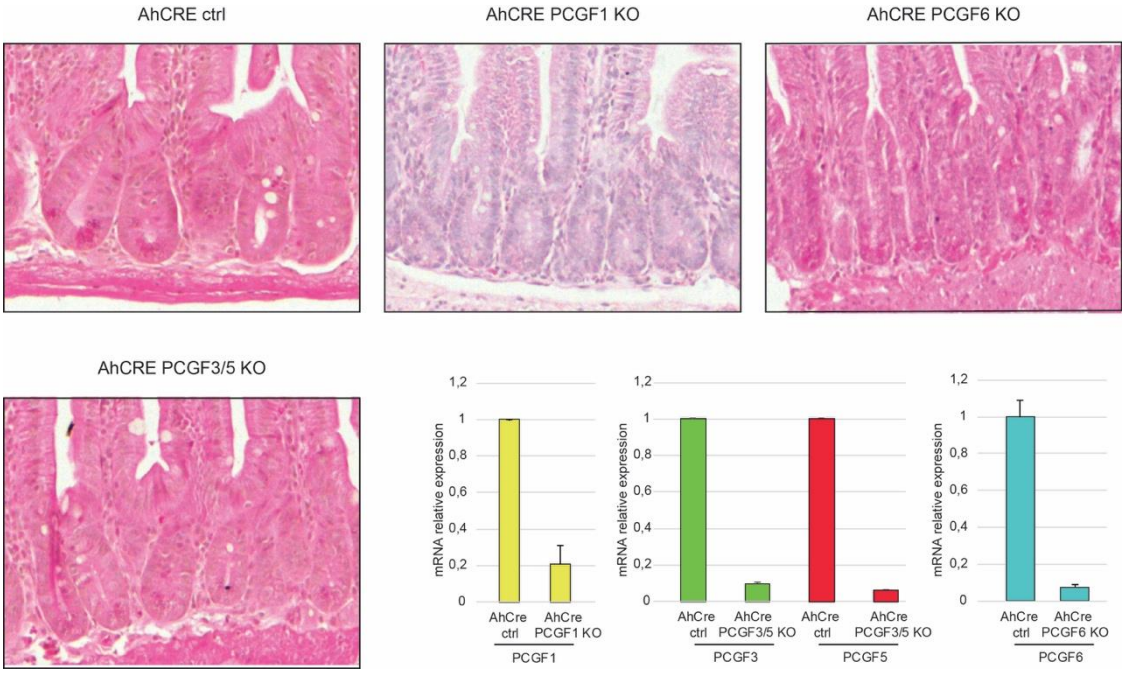

Figure 4.37 Single deletion of PRC1 subcomplexes does not affect intestinal homeostasis

Hematoxylin and Eosin staining of duodenum from AhCre-PCGF1, AhCre-PCGF6 and AhCre-PCGF3/5 KOs and their floxing efficiency, showing that single PRC1 subcomplexes ablation does not affect intestinal homeostasis. Tissues were collected after 15days from first beta-napthoflavon intraperitoneal injection. Graph represent the relative expression plus Standard Deviation of PCGFs transcripts in the respective ctrl and KOs mouse.

PRC1 are reported as activatory-Polycomb complexes, and we show that they share the ability to bind BHLH motifs on different genes. To deeply investigate the activatory

properties of PRC1 complex we are creating mice strains where PRC1.3/5 and PRC1.6 are concomitantly ablated from LGR5 expressing stem cells and whole intestinal epithelium.
These conditional KOs for repressive and activatory PRC1 subcomplexes will be used to perform both phenotypical and molecular analyses in order to dissect the functions in homeostasis and their contribution to PRC1-loss-of-activity phenotype.

As the last part of our characterization we aim to address the ability of the different PCGFs-containing subcomplexes in tissue regeneration upon damage, and in oncogenic transformation.
To address PCGFs role in regeneration we are planning to perform phenotypic and molecular analyses of PCGFs conditional KOs upon different damage induction, such as inflammation and irradiation.
On the other hand, to address the oncogenic potential of PRC1 we will focus on PCGF6-containing PRC1 subcomplex, due to its interaction with MGA and MAX proteins, which are involved in the c-Myc pathway. Of note, c-Myc overexpression is not sufficient to induce tumorigenesis in intestinal epithelium, but it has the ability to expand the staminal compartment during its upregulation (Finch, Soucek et al. 2009). We hypothesize that PCGF6 is able to restrain c-Myc transforming capability in intestinal epithelium, preventing c-myc binding on important genes necessary for transformation. To validate this model, we are breeding AhCre-PCGF6 conditional KO mouse model with Rosa26-LSL-MYCERT2 that allow Myc translocation in the nucleus upon tamoxifen delivery, in this way we can couple PCGF6 KO with active nuclear c-myc function. We first analyzed the oncogenic potential of PCGF6 alone in a protocol of colon cancer induction, that exploits a carcinogen (Azoxymethane) and sequent cycles of colon inflammation with DSS molecule, allowing us to obtain colon adenomas in 60 days (Fig 4.38A). Preliminary results shows that PCGF6 KO is maintained during the whole protocol (Fig 4.38B), suggesting that depleted crypts are not counter selected and it does not have a major effect in tissue maintenance, as demonstrated

by the similar weight curve between AhCre ctrl and PCGF6 KO mice (Fig 4.38C) and from colon cancer adenomas histological sections that were similar in number and dimension along the colon (Fig 4.38D). However, deeper investigation of histological sections and

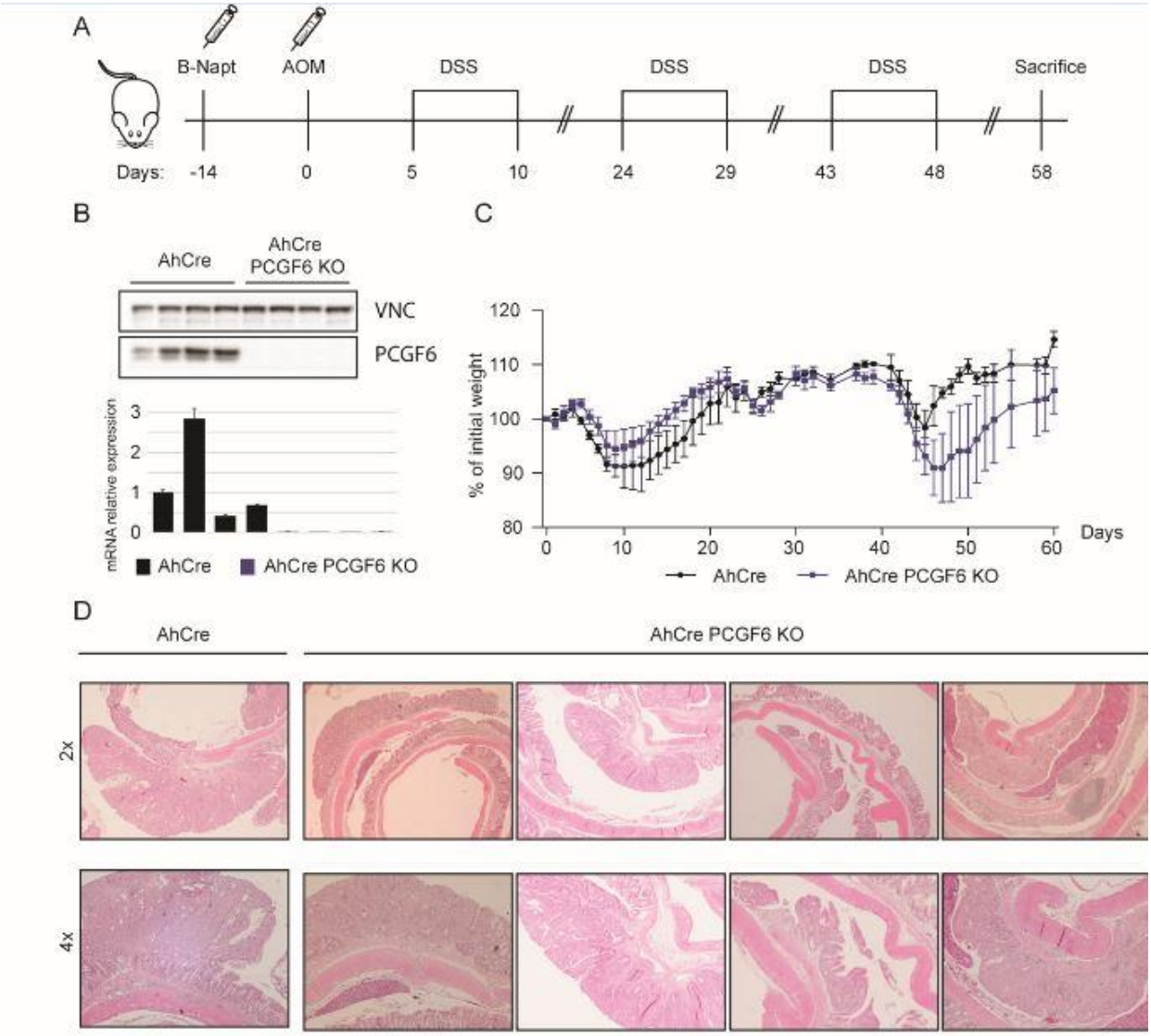

Figure 4.38 PCGF6 KO does not affect adenomas onset and progression

A) schematic view of AOM-DSS protocol used for AhCre WT and PCGF6 mice.
B) Western blot analyses (up) and mRNA RT-qPCR (bottom) of intestinal crypts to validate PCGF6 KO at the end of the protocol.
C) Weight curve showing the percentage of weight loss during the DSS cycles.
D) Hematoxylin and Eosin staining of AhCre ctrl and AhCre-PCGF6 KO mice at the end of the AOM-DSS protocol, showing adenoma formation in the two conditions.

molecular studies are required, as well as is necessary to increase the number of experimental animals, and to carefully monitor the number and the volume of the tumors arising in the two conditions Moreover, we aim to compare the effect of Myc overexpression in the presence or absence of PRC1.6, to validate our hypothesis, thus further analyses will be performed with the Myc inducible mice strains.

5. DISCUSSION

5.1 PROJECT OVERVIEW

Polycomb Groups of Proteins are epigenetic factors involved in development and differentiation. PcG proteins assemble to form two main complexes named PRC1 and PRC2 which roles are widely studied in ESCs and other cultured cell lines since 40 years (Aloia, Di Stefano et al. 2013, Aranda, Mas et al. 2015, Scelfo, Piunti et al. 2015, Poynter and Kadoch 2016). However, a deep characterization of Polycomb complexes function in vivo has begun just few years ago, and a comprehensive view of their roles is still missing. The first studies demonstrated that Polycomb complexes were linked to embryonic development and their alteration leads to several different phenotypic defects spanning from homeotic transformation to pre-implantation death.

Instead, the role of the PcG proteins roles in adult tissue homeostasis is still not known. Importantly tumors are strictly related to adult cells dedifferentiation and loss of identity (Friedmann-Morvinski and Verma 2014, Roy and Hebrok 2015). Adult tissues are maintained throughout life from adult stem cell pools that drive organs regeneration, and, in the past 5 years, it starts to be clear that Polycomb proteins are important regulator of stem cell identity and differentiation also in adult context. We recently reported that PRC1 and PRC2 play crucial roles in supporting intestinal homeostasis governing two different functions, by sustaining stem cell identity and self-renewal, and surveilling the balance among enterocytes and secretory cells by regulating lineage-differentiation genes respectively (Chiacchiera, Rossi et al. 2016, Chiacchiera, Rossi et al. 2016, Chiacchiera and Pasini 2017).

Particularly, PRC1 is critical to maintain ISC and the loss of both RING1A and RING1B catalytic subunits leads to stem cells exhaustion driven by a massive upregulation of different non-lineage-specific transcription factors.

Additionally, PRC1 is composed of several subunits, that generate different subcomplexes which are able to govern different aspects of stem cell maintenance, and these complexes are not studied in adult tissue homeostasis. Indeed, their contribution to PRC1-loss-of-activity phenotype is still obscure. The discovery of their biological function in both homeostatic and pathological condition could also be important to develop novel therapeutic approaches. In fact, deregulation of all complexes could be dangerous for the whole organism, while targeting specific subcomplexes could be more specific and effective to overwhelm tumor growth without influencing healthy tissue. To this end we want to deeply investigate PRC1 subcomplexes in different compartments, in order to have a comprehensive view of their regulation and functions. Nevertheless, from new emerging literature, mostly related to cancer, is clear that the same proteins can behave differently depending from the context. Without going too far from Polycomb proteins, PRC2 complex is found to be mutated in opposite manners depending on the tumoral context (Scelfo, Piunti et al. 2015), highlighting that it is necessary to study proteins in a context dependent manner.

In order to overcome the reported functional and biochemical redundancy, we exploited the use of a mouse model in which both catalytic subunits of PRC1 complexes could be abrogated (del Mar Lorente, Marcos-Gutierrez et al. 2000; de Napoles, Mermoud et al. 2004; Roman-Trufero, Mendez-Gomez et al. 2009). Until tamoxifen delivery our mouse model LGR5-GFP-ires-CreERT2/Ring1a$^{-/-}$/Ring1b$^{fl/fl}$/Rosa26Lox-stop-LoxLacZ only harbor the homozygous excision of *Ring1a* gene. In these conditions we do not notice any severe impairment in hair follicle morphogenesis and regeneration, as demonstrated by their ability to maintain the fur, during development and first anagen, however, we cannot formally

exclude that at least part of the phenotype observed during hair regeneration could be due to *Ring1a* depletion in the surrounding environment.

5.2 PRC1 IS NECESSARY TO MAINTAIN ANAGEN PROGRESSION

Using the LGR5-GFP-ires-CreERT2/Ring1a$^{-/-}$/Ring1b$^{fl/fl}$/Rosa26Lox-stop-Lox LacZ mouse strain we had the unique opportunity to deeply investigate PRC1s role in hair follicles and intestinal adult tissue contexts, which share common features, such as the rapid division of LGR5 stem cell population. These compartments arise from distinct embryonic layers (de Santa Barbara, van den Brink et al. 2003, Liu, Zhang et al. 2013), ectoderm and endoderm respectively, allowing us to analyze whether this fundamental complex plays the same role exploiting the same mechanism or the context influence PRC1 function. Our data revealed that PRC1 is able to repress a common set of genes in ISC and HFSCs, suggesting that its role is fundamental throughout different tissues despite the different embryonic origins. However, in adult life the pools of transcription factors present in a specific cell type, is able to shape the molecular outcome of PRC1 loss.

Differently from ISC, that continuously divide to regenerate the tissue, LGR5-HFSCs encounter cycles of proliferation and resting during their lives. In order to minimize the differences among different HFs related to the cell cycle stages we decided to induce anagen. Loss of PRC1 activity in this context leads to the same phenotypic effect previously observed in the intestinal compartment. We faced an impairment of proliferation that inhibits the correct formation of all the structures that will develop the hairs, ultimately affecting tissue regeneration.

PRC1 is a known epigenetic repressor of *Ink4a-ARF* genomic locus that encode for p16 and p19 mouse proteins that are able to block Cyclin D and MDM2 negative regulator of RB and p53, leading to cell cycle inhibition. However, despite the relief of the transcriptional repression of this locus, it has been demonstrated, both in adult stem cells, in our ISC work, and from a new HF-related paper carried out during morphogenesis, that PRC1-loss-of-activity phenotype is independent from *Ink4a-ARF* locus activation, suggesting that also in our context the early anagen proliferative blocks is induced by other factors apart from p16-p19 pathways (Chiacchiera, Rossi et al. 2016, Cohen, Zhao et al. 2018).

Whether these alternative pathways, which leads to a phenotypic convergence in the absence of PRC1, are the same in different tissues was investigated at molecular levels by comparing ISCs and HFSCs data.

Even though, we faced a great impairment of anagen progression, we could see some anagen features in a reduced number of follicles that partially express beta-galactosidase protein. It has been demonstrated that upon LGR5-HFSCs depletion, CD34-HFSCs, residing in the upper bulge region, start to express LGR5 stemness marker and the follicles are able to correctly proceed through anagen (Hoeck, Biehs et al. 2017). However, it is possible that this mechanism is not happening in our model. In fact, we are not losing LGR5 expression in quiescent follicles, but only the PRC1 associated histone mark, suggesting that, rather than disrupt LGR5-HFSCs population within the hair follicle, PRC1 ablation is able to induce a massive deregulation of the transcriptional landscape without affecting stem cell viability but only their self-renewal potential and identity. In this view, PRC1 depleted cells are still able to divide once, or just a few times, giving rise to LacZ positive progeny but, lacking essential self-renewal related genes and other hair follicle specific transcripts, these cells are not able to sustain the correct hair follicle cycle progression and regeneration.

Analyzing RNA-seq data obtained from LGR5-HFSCs *Ring1a/b* ctrl and dKOs, we found that PRC1 depleted cells show reduced expression of the *Shh* gene. SHH pathway is

necessary to sustain several processes in HF, first of all anagen progression. Remarkably, it has been demonstrated that ablation of the *Shh* gene in K15 expressing cells, that specify for both bulge and HG-HFSCs, leads to the generation of Mx cells that are impaired in anagen progression and failed to proceed after Anagen phase II (Hsu, Li et al. 2014, Zhang, Tsai et al. 2016). Therefore, we hypothesize that PRC1 activity is necessary to sustain *Shh* active transcription and hair follicle cycle progression.

5.3 PRC1 IS NECESSARY FOR TISSUE IDENTITY MAINTENANCE

PRC1 loss induces the deregulation of several different genes, both directly and indirectly. We confirmed that, also in this tissue context, PRC1 activity is necessary to preserve the expression of genes necessary for cell identity maintenance. This is in accordance with Cohen and colleagues (Cohen, Zhao et al. 2018), that observed that PRC1 ablation in epidermal progenitors downregulates epidermal and hair follicle related genes.

Upregulated genes upon PRC1 loss of activity in HFSCs mostly comprise homeotic and development-related transcription factors, and the same is true for the intestinal compartments. Overall, almost the 25% of the upregulated genes were common among the two stem cell populations and, more importantly, in both cases the deregulated transcripts were not specifically expressed in peculiar tissues, but they were widely expressed among an extensive panel of tissues and cell lines, highlighting the crucial role of PRC1 in defining lineage-specificity. The same results were obtained also in epidermal progenitors (Cohen, Zhao et al. 2018) where the *Ring1a/b* dKO shows the upregulation of various genes involved in development and differentiation. These results together underlie the common role in governing identity maintenance that is accomplished by PRC1 in different stem cells, temporally spanning from embryonic stem cells, through more differentiated progenitor stem cells, to adult stem cells.

PRC1 and its PCGFs subunits are mainly studied in mESCs and during embryonic development. Recently Cohen and colleagues investigated PCGFs role in hair follicle morphogenesis. Importantly, they did not identify any defects in hair follicle formation in PCGF1, PCGF3/5 and PCGF6 KO. On the other hand, consistently with PRC1 catalytic mutant, that leads to the upregulation of only few genes and to an increase of Merkel cells within the developing hair follicle and epidermis, PCGF2/4 KO leads to the same phenotype, without affecting hair follicle features. Importantly LGR5 stem cells arise after morphogenesis and they do not address any feature of adult stem cell maintenance.

Remarkably, nothing is known about the specific contribution of different PRC1 sub-complexes in adult homeostasis preservation. To fill this void, we crossed different PCGFs conditional KOs in order to investigate their specific involvement in different homeostatic processes, evaluating both their phenotypic and transcriptional outcome upon loss-of-activity induction. We showed that, consistently with hair follicle morphogenesis, single PCGFs KOs in adult LGR5-ISC, are not sufficient to impair homeostasis. This is highlighted also by the different transcriptomic changes arising from PCGFs depletion, showing how single PRC1 subcomplexes are specifically involved in minor processes, that are not sufficient to induce stem cell self-renewal failure. However, based on transcriptomic and genomic data, we hypothesize that a combination of different PRC1 subcomplexes ablation could phenocopy the drastic *Ring1a/b* dKO previously described.

Additionally, our and Dr. Klose laboratories precisely shown that different combinations of PCGFs KOs are necessary to phenocopy *Ring1a/b* loss and that a single PCGF loss is not sufficient to induce a significative transcriptional deregulation to induce phenotype changes in vitro (Fursova, Blackledge et al. 2019, Scelfo, Fernandez-Perez et al. 2019).

5.4 PROFILING PRC1 BINDING IN STEM CELLS

Carrying out this project we could also compare the binding profile of RING1B in different LGR5 stem cell population. In both hair follicle and intestinal stem cells population PRC1 is mainly found at gene promoters. Comparing RING1B peaks among ISCs and HFSCs, we found that only a subset were common among the two population, meaning that RING1B binds to different genes in different adult stem cells. Remarkably, the shared peaks are related to genes involved in development and differentiation, further highlighting that PRC1 role in cell fate determination and stem cell maintenance is common among different stem cells.

By ChIP-seq experiments in HFSCs, we proved that PRC1 is able to bind both active H3K4me3-marked genes and repressed genes decorated with the H3K27me3 histone mark. Repressed genes were bound by Canonical PRC1 complexes, as demonstrated by the presence of CBX8 subunit, while active target genes display the presence of RYBP, defining the non canonical part of the complexes. Interestingly, we showed that canonical target genes are also marked by high levels of H2AK119Ub1 histone modification compared to non canonical sites that, instead, show only low levels of PRC1 mark, suggesting that non canonical complexes could exert their function independently from their ability to ubiquitinate histone H2A on K119. Importantly this histone modification distribution has been described also in murine ESCs, where PRC1-mediated ubiquitination and PRC2-mediated methylation co-exist at gene promoters bound by CBX7 and RING1B, while RYBP/RING1B co-occupied genes are largely devoid of H2AK119Ub1 (Morey, Aloia et al. 2013). We have also shown that this ability of PRC1 to binds both active and repressed genes is not a peculiar behavior of HFSCs and ESCs but is found also in ISCs. Moreover, this latter observation has also been confirmed by Cohen and colleagues (Cohen, Zhao et al. 2018) indeed expanding the evidence of PRC1 role on active genes also in epidermal progenitors.

In accordance with the recent emerging literature (Zhao, Huang et al. 2017, Cohen, Zhao et al. 2018, Fursova, Blackledge et al. 2019, Scelfo, Fernandez-Perez et al. 2019), we provide further evidences that PRC1 is able to bind active genes *in vivo*, and that this is achieved in the context of RYBP containing non-canonical complexes. However only few of those active PRC1 genes scored among the down-regulated transcripts upon PRC1 loss, both in HFCSs and ISCs, thereby suggesting a marginal role of non-canonical subcomplexes in maintaining the expression of those targets. Therefore, their specific role on active genes remains to be addressed.

This latter observation suggests that stem cells loss of identity and self-renewal impairment, firstly shown in ISCs and now described for HFSCs, could be primarily ascribed to the repressive canonical activity of PRC1. We described that several Polycomb targets become derepressed upon PRC1 depletion, and those upregulated genes can be directly linked to the phenotypic convergence observed in the two stem cells populations, highlighting the general role of PRC1 in maintaining transcriptional repression of non-lineage specific genes.

Additionally, we define that, in intestinal crypts, all non-canonical PRC1 subcomplexes can binds transcriptionally active genes and. Of note, PCGF4, that in the context of PRC1 has been always associated with gene repression, when localized on the chromatin alone is found on active genes. Remarkably, canonical subunit PCGF2 binds only repressed genes, and the concomitant genomic localization of PCGF2 and PCGF4, as well as PCGF1, PCGF2 and PCGF4 is found on transcriptionally silenced genes, leading to the hypothesis that PCGF2 canonical subunits could be primarily involved in gene silencing. Moreover, it is possible that these differences in genomic localization could be part of the dissimilar behavior reported in literature for PCGF2/Mel18 and PCGF4/Bmi1 in tumors (Zhang, Sheng et al. 2010).

5.5 PRC1 GENERAL ACTIVITY IS INFLUENCED BY TFs POOLS.

Importantly, both in ISCs and HFSCs, not all PRC1 repressed targets are transcriptionally activated upon *Ring1a/b* dKO. This evidence points out that, despite the general role of PRC1 previously described is shared among different stem cells of different tissues and arising from different embryonic layers, PRC1 transcriptional outcome is influenced by the tissue context, resulting in a cell type dependent upregulation of different PRC1 target genes. Likely, this specificity is conferred by the TFs repertoire available in the given cells.

Accordingly, while in ISCs we did not found any specifics TFs able to drive a differentiation program, in *Ring1a/b* dKO HFSCs we could appreciate the de-repression of ASCL2, that is known to be sufficient and required for epidermal differentiation (Moriyama, Durham et al. 2008). Deeper analyses of transcriptomic data from PRC1 deficient HFSCs confirmed the activation of an epidermal-specific transcriptional program, that involves the upregulation of different epidermal genes, which could, at least in part, contribute to the loss-of-identity phenotype arising from *Ring1a/b* depletion in HFSCs.

5.6 PRC1 AS A STEM CELL IDENTITY GUARDIAN AND CLINICAL IMPLICATION

Our data sustain the existence of a general role of PRC1, in different populations of adult stem cell, in the preservation of cell identity. PRC1 loss deregulates different genes, which are only partially overlapping in different stem cell populations, that ultimately converge to the same phenotypic effect through different cell-type specific mechanisms.

This observation is particularly important non only to elucidate PRC1, and more in general Polycomb proteins, roles in shaping adult tissues and homeostasis maintenance, but also to analyze these epigenetic factors in several pathological conditions, primarily in cancer, in

which Polycomb complexes are directly involved and play different roles. Several reports show how PcG are required for tumor development and progression, as well as for its prevention depending on the contexts (Richly, Aloia et al. 2011, Scelfo, Piunti et al. 2015) and some new molecules that act as Polycomb inhibitors have already entered clinical trials (Richly, Aloia et al. 2011, Pasini and Di Croce 2016). Taking into account the context dependency highlighted from our works in adult stem cells, it is possible that the efficacy and the consequences of PcG inhibition could be cell type specific, linked to the TF pools and the signaling pathways of the different cells, underlying the necessity to carefully analyze data in context and specific situations.

6. BIBLIOGRAPHY

Akasaka, T., M. Kanno, R. Balling, M. A. Mieza, M. Taniguchi and H. Koseki (1996). "A role for mel-18, a Polycomb group-related vertebrate gene, during theanteroposterior specification of the axial skeleton." Development **122**(5): 1513-1522.

Alkema, M. J., N. M. van der Lugt, R. C. Bobeldijk, A. Berns and M. van Lohuizen (1995). "Transformation of axial skeleton due to overexpression of bmi-1 in transgenic mice." Nature **374**(6524): 724-727.

Aloia, L., B. Di Stefano and L. Di Croce (2013). "Polycomb complexes in stem cells and embryonic development." Development **140**(12): 2525-2534
.

Anders, S., P. T. Pyl and W. Huber (2015). "HTSeq--a Python framework to work with high-throughput sequencing data." Bioinformatics **31**(2): 166-169.

Andl, T., S. T. Reddy, T. Gaddapara and S. E. Millar (2002). "WNT signals are required for the initiation of hair follicle development." Dev Cell **2**(5): 643-653.

Aranda, S., G. Mas and L. Di Croce (2015). "Regulation of gene transcription by Polycomb proteins." Sci Adv **1**(11): e1500737.

Arnaudo, A. M. and B. A. Garcia (2013). "Proteomic characterization of novel histone post-translational modifications." Epigenetics Chromatin **6**(1): 24.

Ballare, C., M. Lange, A. Lapinaite, G. M. Martin, L. Morey, G. Pascual, R. Liefke, B. Simon, Y. Shi, O. Gozani, T. Carlomagno, S. A. Benitah and L. Di Croce (2012). "Phf19 links methylated Lys36 of histone H3 to regulation of Polycomb activity." Nat Struct Mol Biol **19**(12): 1257-1265.

Bannister, A. J. and T. Kouzarides (2011). "Regulation of chromatin by histone modifications." Cell Res **21**(3): 381-395.

Barker, N. (2014). "Adult intestinal stem cells: critical drivers of epithelial homeostasis and regeneration." Nat Rev Mol Cell Biol **15**(1): 19-33.

Barker, N., J. H. van Es, V. Jaks, M. Kasper, H. Snippert, R. Toftgard and H. Clevers (2008). "Very long-term self-renewal of small intestine, colon, and hair follicles from cycling Lgr5+ve stem cells." Cold Spring Harb Symp Quant Biol **73**: 351-356.

Barker, N., J. H. van Es, J. Kuipers, P. Kujala, M. van den Born, M. Cozijnsen, A. Haegebarth, J. Korving, H. Begthel, P. J. Peters and H. Clevers (2007). "Identification of stem cells in small intestine and colon by marker gene Lgr5." Nature **449**(7165): 1003-1007.

Barker, N., A. van Oudenaarden and H. Clevers (2012). "Identifying the stem cell of the intestinal crypt: strategies and pitfalls." Cell Stem Cell **11**(4): 452-460.

Barrero, M. J. and J. C. Izpisua Belmonte (2013). "Polycomb complex recruitment in pluripotent stem cells." Nat Cell Biol **15**(4): 348-350.

Barsh, G. (1999). "Of ancient tales and hairless tails." Nat Genet **22**(4): 315-316.

Bernstein, B. E., T. S. Mikkelsen, X. Xie, M. Kamal, D. J. Huebert, J. Cuff, B. Fry, A. Meissner, M. Wernig, K. Plath, R. Jaenisch, A. Wagschal, R. Feil, S. L. Schreiber and E. S. Lander (2006). "A bivalent chromatin structure marks key developmental genes in embryonic stem cells." Cell **125**(2): 315-326.

Beumer, J. and H. Clevers (2016). "Regulation and plasticity of intestinal stem cells during homeostasis and regeneration." Development **143**(20): 3639-3649.

Bevins, C. L. and N. H. Salzman (2011). "Paneth cells, antimicrobial peptides and maintenance of intestinal homeostasis." Nat Rev Microbiol **9**(5): 356-368.

Birchenough, G. M., M. E. Johansson, J. K. Gustafsson, J. H. Bergstrom and G. C. Hansson (2015). "New developments in goblet cell mucus secretion and function." Mucosal Immunol **8**(4): 712-719.

Bjerknes, M. and H. Cheng (1999). "Clonal analysis of mouse intestinal epithelial progenitors." Gastroenterology **116**(1): 7-14.

Blackledge, N. P., J. C. Zhou, M. Y. Tolstorukov, A. M. Farcas, P. J. Park and R. J. Klose (2010). "CpG islands recruit a histone H3 lysine 36 demethylase." Mol Cell **38**(2): 179-190.

Blanpain, C., W. E. Lowry, A. Geoghegan, L. Polak and E. Fuchs (2004). "Self-renewal, multipotency, and the existence of two cell populations within an epithelial stem cell niche." Cell **118**(5): 635-648.

Boukarabila, H., A. J. Saurin, E. Batsche, N. Mossadegh, M. van Lohuizen, A. P. Otte, J. Pradel, C. Muchardt, M. Sieweke and E. Duprez (2009). "The PRC1 Polycomb group complex interacts with PLZF/RARA to mediate leukemic transformation." Genes Dev **23**(10): 1195-1206.

Boyer, L. A., K. Plath, J. Zeitlinger, T. Brambrink, L. A. Medeiros, T. I. Lee, S. S. Levine, M. Wernig, A. Tajonar, M. K. Ray, G. W. Bell, A. P. Otte, M. Vidal, D. K. Gifford, R. A. Young and R. Jaenisch (2006). "Polycomb complexes repress developmental regulators in murine embryonic stem cells." Nature **441**(7091): 349-353.

Bracken, A. P., N. Dietrich, D. Pasini, K. H. Hansen and K. Helin (2006). "Genome-wide mapping of Polycomb target genes unravels their roles in cell fate transitions." Genes Dev **20**(9): 1123-1136.

Braun, K. M., C. Niemann, U. B. Jensen, J. P. Sundberg, V. Silva-Vargas and F. M. Watt (2003). "Manipulation of stem cell proliferation and lineage commitment: visualisation of label-retaining cells in wholemounts of mouse epidermis." Development **130**(21): 5241-5255.

Brookes, E., I. de Santiago, D. Hebenstreit, K. J. Morris, T. Carroll, S. Q. Xie, J. K. Stock, M. Heidemann, D. Eick, N. Nozaki, H. Kimura, J. Ragoussis, S. A. Teichmann and A. Pombo (2012). "Polycomb associates genome-wide with a specific RNA polymerase II variant, and regulates metabolic genes in ESCs." Cell Stem Cell **10**(2): 157-170.

Buczacki, S. J., H. I. Zecchini, A. M. Nicholson, R. Russell, L. Vermeulen, R. Kemp and D. J. Winton (2013). "Intestinal label-retaining cells are secretory precursors expressing Lgr5." Nature **495**(7439): 65-69.

Busturia, A. and M. Bienz (1993). "Silencers in abdominal-B, a homeotic Drosophila gene." EMBO J **12**(4): 1415-1425.

Cales, C., M. Roman-Trufero, L. Pavon, I. Serrano, T. Melgar, M. Endoh, C. Perez, H. Koseki and M. Vidal (2008). "Inactivation of the polycomb group protein Ring1B unveils an antiproliferative role in hematopoietic cell expansion and cooperation with tumorigenesis associated with Ink4a deletion." Mol Cell Biol **28**(3): 1018-1028.

Cao, R., Y. Tsukada and Y. Zhang (2005). "Role of Bmi-1 and Ring1A in H2A ubiquitylation and Hox gene silencing." Mol Cell **20**(6): 845-854.

Cao, R., H. Wang, J. He, H. Erdjument-Bromage, P. Tempst and Y. Zhang (2008). "Role of hPHF1 in H3K27 methylation and Hox gene silencing." Mol Cell Biol **28**(5): 1862-1872.

Cao, R., L. Wang, H. Wang, L. Xia, H. Erdjument-Bromage, P. Tempst, R. S. Jones and Y. Zhang (2002). "Role of histone H3 lysine 27 methylation in Polycomb-group silencing." Science **298**(5595): 1039-1043.

Cao, R. and Y. Zhang (2004). "SUZ12 is required for both the histone methyltransferase activity and the silencing function of the EED-EZH2 complex." Mol Cell **15**(1): 57-67.

Carbone, M., H. Yang, H. I. Pass, T. Krausz, J. R. Testa and G. Gaudino (2013). "BAP1 and cancer." Nat Rev Cancer **13**(3): 153-159.

Chen, D., A. Jarrell, C. Guo, R. Lang and R. Atit (2012). "Dermal beta-catenin activity in response to epidermal Wnt ligands is required for fibroblast proliferation and hair follicle initiation." Development **139**(8): 1522-1533.

Chen, H. and P. C. Boutros (2011). "VennDiagram: a package for the generation of highly-customizable Venn and Euler diagrams in R." BMC Bioinformatics **12**: 35.

Cheng, H. and C. P. Leblond (1974). "Origin, differentiation and renewal of the four main epithelial cell types in the mouse small intestine. I. Columnar cell." Am J Anat **141**(4): 461-479.

Cheung, P., C. D. Allis and P. Sassone-Corsi (2000). "Signaling to chromatin through histone modifications." Cell **103**(2): 263-271.

Chiacchiera, F. and D. Pasini (2017). "Control of adult intestinal identity by the Polycomb repressive machinery." Cell Cycle **16**(3): 243-244.

Chiacchiera, F., A. Rossi, S. Jammula, A. Piunti, A. Scelfo, P. Ordonez-Moran, J. Huelsken, H. Koseki and D. Pasini (2016). "Polycomb Complex PRC1 Preserves Intestinal Stem Cell Identity by Sustaining Wnt/beta-Catenin Transcriptional Activity." Cell Stem Cell **18**(1): 91-103.

Chiacchiera, F., A. Rossi, S. Jammula, M. Zanotti and D. Pasini (2016). "PRC2 preserves intestinal progenitors and restricts secretory lineage commitment." EMBO J **35**(21): 2301-2314.

Chiang, C., R. Z. Swan, M. Grachtchouk, M. Bolinger, Y. Litingtung, E. K. Robertson, M. K. Cooper, W. Gaffield, H. Westphal, P. A. Beachy and A. A. Dlugosz (1999). "Essential role for Sonic hedgehog during hair follicle morphogenesis." Dev Biol **205**(1): 1-9.

Cohen, I., D. Zhao, C. Bar, V. J. Valdes, K. L. Dauber-Decker, M. B. Nguyen, M. Nakayama, M. Rendl, W. A. Bickmore, H. Koseki, D. Zheng and E. Ezhkova (2018). "PRC1 Fine-tunes Gene Repression and Activation to Safeguard Skin Development and Stem Cell Specification." Cell Stem Cell **22**(5): 726-739 e727.

Cohen, I., D. Zhao, G. Menon, M. Nakayama, H. Koseki, D. Zheng and E. Ezhkova (2019). "PRC1 preserves epidermal tissue integrity independently of PRC2." Genes Dev **33**(1-2): 55-60.

Cohen, M., A. Kicheva, A. Ribeiro, R. Blassberg, K. M. Page, C. P. Barnes and J. Briscoe (2015). "Ptch1 and Gli regulate Shh signalling dynamics via multiple mechanisms." Nat Commun **6**: 6709.

Cotsarelis, G. (2006). "Epithelial stem cells: a folliculocentric view." J Invest Dermatol **126**(7): 1459-1468.

Cotsarelis, G., T. T. Sun and R. M. Lavker (1990). "Label-retaining cells reside in the bulge area of pilosebaceous unit: implications for follicular stem cells, hair cycle, and skin carcinogenesis." Cell **61**(7): 1329-1337.

Dauber, K. L., C. N. Perdigoto, V. J. Valdes, F. J. Santoriello, I. Cohen and E. Ezhkova (2016). "Dissecting the Roles of Polycomb Repressive Complex 2 Subunits in the Control of Skin Development." J Invest Dermatol **136**(8): 1647-1655.

de Lau, W., W. C. Peng, P. Gros and H. Clevers (2014). "The R-spondin/Lgr5/Rnf43 module: regulator of Wnt signal strength." Genes Dev **28**(4): 305-316.

de Napoles, M., J. E. Mermoud, R. Wakao, Y. A. Tang, M. Endoh, R. Appanah, T. B. Nesterova, J. Silva, A. P. Otte, M. Vidal, H. Koseki and N. Brockdorff (2004). "Polycomb group proteins Ring1A/B link ubiquitylation of histone H2A to heritable gene silencing and X inactivation." Dev Cell **7**(5): 663-676.

de Santa Barbara, P., G. R. van den Brink and D. J. Roberts (2003). "Development and differentiation of the intestinal epithelium." Cell Mol Life Sci **60**(7): 1322-1332.

Dekaney, C. M., A. S. Gulati, A. P. Garrison, M. A. Helmrath and S. J. Henning (2009). "Regeneration of intestinal stem/progenitor cells following doxorubicin treatment of mice." Am J Physiol Gastrointest Liver Physiol **297**(3): G461-470.

del Mar Lorente, M., C. Marcos-Gutierrez, C. Perez, J. Schoorlemmer, A. Ramirez, T. Magin and M. Vidal (2000). "Loss- and gain-of-function mutations show a polycomb group function for Ring1A in mice." Development **127**(23): 5093-5100.

Desta, Z., B. A. Ward, N. V. Soukhova and D. A. Flockhart (2004). "Comprehensive evaluation of tamoxifen sequential biotransformation by the human cytochrome P450 system in vitro: prominent roles for CYP3A and CYP2D6." J Pharmacol Exp Ther **310**(3): 1062-1075.

Dominski, Z. and W. F. Marzluff (2007). "Formation of the 3' end of histone mRNA: getting closer to the end." Gene **396**(2): 373-390.

Driskell, R. R., C. Clavel, M. Rendl and F. M. Watt (2011). "Hair follicle dermal papilla cells at a glance." J Cell Sci **124**(Pt 8): 1179-1182.

Elliott, E. N. and K. H. Kaestner (2015). "Epigenetic regulation of the intestinal epithelium." Cell Mol Life Sci **72**(21): 4139-4156.

Endoh, M., T. A. Endo, T. Endoh, Y. Fujimura, O. Ohara, T. Toyoda, A. P. Otte, M. Okano, N. Brockdorff, M. Vidal and H. Koseki (2008). "Polycomb group proteins Ring1A/B are functionally linked to the core transcriptional regulatory circuitry to maintain ES cell identity." Development **135**(8): 1513-1524.

Endoh, M., T. A. Endo, J. Shinga, K. Hayashi, A. Farcas, K. W. Ma, S. Ito, J. Sharif, T. Endoh, N. Onaga, M. Nakayama, T. Ishikura, O. Masui, B. M. Kessler, T. Suda, O. Ohara, A. Okuda, R. Klose and H. Koseki (2017). "PCGF6-PRC1 suppresses premature differentiation of mouse embryonic stem cells by regulating germ cell-related genes." Elife **6**.

Ernst, T., A. J. Chase, J. Score, C. E. Hidalgo-Curtis, C. Bryant, A. V. Jones, K. Waghorn, K. Zoi, F. M. Ross, A. Reiter, A. Hochhaus, H. G. Drexler, A. Duncombe, F. Cervantes, D. Oscier, J. Boultwood, F. H. Grand and N. C. Cross (2010). "Inactivating mutations of the histone methyltransferase gene EZH2 in myeloid disorders." Nat Genet **42**(8): 722-726.

Ezhkova, E., W. H. Lien, N. Stokes, H. A. Pasolli, J. M. Silva and E. Fuchs (2011). "EZH1 and EZH2 cogovern histone H3K27 trimethylation and are essential for hair follicle homeostasis and wound repair." Genes Dev **25**(5): 485-498.

Ezhkova, E., H. A. Pasolli, J. S. Parker, N. Stokes, I. H. Su, G. Hannon, A. Tarakhovsky and E. Fuchs (2009). "Ezh2 orchestrates gene expression for the stepwise differentiation of tissue-specific stem cells." Cell **136**(6): 1122-1135.

Faust, C., A. Schumacher, B. Holdener and T. Magnuson (1995). "The eed mutation disrupts anterior mesoderm production in mice." Development **121**(2): 273-285.

Ferrai, C., E. Torlai Triglia, J. R. Risner-Janiczek, T. Rito, O. J. Rackham, I. de Santiago, A. Kukalev, M. Nicodemi, A. Akalin, M. Li, M. A. Ungless and A. Pombo (2017). "RNA

polymerase II primes Polycomb-repressed developmental genes throughout terminal neuronal differentiation." Mol Syst Biol **13**(10): 946.

Ferrari, K. J., A. Scelfo, S. Jammula, A. Cuomo, I. Barozzi, A. Stutzer, W. Fischle, T. Bonaldi and D. Pasini (2014). "Polycomb-dependent H3K27me1 and H3K27me2 regulate active transcription and enhancer fidelity." Mol Cell **53**(1): 49-62.

Festa, E., J. Fretz, R. Berry, B. Schmidt, M. Rodeheffer, M. Horowitz and V. Horsley (2011). "Adipocyte lineage cells contribute to the skin stem cell niche to drive hair cycling." Cell **146**(5): 761-771.

Fevr, T., S. Robine, D. Louvard and J. Huelsken (2007). "Wnt/beta-catenin is essential for intestinal homeostasis and maintenance of intestinal stem cells." Mol Cell Biol **27**(21): 7551-7559.

Finch, A. J., L. Soucek, M. R. Junttila, L. B. Swigart and G. I. Evan (2009). "Acute overexpression of Myc in intestinal epithelium recapitulates some but not all the changes elicited by Wnt/beta-catenin pathway activation." Mol Cell Biol **29**(19): 5306-5315.

Forzati, F., A. Federico, P. Pallante, A. Abbate, F. Esposito, U. Malapelle, R. Sepe, G. Palma, G. Troncone, M. Scarfo, C. Arra, M. Fedele and A. Fusco (2012). "CBX7 is a tumor suppressor in mice and humans." J Clin Invest **122**(2): 612-623.

Foster, A. R., C. Nicu, M. R. Schneider, E. Hinde and R. Paus (2018). "Dermal white adipose tissue undergoes major morphological changes during the spontaneous and induced murine hair follicle cycling: a reappraisal." Arch Dermatol Res **310**(5): 453-462.

Friedmann-Morvinski, D. and I. M. Verma (2014). "Dedifferentiation and reprogramming: origins of cancer stem cells." EMBO Rep **15**(3): 244-253.

Fuchs, E. (2007). "Scratching the surface of skin development." Nature **445**(7130): 834-842.

Fuchs, E. (2008). "Skin stem cells: rising to the surface." J Cell Biol **180**(2): 273-284.

Fuchs, E. (2016). "Epithelial Skin Biology: Three Decades of Developmental Biology, a Hundred Questions Answered and a Thousand New Ones to Address." Curr Top Dev Biol **116**: 357-374.

Fursova, N. A., N. P. Blackledge, M. Nakayama, S. Ito, Y. Koseki, A. M. Farcas, H. W. King, H. Koseki and R. J. Klose (2019). "Synergy between Variant PRC1 Complexes Defines Polycomb-Mediated Gene Repression." Mol Cell **74**(5): 1020-1036 e1028.

Gao, Z., P. Lee, J. M. Stafford, M. von Schimmelmann, A. Schaefer and D. Reinberg (2014). "An AUTS2-Polycomb complex activates gene expression in the CNS." Nature **516**(7531): 349-354.

Gao, Z., J. Zhang, R. Bonasio, F. Strino, A. Sawai, F. Parisi, Y. Kluger and D. Reinberg (2012). "PCGF homologs, CBX proteins, and RYBP define functionally distinct PRC1 family complexes." Mol Cell **45**(3): 344-356.

Gehart, H. and H. Clevers (2019). "Tales from the crypt: new insights into intestinal stem cells." Nat Rev Gastroenterol Hepatol **16**(1): 19-34.

Genander, M., P. J. Cook, D. Ramskold, B. E. Keyes, A. F. Mertz, R. Sandberg and E. Fuchs (2014). "BMP signaling and its pSMAD1/5 target genes differentially regulate hair follicle stem cell lineages." Cell Stem Cell **15**(5): 619-633.

Greco, V., T. Chen, M. Rendl, M. Schober, H. A. Pasolli, N. Stokes, J. Dela Cruz-Racelis and E. Fuchs (2009). "A two-step mechanism for stem cell activation during hair regeneration." Cell Stem Cell **4**(2): 155-169.

Grinberg, I. and K. J. Millen (2005). "The ZIC gene family in development and disease." Clin Genet **67**(4): 290-296.

Guruharsha, K. G., M. W. Kankel and S. Artavanis-Tsakonas (2012). "The Notch signalling system: recent insights into the complexity of a conserved pathway." Nat Rev Genet **13**(9): 654-666.

Hanahan, D. and R. A. Weinberg (2000). "The hallmarks of cancer." Cell **100**(1): 57-70.

Hanahan, D. and R. A. Weinberg (2011). "Hallmarks of cancer: the next generation." Cell **144**(5): 646-674.

Hargreaves, D. C. and G. R. Crabtree (2011). "ATP-dependent chromatin remodeling: genetics, genomics and mechanisms." Cell Res **21**(3): 396-420.

Haupt, Y., W. S. Alexander, G. Barri, S. P. Klinken and J. M. Adams (1991). "Novel zinc finger gene implicated as myc collaborator by retrovirally accelerated lymphomagenesis in E mu-myc transgenic mice." Cell **65**(5): 753-763.

Haupt, Y., M. L. Bath, A. W. Harris and J. M. Adams (1993). "bmi-1 transgene induces lymphomas and collaborates with myc in tumorigenesis." Oncogene **8**(11): 3161-3164.

He, J., L. Shen, M. Wan, O. Taranova, H. Wu and Y. Zhang (2013). "Kdm2b maintains murine embryonic stem cell status by recruiting PRC1 complex to CpG islands of developmental genes." Nat Cell Biol **15**(4): 373-384.

He, X. C., J. Zhang, W. G. Tong, O. Tawfik, J. Ross, D. H. Scoville, Q. Tian, X. Zeng, X. He, L. M. Wiedemann, Y. Mishina and L. Li (2004). "BMP signaling inhibits intestinal stem cell self-renewal through suppression of Wnt-beta-catenin signaling." Nat Genet **36**(10): 1117-1121.

Headon, D. J. and P. A. Overbeek (1999). "Involvement of a novel Tnf receptor homologue in hair follicle induction." Nat Genet **22**(4): 370-374.

Hebert, J. M., T. Rosenquist, J. Gotz and G. R. Martin (1994). "FGF5 as a regulator of the hair growth cycle: evidence from targeted and spontaneous mutations." Cell **78**(6): 1017-1025.

Helin, K. and D. Dhanak (2013). "Chromatin proteins and modifications as drug targets." Nature **502**(7472): 480-488.

Hirabayashi, Y., N. Suzki, M. Tsuboi, T. A. Endo, T. Toyoda, J. Shinga, H. Koseki, M. Vidal and Y. Gotoh (2009). "Polycomb limits the neurogenic competence of neural precursor cells to promote astrogenic fate transition." Neuron **63**(5): 600-613.

Hoeck, J. D., B. Biehs, A. V. Kurtova, N. M. Kljavin, E. M. F. de Sousa, B. Alicke, H. Koeppen, Z. Modrusan, R. Piskol and F. J. de Sauvage (2017). "Stem cell plasticity enables hair regeneration following Lgr5(+) cell loss." Nat Cell Biol **19**(6): 666-676.

Howitt, M. R., S. Lavoie, M. Michaud, A. M. Blum, S. V. Tran, J. V. Weinstock, C. A. Gallini, K. Redding, R. F. Margolskee, L. C. Osborne, D. Artis and W. S. Garrett (2016). "Tuft cells, taste-chemosensory cells, orchestrate parasite type 2 immunity in the gut." Science **351**(6279): 1329-1333.

Hsu, Y. C., L. Li and E. Fuchs (2014). "Emerging interactions between skin stem cells and their niches." Nat Med **20**(8): 847-856.

Hsu, Y. C., L. Li and E. Fuchs (2014). "Transit-amplifying cells orchestrate stem cell activity and tissue regeneration." Cell **157**(4): 935-949.

Hsu, Y. C., H. A. Pasolli and E. Fuchs (2011). "Dynamics between stem cells, niche, and progeny in the hair follicle." Cell **144**(1): 92-105.

Huang da, W., B. T. Sherman and R. A. Lempicki (2009). "Systematic and integrative analysis of large gene lists using DAVID bioinformatics resources." Nat Protoc **4**(1): 44-57.

Huelsken, J., R. Vogel, B. Erdmann, G. Cotsarelis and W. Birchmeier (2001). "beta-Catenin controls hair follicle morphogenesis and stem cell differentiation in the skin." Cell **105**(4): 533-545.

Huh, S. H., K. Narhi, P. H. Lindfors, O. Haara, L. Yang, D. M. Ornitz and M. L. Mikkola (2013). "Fgf20 governs formation of primary and secondary dermal condensations in developing hair follicles." Genes Dev **27**(4): 450-458.

Illingworth, R. S. and A. P. Bird (2009). "CpG islands--'a rough guide'." FEBS Lett **583**(11): 1713-1720.

Ingham, P. W. (1983). "Differential expression of bithorax complex genes in the absence of the extra sex combs and trithorax genes." Nature **306**(5943): 591-593.

Ingham, P. W. (1985). "A clonal analysis of the requirement for the trithorax gene in the diversification of segments in Drosophila." J Embryol Exp Morphol **89**: 349-365.

Ingham, P. W. (1985). "Genetic control of the spatial pattern of selector gene expression in Drosophila." Cold Spring Harb Symp Quant Biol **50**: 201-208.

Ireland, H., R. Kemp, C. Houghton, L. Howard, A. R. Clarke, O. J. Sansom and D. J. Winton (2004). "Inducible Cre-mediated control of gene expression in the murine gastrointestinal tract: effect of loss of beta-catenin." Gastroenterology **126**(5): 1236-1246.

Ito, M., K. Kizawa, K. Hamada and G. Cotsarelis (2004). "Hair follicle stem cells in the lower bulge form the secondary germ, a biochemically distinct but functionally equivalent progenitor cell population, at the termination of catagen." Differentiation **72**(9-10): 548-557.

Jadhav, U., K. Nalapareddy, M. Saxena, N. K. O'Neill, L. Pinello, G. C. Yuan, S. H. Orkin and R. A. Shivdasani (2016). "Acquired Tissue-Specific Promoter Bivalency Is a Basis for PRC2 Necessity in Adult Cells." Cell **165**(6): 1389-1400.

Jaks, V., N. Barker, M. Kasper, J. H. van Es, H. J. Snippert, H. Clevers and R. Toftgard (2008). "Lgr5 marks cycling, yet long-lived, hair follicle stem cells." Nat Genet **40**(11): 1291-1299.

Jensen, J., E. E. Pedersen, P. Galante, J. Hald, R. S. Heller, M. Ishibashi, R. Kageyama, F. Guillemot, P. Serup and O. D. Madsen (2000). "Control of endodermal endocrine development by Hes-1." Nat Genet **24**(1): 36-44.

Jenuwein, T. and C. D. Allis (2001). "Translating the histone code." Science **293**(5532): 1074-1080.

Jones, P. A. and S. B. Baylin (2007). "The epigenomics of cancer." Cell **128**(4): 683-692.

Joost, S., A. Zeisel, T. Jacob, X. Sun, G. La Manno, P. Lonnerberg, S. Linnarsson and M. Kasper (2016). "Single-Cell Transcriptomics Reveals that Differentiation and Spatial Signatures Shape Epidermal and Hair Follicle Heterogeneity." Cell Syst **3**(3): 221-237 e229.

Kayahara, T., M. Sawada, S. Takaishi, H. Fukui, H. Seno, H. Fukuzawa, K. Suzuki, H. Hiai, R. Kageyama, H. Okano and T. Chiba (2003). "Candidate markers for stem and early progenitor cells, Musashi-1 and Hes1, are expressed in crypt base columnar cells of mouse small intestine." FEBS Lett **535**(1-3): 131-135.

Kennison, J. A. and J. W. Tamkun (1988). "Dosage-dependent modifiers of polycomb and antennapedia mutations in Drosophila." Proc Natl Acad Sci U S A **85**(21): 8136-8140.

Ketel, C. S., E. F. Andersen, M. L. Vargas, J. Suh, S. Strome and J. A. Simon (2005). "Subunit contributions to histone methyltransferase activities of fly and worm polycomb group complexes." Mol Cell Biol **25**(16): 6857-6868.

Klauke, K., V. Radulovic, M. Broekhuis, E. Weersing, E. Zwart, S. Olthof, M. Ritsema, S. Bruggeman, X. Wu, K. Helin, L. Bystrykh and G. de Haan (2013). "Polycomb Cbx family members mediate the balance between haematopoietic stem cell self-renewal and differentiation." Nat Cell Biol **15**(4): 353-362.

Kleer, C. G., Q. Cao, S. Varambally, R. Shen, I. Ota, S. A. Tomlins, D. Ghosh, R. G. Sewalt, A. P. Otte, D. F. Hayes, M. S. Sabel, D. Livant, S. J. Weiss, M. A. Rubin and A. M. Chinnaiyan (2003). "EZH2 is a marker of aggressive breast cancer and promotes neoplastic transformation of breast epithelial cells." Proc Natl Acad Sci U S A **100**(20): 11606-11611.
Kornberg, R. D. (1974). "Chromatin structure: a repeating unit of histones and DNA." Science **184**(4139): 868-871.

Kornberg, R. D. and J. O. Thomas (1974). "Chromatin structure; oligomers of the histones." Science **184**(4139): 865-868.

Kouzarides, T. (2007). "Chromatin modifications and their function." Cell **128**(4): 693-705.

Ku, M., R. P. Koche, E. Rheinbay, E. M. Mendenhall, M. Endoh, T. S. Mikkelsen, A. Presser, C. Nusbaum, X. Xie, A. S. Chi, M. Adli, S. Kasif, L. M. Ptaszek, C. A. Cowan, E. S. Lander, H. Koseki and B. E. Bernstein (2008). "Genomewide analysis of PRC1 and PRC2 occupancy identifies two classes of bivalent domains." PLoS Genet **4**(10): e1000242.

Langmead, B., C. Trapnell, M. Pop and S. L. Salzberg (2009). "Ultrafast and memory-efficient alignment of short DNA sequences to the human genome." Genome Biol **10**(3): R25.

Lee, D., M. Yu, E. Lee, H. Kim, Y. Yang, K. Kim, C. Pannicia, J. M. Kurie and D. W. Threadgill (2009). "Tumor-specific apoptosis caused by deletion of the ERBB3 pseudo-kinase in mouse intestinal epithelium." J Clin Invest **119**(9): 2702-2713.

Leung, C., S. H. Tan and N. Barker (2018). "Recent Advances in Lgr5(+) Stem Cell Research." Trends Cell Biol **28**(5): 380-391.

Levine, M. and R. Tjian (2003). "Transcription regulation and animal diversity." Nature **424**(6945): 147-151.

Lewis, E. B. (1978). "A gene complex controlling segmentation in Drosophila." Nature **276**(5688): 565-570.

Li, E. (2002). "Chromatin modification and epigenetic reprogramming in mammalian development." Nat Rev Genet **3**(9): 662-673.

Li, G., R. Margueron, M. Ku, P. Chambon, B. E. Bernstein and D. Reinberg (2010). "Jarid2 and PRC2, partners in regulating gene expression." Genes Dev **24**(4): 368-380.

Lien, W. H., X. Guo, L. Polak, L. N. Lawton, R. A. Young, D. Zheng and E. Fuchs (2011). "Genome-wide maps of histone modifications unwind in vivo chromatin states of the hair follicle lineage." Cell Stem Cell **9**(3): 219-232.

Lien, W. H., L. Polak, M. Lin, K. Lay, D. Zheng and E. Fuchs (2014). "In vivo transcriptional governance of hair follicle stem cells by canonical Wnt regulators." Nat Cell Biol **16**(2): 179-190.

Lin, K. K., D. Chudova, G. W. Hatfield, P. Smyth and B. Andersen (2004). "Identification of hair cycle-associated genes from time-course gene expression profile data by using replicate variance." Proc Natl Acad Sci U S A **101**(45): 15955-15960.

Liu, S., H. Zhang and E. Duan (2013). "Epidermal development in mammals: key regulators, signals from beneath, and stem cells." Int J Mol Sci **14**(6): 10869-10895.

Love, M. I., W. Huber and S. Anders (2014). "Moderated estimation of fold change and dispersion for RNA-seq data with DESeq2." Genome Biol **15**(12): 550.

Lynch, M. D., A. J. Smith, M. De Gobbi, M. Flenley, J. R. Hughes, D. Vernimmen, H. Ayyub, J. A. Sharpe, J. A. Sloane-Stanley, L. Sutherland, S. Meek, T. Burdon, R. J. Gibbons, D. Garrick and D. R. Higgs (2012). "An interspecies analysis reveals a key role for unmethylated CpG dinucleotides in vertebrate Polycomb complex recruitment." EMBO J **31**(2): 317-329.

Mallo, M. and C. R. Alonso (2013). "The regulation of Hox gene expression during animal development." Development **140**(19): 3951-3963.

Margueron, R., N. Justin, K. Ohno, M. L. Sharpe, J. Son, W. J. Drury, 3rd, P. Voigt, S. R. Martin, W. R. Taylor, V. De Marco, V. Pirrotta, D. Reinberg and S. J. Gamblin (2009). "Role of the polycomb protein EED in the propagation of repressive histone marks." Nature **461**(7265): 762-767.

Margueron, R., G. Li, K. Sarma, A. Blais, J. Zavadil, C. L. Woodcock, B. D. Dynlacht and D. Reinberg (2008). "Ezh1 and Ezh2 maintain repressive chromatin through different mechanisms." Mol Cell **32**(4): 503-518.

Margueron, R. and D. Reinberg (2011). "The Polycomb complex PRC2 and its mark in life." Nature **469**(7330): 343-349.

Marzluff, W. F. and R. J. Duronio (2002). "Histone mRNA expression: multiple levels of cell cycle regulation and important developmental consequences." Curr Opin Cell Biol **14**(6): 692-699.

Mendenhall, E. M., R. P. Koche, T. Truong, V. W. Zhou, B. Issac, A. S. Chi, M. Ku and B. E. Bernstein (2010). "GC-rich sequence elements recruit PRC2 in mammalian ES cells." PLoS Genet **6**(12): e1001244.

Metcalfe, C., N. M. Kljavin, R. Ybarra and F. J. de Sauvage (2014). "Lgr5+ stem cells are indispensable for radiation-induced intestinal regeneration." Cell Stem Cell **14**(2): 149-159.

Miettinen, P. J., J. E. Berger, J. Meneses, Y. Phung, R. A. Pedersen, Z. Werb and R. Derynck (1995). "Epithelial immaturity and multiorgan failure in mice lacking epidermal growth factor receptor." Nature **376**(6538): 337-341.

Mikkelsen, T. S., M. Ku, D. B. Jaffe, B. Issac, E. Lieberman, G. Giannoukos, P. Alvarez, W. Brockman, T. K. Kim, R. P. Koche, W. Lee, E. Mendenhall, A. O'Donovan, A. Presser, C. Russ, X. Xie, A. Meissner, M. Wernig, R. Jaenisch, C. Nusbaum, E. S. Lander and B. E. Bernstein (2007). "Genome-wide maps of chromatin state in pluripotent and lineage-committed cells." Nature **448**(7153): 553-560.

Mohammad, H. P. and S. B. Baylin (2010). "Linking cell signaling and the epigenetic machinery." Nat Biotechnol **28**(10): 1033-1038.

Mohn, F., M. Weber, M. Rebhan, T. C. Roloff, J. Richter, M. B. Stadler, M. Bibel and D. Schubeler (2008). "Lineage-specific polycomb targets and de novo DNA methylation define restriction and potential of neuronal progenitors." Mol Cell **30**(6): 755-766.

Mohty, M., A. S. Yong, R. M. Szydlo, J. F. Apperley and J. V. Melo (2007). "The polycomb group BMI1 gene is a molecular marker for predicting prognosis of chronic myeloid leukemia." Blood **110**(1): 380-383.

Montgomery, R. K., D. L. Carlone, C. A. Richmond, L. Farilla, M. E. Kranendonk, D. E. Henderson, N. Y. Baffour-Awuah, D. M. Ambruzs, L. K. Fogli, S. Algra and D. T. Breault (2011). "Mouse telomerase reverse transcriptase (mTert) expression marks slowly cycling intestinal stem cells." Proc Natl Acad Sci U S A **108**(1): 179-184.

Morey, L., L. Aloia, L. Cozzuto, S. A. Benitah and L. Di Croce (2013). "RYBP and Cbx7 define specific biological functions of polycomb complexes in mouse embryonic stem cells." Cell Rep **3**(1): 60-69.

Morey, L. and K. Helin (2010). "Polycomb group protein-mediated repression of transcription." Trends Biochem Sci **35**(6): 323-332.

Morey, L., G. Pascual, L. Cozzuto, G. Roma, A. Wutz, S. A. Benitah and L. Di Croce (2012). "Nonoverlapping functions of the Polycomb group Cbx family of proteins in embryonic stem cells." Cell Stem Cell **10**(1): 47-62.

Morgan, B. A. (2008). "A glorious revolution in stem cell biology." Nat Genet **40**(11): 1269-1270.

Morin, R. D., N. A. Johnson, T. M. Severson, A. J. Mungall, J. An, R. Goya, J. E. Paul, M. Boyle, B. W. Woolcock, F. Kuchenbauer, D. Yap, R. K. Humphries, O. L. Griffith, S. Shah, H. Zhu, M. Kimbara, P. Shashkin, J. F. Charlot, M. Tcherpakov, R. Corbett, A. Tam, R. Varhol, D. Smailus, M. Moksa, Y. Zhao, A. Delaney, H. Qian, I. Birol, J. Schein, R. Moore, R. Holt, D. E. Horsman, J. M. Connors, S. Jones, S. Aparicio, M. Hirst, R. D. Gascoyne and M. A. Marra (2010). "Somatic mutations altering EZH2 (Tyr641) in follicular and diffuse large B-cell lymphomas of germinal-center origin." Nat Genet **42**(2): 181-185.

Moriyama, M., A. D. Durham, H. Moriyama, K. Hasegawa, S. Nishikawa, F. Radtke and M. Osawa (2008). "Multiple roles of Notch signaling in the regulation of epidermal development." Dev Cell **14**(4): 594-604.

Morris, R. J., Y. Liu, L. Marles, Z. Yang, C. Trempus, S. Li, J. S. Lin, J. A. Sawicki and G. Cotsarelis (2004). "Capturing and profiling adult hair follicle stem cells." Nat Biotechnol **22**(4): 411-417.

Mortimer, T., E. N. Wainwright, H. Patel, B. M. Siow, Z. Jaunmuktane, S. Brandner and P. Scaffidi (2019). "Redistribution of EZH2 promotes malignant phenotypes by rewiring developmental programmes." EMBO Rep: e48155.

Mousavi, K., H. Zare, A. H. Wang and V. Sartorelli (2012). "Polycomb protein Ezh1 promotes RNA polymerase II elongation." Mol Cell **45**(2): 255-262.

Muller, J., C. M. Hart, N. J. Francis, M. L. Vargas, A. Sengupta, B. Wild, E. L. Miller, M. B. O'Connor, R. E. Kingston and J. A. Simon (2002). "Histone methyltransferase activity of a Drosophila Polycomb group repressor complex." Cell **111**(2): 197-208.

Muller-Rover, S., B. Handjiski, C. van der Veen, S. Eichmuller, K. Foitzik, I. A. McKay, K. S. Stenn and R. Paus (2001). "A comprehensive guide for the accurate classification of murine hair follicles in distinct hair cycle stages." J Invest Dermatol **117**(1): 3-15.

Murali, R., T. Wiesner and R. A. Scolyer (2013). "Tumours associated with BAP1 mutations." Pathology **45**(2): 116-126.

Narhi, K., E. Jarvinen, W. Birchmeier, M. M. Taketo, M. L. Mikkola and I. Thesleff (2008). "Sustained epithelial beta-catenin activity induces precocious hair development but disrupts hair follicle down-growth and hair shaft formation." Development **135**(6): 1019-1028.

Nowak, J. A., L. Polak, H. A. Pasolli and E. Fuchs (2008). "Hair follicle stem cells are specified and function in early skin morphogenesis." Cell Stem Cell **3**(1): 33-43.

Ntziachristos, P., A. Tsirigos, P. Van Vlierberghe, J. Nedjic, T. Trimarchi, M. S. Flaherty, D. Ferres-Marco, V. da Ros, Z. Tang, J. Siegle, P. Asp, M. Hadler, I. Rigo, K. De Keersmaecker, J. Patel, T. Huynh, F. Utro, S. Poglio, J. B. Samon, E. Paietta, J. Racevskis, J. M. Rowe, R. Rabadan, R. L. Levine, S. Brown, F. Pflumio, M. Dominguez, A. Ferrando and I. Aifantis (2012). "Genetic inactivation of the polycomb repressive complex 2 in T cell acute lymphoblastic leukemia." Nat Med **18**(2): 298-301.

Nusse, R. and H. Clevers (2017). "Wnt/beta-Catenin Signaling, Disease, and Emerging Therapeutic Modalities." Cell **169**(6): 985-999.

O'Carroll, D., S. Erhardt, M. Pagani, S. C. Barton, M. A. Surani and T. Jenuwein (2001). "The polycomb-group gene Ezh2 is required for early mouse development." Mol Cell Biol **21**(13): 4330-4336.

O'Loghlen, A., A. M. Munoz-Cabello, A. Gaspar-Maia, H. A. Wu, A. Banito, N. Kunowska, T. Racek, H. N. Pemberton, P. Beolchi, F. Lavial, O. Masui, M. Vermeulen, T. Carroll, J. Graumann, E. Heard, N. Dillon, V. Azuara, A. P. Snijders, G. Peters, E. Bernstein and J. Gil (2012). "MicroRNA regulation of Cbx7 mediates a switch of Polycomb orthologs during ESC differentiation." Cell Stem Cell **10**(1): 33-46.

Ogawa, H., K. Ishiguro, S. Gaubatz, D. M. Livingston and Y. Nakatani (2002). "A complex with chromatin modifiers that occupies E2F- and Myc-responsive genes in G0 cells." Science **296**(5570): 1132-1136.

Oguro, H., J. Yuan, H. Ichikawa, T. Ikawa, S. Yamazaki, H. Kawamoto, H. Nakauchi and A. Iwama (2010). "Poised lineage specification in multipotential hematopoietic stem and progenitor cells by the polycomb protein Bmi1." Cell Stem Cell **6**(3): 279-286.

Okano, M., D. W. Bell, D. A. Haber and E. Li (1999). "DNA methyltransferases Dnmt3a and Dnmt3b are essential for de novo methylation and mammalian development." Cell **99**(3): 247-257.

Okano, M., S. Xie and E. Li (1998). "Dnmt2 is not required for de novo and maintenance methylation of viral DNA in embryonic stem cells." Nucleic Acids Res **26**(11): 2536-2540.

Orkin, S. H. and K. Hochedlinger (2011). "Chromatin connections to pluripotency and cellular reprogramming." Cell **145**(6): 835-850.

Oshima, H., A. Rochat, C. Kedzia, K. Kobayashi and Y. Barrandon (2001). "Morphogenesis and renewal of hair follicles from adult multipotent stem cells." Cell **104**(2): 233-245.

Oumard, A., J. Qiao, T. Jostock, J. Li and J. Bode (2006). "Recommended Method for Chromosome Exploitation: RMCE-based Cassette-exchange Systems in Animal Cell Biotechnology." Cytotechnology **50**(1-3): 93-108.

Park, I. K., D. Qian, M. Kiel, M. W. Becker, M. Pihalja, I. L. Weissman, S. J. Morrison and M. F. Clarke (2003). "Bmi-1 is required for maintenance of adult self-renewing haematopoietic stem cells." Nature **423**(6937): 302-305.

Pasini, D., A. P. Bracken, J. B. Hansen, M. Capillo and K. Helin (2007). "The polycomb group protein Suz12 is required for embryonic stem cell differentiation." Mol Cell Biol **27**(10): 3769-3779.

Pasini, D., A. P. Bracken, M. R. Jensen, E. Lazzerini Denchi and K. Helin (2004). "Suz12 is essential for mouse development and for EZH2 histone methyltransferase activity." EMBO J **23**(20): 4061-4071.

Pasini, D., P. A. Cloos, J. Walfridsson, L. Olsson, J. P. Bukowski, J. V. Johansen, M. Bak, N. Tommerup, J. Rappsilber and K. Helin (2010). "JARID2 regulates binding of the Polycomb repressive complex 2 to target genes in ES cells." Nature **464**(7286): 306-310.

Pasini, D. and L. Di Croce (2016). "Emerging roles for Polycomb proteins in cancer." Curr Opin Genet Dev **36**: 50-58.

Paus, R. and K. Foitzik (2004). "In search of the "hair cycle clock": a guided tour." Differentiation **72**(9-10): 489-511.

Paus, R., S. Muller-Rover, C. Van Der Veen, M. Maurer, S. Eichmuller, G. Ling, U. Hofmann, K. Foitzik, L. Mecklenburg and B. Handjiski (1999). "A comprehensive guide for the recognition and classification of distinct stages of hair follicle morphogenesis." J Invest Dermatol **113**(4): 523-532.

Picelli, S., O. R. Faridani, A. K. Bjorklund, G. Winberg, S. Sagasser and R. Sandberg (2014). "Full-length RNA-seq from single cells using Smart-seq2." Nat Protoc **9**(1): 171-181.

Pickart, C. M. (2001). "Mechanisms underlying ubiquitination." Annu Rev Biochem **70**: 503-533.

Pivetti, S., D. Fernandez-Perez, A. D'Ambrosio, C. M. Barbieri, D. Manganaro, A. Rossi, L. Barnabei, M. Zanotti, A. Scelfo, F. Chiacchiera and D. Pasini (2019). "Loss of PRC1 activity in different stem cell compartments activates a common transcriptional program with cell type-dependent outcomes." Sci Adv **5**(5): eaav1594.

Plikus, M. V., J. A. Mayer, D. de la Cruz, R. E. Baker, P. K. Maini, R. Maxson and C. M. Chuong (2008). "Cyclic dermal BMP signalling regulates stem cell activation during hair regeneration." Nature **451**(7176): 340-344.

Potten, C. S. (1977). "Extreme sensitivity of some intestinal crypt cells to X and gamma irradiation." Nature **269**(5628): 518-521.

Powell, A. E., Y. Wang, Y. Li, E. J. Poulin, A. L. Means, M. K. Washington, J. N. Higginbotham, A. Juchheim, N. Prasad, S. E. Levy, Y. Guo, Y. Shyr, B. J. Aronow, K. M.

Haigis, J. L. Franklin and R. J. Coffey (2012). "The pan-ErbB negative regulator Lrig1 is an intestinal stem cell marker that functions as a tumor suppressor." Cell **149**(1): 146-158.

Poynter, S. T. and C. Kadoch (2016). "Polycomb and trithorax opposition in development and disease." Wiley Interdiscip Rev Dev Biol **5**(6): 659-688.

Qi, Z., Y. Li, B. Zhao, C. Xu, Y. Liu, H. Li, B. Zhang, X. Wang, X. Yang, W. Xie, B. Li, J. J. Han and Y. G. Chen (2017). "BMP restricts stemness of intestinal Lgr5(+) stem cells by directly suppressing their signature genes." Nat Commun **8**: 13824.

Raaphorst, F. M. (2005). "Deregulated expression of Polycomb-group oncogenes in human malignant lymphomas and epithelial tumors." Hum Mol Genet **14 Spec No 1**: R93-R100.

Ramirez, F., D. P. Ryan, B. Gruning, V. Bhardwaj, F. Kilpert, A. S. Richter, S. Heyne, F. Dundar and T. Manke (2016). "deepTools2: a next generation web server for deep-sequencing data analysis." Nucleic Acids Res **44**(W1): W160-165.

Rendl, M., L. Lewis and E. Fuchs (2005). "Molecular dissection of mesenchymal-epithelial interactions in the hair follicle." PLoS Biol **3**(11): e331.

Rezza, A., Z. Wang, R. Sennett, W. Qiao, D. Wang, N. Heitman, K. W. Mok, C. Clavel, R. Yi, P. Zandstra, A. Ma'ayan and M. Rendl (2016). "Signaling Networks among Stem Cell Precursors, Transit-Amplifying Progenitors, and their Niche in Developing Hair Follicles." Cell Rep **14**(12): 3001-3018.

Rhee, H., L. Polak and E. Fuchs (2006). "Lhx2 maintains stem cell character in hair follicles." Science **312**(5782): 1946-1949.

Richly, H., L. Aloia and L. Di Croce (2011). "Roles of the Polycomb group proteins in stem cells and cancer." Cell Death Dis **2**: e204.

Richmond, T. J. and C. A. Davey (2003). "The structure of DNA in the nucleosome core." Nature **423**(6936): 145-150.

Riising, E. M., I. Comet, B. Leblanc, X. Wu, J. V. Johansen and K. Helin (2014). "Gene silencing triggers polycomb repressive complex 2 recruitment to CpG islands genome wide." Mol Cell **55**(3): 347-360.

Rinaldi, L. and S. A. Benitah (2015). "Epigenetic regulation of adult stem cell function." FEBS J **282**(9): 1589-1604.

Rinn, J. L., M. Kertesz, J. K. Wang, S. L. Squazzo, X. Xu, S. A. Brugmann, L. H. Goodnough, J. A. Helms, P. J. Farnham, E. Segal and H. Y. Chang (2007). "Functional demarcation of active and silent chromatin domains in human HOX loci by noncoding RNAs." Cell **129**(7): 1311-1323.

Rodriguez-Colman, M. J., M. Schewe, M. Meerlo, E. Stigter, J. Gerrits, M. Pras-Raves, A. Sacchetti, M. Hornsveld, K. C. Oost, H. J. Snippert, N. Verhoeven-Duif, R. Fodde and B. M. Burgering (2017). "Interplay between metabolic identities in the intestinal crypt supports stem cell function." Nature **543**(7645): 424-427.

Rohs, R., S. M. West, A. Sosinsky, P. Liu, R. S. Mann and B. Honig (2009). "The role of DNA shape in protein-DNA recognition." Nature **461**(7268): 1248-1253.

Roman-Trufero, M., H. R. Mendez-Gomez, C. Perez, A. Hijikata, Y. Fujimura, T. Endo, H. Koseki, C. Vicario-Abejon and M. Vidal (2009). "Maintenance of undifferentiated state and self-renewal of embryonic neural stem cells by Polycomb protein Ring1B." Stem Cells **27**(7): 1559-1570.

Rompolas, P., K. R. Mesa and V. Greco (2013). "Spatial organization within a niche as a determinant of stem-cell fate." Nature **502**(7472): 513-518.

Rosen, E. D. and B. M. Spiegelman (2014). "What we talk about when we talk about fat." Cell **156**(1-2): 20-44.

Ross, K., A. K. Sedello, G. P. Todd, M. Paszkowski-Rogacz, A. W. Bird, L. Ding, T. Grinenko, K. Behrens, N. Hubner, M. Mann, C. Waskow, C. Stocking and F. Buchholz (2012). "Polycomb group ring finger 1 cooperates with Runx1 in regulating differentiation and self-renewal of hematopoietic cells." Blood **119**(18): 4152-4161.

Rothbart, S. B. and B. D. Strahl (2014). "Interpreting the language of histone and DNA modifications." Biochim Biophys Acta **1839**(8): 627-643.

Roy, N. and M. Hebrok (2015). "Regulation of Cellular Identity in Cancer." Dev Cell **35**(6): 674-684.

Sancho, R., C. A. Cremona and A. Behrens (2015). "Stem cell and progenitor fate in the mammalian intestine: Notch and lateral inhibition in homeostasis and disease." EMBO Rep **16**(5): 571-581.

Sangiorgi, E. and M. R. Capecchi (2008). "Bmi1 is expressed in vivo in intestinal stem cells." Nat Genet **40**(7): 915-920.

Sato, T., J. H. van Es, H. J. Snippert, D. E. Stange, R. G. Vries, M. van den Born, N. Barker, N. F. Shroyer, M. van de Wetering and H. Clevers (2011). "Paneth cells constitute the niche for Lgr5 stem cells in intestinal crypts." Nature **469**(7330): 415-418.

Saxena, N., K. W. Mok and M. Rendl (2019). "An updated classification of hair follicle morphogenesis." Exp Dermatol **28**(4): 332-344.

Scelfo, A., D. Fernandez-Perez, S. Tamburri, M. Zanotti, E. Lavarone, M. Soldi, T. Bonaldi, K. J. Ferrari and D. Pasini (2019). "Functional Landscape of PCGF Proteins Reveals Both RING1A/B-Dependent-and RING1A/B-Independent-Specific Activities." Mol Cell **74**(5): 1037-1052 e1037.

Scelfo, A., A. Piunti and D. Pasini (2015). "The controversial role of the Polycomb group proteins in transcription and cancer: how much do we not understand Polycomb proteins?" FEBS J **282**(9): 1703-1722.

Scheuermann, J. C., A. G. de Ayala Alonso, K. Oktaba, N. Ly-Hartig, R. K. McGinty, S. Fraterman, M. Wilm, T. W. Muir and J. Muller (2010). "Histone H2A deubiquitinase activity of the Polycomb repressive complex PR-DUB." Nature **465**(7295): 243-247.

Schmidt-Ullrich, R., D. J. Tobin, D. Lenhard, P. Schneider, R. Paus and C. Scheidereit (2006). "NF-kappaB transmits Eda A1/EdaR signalling to activate Shh and cyclin D1

expression, and controls post-initiation hair placode down growth." Development **133**(6): 1045-1057.

Schneider, M. R., R. Schmidt-Ullrich and R. Paus (2009). "The hair follicle as a dynamic miniorgan." Curr Biol **19**(3): R132-142.

Schoeftner, S., A. K. Sengupta, S. Kubicek, K. Mechtler, L. Spahn, H. Koseki, T. Jenuwein and A. Wutz (2006). "Recruitment of PRC1 function at the initiation of X inactivation independent of PRC2 and silencing." EMBO J **25**(13): 3110-3122.

Schuettengruber, B., H. M. Bourbon, L. Di Croce and G. Cavalli (2017). "Genome Regulation by Polycomb and Trithorax: 70 Years and Counting." Cell **171**(1): 34-57.

Schwartz, Y. B. and V. Pirrotta (2013). "A new world of Polycombs: unexpected partnerships and emerging functions." Nat Rev Genet **14**(12): 853-864.

Schwartz, Y. B. and V. Pirrotta (2014). "Ruled by ubiquitylation: a new order for polycomb recruitment." Cell Rep **8**(2): 321-325.

Scott, C. L., J. Gil, E. Hernando, J. Teruya-Feldstein, M. Narita, D. Martinez, T. Visakorpi, D. Mu, C. Cordon-Cardo, G. Peters, D. Beach and S. W. Lowe (2007). "Role of the chromobox protein CBX7 in lymphomagenesis." Proc Natl Acad Sci U S A **104**(13): 5389-5394.

Scoville, D. H., T. Sato, X. C. He and L. Li (2008). "Current view: intestinal stem cells and signaling." Gastroenterology **134**(3): 849-864.

Sengupta, A. K., A. Kuhrs and J. Muller (2004). "General transcriptional silencing by a Polycomb response element in Drosophila." Development **131**(9): 1959-1965.

Shafaroudi, A. M., S. J. Mowla, S. A. Ziaee, A. R. Bahrami, Y. Atlasi and M. Malakootian (2008). "Overexpression of BMI1, a polycomb group repressor protein, in bladder tumors: a preliminary report." Urol J **5**(2): 99-105.

Shilatifard, A. (2012). "The COMPASS family of histone H3K4 methylases: mechanisms of regulation in development and disease pathogenesis." Annu Rev Biochem **81**: 65-95.

Shinjo, K., Y. Yamashita, E. Yamamoto, S. Akatsuka, N. Uno, A. Kamiya, K. Niimi, Y. Sakaguchi, T. Nagasaka, T. Takahashi, K. Shibata, H. Kajiyama, F. Kikkawa and S. Toyokuni (2014). "Expression of chromobox homolog 7 (CBX7) is associated with poor prognosis in ovarian clear cell adenocarcinoma via TRAIL-induced apoptotic pathway regulation." Int J Cancer **135**(2): 308-318.

Slominski, A., R. Paus and R. Costantino (1991). "Differential expression and activity of melanogenesis-related proteins during induced hair growth in mice." J Invest Dermatol **96**(2): 172-179.

Smits, A. H., P. W. Jansen, I. Poser, A. A. Hyman and M. Vermeulen (2013). "Stoichiometry of chromatin-associated protein complexes revealed by label-free quantitative mass spectrometry-based proteomics." Nucleic Acids Res **41**(1): e28.

Sneeringer, C. J., M. P. Scott, K. W. Kuntz, S. K. Knutson, R. M. Pollock, V. M. Richon and R. A. Copeland (2010). "Coordinated activities of wild-type plus mutant EZH2 drive tumor-associated hypertrimethylation of lysine 27 on histone H3 (H3K27) in human B-cell lymphomas." Proc Natl Acad Sci U S A **107**(49): 20980-20985.

Sparmann, A. and M. van Lohuizen (2006). "Polycomb silencers control cell fate, development and cancer." Nat Rev Cancer **6**(11): 846-856.

St-Jacques, B., H. R. Dassule, I. Karavanova, V. A. Botchkarev, J. Li, P. S. Danielian, J. A. McMahon, P. M. Lewis, R. Paus and A. P. McMahon (1998). "Sonic hedgehog signaling is essential for hair development." Curr Biol **8**(19): 1058-1068.

Stielow, B., F. Finkernagel, T. Stiewe, A. Nist and G. Suske (2018). "MGA, L3MBTL2 and E2F6 determine genomic binding of the non-canonical Polycomb repressive complex PRC1.6." PLoS Genet **14**(1): e1007193.

Stock, J. K., S. Giadrossi, M. Casanova, E. Brookes, M. Vidal, H. Koseki, N. Brockdorff, A. G. Fisher and A. Pombo (2007). "Ring1-mediated ubiquitination of H2A restrains poised RNA polymerase II at bivalent genes in mouse ES cells." Nat Cell Biol **9**(12): 1428-1435.

Struhl, G. and M. Akam (1985). "Altered distributions of Ultrabithorax transcripts in extra sex combs mutant embryos of Drosophila." EMBO J **4**(12): 3259-3264.

Subramanian, A., P. Tamayo, V. K. Mootha, S. Mukherjee, B. L. Ebert, M. A. Gillette, A. Paulovich, S. L. Pomeroy, T. R. Golub, E. S. Lander and J. P. Mesirov (2005). "Gene set enrichment analysis: a knowledge-based approach for interpreting genome-wide expression profiles." Proc Natl Acad Sci U S A **102**(43): 15545-15550.

Sudarsanam, P. and F. Winston (2000). "The Swi/Snf family nucleosome-remodeling complexes and transcriptional control." Trends Genet **16**(8): 345-351.

Suzuki, K., H. Fukui, T. Kayahara, M. Sawada, H. Seno, H. Hiai, R. Kageyama, H. Okano and T. Chiba (2005). "Hes1-deficient mice show precocious differentiation of Paneth cells in the small intestine." Biochem Biophys Res Commun **328**(1): 348-352.

Szenker, E., D. Ray-Gallet and G. Almouzni (2011). "The double face of the histone variant H3.3." Cell Res **21**(3): 421-434.

Takebe, N., P. J. Harris, R. Q. Warren and S. P. Ivy (2011). "Targeting cancer stem cells by inhibiting Wnt, Notch, and Hedgehog pathways." Nat Rev Clin Oncol **8**(2): 97-106.

Takeda, N., R. Jain, M. R. LeBoeuf, Q. Wang, M. M. Lu and J. A. Epstein (2011). "Interconversion between intestinal stem cell populations in distinct niches." Science **334**(6061): 1420-1424.

Takeuchi, T., Y. Yamazaki, Y. Katoh-Fukui, R. Tsuchiya, S. Kondo, J. Motoyama and T. Higashinakagawa (1995). "Gene trap capture of a novel mouse gene, jumonji, required for neural tube formation." Genes Dev **9**(10): 1211-1222.

Talbert, P. B. and S. Henikoff (2017). "Histone variants on the move: substrates for chromatin dynamics." Nat Rev Mol Cell Biol **18**(2): 115-126.

Tavares, L., E. Dimitrova, D. Oxley, J. Webster, R. Poot, J. Demmers, K. Bezstarosti, S. Taylor, H. Ura, H. Koide, A. Wutz, M. Vidal, S. Elderkin and N. Brockdorff (2012). "RYBP-

PRC1 complexes mediate H2A ubiquitylation at polycomb target sites independently of PRC2 and H3K27me3." Cell **148**(4): 664-678.

Tetteh, P. W., H. F. Farin and H. Clevers (2015). "Plasticity within stem cell hierarchies in mammalian epithelia." Trends Cell Biol **25**(2): 100-108.

Threadgill, D. W., A. A. Dlugosz, L. A. Hansen, T. Tennenbaum, U. Lichti, D. Yee, C. LaMantia, T. Mourton, K. Herrup, R. C. Harris and et al. (1995). "Targeted disruption of mouse EGF receptor: effect of genetic background on mutant phenotype." Science **269**(5221): 230-234.

Tian, H., B. Biehs, S. Warming, K. G. Leong, L. Rangell, O. D. Klein and F. J. de Sauvage (2011). "A reserve stem cell population in small intestine renders Lgr5-positive cells dispensable." Nature **478**(7368): 255-259.

Tomann, P., R. Paus, S. E. Millar, C. Scheidereit and R. Schmidt-Ullrich (2016). "Lhx2 is a direct NF-kappaB target gene that promotes primary hair follicle placode down-growth." Development **143**(9): 1512-1522.

Trapnell, C., L. Pachter and S. L. Salzberg (2009). "TopHat: discovering splice junctions with RNA-Seq." Bioinformatics **25**(9): 1105-1111.

Trempus, C. S., R. J. Morris, C. D. Bortner, G. Cotsarelis, R. S. Faircloth, J. M. Reece and R. W. Tennant (2003). "Enrichment for living murine keratinocytes from the hair follicle bulge with the cell surface marker CD34." J Invest Dermatol **120**(4): 501-511.

Trojer, P., A. R. Cao, Z. Gao, Y. Li, J. Zhang, X. Xu, G. Li, R. Losson, H. Erdjument-Bromage, P. Tempst, P. J. Farnham and D. Reinberg (2011). "L3MBTL2 protein acts in concert with PcG protein-mediated monoubiquitination of H2A to establish a repressive chromatin structure." Mol Cell **42**(4): 438-450.

Trojer, P. and D. Reinberg (2007). "Facultative heterochromatin: is there a distinctive molecular signature?" Mol Cell **28**(1): 1-13.

Tumbar, T., G. Guasch, V. Greco, C. Blanpain, W. E. Lowry, M. Rendl and E. Fuchs (2004). "Defining the epithelial stem cell niche in skin." Science **303**(5656): 359-363.

Ueo, T., I. Imayoshi, T. Kobayashi, T. Ohtsuka, H. Seno, H. Nakase, T. Chiba and R. Kageyama (2012). "The role of Hes genes in intestinal development, homeostasis and tumor formation." Development **139**(6): 1071-1082.

van der Lugt, N. M., J. Domen, K. Linders, M. van Roon, E. Robanus-Maandag, H. te Riele, M. van der Valk, J. Deschamps, M. Sofroniew, M. van Lohuizen and et al. (1994). "Posterior transformation, neurological abnormalities, and severe hematopoietic defects in mice with a targeted deletion of the bmi-1 proto-oncogene." Genes Dev **8**(7): 757-769.

van Es, J. H., A. Haegebarth, P. Kujala, S. Itzkovitz, B. K. Koo, S. F. Boj, J. Korving, M. van den Born, A. van Oudenaarden, S. Robine and H. Clevers (2012). "A critical role for the Wnt effector Tcf4 in adult intestinal homeostatic self-renewal." Mol Cell Biol **32**(10): 1918-1927.

van Es, J. H., P. Jay, A. Gregorieff, M. E. van Gijn, S. Jonkheer, P. Hatzis, A. Thiele, M. van den Born, H. Begthel, T. Brabletz, M. M. Taketo and H. Clevers (2005). "Wnt signalling induces maturation of Paneth cells in intestinal crypts." Nat Cell Biol **7**(4): 381-386.

VanDussen, K. L. and L. C. Samuelson (2010). "Mouse atonal homolog 1 directs intestinal progenitors to secretory cell rather than absorptive cell fate." Dev Biol **346**(2): 215-223.

Varjosalo, M. and J. Taipale (2008). "Hedgehog: functions and mechanisms." Genes Dev **22**(18): 2454-2472.

Vermeulen, L., E. M. F. De Sousa, M. van der Heijden, K. Cameron, J. H. de Jong, T. Borovski, J. B. Tuynman, M. Todaro, C. Merz, H. Rodermond, M. R. Sprick, K. Kemper, D. J. Richel, G. Stassi and J. P. Medema (2010). "Wnt activity defines colon cancer stem cells and is regulated by the microenvironment." Nat Cell Biol **12**(5): 468-476.

Vogelstein, B., N. Papadopoulos, V. E. Velculescu, S. Zhou, L. A. Diaz, Jr. and K. W. Kinzler (2013). "Cancer genome landscapes." Science **339**(6127): 1546-1558.

Voigt, P., W. W. Tee and D. Reinberg (2013). "A double take on bivalent promoters." Genes Dev **27**(12): 1318-1338.

Voncken, J. W., B. A. Roelen, M. Roefs, S. de Vries, E. Verhoeven, S. Marino, J. Deschamps and M. van Lohuizen (2003). "Rnf2 (Ring1b) deficiency causes gastrulation arrest and cell cycle inhibition." Proc Natl Acad Sci U S A **100**(5): 2468-2473.

Wagner, E. J. and P. B. Carpenter (2012). "Understanding the language of Lys36 methylation at histone H3." Nat Rev Mol Cell Biol **13**(2): 115-126.

Wang, H., L. Wang, H. Erdjument-Bromage, M. Vidal, P. Tempst, R. S. Jones and Y. Zhang (2004). "Role of histone H2A ubiquitination in Polycomb silencing." Nature **431**(7010): 873-878.

Wang, S., F. He, W. Xiong, S. Gu, H. Liu, T. Zhang, X. Yu and Y. Chen (2007). "Polycomblike-2-deficient mice exhibit normal left-right asymmetry." Dev Dyn **236**(3): 853-861.

Wiederschain, D., L. Chen, B. Johnson, K. Bettano, D. Jackson, J. Taraszka, Y. K. Wang, M. D. Jones, M. Morrissey, J. Deeds, R. Mosher, P. Fordjour, C. Lengauer and J. D. Benson (2007). "Contribution of polycomb homologues Bmi-1 and Mel-18 to medulloblastoma pathogenesis." Mol Cell Biol **27**(13): 4968-4979.

Worthington, J. J., F. Reimann and F. M. Gribble (2018). "Enteroendocrine cells-sensory sentinels of the intestinal environment and orchestrators of mucosal immunity." Mucosal Immunol **11**(1): 3-20.

Xu, B., D. M. On, A. Ma, T. Parton, K. D. Konze, S. G. Pattenden, D. F. Allison, L. Cai, S. Rockowitz, S. Liu, Y. Liu, F. Li, M. Vedadi, S. V. Frye, B. A. Garcia, D. Zheng, J. Jin and G. G. Wang (2015). "Selective inhibition of EZH2 and EZH1 enzymatic activity by a small molecule suppresses MLL-rearranged leukemia." Blood **125**(2): 346-357.

Yan, Y., W. Zhao, Y. Huang, H. Tong, Y. Xia, Q. Jiang and J. Qin (2017). "Loss of Polycomb Group Protein Pcgf1 Severely Compromises Proper Differentiation of Embryonic Stem Cells." Sci Rep **7**: 46276.

Yang, Q., N. A. Bermingham, M. J. Finegold and H. Y. Zoghbi (2001). "Requirement of Math1 for secretory cell lineage commitment in the mouse intestine." Science **294**(5549): 2155-2158.

Yu, J., J. Yu, R. S. Mani, Q. Cao, C. J. Brenner, X. Cao, X. Wang, L. Wu, J. Li, M. Hu, Y. Gong, H. Cheng, B. Laxman, A. Vellaichamy, S. Shankar, Y. Li, S. M. Dhanasekaran, R. Morey, T. Barrette, R. J. Lonigro, S. A. Tomlins, S. Varambally, Z. S. Qin and A. M. Chinnaiyan (2010). "An integrated network of androgen receptor, polycomb, and TMPRSS2-ERG gene fusions in prostate cancer progression." Cancer Cell **17**(5): 443-454.

Zhang, B., P. C. Tsai, M. Gonzalez-Celeiro, O. Chung, B. Boumard, C. N. Perdigoto, E. Ezhkova and Y. C. Hsu (2016). "Hair follicles' transit-amplifying cells govern concurrent dermal adipocyte production through Sonic Hedgehog." Genes Dev **30**(20): 2325-2338.

Zhang, X. W., Y. P. Sheng, Q. Li, W. Qin, Y. W. Lu, Y. F. Cheng, B. Y. Liu, F. C. Zhang, J. Li, G. P. Dimri and W. J. Guo (2010). "BMI1 and Mel-18 oppositely regulate carcinogenesis and progression of gastric cancer." Mol Cancer **9**: 40.

Zhang, Y. (2003). "Transcriptional regulation by histone ubiquitination and deubiquitination." Genes Dev **17**(22): 2733-2740.

Zhang, Y., T. Liu, C. A. Meyer, J. Eeckhoute, D. S. Johnson, B. E. Bernstein, C. Nusbaum, R. M. Myers, M. Brown, W. Li and X. S. Liu (2008). "Model-based analysis of ChIP-Seq (MACS)." Genome Biol **9**(9): R137.

Zhang, Y., P. Tomann, T. Andl, N. M. Gallant, J. Huelsken, B. Jerchow, W. Birchmeier, R. Paus, S. Piccolo, M. L. Mikkola, E. E. Morrisey, P. A. Overbeek, C. Scheidereit, S. E. Millar and R. Schmidt-Ullrich (2009). "Reciprocal requirements for EDA/EDAR/NF-kappaB and Wnt/beta-catenin signaling pathways in hair follicle induction." Dev Cell **17**(1): 49-61.

Zhao, C., A. Chen, C. H. Jamieson, M. Fereshteh, A. Abrahamsson, J. Blum, H. Y. Kwon, J. Kim, J. P. Chute, D. Rizzieri, M. Munchhof, T. VanArsdale, P. A. Beachy and T. Reya (2009). "Hedgehog signalling is essential for maintenance of cancer stem cells in myeloid leukaemia." Nature **458**(7239): 776-779.

Zhao, W., Y. Huang, J. Zhang, M. Liu, H. Ji, C. Wang, N. Cao, C. Li, Y. Xia, Q. Jiang and J. Qin (2017). "Polycomb group RING finger proteins 3/5 activate transcription via an interaction with the pluripotency factor Tex10 in embryonic stem cells." J Biol Chem **292**(52): 21527-21537.

Zhou, W., X. Wang and M. G. Rosenfeld (2009). "Histone H2A ubiquitination in transcriptional regulation and DNA damage repair." Int J Biochem Cell Biol **41**(1): 12-15.

Zhou, W., P. Zhu, J. Wang, G. Pascual, K. A. Ohgi, J. Lozach, C. K. Glass and M. G. Rosenfeld (2008). "Histone H2A monoubiquitination represses transcription by inhibiting RNA polymerase II transcriptional elongation." Mol Cell **29**(1): 69-80.

Zhu, L. J., C. Gazin, N. D. Lawson, H. Pages, S. M. Lin, D. S. Lapointe and M. R. Green (2010). "ChIPpeakAnno: a Bioconductor package to annotate ChIP-seq and ChIP-chip data." BMC Bioinformatics **11**: 237.

7. APPENDIX: Publication

MOLECULAR BIOLOGY

Loss of PRC1 activity in different stem cell compartments activates a common transcriptional program with cell type–dependent outcomes

Silvia Pivetti[1], Daniel Fernandez-Perez[1], Alessandro D'Ambrosio[1], Caterina Maria Barbieri[1], Daria Manganaro[1], Alessandra Rossi[1], Laura Barnabei[1]*, Marika Zanotti[1], Andrea Scelfo[1], Fulvio Chiacchiera[1,2†‡], Diego Pasini[1,3†‡]

Polycomb repressive complexes are evolutionarily conserved complexes that maintain transcriptional repression during development and differentiation to establish and preserve cell identity. We recently described the fundamental role of PRC1 in preserving intestinal stem cell identity through the inhibition of non–lineage-specific transcription factors. To further elucidate the role of PRC1 in adult stem cell maintenance, we now investigated its role in LGR5$^+$ hair follicle stem cells during regeneration. We show that PRC1 depletion severely affects hair regeneration and, different from intestinal stem cells, derepression of its targets induces the ectopic activation of an epidermal-specific program. Our data support a general role of PRC1 in preserving stem cell identity that is shared between different compartments. However, the final outcome of the ectopic activation of non–lineage-specific transcription factors observed upon loss of PRC1 is largely context-dependent and likely related to the transcription factors repertoire and specific epigenetic landscape of different cellular compartments.

INTRODUCTION

Cellular identity is preserved by different layers of transcriptional control. Among the factors and molecular circuits involved in establishing and maintaining cell type–specific transcriptional profiles, epigenetic regulators play a pivotal role. Alterations in these mechanisms are one of the leading causes of different pathologies, such as cancer (*1*, *2*). Polycomb group (PcG) proteins are a class of evolutionarily conserved molecules required to maintain transcriptional repression during development and differentiation (*3*). PcG proteins assemble into two major complexes named Polycomb repressive complex 2 (PRC2) and PRC1. PRC1 and PRC2 share the vast majority of their targets, characterized by CpG-rich regions at promoters, where they are recruited sequentially. The core of PRC2 is composed of the mutually exclusive catalytic subunits EZH1 and EZH2, which deposit the mono-, di-, and trimethylation on lysine 27 of histone H3 (H3K27me3), and of two structural proteins SUZ12 and EED, which are necessary for complex formation and stabilization (*4*, *5*). PRC1 is responsible for the deposition of a single ubiquitin moiety on lysine 119 of histone H2A (H2AK119Ub1) through the catalytic subunits RING1A or RING1B. In addition, it has been described that PRC1 exists in several different forms characterized by the presence of different mutually exclusive Polycomb group ring finger (PCGF) proteins (*6*). These different complexes have been defined as "canonical" or "noncanonical" depending on their ability to associate with chromobox (CBX) proteins. While CBX-containing canonical PRC1 complexes are tethered to chromatin by PRC2-dependent deposition of H3K27me3, the recruitment of noncanonical complexes remains independent of PRC2 activity.

The activity and biological function of PRC1 and PRC2 has been intensively investigated in the past 20 years during embryonic development and using embryonic stem cells (ESCs) (*3*, *5*), while their role in adult stem cells and tissue homeostasis has only recently attracted attention (*7*–*14*). Adult tissues are constantly regenerated and maintained by a pool of stem cells, which are able to compensate for cell loss and tissue damage while preserving stem cell pools (*15*). We recently uncovered the central role of PRC1 activity in preserving intestinal stem cell (ISC) identity through the transcriptional repression of non–lineage-specific transcription factors (TFs), which are able to interfere with the transcriptional program stimulated by the Wnt pathway required for the maintenance of the ISC pool (*9*). With the aim to uncover whether this is a general PcG role in adult stem cells, we now investigated the consequences of PRC1 loss of activity in a stem cell compartment from a different tissue with a distinct developmental origin—hair follicle stem cells (HFSCs).

The skin is the largest organ of the body. It is the first barrier against external insults such as bacteria and virus infections, toxic agents, and ultraviolet radiation, preserving, at the same time, water and temperature homeostasis. In mammals, the epidermis comprises the interfollicular epidermis and the pilosebaceous unit composed of the hair follicle (HF) and the sebaceous gland. During morphogenesis, which begins after delivery, HFs grow downward in the dermal compartment of the skin from the hair bulge and its associated germ (*16*). Hair regeneration is fueled by two different stem cell pools located in the bulge and hair germ. The bulge contains both CD34$^+$ and LGR5$^+$ (Leucine Rich Repeat Containing G Protein-coupled-receptor-5) stem cells, while the hair germ is exclusively colonized by LGR5$^+$ stem cells (*17*, *18*). Throughout life, HFs cycle between proliferation (anagen), destruction (catagen), and resting (telogen) phases (*19*). Anagen onset is activated when WNT proliferative signals overcome a bone morphogenetic protein threshold (*20*, *21*), and LGR5$^+$ HFSCs are essential during anagen to sustain HF growth (*22*). These cells first proliferate to form multipotent progenitors that briefly divide and give rise to matrix cells that will generate all the inner layers of the differentiating

[1]European Institute of Oncology–IRCCS, Department of Experimental Oncology, Milan, Italy. [2]University of Trento, Department of Cellular, Computational and Integrative Biology–CIBIO, Trento, Italy. [3]University of Milan, Department of Health Sciences, Milan, Italy.
*Present address: Imagine Institute, Paris, France.
†These authors contributed equally to this work.
‡Corresponding author. Email: fulvio.chiacchiera@unitn.it (F.C.); diego.pasini@ieo.it (D.P.)

HF (*23*, *24*). During anagen progression, LGR5$^+$ stem cells expand downward to constitute the outer root sheet (ORS) that delimitates the follicle. During anagen phase, LGR5$^+$ HFSCs appear to be functionally similar to LGR5$^+$ ISCs, being actively proliferating stem cells supporting a renewing tissue. For these reasons, they represent a good system to uncover general, stem cell–specific PRC1 activities.

Here, we report that the activity of PRC1 is essential to sustain LGR5$^+$ HFSC and general HF regeneration. We further characterized the direct molecular circuits triggered by PRC1 loss of function and found that, despite the fact that a large part of PRC1 activity is associated with active gene expression, the phenotypic outcome of its loss of function can be primarily ascribed to its canonical repressive functions. In this context, PRC1 is directly involved in suppressing an epidermal transcriptional program maintaining silencing of the master epidermal regulator *Ascl2*. Taking advantage of parallel data generated in ISCs, we further show that, despite the fact that PRC1 retains a general role in suppressing developmental programs across tissue and stem cell compartments, the molecular phenotypes triggered by PRC1 loss of function are strongly dependent on the cellular context, and therefore, by the repertoire of the expressed TFs in any given cell.

RESULTS

PRC1-dependent H2AK119Ub1 is required for HF regeneration

To uncover the general mechanisms by which PRC1 activity contributes to lineage identity in different adult stem cell populations, we took advantage of the *LGR5-GFP-ires-CreERT2/Ring1a*$^{-/-}$*/Ring1b*$^{fl/fl}$*/Rosa26lox-stop-lox LacZ* compound model (hereof *Ring1a/b* ctrl or dKO upon tamoxifen treatment) that we have previously generated (fig. S1A) (*9*). The *Lgr5* transgene is homogenously expressed in a population of actively cycling and long-lived HFSCs that, from the base of the hair bulb, gradually expand through the ORS, contributing to the regeneration of the follicle (*18*). We used this genetic model to acutely abrogate PRC1 activity in 8 to 12 weeks, sex-matched mice and showed that four daily tamoxifen injections are sufficient to abolish PRC1 activity in LGR5$^+$ [green fluorescent protein–positive (GFP$^+$)] HFSCs, as shown by the loss of H2AK119Ub1 in GFP$^+$ cells of telogen HFs (Fig. 1, A and B).

HF regeneration in adult mice is a critical mechanism through which fur is maintained during the entire life span. HFs cycle synchronously during the first 10 to 11 weeks of age and then gradually loose synchrony, despite maintaining the same regenerating capabilities (fig. S1B) (*18*, *19*, *25*). To investigate the role of PRC1 in adult HFSCs during HF regeneration, we exploited the possibility to resynchronize HFs by means of follicles plucking. As soon as the hair is removed, follicles rapidly and synchronously enter into anagen phase and start to cycle (*25*). To abrogate PRC1 activity from the first phases of HF regeneration, we administered tamoxifen in adult mice 1 day before waxing the back skin (Fig. 1C). After 12 days from waxing, while the fur of *Ring1a/b* ctrl mice was completely regenerated (Fig. 1D, top), we severely delayed follicle regeneration in *Ring1a/b* dKO mice in the absence of PRC1 activity (Fig. 1D, bottom). We further confirmed this result by lineage-tracing analyses, taking advantage of a *Rosa26lox-stop-lox LacZ* allele to follow LACZ expression in the progeny of LGR5$^+$ stem cells. Twelve days after waxing, we markedly reduced the number of β-galactosidase (β-Gal)–expressing HFs in *Ring1a/b* dKO animals, suggesting that the residual hair growth is derived from wild-type HFs (Fig. 1E).

PRC1 depletion affects the onset of anagen phase and the HF cycle

To elucidate whether PRC1 activity is required for entering into or to progress through the anagen phase, we activated Cre-mediated recombination at P49 to induce Ring1b loss of function during the long telogen period. After 2 weeks from tamoxifen exposure, we synchronized HFs by waxing and then collected the back skin after 8 and 12 days (Fig. 2A and fig. S2A) to perform histological analyses and β-Gal staining to trace PRC1-null progeny. After 8 days from waxing, we observed a substantial delay in hair growth in *Ring1a/b* dKO mice (fig. S2B). This was further confirmed by histological analysis showing shorter HFs, blocked in the early anagen phases (I and II) [fig. S2, C (top) and D] (*25*). At 8 days from waxing, the total number β-Gal$^+$ HFs was strongly reduced in *Ring1a/b* dKOs [fig. S2, C (bottom) and E]. It is well established that the hypodermal adipocyte layer fluctuates in thickness during the hair cycle (*25*, *26*). This increases during anagen and reduces throughout catagen to reach a resting phase until a new hair cycle begins. *Ring1a/b* dKOs displayed a clear imbalance of hypodermis fat (fig. S2F) and dermis thickness (fig. S2G), despite the fact that the total skin showed a similar width (fig. S2H). This reinforces evidence that PRC1 loss severely affects HF regeneration. This phenotype was confirmed and enhanced after 12 days from waxing (Fig. 2B). According to Müller-Röver *et al.* (*25*) classification, at this time point, while *Ring1a/b* ctrl mice showed all features of full anagen (anagen phase VI), *Ring1a/b* dKO follicles still resembled primary stages of the hair cycle (anagen phases II and III; Fig. 2C, top). Lineage tracing of LGR5$^+$ stem cell progeny showed a marked reduction of cells derived from *Ring1a/b* dKO stem cells, as demonstrated by the severe lack of β-Gal staining compared to ctrl follicles [Fig. 2, C (bottom) and D]. Consistently, the differences in follicles length, hypodermis, and dermis thickness were further increased at 12 versus 8 days after waxing, with a similar reduced number of HFs (Fig. 2, E to H, and fig. S2, I to L). Together, these data suggest that the loss of PRC1 activity does not fully prevent entry into the anagen phase but rather impairs the regenerative potential of LGR5$^+$ stem cells.

Conserved PRC1-repressed transcriptional programs are required to preserve HFSCs and ISCs

Our results suggest that the loss of PRC1 induces similar phenotypic outcomes in HFSCs compared to our previous results with ISCs (*9*). Whether this involves common or cell type–specific pathways remains an important open question. To investigate the transcriptional changes induced by PRC1 loss of function in anagen-activated LGR5$^+$ stem cells, we collected the skin of *Ring1a/b* dKO and ctrl adult mice 8 days from waxing (Fig. 3A). HFs were isolated and reduced at single cells, and LGR5$^+$ cells were isolated by fluorescence-activated cell sorting (FACS) to perform RNA sequencing (RNA-seq) analyses. FACS analysis on the same cells stained for H2AK119Ub1 demonstrated that tamoxifen treatment results in >70% loss of PRC1 activity in LGR5$^+$ (GFP$^+$) cells (Fig. 3B). RNA-seq analysis in these cell populations revealed a >5-fold bias in genes up-regulation (1066 up-regulated versus 187 down-regulated genes) that is consistent with the general PRC1 role as transcriptional repressor also in the HF compartment (Fig. 3C). Gene ontology (GO) analysis on differentially expressed genes showed that up-regulated genes are primarily associated with general developmental processes (Fig. 3D). In contrast, down-regulated genes were specifically enriched by factors involved in HF morphogenesis, HFSC maintenance, and hair cycle progression (Fig. 3E), such as Sonic hedgehog (*23*, *27*). Moreover,

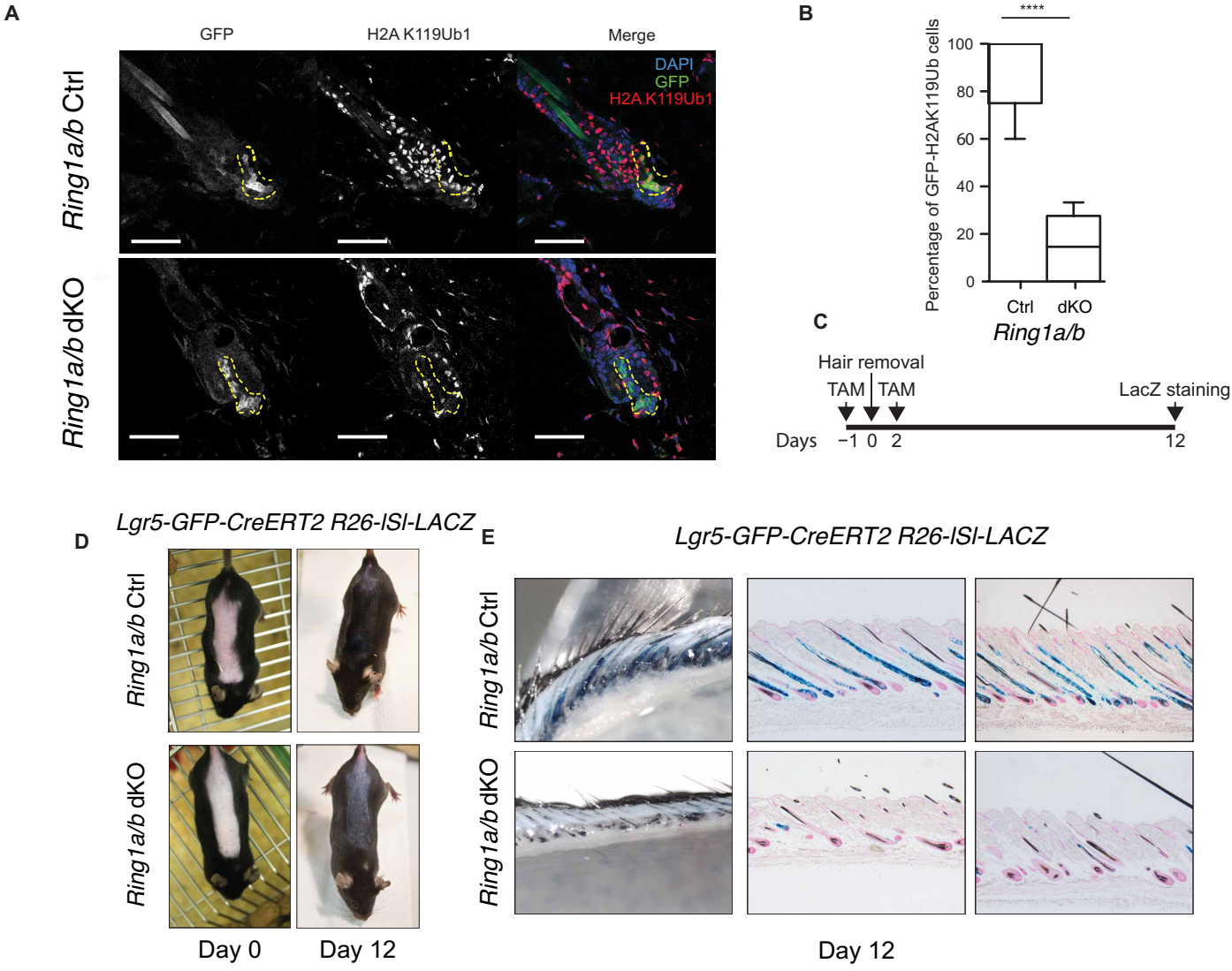

Fig. 1. PRC1 activity is required to sustain HF regeneration. (**A**) Immunostaining using H2AK119Ub1 (red) and 4′,6-diamidino-2-phenylindole dihydrochloride (DAPI; blue) of HF from LGR5-eGFP-ires-CREERT2 HFSCs in *Ring1a/b*$^{+/+}$ and *Ring1a/b*$^{-/-}$ mice . Scale bars, 50 μm. (Photo credit: F.C. and S.P., European Institute of Oncology). (**B**) Quantification of H2AK119Ub1^{+} HFSCs in *Ring1a/b*$^{+/+}$ and *Ring1a/b*$^{-/-}$ mice. ****$P < 0.0001$ (P values were calculated with two side t test). TAM, tamoxifen. (**C**) Schematic representation of the protocol used in (D) and (E). (**D**) Representative pictures of *Ring1a/b*$^{+/+}$ and *Ring1a/b*$^{-/-}$ mice immediately after hair removal and after 12 days. (Photo credit: F.C., European Institute of Oncology). (**E**) In vivo lineage tracing of HFSCs. Mice were treated as described in (C), and skin was collected at indicated time point. Samples were stained with X-Gal. Whole tissues were imaged before paraffin embedding, and the sections obtained were counterstained using neutral red. (Photo credit: F.C., European Institute of Oncology).

functional annotation revealed that DNA binding TFs, and particularly homeotic TFs, were overrepresented among the genes up-regulated in *Ring1a/b* dKO (fig. S3A). The additional comparison in respect to transcriptional data obtained from several tissues (ENCODE; fig. S3B, bottom) highlighted that the loss of PRC1 activity results in the transcriptional activation of non–lineage-specific genes that are preferentially expressed in distinct tissue compartments. In contrast, down-regulated genes were primarily expressed in activated LGR5^{+} HFSCs (fig. S3B, top), further corroborating impaired activation of HFSC regenerative capabilities in the absence of PRC1 activity. These data are in agreement with our previous finding in ISCs (*9*), further highlighting the conserved essential role of PRC1 in maintaining lineage identity within adult tissues. Whether this involves common or specific mechanisms remains an open question. Thus, we searched for common classes of genes that could be potentially involved with the loss of cell identity in ISCs versus HFSCs upon PRC1 inactivation. We compared RNA-seq profiles in both stem cell compartments and found that none of the down-regulated genes were in common in accordance with the distinct identity of the two stem cell populations (fig. S3C). In contrast, we found approximately one-fourth of the up-regulated genes (255 genes, ≈25%) in common between ISC and HFSC (fig. S3D). This group of genes was enriched by mainly homeobox-containing TFs involved in regulating general developmental processes (fig. S3E). Several ZIC (Zinc finger protein of the cerebellum) TFs (*Zic1*, *Zic4*, and *Zic5*; fig. S3F), as well as *Sox7*, *Hoxa10*, and *Hoxb13* (fig. S3G), were present within this list. Together, these data suggest that

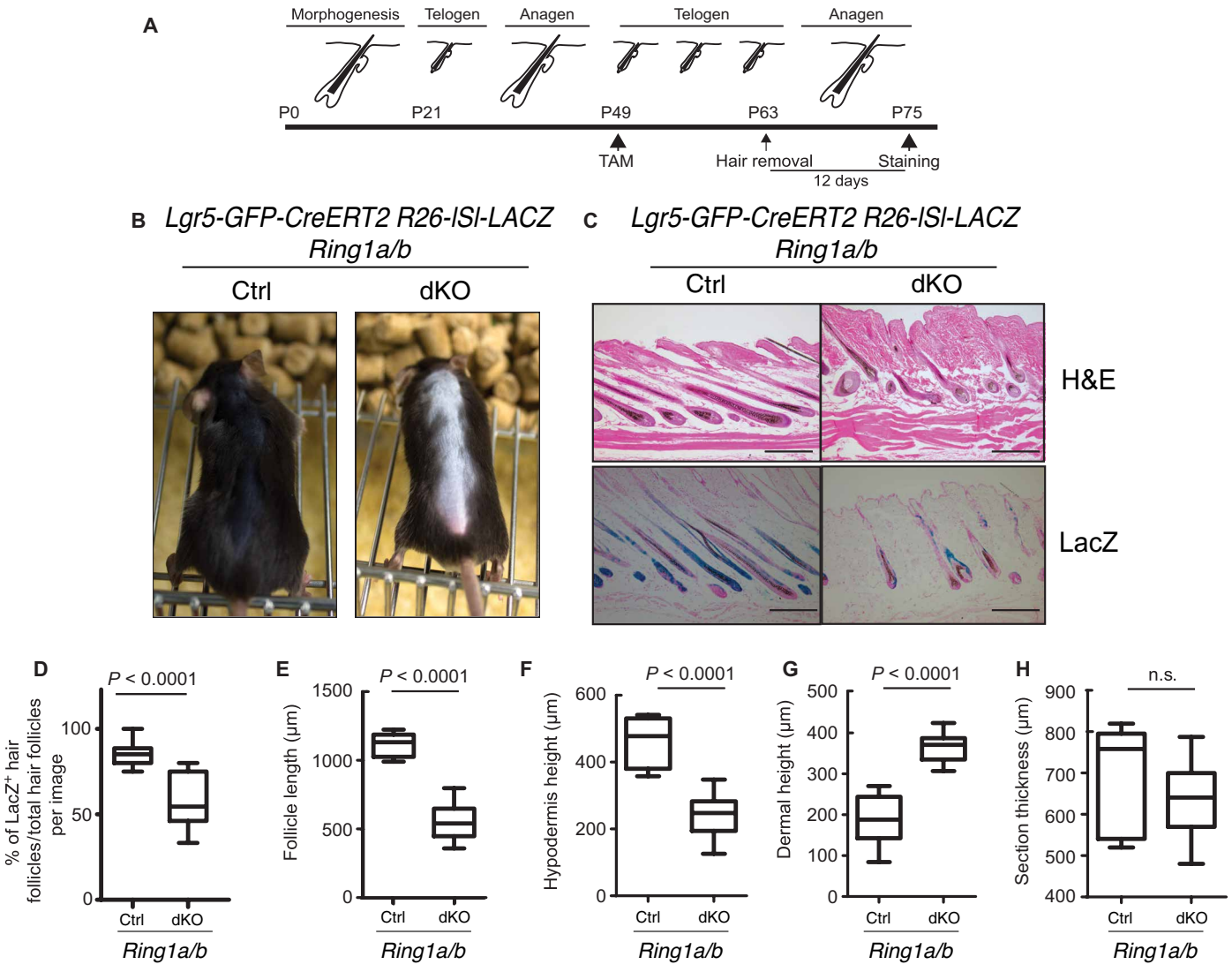

Fig. 2. PRC1 activity is required for anagen onset and progression. (**A**) Schematic representation of the experiment. Tamoxifen was delivered intraperitoneally once a day for four consecutive days during the long telogen phase. At 63 days, postdelivery hairs were removed, and samples were collected after 12 days. (**B**) Representative pictures of *Ring1a/b*$^{+/+}$ and *Ring1a/b*$^{-/-}$ mice immediately after hair removal and after 12 days. (Photo credit: S.P., European Institute of Oncology). (**C**) Histological analysis and in vivo lineage tracing of HFSCs. Mice were treated as described in (A). Skin was collected at the indicated time points. All collected sample were paraffin-embedded and stained with either X-Gal or hematoxylin and eosin (H&E). Scale bars, 250 μm. (Photo credit: S.P., European Institute of Oncology). (**D**) Quantification of β-Gal^{+} HFs, (**E**) HF length, (**F**) hypodermis, (**G**) dermal height, and (**H**) total section thickness at 12 days after waxing in *Ring1a/b*$^{+/+}$ and *Ring1a/b*$^{-/-}$ mice. All *P* values were calculated with two-side *t* test. n.s., not significant.

PRC1 plays a common general role in distinct stem cell compartments to prevent activation of non–lineage-specific, homeobox-containing TFs.

Transcriptional repression of a subset of canonical PRC1 targets preserves stem cell identity

Recently, two major classes of PRC1 complexes have been described (*6*) on the basis of their biochemical composition. Canonical PRC1, which contains CBX proteins, is recruited on their targets in a PRC2-dependent manner. Noncanonical PRC1 complexes do not contain the CBX-containing subunits and are recruited independently from PRC2. They are characterized by the presence of different PCGF subunits and share the subunits RYBP (RING1 and YY1 Binding Protein) or YAF2 (YY1 Associated Factor 2). Different components of canonical and noncanonical PRC1 complexes are expressed in HFSCs (fig. S4A). To investigate the ability of RING1B to enter both canonical and noncanonical complexes in HFSCs, we performed proximity ligation assay (PLA). Wild-type and dKO LGR5^{+} HFSCs from waxed mice have been sorted (fig. S4, B and C) and used to investigate the ability of RING1B to interact with RYBP (Fig. 3, F and G) or BMI1 (Fig. 3, H and I). Our data indicate that in HFSCs, both canonical and noncanonical complexes assemble, suggesting that the phenotype observed in dKO HFSCs could be the result of the impaired activity of different complexes.

To identify the common mechanisms through which PRC1 regulates cell fate determination in different stem cell populations, we performed chromatin immunoprecipitation sequencing (ChIP-seq)

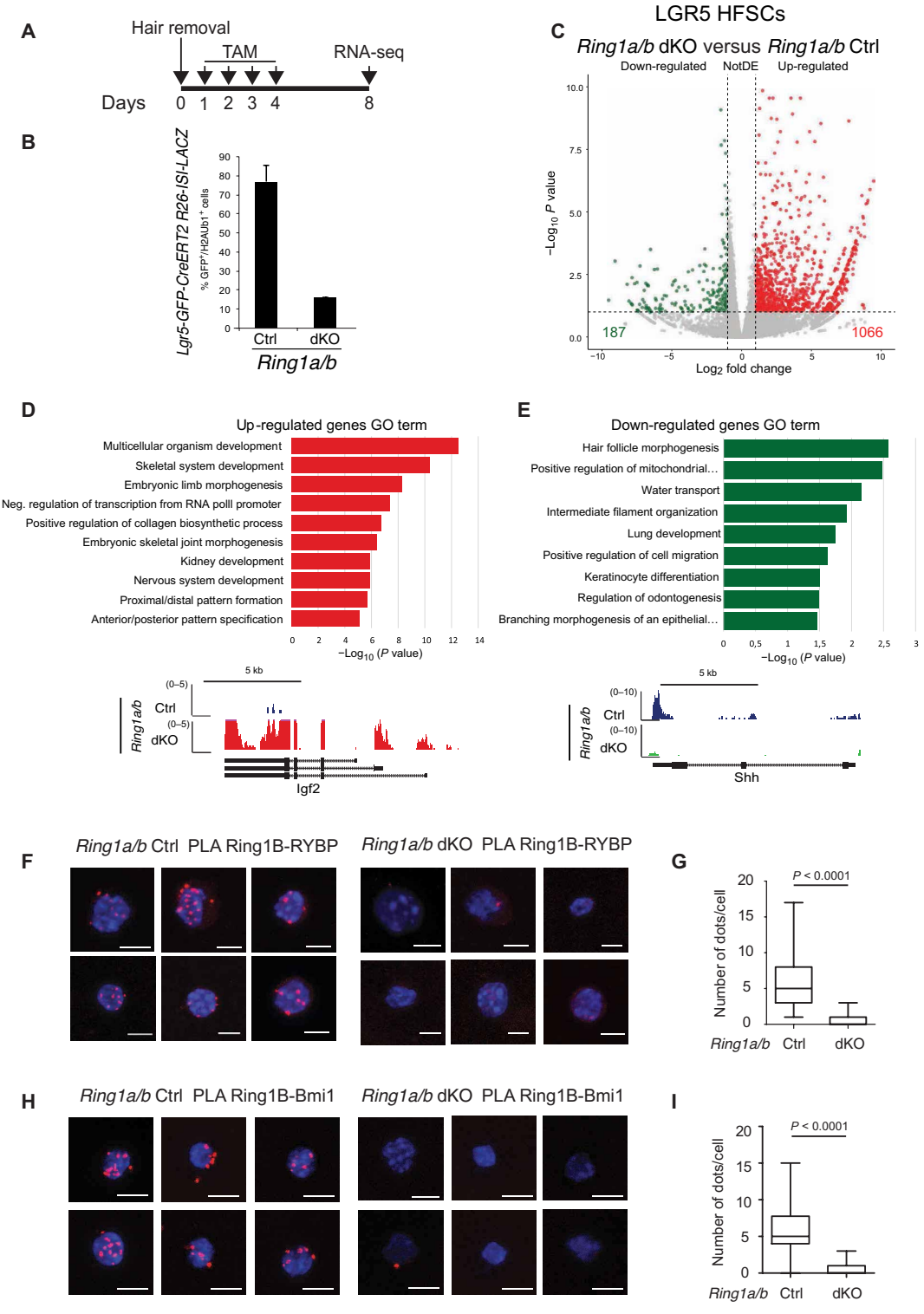

Fig. 3. Loss of PCR1 activity affects HFSCs transcriptional landscape. (**A**) Schematic view of the experiment. (**B**) Quantification of H2AK119Ub1^{+} HFSCs used for RNA-seq experiments in *Ring1a/b*$^{+/+}$ and *Ring1a/b*$^{-/-}$ mice. HFs were collected 8 days after waxing. Single-cell suspension was stained using anti-H2Ak119Ub1 and analyzed by FACS. (**C**) Volcano plot of differentially expressed genes between *Ring1a/b*$^{+/+}$ and *Ring1a/b*$^{-/-}$ mice. Log_2 fold change, ≥1. (**D**) GO analysis of up-regulated and (**E**) down-regulated genes in *Ring1a/b*$^{-/-}$ mice (log_2 fold change, ≥1) representative snapshots of modulated genes is shown. Shh, Sonic hedgehog. (**F**) PLA between RING1B and RYBP on *Ring1a/b*$^{+/+}$ and *Ring1a/b*$^{-/-}$ HFSCs. (Photo credit: S.P. and A.D., European Institute of Oncology). (**G**) Quantification of RING1B-RYBP PLA dots per cell in *Ring1a/b*$^{+/+}$ and *Ring1a/b*$^{-/-}$ HFSCs. (**H**) PLA between RING1B and BMI1 on *Ring1a/b*$^{+/+}$ and *Ring1a/b*$^{-/-}$ HFSCs. (Photo credit: S.P. and A.D., European Institute of Oncology). (**I**) Quantification of RING1B-BMI1 PLA dots per cell in *Ring1a/b*$^{+/+}$ and *Ring1a/b*$^{-/-}$ HFSCs. Scale bars, 5 μm. All *P* values were calculated with two-side *t* test.

analysis for RING1B in FACS-sorted activated LGR5$^+$ stem cells purified 8 days from waxing (Fig. 4, A and B). This analysis identified nearly 3900 RING1B significant peaks that were mainly associated with promoter regions (Fig. 4C). This distribution closely resembles the RING1B chromatin association that we have found in ISCs (Fig. 4D). Since RING1A or RING1B can form distinct functional complexes that may localize differently along the genome (*6*), we first compared the genomic localization of RING1B in both HFSCs and ISCs in respect to the deposition of H3K27me3 to define Polycomb-repressed domains (*9*, *28*). We restricted the extent of overlap with the canonical PcG-repressed domains only to 20% of RING1B sites in HFSCs (Fig. 4E) and to 10% in ISCs (Fig. 4F), suggesting that a large fraction of RING1B activity is exerted independently of PRC2. In ESCs, H3K27me3 is enriched at promoters of developmental-related genes concomitantly with the deposition of the transcriptional activatory modification H3K4me3. This promoter status has been defined as "bivalent" or "poised" (*29*). Bivalency is resolved when ESCs are triggered to differentiate by the acquisition of a purely active (H3K4me3 only) or repressed (H3K27me3 only) state. We found that, while only 30% of H3K27me3 sites in HFSC are bivalent (coenriched with H3K4me3), this proportion expands in ISCs where it reaches 80% of all RING1B target promoters enriched for H3K27me3 (Fig. 4, G and H). We also observed a large fraction of RING1B-bound sites that lacks H3K27me3 but presents H3K4me3 deposition (Fig. 4, I and J). Accordingly, with the ability of RING1B to interact with subunits of both canonical and noncanonical complexes, we observed that in HFSCs, nearly 70% of RYBP peaks colocalize with RING1B (Fig. 4K), but only a small percentage (11%) of the co-occupied regions harbor H2AK119Ub (Fig. 4L). Those regions characterized by the presence of RING1B and H2AK119Ub are also occupied by CBX8, a canonical PRC1 subunit, and are decorated by PRC2-dependent H3K27me3 mark (Fig. 4, M and N). These data suggest that both canonical and noncanonical PRC1 activities, which are not associated with H3K27me3 and H2AK119Ub, could contribute in the maintenance of stem cell identity.

To address this issue, we ranked all RING1B target promoters based on their expression in wild-type cells, and we compared their expression in PRC1-defective HFSCs and ISCs (Fig. 4O and fig. S5A). This analysis identified four classes of genes. Repressed genes in wild-type cells defined cluster 1 and were enriched for transcriptionally activated genes in *Ring1a/b* dKO HFSCs and ISCs. Genes with intermediate expression (clusters 2 and 3) showed no difference (Fig. 4O) or slightly decreased expression (fig. S5A) in *Ring1a/b* dKO cells. Highly expressed genes (cluster 4) were slightly downregulated in *Ring1a/b* dKO HFSC. The distribution of H3K27me3, H2AK119Ub, and H3K4me3 (Fig. 4P and fig. S5B) identified genes belonging to cluster 1 as fully silenced through canonical Polycomb activities, as demonstrated by the presence of CBX8 (Fig. 4P). These sites are devoid of H3K4me3, which is instead enriched at all the other clusters (Fig. 4P and fig. S5B) where colocalizes with RING1B and RYBP (Fig. 4P). Accordingly, genes involved in development and differentiation were only enriched in cluster 1 (Fig. 4Q and fig. S5, C, E, and F). Despite the fact that these data support a prominent role for canonical versus noncanonical activities in maintaining cell identity in HFSCs and ISCs, it is important to stress that only a subset of RING1B$^+$/H3K27me3$^+$/H2AK119Ub targets become derepressed upon the loss of PRC1 activity in HFSCs and ISCs (Fig. 4R and fig. S5D). This suggests, first, that H3K27me3 is largely sufficient to prevent TF accessibility and activation of PcG targets and, second, that only a small proportion of PcG target genes contribute to the observed phenotypes.

Loss of PRC1 activity activates epidermal-specific program

To uncover direct mechanisms associated with PRC1 loss of activity, we focused our attention on RING1B targets that became derepressed in *Ring1a/b* dKO. This includes *Ascl2* (Fig. 5A), which encodes for a TF previously shown to be sufficient and required to drive epidermal differentiation (*30*). To investigate whether a specific differentiation program is initiated upon PRC1 activity loss, we performed gene set enrichment analysis (GSEA) comparing signatures from different cells belonging to distinct skin compartments (*31*) against *Ring1a/b* dKO versus ctrl transcriptional outcome in HFSCs. This analysis showed that, together with the stem cell signature, genes involved in epidermal-specific transcriptional program became enriched in *Ring1a/b* dKO mice (Fig. 5B). Among them, *Satb1*, *Krtdap*, *Calm5*, *Itgam*, and *Gdpd2*, together with *Ascl2*, were some of the known epidermal markers that are highly activated (Fig. 5, A, C, and D). We further scanned the *Ascl2* promoter with LASAGNA-Search 2.0 (*32*) for putative TFs responsible for its activation and found several binding motifs that are recognized by the family of ZIC TFs (Fig. 5E). Note that different members of this TF family are also directly bound and derepressed in *Ring1a/b* dKO HFSCs (fig. S3F), establishing a positive feedback loop driving epidermal identity. Together, these results support a model in which PRC1 directly suppresses an epidermal-specific transcriptional program via suppression of master regulators of lineage specification, thus contributing to preserve HF identity.

DISCUSSION

The role of Polycomb complexes in maintaining adult stem cell identity has been investigated by several groups during the past 5 years. We recently reported that PRC1 and PRC2 play a crucial role in supporting intestinal homeostasis (*8*–*10*). Along the crypt-to-villus axis, the balance between secretory cells and enterocytes differentiation, transit-amplifying cell proliferation and stem cell maintenance are preserved by Polycomb complexes. In particular, PRC1 is critically required for ISC maintenance, and the loss of RING1A/B subunits leads to stem cell exhaustion. Its activity is required to maintain repressed non–lineage-specific TFs, some of which are able to interfere with the ISC-specific transcriptional programs. Stem cell loss observed in RING1A/B-deficient intestinal epithelium can therefore be ascribed not to the initiation of a defined transcriptional program but to the loss of stem cell–specific ones. To unveil general mechanisms underlying PRC1-dependent adult stem cell maintenance, we extended its analysis in proliferating HFSCs. Similar to what we previously described for ISCs, the loss of RING1A/B in HFSCs markedly affects HF regeneration. This phenotypic convergence is mirrored at a transcriptional level by the up-regulation of non–lineage-specific genes, enriched for DNA binding TFs. We provide evidence that PRC1 associates at H3K27Me3$^+$ promoters of repressed genes in the context of canonical complexes, characterized by the presence of CBX8 subunit and H2AK119Ub. At promoters of active genes, RING1B occupancy coincides with RYBP and low or undetectable H2AK119Ub levels, suggesting that noncanonical PRC1 complexes could play a role at these promoters that is largely independent from their ability to modify histone H2A. A similar

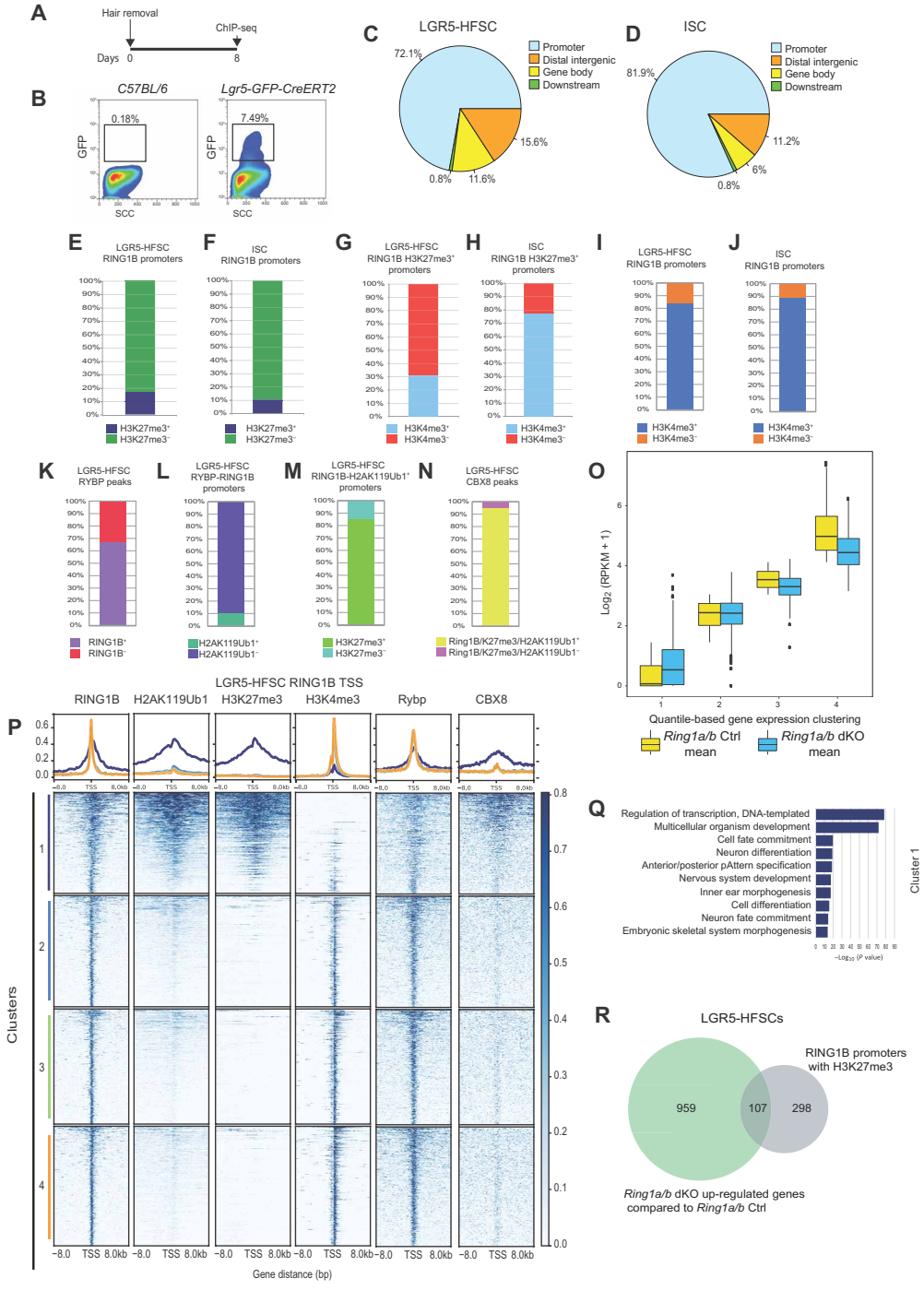

Fig. 4. Genomic distribution of PRC1 binding in HFSCs and ISCs. (**A**) Schematic view of ChIP-seq experiment. (**B**) Gating strategy used to sort HFSCs used in ChIP-seq experiments. (**C**) Genomic distribution of RING1B-bound sites in LGR5$^+$ HFSCs. (**D**) Genomic distribution of RING1B-bound sites in LGR5$^+$ ISCs. (**E**) Bar plots showing the fraction of RING1B-bound promoters marked by H3K27me3 in HFSCs. (**F**) Bar plots showing the fraction of RING1B-bound promoters marked by H3K27me3 in ISCs. (**G**) Bar plots showing the fraction of RING1B-bound H3K27Me3$^+$ promoters marked by H3K4Me3 in HFSCs. (**H**) Bar plots showing the fraction of RING1B-bound H3K27Me3$^+$ promoters marked by H3K4Me3 in ISCs. (**I**) Bar plots showing the fraction of RING1B-bound promoters marked by H3K4me3 in HFSCs. (**J**) Bar plots showing the fraction of RING1B-bound promoters marked by H3K4me3 in ISCs. (**K**) Bar plot showing the fraction of RYBP peaks overlapping with RING1B peaks in HFSCs. (**L**) Bar plot representing the percentage of promoters occupied by RYBP and RING1B marked by H2AK119Ub1 in HFSCs. (**M**) Bar plot showing the percentage of promoters occupied by RING1B and H2AK119Ub marked by H3K27Me3 in HFSCs. (**N**) Bar plot showing the percentage of CBX8 peaks overlapping with RING1B, H3K27Me3, and H2AK119Ub triple-positive peaks in HFSCs. (**O**) Quartile-based gene expression clustering performed using *Ring1a/b*$^{+/+}$ RNA-seq data, showing expression variations between *Ring1a/b*$^{+/+}$ and *Ring1a/b*$^{-/-}$ HFSCs. (**P**) Heatmap representing normalized RING1B, H3K27me3, H3K4Me3, H2AK119Ub1, CBX8, and RYBP ChIP-seq intensities of ±8 kb from TSS of RING1B target genes in HFSCs. Clusters were made according to Fig. 4O. bp, base pair. (**Q**) GO analyses of genes belonging to cluster 1. (**R**) Venn diagram showing the overlap between up-regulated genes in *Ring1a/b*$^{-/-}$ mice with total RING1B/H3K27me3-enriched regions.

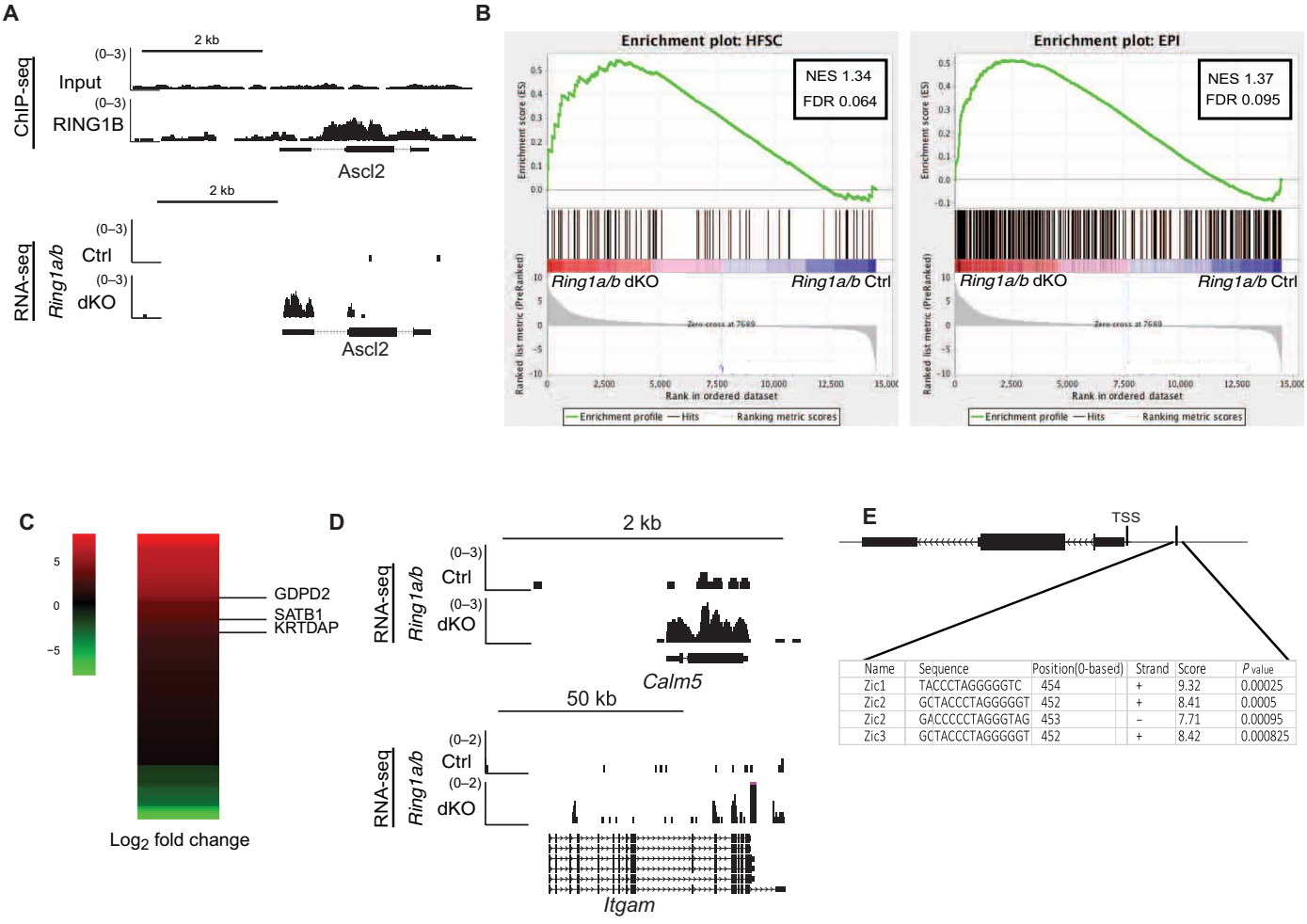

Name	Sequence	Position(0-based)	Strand	Score	P value
Zic1	TACCCTAGGGGGTC	454	+	9.32	0.00025
Zic2	GCTACCCTAGGGGGT	452	+	8.41	0.0005
Zic2	GACCCCCTAGGGTAG	453	–	7.71	0.00095
Zic3	GCTACCCTAGGGGGT	452	+	8.42	0.000825

Fig. 5. PRC1 activity is required to maintained repressed the epidermal-specific transcriptional program in HFSCs. (**A**) RING1B occupancy at ASCL2 locus and transcriptional activation of ASCL2 in *Ring1a/b*$^{-/-}$. (**B**) GSEAs performed on *Ring1a/b*$^{-/-}$ HFSCs using signatures specific for 14 major skin and HF cell populations (*31*). FDR, false discovery rate; NES, normalized enriched stone; EPI, epidermis. (**C**) Heatmap representing epidermal-specific genes differentially regulated in *Ring1a/b*$^{-/-}$ HFSCs (log_2 fold change). (**D**) Genomic snapshots of RNA-seq for *Calm5* and *Itgam* genes that are involved in epidermal differentiation. Chr13, chromosome 13. (**E**) Motif enrichment analyses on *Ascl2* promoter performed using LASAGNA-search 2.0 (*32*).

distribution has also been reported in murine ESCs, where H2AK119Ub1 and PRC2 co-occupy genes bound by CBX7/RING1B and are largely excluded by those regions exclusively bound by RYBP/RING1B (*33*). Note that, similar to ESCs, PRC1 localized on both repressed (canonical PcG targets) and active genes in both ISCs and HFSCs. This latter observation is in line with another recent report demonstrating a pivotal role of PRC1 during skin development (*11*). However, despite the fact that RYBP-containing PRC1 localizes to active promoters in both ISCs and HFSCs, very few of those active PRC1 targets score among the down-regulated genes, suggesting a marginal role of noncanonical complexes in preserving the expression of these target genes. This further restricts the specific phenotypes firstly described in ISCs and now documented in HFSCs to a more canonical PRC1 repressive activity. Our data demonstrate that several PcG direct targets became derepressed upon PRC1 loss of function and several of these targets can be directly linked to the observed phenotypic convergence. However, in HFSCs and ISCs, not all the PRC1 bound targets became activated upon RING1A/B loss. This suggests that, despite the idea that a general PRC1 role in maintaining repression of non–lineage-specific genes is, to some extent, conserved in cells of different developmental origin and tissues (i.e., HFSC, ESCs, and ISC), the transcriptional program triggered by its loss of function remains cell type dependent. This is likely due to the repertoire of available TFs in any given cell. Accordingly, among the different derepressed genes in *Ring1a/b* dKO HFSC, we found ASCL2, a DNA binding TF sufficient and required for epidermal differentiation (*30*). Further analysis of the transcriptome of PRC1-deficient HFSCs confirmed the activation of an ectopic, epidermal-specific, transcriptional program that could likely contribute for the observed phenotype.

Together, our data ultimately support the existence of a general role played by PRC1 to maintain adult stem cell identity that converge into a common phenotype with distinct cell type–specific mechanisms. This observation is of crucial importance not only to understand the role of Polycomb complexes in shaping adult tissues but also in different pathological settings, such as cancer, in which PcG is directly involved. The requirement of PcG during tumor development and progression, where a high level of cell heterogeneity can be observed, has been extensively reported, and several PcG

inhibitors entered clinical trials (*1*, *34*). In this context, the efficacy (i.e., the consequences) of PcG inhibition could be cell type specific, as we describe for adult stem cells, and possibly dependent on the integrity of the signaling pathways and on the TF repertoire of the different cells.

MATERIALS AND METHODS

Mouse models

Lgr5-specific conditional knockout mice were generated by crossing Ring1A$^{-/-}$ Ring1B$^{fl/fl}$ (*35*), with LGR5-eGFP-IRES-CreERT2 mice (*36*). These mice were crossed with Rosa26lox-stop-lox LacZ transgenic mice for in vivo lineage tracing (*37*). Genotyping was confirmed by polymerase chain reaction (PCR) of tail skin DNA. Cre-dependent recombination was induced performing three intraperitoneal injections of tamoxifen (Sigma-Aldrich) at 75 mg/kg.

Mice were maintained accordingly to the guidelines set out in Commission Recommendation 2007/526/EC, 18 June 2007, on guidelines for the accommodation and care of animals used for experimental and other scientific purposes. All experiments were performed in accordance with the Italian Laws (D.L.vo 116/92 and following additions), which enforces EU Directive 86/609 (Council Directive 86/609/EEC of 24 November 1986 on the approximation of laws, regulations, and administrative provisions of the member states regarding the protection of animals used for experimental and other scientific purposes).

HF purification

LGR5$^+$ cells were purified from back skin of treated mice at different time points. Subcutaneous fat and the blood vessels were removed, and the skin was digested using collagenase (2.5 mg/ml) in Dulbecco's modified Eagle's medium (DMEM) for 45 min. HFs were scraped off and incubated for 10 min at 37°C with 2.5% trypsin in phosphate-buffered saline (PBS) and deoxyribonuclease 1 (DNase1; 1600 U/ml). Fetal bovine serum was added to neutralize trypsin. Cells were washed with PBS and filtered with 70-μm cell strainer.

Flow cytometry and FACS

Single-cell suspension were washed and resuspended in sorting medium [DMEM; 1:100 penicillin and streptomicin (17-602F, Lonza), 1:100 L-glutamine (17-605E, Lonza), Hepes, 2 mM EDTA, DNase1 (800 U/ml), and 10 uM Y27632 (Selleck Chemicals)]. Single GFP$^+$ cells were FACS-sorted using either FACSMelody or FACSJazz cell sorters (BD Biosciences). Living cells were discriminated by propidium iodide exclusion staining.

Immunofluorescence

Back skin was harvested at the described time points, fixed with 4% paraformaldehyde (PFA) for 3 hours at 4°C, and cryopreserved in 30% sucrose overnight, followed by O.C.T. embedding (Tissue-TEK 4583). Embedded tissues were cut at 7 μm in thickness. Sections were washed in tris-buffered saline–0.1% Tween 20 (TBS-T) and blocked with 5% donkey serum at room temperature for 1 hour. Section were incubated with anti-H2AK119Ub (D27C4, Cell Signaling Technology) overnight at 4°C, washed in TBS-T, incubated for 1 hour at room temperature with secondary antibody [715-165-147, Cy3 AffiniPure Donkey Anti-Rabbit IgG (H+L), Jackson ImmunoResearch] and 4′,6-diamidino-2-phenylindole dihydrochloride (32670, Sigma-Aldrich), and mounted with Mowiol 4-88 (81381, Sigma-Aldrich). Images were taken with Leica Sp8 confocal microscope.

Proximity ligation assay

Anagen-induced sorted LGR5 HFSCs were spotted in Cell-Tak (Corning)–coated coverslip, and PLA was performed using Sigma-Aldrich Duolink In Situ Orange Starter Kit Mouse/Rabbit following the manufacturer's instruction protocol. Anti-RING1B antibody (homemade), anti-RYBP (AB3637, Millipore), and anti-BMI1 (homemade) primary antibodies were used.

Histology and lineage tracing

Freshly obtained back skin samples were collected at the indicated time point and were immediately prefixed for 30 min at room temperature in PBS containing 0.2% gluteraldehyde, 0.02% NP-40, and 2% PFA. Samples were washed three times for 10 min each with PBS and incubated for 30 min with the equilibration buffer (2 mM $MgCl_2$, 0.02 NP-40, and 0.1% sodium deoxycholate in PBS). Samples were stained overnight at room temperature using 5 mM $K_3Fe(CN)_6$, 5 mM $K_4Fe(CN)_6$, and X-Gal (1 mg/ml) in equilibration buffer. Stained skin were washed abundantly with PBS at room temperature and then fixed overnight in 4% PFA in PBS before paraffin embedding. Five-micrometer sections were obtained, rehydrated, and nuclei-counterstained with Nuclear Fast Red solution for 10 min at room temperature. For histological analysis, freshly isolated back skin samples were fixed in 4% formaldehyde overnight, paraffin-embedded, and stained with hematoxylin and eosin Y. Images were acquired using Olympus BX51 or Leica DM6 widefield microscope.

RNA sequencing

FACS-sorted cells were collected in 0.5-ml tubes and processed directly following Smart-seq2 protocol (*38*) with minor modifications. Briefly, 3000 cells per sample were collected directly and lysed in 2 μl of lysis buffer [0.2% Triton X-100 and ribonuclease inhibitor (4 U/μl)]. One microliter of 10 μM oligo-dT30Vn and 1 μl of 10 mM deoxynucleotide triphosphate were added, and the samples were incubated for 3 min at 72°C. Reverse transcriptase step was performed using SuperScript III reverse transcriptase enzyme (Invitrogen). Preamplification of the obtained complementary DNA (cDNA) was performed using KAPA Taq HotStart enzyme with High-Fidelity Buffer. Preamplified cDNA was purified using AMPure beads (Agencourt AMPure XP, Beckman Coulter), and the quality was checked using Bioanalyzer (Agilent). Two nanograms of cDNA was tagmented with 100 ng of homemade Tn5 enzyme and further amplified using KAPA HiFi HotStart Kit. Tagmented, amplified DNA was sequenced using Illumina HiSeq2000.

ChIP sequencing

LGR5$^+$ HFSCs were purified as previously described from anagen-synchronized HFs of Ring1a/b$^{+/+}$ mice and were extracted following the protocol previously described. A total of 2.5 million cells were used for ChIP-seq as previously described (*9*). Sonicated chromatin was incubated with 10 μg of rabbit anti-RING1B antibody (homemade), anti-H2AK119Ub1 (8240, Cell Signaling Technology), anti-RYBP (AB3637, Millipore), and anti-CBX8 (*39*) overnight, and the immunocomplexes recovered using protein A–conjugated magnetic beads (Dynabeads, Life Technologies). Purified chromatin was decross-linked overnight in 0.1 M $NaHCO_3$ and 1% SDS. Decross-linked DNA was purified. ISC-specific H3K4me3 ChIP-seq profile was obtained as previously described (*9*) using 5 μg of anti-H3K4Me3 antibody (catalog no. 39159, Active Motif).

RNA-seq analysis

Reads were aligned to the mouse reference genome mm9 using TopHat v2.1.1 (*40*) with parameters *--no-coverage-search* and *--library-type fr-unstranded*. PCR duplicates were removed using Picard (http://broadinstitute.github.io/picard/). Gene counts were calculated using HTSeq-count v0.8.0 (*41*) with parameters *--stranded=no --mode=intersection-nonempty* using RefSeq mm9 annotation downloaded from the University of California, Santa Cruz. Differential expression analyses were performed using the R package DESeq2 v1.20 (*42*) using default parameters. Genes with an absolute $\log_2$ fold change of 1 and false discovery rate of <0.1 were considered as differentially expressed. Gene enrichment analysis on down- and up-regulated genes was performed using DAVID 6.8 (*43*). A preranked GSEA (*44*) was performed using gene lists (Signature Gene Lists) from multiple skin cell populations obtained from (*31*). The analysis was performed using default parameters (weighted as enrichment statistic) and ranking the input gene list using $\log_2$ fold-change data obtained from DESeq2.

To assess the expression of differentially expressed genes in Ring1A/B$^{-/-}$ versus wild-type HFSC in other mouse tissues, we used public RNA-seq data (bam files) deposited by ENCODE at (http://hgdownload.soe.ucsc.edu/goldenPath/mm9/encodeDCC/wgEncodeLicrRnaSeq/). Bam files were processed with the pipeline described previously, and RPKM (Read Per Kilobase of Milion Mapped Reads) data were normalized with the function normalize.quantiles() from the R package preprocessCore (https://github.com/bmbolstad/preprocessCore).

ChIP-seq analysis

Reads were aligned to the mouse reference genome mm9 using Bowtie v1.2.2 (*45*) with default parameters and not allowing multimapping (-m1). PCR duplicates were removed using Picard (http://broadinstitute.github.io/picard/). Peaks were called using MACS2 v2.1.1 (*46*) with parameters *-g mm --nomodel -p 1e-10 –B*. Genomic peak annotation was performed using the R package ChIPpeakAnno v3.15 (*47*), considering the promoter region of ±2.5 kb around the TSS (Transcription Start Site). Overlaps of ChIP-seq targets were performed as following: Genes with peaks in their promoter regions (±2.5 kb around TSS) were considered as targets. Then, the overlap between target gene lists was performed using the R package VennDiagram v1.6.20 (*48*).

For heatmap representation of ChIP-seq signal, bigwig files, with input signal subtracted, were generated using the function bamCompare from deepTools 2.0 (*49*) with parameters *--ratio subtract –bs 30 --extendReads 200*. To normalize for differences in sample library size, a scaling factor for each sample was calculated as (1/total mapped reads) × 1 million and applied during bigwig file generation with the parameter *–scaleFactors* from bamCompare.

Ring1b ChIP-seq targets were clustered in four groups according to their RPKM expression using the *dplyr* function *ntile()*. Tracks for H3K27me3 from ISC and HFSC were obtained from (*9*) and (*28*), respectively, and processed with the pipeline described previously.

SUPPLEMENTARY MATERIALS

Supplementary material for this article is available at http://advances.sciencemag.org/cgi/content/full/5/5/eaav1594/DC1

Fig. S1. Mouse model of PRC1 activity abrogation.
Fig. S2. PRC1 loss severely affects anagen onset and progression.
Fig. S3. PRC1 loss has different transcriptional effects among tissues.
Fig. S4. Expression of core PRC1 subunits in HFSCs.
Fig. S5. Genomic distribution of PRC1 in ISCs resembles HFSCs.

REFERENCES AND NOTES

1. D. Pasini, L. Di Croce, Emerging roles for Polycomb proteins in cancer. *Curr. Opin. Genet. Dev.* **36**, 50–58 (2016).
2. B. Vogelstein, N. Papadopoulos, V. E. Velculescu, S. Zhou, L. A. Diaz Jr., K. W. Kinzler, Cancer genome landscapes. *Science* **339**, 1546–1558 (2013).
3. L. Di Croce, K. Helin, Transcriptional regulation by Polycomb group proteins. *Nat. Struct. Mol. Biol.* **20**, 1147–1155 (2013).
4. S. Aranda, G. Mas, L. Di Croce, Regulation of gene transcription by Polycomb proteins. *Sci. Adv.* **1**, e1500737 (2015).
5. A. Scelfo, A. Piunti, D. Pasini, The controversial role of the Polycomb group proteins in transcription and cancer: How much do we not understand Polycomb proteins? *FEBS J.* **282**, 1703–1722 (2015).
6. Z. Gao, J. Zhang, R. Bonasio, F. Strino, A. Sawai, F. Parisi, Y. Kluger, D. Reinberg, PCGF homologs, CBX proteins, and RYBP define functionally distinct PRC1 family complexes. *Mol. Cell* **45**, 344–356 (2012).
7. E. S. Bardot, V. J. Valdes, J. Zhang, C. N. Perdigoto, S. Nicolis, S. A. Hearn, J. M. Silva, E. Ezhkova, Polycomb subunits Ezh1 and Ezh2 regulate the Merkel cell differentiation program in skin stem cells. *EMBO J.* **32**, 1990–2000 (2013).
8. F. Chiacchiera, D. Pasini, Control of adult intestinal identity by the Polycomb repressive machinery. *Cell Cycle* **16**, 243–244 (2017).
9. F. Chiacchiera, A. Rossi, S. Jammula, A. Piunti, A. Scelfo, P. Ordóñez-Morán, J. Huelsken, H. Koseki, D. Pasini, Polycomb complex PRC1 preserves intestinal stem cell identity by sustaining Wnt/β-catenin transcriptional activity. *Cell Stem Cell* **18**, 91–103 (2016).
10. F. Chiacchiera, A. Rossi, S. Jammula, M. Zanotti, D. Pasini, PRC2 preserves intestinal progenitors and restricts secretory lineage commitment. *EMBO J.* **35**, 2301–2314 (2016).
11. I. Cohen, D. Zhao, C. Bar, V. J. Valdes, K. L. Dauber-Decker, M. B. Nguyen, M. Nakayama, M. Rendl, W. A. Bickmore, H. Koseki, D. Zheng, E. Ezhkova, PRC1 fine-tunes gene repression and activation to safeguard skin development and stem cell specification. *Cell Stem Cell* **22**, 726–739.e7 (2018).
12. K. L. Dauber, C. N. Perdigoto, V. J. Valdes, F. J. Santoriello, I. Cohen, E. Ezhkova, Dissecting the roles of Polycomb repressive complex 2 subunits in the control of skin development. *J. Invest. Dermatol.* **136**, 1647–1655 (2016).
13. E. Ezhkova, W.-H. Lien, N. Stokes, H. A. Pasolli, J. M. Silva, E. Fuchs, EZH1 and EZH2 cogovern histone H3K27 trimethylation and are essential for hair follicle homeostasis and wound repair. *Genes Dev.* **25**, 485–498 (2011).
14. M. Vidal, K. Starowicz, Polycomb complexes PRC1 and their function in hematopoiesis. *Exp. Hematol.* **48**, 12–31 (2017).
15. N. Barker, S. Bartfeld, H. Clevers, Tissue-resident adult stem cell populations of rapidly self-renewing organs. *Cell Stem Cell* **7**, 656–670 (2010).
16. E. Fuchs, Epithelial skin biology: Three decades of developmental biology, a hundred questions answered and a thousand new ones to address. *Curr. Top. Dev. Biol.* **116**, 357–374 (2016).
17. A. Haegebarth, H. Clevers, Wnt signaling, Lgr5, and stem cells in the intestine and skin. *Am. J. Pathol.* **174**, 715–721 (2009).
18. V. Jaks, N. Barker, M. Kasper, J. H. van Es, H. J. Snippert, H. Clevers, R. Toftgård, Lgr5 marks cycling, yet long-lived, hair follicle stem cells. *Nat. Genet.* **40**, 1291–1299 (2008).
19. R. Paus, S. Müller-Röver, C. van der Veen, M. Maurer, S. Eichmüller, G. Ling, U. Hofmann, K. Foitzik, L. Mecklenburg, B. Handjiski, A comprehensive guide for the recognition and classification of distinct stages of hair follicle morphogenesis. *J. Invest. Dermatol.* **113**, 523–532 (1999).
20. R. C. Adam, H. Yang, Y. Ge, W.-H. Lien, P. Wang, Y. Zhao, L. Polak, J. Levorse, S. C. Baksh, D. Zheng, E. Fuchs, Temporal layering of signaling effectors drives chromatin remodeling during hair follicle stem cell lineage progression. *Cell Stem Cell* **22**, 398–413.e7 (2018).
21. V. Greco, T. Chen, M. Rendl, M. Schober, H. A. Pasolli, N. Stokes, J. dela Cruz-Racelis, E. Fuchs, A two-step mechanism for stem cell activation during hair regeneration. *Cell Stem Cell* **4**, 155–169 (2009).
22. J. D. Hoeck, B. Biehs, A. V. Kurtova, N. M. Kljavin, F. de Sousa e Melo, B. Alicke, H. Koeppen, Z. Modrusan, R. Piskol, F. J. de Sauvage, Stem cell plasticity enables hair regeneration following *Lgr5*$^{+}$ cell loss. *Nat. Cell Biol.* **19**, 666–676 (2017).
23. Y.-C. Hsu, L. Li, E. Fuchs, Transit-amplifying cells orchestrate stem cell activity and tissue regeneration. *Cell* **157**, 935–949 (2014).
24. H. Yang, R. C. Adam, Y. Ge, Z. L. Hua, E. Fuchs, Epithelial-mesenchymal micro-niches govern stem cell lineage choices. *Cell* **169**, 483–496.e13 (2017).
25. S. Müller-Röver, K. Foitzik, R. Paus, B. Handjiski, C. der Veen, S. Eichmüller, I. A. McKay, K. S. Stenn, A comprehensive guide for the accurate classification of murine hair follicles in distinct hair cycle stages. *J. Invest. Dermatol.* **117**, 3–15 (2001).
26. A. R. Foster, C. Nicu, M. R. Schneider, E. Hinde, R. Paus, Dermal white adipose tissue undergoes major morphological changes during the spontaneous and induced murine hair follicle cycling: A reappraisal. *Arch. Dermatol. Res.* **310**, 453–462 (2018).

27. B. St-Jacques, H. R. Dassule, I. Karavanova, V. A. Botchkarev, J. Li, P. S. Danielian, J. A. McMahon, P. M. Lewis, R. Paus, A. P. McMahon, Sonic hedgehog signaling is essential for hair development. *Curr. Biol.* **8**, 1058–1069 (1998).
28. W. H. Lien, X. Guo, L. Polak, L. N. Lawton, R. A. Young, D. Zheng, E. Fuchs, Genome-wide maps of histone modifications unwind in vivo chromatin states of the hair follicle lineage. *Cell Stem Cell* **9**, 219–232 (2011).
29. B. E. Bernstein, T. S. Mikkelsen, X. Xie, M. Kamal, D. J. Huebert, J. Cuff, B. Fry, A. Meissner, M. Wernig, K. Plath, R. Jaenisch, A. Wagschal, R. Feil, S. L. Schreiber, E. S. Lander, A bivalent chromatin structure marks key developmental genes in embryonic stem cells. *Cell* **125**, 315–326 (2006).
30. M. Moriyama, A.-D. Durham, H. Moriyama, K. Hasegawa, S.-I. Nishikawa, F. Radtke, M. Osawa, Multiple roles of Notch signaling in the regulation of epidermal development. *Dev. Cell* **14**, 594–604 (2008).
31. A. Rezza, Z. Wang, R. Sennett, W. Qiao, D. Wang, N. Heitman, K. W. Mok, C. Clavel, R. Yi, P. Zandstra, A. Ma'ayan, M. Rendl, Signaling networks among stem cell precursors, transit-amplifying progenitors, and their niche in developing hair follicles. *Cell Rep.* **14**, 3001–3018 (2016).
32. C. Lee, C.-H. Huang, LASAGNA-Search 2.0: Integrated transcription factor binding site search and visualization in a browser. *Bioinformatics* **30**, 1923–1925 (2014).
33. L. Morey, L. Aloia, L. Cozzuto, S. A. Benitah, L. Di Croce, RYBP and Cbx7 define specific biological functions of polycomb complexes in mouse embryonic stem cells. *Cell Rep.* **3**, 60–69 (2013).
34. H. Richly, L. Aloia, L. Di Croce, Roles of the Polycomb group proteins in stem cells and cancer. *Cell Death Dis.* **2**, e204 (2011).
35. M. de Napoles, J. E. Mermoud, R. Wakao, Y. A. Tang, M. Endoh, R. Appanah, T. B. Nesterova, J. Silva, A. P. Otte, M. Vidal, H. Koseki, N. Brockdorff, Polycomb group proteins Ring1A/B link ubiquitylation of histone H2A to heritable gene silencing and X inactivation. *Dev. Cell* **7**, 663–676 (2004).
36. N. Barker, J. H. van Es, J. Kuipers, P. Kujala, M. van den Born, M. Cozijnsen, A. Haegebarth, J. Korving, H. Begthel, P. J. Peters, H. Clevers, Identification of stem cells in small intestine and colon by marker gene *Lgr5*. *Nature* **449**, 1003–1007 (2007).
37. P. Soriano, Generalized *lacZ* expression with the ROSA26 Cre reporter strain. *Nat. Genet.* **21**, 70–71 (1999).
38. S. Picelli, O. R. Faridani, Å. K. Björklund, G. Winberg, S. Sagasser, R. Sandberg, Full-length RNA-seq from single cells using Smart-seq2. *Nat. Protoc.* **9**, 171–181 (2014).
39. A. P. Bracken, N. Dietrich, D. Pasini, K. H. Hansen, K. Helin, Genome-wide mapping of Polycomb target genes unravels their roles in cell fate transitions. *Genes Dev.* **20**, 1123–1136 (2006).
40. C. Trapnell, L. Pachter, S. L. Salzberg, TopHat: Discovering splice junctions with RNA-seq. *Bioinformatics* **25**, 1105–1111 (2009).
41. S. Anders, P. T. Pyl, W. Huber, HTSeq—A Python framework to work with high-throughput sequencing data. *Bioinformatics* **31**, 166–169 (2015).
42. M. I. Love, W. Huber, S. Anders, Moderated estimation of fold change and dispersion for RNA-seq data with DESeq2. *Genome Biol.* **15**, 550 (2014).
43. D. W. Huang, B. T. Sherman, R. A. Lempicki, Systematic and integrative analysis of large gene lists using DAVID bioinformatics resources. *Nat. Protoc.* **4**, 44–57 (2009).
44. A. Subramanian, P. Tamayo, V. K. Mootha, S. Mukherjee, B. L. Ebert, M. A. Gillette, A. Paulovich, S. L. Pomeroy, T. R. Golub, E. S. Lander, J. P. Mesirov, Gene set enrichment analysis: A knowledge-based approach for interpreting genome-wide expression profiles. *Proc. Natl. Acad. Sci. U.S.A.* **102**, 15545–15550 (2005).
45. B. Langmead, C. Trapnell, M. Pop, S. L. Salzberg, Ultrafast and memory-efficient alignment of short DNA sequences to the human genome. *Genome Biol.* **10**, R25 (2009).
46. Y. Zhang, T. Liu, C. A. Meyer, J. Eeckhoute, D. S. Johnson, B. E. Bernstein, C. Nusbaum, R. M. Myers, M. Brown, W. Li, X. S. Liu, Model-based Analysis of ChIP-Seq (MACS). *Genome Biol.* **9**, R137 (2008).
47. L. J. Zhu, C. Gazin, N. D. Lawson, H. Pagès, S. M. Lin, D. S. Lapointe, M. R. Green, ChIPpeakAnno: A Bioconductor package to annotate ChIP-seq and ChIP-chip data. *BMC Bioinf.* **11**, 237 (2010).
48. H. Chen, P. C. Boutros, VennDiagram: A package for the generation of highly-customizable Venn and Euler diagrams in R. *BMC Bioinf.* **12**, 35 (2011).
49. F. Ramírez, D. P. Ryan, B. Grüning, V. Bhardwaj, F. Kilpert, A. S. Richter, S. Heyne, F. Dündar, T. Manke, deepTools2: A next generation web server for deep-sequencing data analysis. *Nucleic Acids Res.* **44**, W160–W165 (2016).

Acknowledgments: We thank M. Vidal and H. Koseki for the *Ring1a*$^{-/-}$ *Ring1b*$^{fl/fl}$ mice. We thank all members of the DP group for helpful discussions. **Funding:** The work in the DP laboratory was supported by grants from the Italian Association for Cancer Research (AIRC), the Italian Ministry of Health, the EMBO young investigator, and the European Research Council (ERC). S.P. was supported by fellowship from the AIRC. F.C. is supported by a grant from the AIRC (grant no. 20344) and by IEO-CCM Foundation (FIEO). **Author contributions:** S.P., A.D., A.R., D.M., L.B., M.Z., and F.C. performed experimental work. D.F.-P and C.M.B. performed the bioinformatics analysis. A.S. produced anti-BMI1 antibody. S.P., D.F.-P, C.M.B., F.C., and D.P. analyzed the data. F.C. and D.P. conceived the experiments. S.P., F.C., and D.P. wrote the manuscript. **Competing interests:** The authors declare that they have no competing interests. **Data and materials availability:** All data needed to evaluate the conclusions in the paper are present in the paper and/or the Supplementary Materials. Additional data related to this paper may be requested from the authors.

Submitted 20 August 2018
Accepted 2 April 2019
Published 15 May 2019
10.1126/sciadv.aav1594

Citation: S. Pivetti, D. Fernandez-Perez, A. D'Ambrosio, C. M. Barbieri, D. Manganaro, A. Rossi, L. Barnabei, M. Zanotti, A. Scelfo, F. Chiacchiera, D. Pasini, Loss of PRC1 activity in different stem cell compartments activates a common transcriptional program with cell type–dependent outcomes. *Sci. Adv.* **5**, eaav1594 (2019).

Loss of PRC1 activity in different stem cell compartments activates a common transcriptional program with cell type–dependent outcomes

Silvia Pivetti, Daniel Fernandez-Perez, Alessandro D'Ambrosio, Caterina Maria Barbieri, Daria Manganaro, Alessandra Rossi, Laura Barnabei, Marika Zanotti, Andrea Scelfo, Fulvio Chiacchiera and Diego Pasini

Sci Adv **5** (5), eaav1594.
DOI: 10.1126/sciadv.aav1594

ACKNOWLEDGMENTS

I would like to thank my Supervisor Dr. Diego Pasini for giving me the opportunity to join this excellent research place and his laboratory, and to work on challenging but exciting projects.

I would like to thank all the Pasini's lab members, both present and former members, for these four intense years of work, and life. I really appreciated the possibility to learn something from each of you.

A special thank goes to Fulvio, now Prof. Chiacchiera. Thank you for helping me, sustaining me and teaching me during these years. I wish you all the best for your new exciting future.

Thanks to Daria, Cecilia, Laura, Debora, Luciano, Daniel, Annachiara and Simona, more than just colleagues, for supporting and understanding me, particularly in the last year. We had a lot of great moments together that I will never forget. Everything is better with you.

Thanks to Loris, we met at the high school and we pursued this career together, you inspired and sustained me during all these years.

Thanks to all of my friends, especially to Alice and Luca. We shared a lot of time together and all of our fantastic adventures helped me during these years.

Thanks to my family, for their unlimited support. You sustained me more than anyone, I am who I am because of you.

Finally, thanks to Nicola, you were always right beside me during all these years, sharing with me all the good and the bad times of this PhD. We did it together, and I would never have chosen anyone but you to reach this goal. This is for you, and for our new family.

“One, remember to look up at the stars and not down at your feet. Two, never give up work. Work gives you meaning and purpose and life is empty without it. Three, if you are lucky enough to find love, remember it is there and don't throw it away.”

— Stephen Hawking

“The important thing is not to stop questioning. Curiosity has its own reason for existence. One cannot help but be in awe when he contemplates the mysteries of eternity, of life, of the marvelous structure of reality. It is enough if one tries merely to comprehend a little of this mystery each day.”

—"Old Man's Advice to Youth: 'Never Lose a Holy Curiosity.'" LIFE Magazine (2 May 1955) p. 64” — Albert Einstein